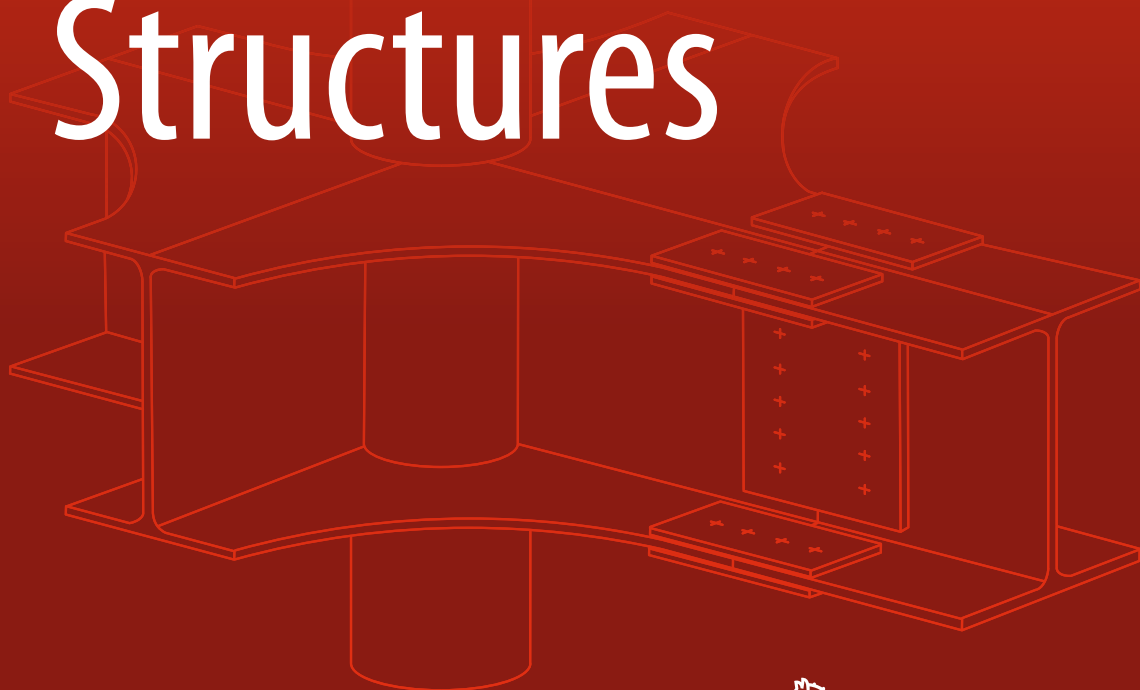


József Farkas  
Károly Jármai

# Optimum Design of Steel Structures



Springer

# Optimum Design of Steel Structures

József Farkas and Károly Jármai

# Optimum Design of Steel Structures

 Springer

Dr. József Farkas  
Professor Emeritus of Metal Structures  
University of Miskolc  
Hungary

Dr. Károly Jármai  
Professor of Structural Engineering  
University of Miskolc  
Hungary

ISBN 978-3-642-36867-7

ISBN 978-3-642-36868-4 (eBook)

DOI 10.1007/978-3-642-36868-4

Springer Heidelberg New York Dordrecht London

Library of Congress Control Number: 2013932222

© Springer-Verlag Berlin Heidelberg 2013

This work is subject to copyright. All rights are reserved by the Publisher, whether the whole or part of the material is concerned, specifically the rights of translation, reprinting, reuse of illustrations, recitation, broadcasting, reproduction on microfilms or in any other physical way, and transmission or information storage and retrieval, electronic adaptation, computer software, or by similar or dissimilar methodology now known or hereafter developed. Exempted from this legal reservation are brief excerpts in connection with reviews or scholarly analysis or material supplied specifically for the purpose of being entered and executed on a computer system, for exclusive use by the purchaser of the work. Duplication of this publication or parts thereof is permitted only under the provisions of the Copyright Law of the Publisher's location, in its current version, and permission for use must always be obtained from Springer. Permissions for use may be obtained through RightsLink at the Copyright Clearance Center. Violations are liable to prosecution under the respective Copyright Law.

The use of general descriptive names, registered names, trademarks, service marks, etc. in this publication does not imply, even in the absence of a specific statement, that such names are exempt from the relevant protective laws and regulations and therefore free for general use.

While the advice and information in this book are believed to be true and accurate at the date of publication, neither the authors nor the editors nor the publisher can accept any legal responsibility for any errors or omissions that may be made. The publisher makes no warranty, express or implied, with respect to the material contained herein.

Printed on acid-free paper

Springer is part of Springer Science+Business Media ([www.springer.com](http://www.springer.com))

# Preface

The cost plays an important role in the design of engineering structures. This role can be illustrated by an example. In the design of a crossing over a big river the designer has two possibilities: design a number of small-span bridges with a number of basements or build a large-span bridge with only two basements. The cost comparison helps designers to select the cheaper version since the cost of basements depends on the quality of soil.

In the case of welded structures the cost comparison helps to select the most economic structural version since the welding is an expensive fabrication technology. Our research has been focused on the use of the optimum design methods to minimize the cost of welded structures. This systematic research resulted in optimized structural types using realistic numerical problems.

This book contains studies worked out during last five years and is a continuation of or books published in years 1984, 1997, 2003 and 2008. Studies on beams, tubular trusses, frames, stiffened plates and shells are grouped in separate chapters. Chapter 1 gives a survey on our experiences in the field of structural optimization. Separate chapters deal with the mathematical function minimization methods and the cost calculation.

Our aim is to transfer the results of our research relating to the optimum design of steel structures, the ways to select the most suitable structural versions. This transfer is enabled by abstracts and conclusions of each section.

The following studies on the optimum design for minimum weight or cost can be brought into prominence: Chapter 4: fire design of a welded box beam, Chapter 5: transmission line tower constructed as a welded tubular truss, Chapter 6: earthquake-resistant design of braced frames, Chapter 7: storage tank roof constructed from welded stiffened sectorial plates, Chapter 8: ring-stiffened cylindrical and conical shells.

Structural optimization is a design system for searching better solutions, which better fulfil engineering requirements. The main requirements of a modern load-carrying structure are the safety, fitness for production and economy. The safety and producibility are guaranteed by design and fabrication constraints, and economy can be achieved by minimization of a cost function.

The main aim of this book is to give designers and fabricators aspects for selection of the best structural solution. A lot of structural versions fulfil the design and fabrication constraints and designers should select from these possibilities the best ones. A suitable cost function helps this selection, since a modern structure should be not only safe and fit for production but also economic.

In most cases, treated in this book, much more unknowns should be varied to find the best solution. In these cases one needs special mathematical methods, some of them are treated in this book as well.

The optimum design procedure can be formulated mathematically as follows: the objective function should be minimized

$$f(x) \rightarrow \min, x = (x_1, \dots, x_n)$$

subject to constraints

$$g_j(x) \leq 0, j = 1 \dots p$$

where  $n$  is the number of unknowns and  $p$  is the number of constraints.

The solution of this constrained function minimization problem needs effective mathematical methods.

The above description shows that the structural optimization has four main components:

- (1) *design constraints* relate to stress, stability, deformation, eigenfrequency, damping,
- (2) *fabrication constraints* formulate the limitation of residual welding distortions, requirements for welding technology, limitations of plate thicknesses and main structural dimensions, definition of available profile series,
- (3) *a cost function* is formulated according to the fabrication sequence and contains the cost of materials, assembly, welding, cutting and painting,
- (4) *mathematical methods*.

In our systematic research we have developed suitable means for these main components. Design constraints are formulated according to relevant Eurocodes or design rules of American Petroleum Institute (API), Det Norske Veritas (DNV) and European Convention for Constructional Steelwork (ECCS).

We have worked out a calculation method for residual welding stresses and distortions, for the cost function we have created a calculation method mainly for welded structures and we use several effective mathematical algorithms.

We have solved a lot of structural optimization problems for various structural models. Since these models are the main components of industrial structures, designers can use them in their work. The cost estimation in design stage is a good basis for the comparison of candidate structural versions.

Our structural models of welded I- and box-beams, tubular trusses, steel frames, stiffened plates and shells can be used in all industrial applications i.e. in bridges, buildings, roofs, columns, towers, ships, cranes, offshore structures, belt-conveyor bridges, machine structures, vehicles, etc.

Since the functions are highly nonlinear only numerical problems can be treated. Therefore, the conclusions are not completely general. In spite of this the solutions give valuable aspects for optimum design, because the numerical data are selected realistically.

The first step of the optimization procedure is the selection of variables. For this selection we need to know the main characteristics of a typical structure as follows: materials, loads, geometry, topology, profiles, fabrication

technology, joints, costs. The better solutions can be obtained by changing these characteristics.

Summarizing: the general aspect of our book is the cost comparison, which is an effective means to select the most suitable structural versions.

We participate continuously in the following conference series: Annual Assemblies International Institute of Welding (IIW), World Congresses of ISSMO (International Society of Structural and Multidisciplinary Optimization), Eurosteel European Conferences of Steel Structures, Tubular Structures Symposia (organized by the IIW subcommission XV-E).

Beside the Conference Proceedings, we publish our studies also in well-known international engineering journals i.e. Structural and Multidisciplinary Optimization, Welding in the World, Computers and Structures, Engineering Optimization, Engineering Structures, Thin-walled Structures, Journal of Constructional Steel Research etc.

We hope that this book can help designers, students, researchers, manufacturers with the aspects shown in realistic models to find better, optimal, competitive structural solutions.

# Acknowledgements

The authors would like to acknowledge the co-operation and help of the following organizations

- Foundation for the Structural Optimization at the University of Miskolc,
- Hungarian Scientific Research Fund OTKA T 75678 project
- TÁMOP 4.2.1.B-10/2/KONV-2010-0001 entitled “Increasing the quality of higher education through the development of research - development and innovation program at the University of Miskolc supported by the European Union, co-financed by the European Social Fund.”

and last but not least the

- University of Miskolc, Hungary, our university.

The authors would like to acknowledge the help of the following persons:

- Dr. László Kota, research fellow,
- Dr. György Kovács, associate professor,
- Dr. Zoltán Virág, associate professor,
- former PhD. students,
- Csaba Barcsák, BSc. student,
- László Daróczy, former MSc. student,

and Dr. Ferenc Orbán professor for the finite element calculations from the University of Pécs.

Last but not least many-many thanks for our family members, who helped a lot everyday.

József Farkas  
Károly Jármai  
University of Miskolc, April, 2013



# Contents

<b>Preface .....</b>	<b>V</b>
<b>Acknowledgements .....</b>	<b>IX</b>
<b>About the Authors .....</b>	<b>XIX</b>
<b>List of Symbols.....</b>	<b>XXI</b>
<b>Abbreviations .....</b>	<b>XXV</b>
<b>1 Experiences with the Optimum Design of Steel Structures .....</b>	<b>1</b>
1.1 Introduction .....	1
1.2 Foundation of the School for Structural Optimization at the University of Miskolc .....	2
1.3 Derivation of the Structural Optimization System.....	2
1.4 Advantages and Disadvantages of Two Different Design Methods .....	5
1.4.1 Design by Routine.....	5
1.4.2 Optimum Design .....	6
1.5 The Problem of the Interaction of Two Instabilities .....	6
1.6 Detailed Results for Different Structural Types.....	7
1.6.1 Compressed and Bent Columns Constructed from Stiffened Shell or from Square Box Walls of Stiffened Plates .....	7
1.6.2 Stiffened or Cellular Plate Supported at Four Corners Subject to a Uniformly Distributed Normal Load (Fig.1.4) .....	9
1.6.3 A Wind Turbine Tower Constructed as a Shell or Tubular Truss Structure .....	9
1.7 Survey of Selected Literature of the Optimum Design of Steel Structures .....	11
1.7.1 Truss Structures.....	11
1.7.2 Building Frames .....	11
1.7.3 Industrial Applications .....	11
1.8 Conclusions .....	13
<b>2 Newer Mathematical Methods in Structural Optimization .....</b>	<b>15</b>
2.1 Introduction .....	15
2.2 Firefly Algorithm.....	16
2.3 Particle Swarm Optimization Algorithm .....	19
2.3.1 The PSO Algorithm.....	19
2.3.2 Modification of PSO Algorithm with Gradient Estimation.....	21
2.3.3 Comparing the Standard PSO and the Modified PSO (GPSO) .....	23
2.4 The IOSO Technique .....	24

2.4.1	Main Features of IOSO Technology .....	24
2.4.2	Testing of the Method .....	25
2.4.3	Novelty and Distinctive Features of IOSO.....	27
<b>3</b>	<b>Cost Calculations .....</b>	<b>29</b>
3.1	Introduction .....	29
3.2	The Cost Function.....	29
3.2.1	The Cost of Materials.....	30
3.2.2	The Fabrication Cost in General .....	30
3.2.2.1	Fabrication Times for Welding .....	30
3.2.2.2	Thermal and Waterjet Cutting .....	32
3.2.2.3	Time for Flattening Plates .....	39
3.2.2.4	Surface Preparation Time .....	39
3.2.2.5	Painting Time .....	40
3.2.2.6	Times of Hand Cutting and Machine Grinding of Strut Ends.....	40
3.2.2.7	Cost of Intumescent Painting .....	40
3.2.3	Total Cost Function.....	40
3.3	Conclusion .....	41
<b>4</b>	<b>Beams and Columns .....</b>	<b>43</b>
4.1	Comparison of Minimum Volume and Minimum Cost Design of a Welded Box Beam.....	43
4.1.1	Introduction.....	43
4.1.2	Minimum Cross-Sectional Area Design .....	44
4.1.3	Minimum Cost Design.....	46
4.1.4	Numerical Data and Results .....	46
4.2	Minimum Cost Design for Fire Resistance of a Welded Box Column and a Welded Box Beam.....	47
4.2.1	Introduction.....	47
4.2.2	The Critical Temperature Method .....	48
4.2.3	A Centrally Compressed Column with Pinned Ends of Welded Square Box Cross-Section .....	50
4.2.3.1	Overall Buckling Constraint for Ambient Temperature.....	51
4.2.3.2	Overall Buckling Constraint in Fire .....	51
4.2.3.3	Local Buckling Constraint.....	52
4.2.3.4	Cost Function.....	52
4.2.3.5	Numerical Data and Results .....	53
4.2.3.6	Cost Including Protection .....	53
4.2.4	A Simply Supported Uniformly Loaded Welded Box Beam.....	54
4.2.4.1	Optimum Design .....	54
4.2.4.2	Optimum Design of Unprotected Beam with Stress Constraint .....	55
4.2.4.3	Optimum Design of the Protected Beam with Stress Constraint .....	57

4.2.4.4	Optimum Design of Unprotected Beam with Deflection Constraint .....	57
4.2.4.5	Optimum Design of the Protected Beam with Deflection Constraint .....	58
4.2.5	Conclusions.....	58
<b>5</b>	<b>Tubular Trusses.....</b>	<b>61</b>
5.1	Survey of Selected Literature.....	62
5.2	Comparison of Minimum Volume and Minimum Cost Design of a Welded Tubular Truss .....	63
5.2.1	Introduction.....	63
5.2.2	Minimum Volume Design .....	63
5.2.3	Minimum Cost Design.....	66
5.2.4	Numerical Data and Results .....	67
5.2.5	Conclusions.....	68
5.3	Optimum Design of Tubular Trusses for Displacement Constraint.....	68
5.3.1	Introduction.....	69
5.3.2	The Displacement Constraint.....	69
5.3.3	Design for Overall Buckling.....	69
5.3.4	A Truss Column with Parallel Chords (Fig. 5.2) .....	70
5.3.5	A Truss Column with Non-parallel Chords (Fig. 5.3) .....	72
5.4	Volume and Cost Minimization of a Tubular Truss with Non-parallel Chords in the Case of a Displacement-Constraint .....	75
5.4.1	Introduction.....	75
5.4.2	Minimum Volume Design of the Tubular Truss with Non-parallel Chords.....	76
5.4.3	Check of the Compression Rods for Overall Buckling.....	80
5.4.4	The Cost Function.....	80
5.4.5	Numerical Data .....	82
5.4.6	The Optimization Process .....	82
5.4.7	Results of the Optimization .....	82
5.4.8	Check of Strength of a Tubular Joint.....	83
5.4.9	Conclusions.....	85
5.5	Minimum Cost Design and Comparison of Tubular Trusses with N- and Cross-(Rhombic)-Bracing .....	86
5.5.1	Introduction.....	86
5.5.2	The Optimization Process .....	87
5.5.3	Optimum Design of an N-Type Planar Tubular Truss.....	88
5.5.3.1	Optimum Height and Cross-Sectional Areas for Stress and Overall Buckling Constraints.....	88
5.5.3.2	Optimum Height and Cross-Sectional Areas for Deflection Constraint .....	90
5.5.4	Optimum Design of a Rhombic-Type Planar Tubular Truss .....	91
5.5.4.1	Optimum Height and Cross-Sectional Areas for Stress and Overall Buckling Constraints.....	91

5.5.4.2	Check of a Truss Joint with Available Tubular Profiles.....	94
5.5.4.3	Optimum Height and Cross-Sectional Areas for Deflection Constraint .....	95
5.5.5	Comparison of the Two Bracing Types .....	97
5.5.6	Conclusions.....	97
5.6	Optimum Design of a Transmission Line Tower Constructed from Welded Tubular Truss.....	98
5.6.1	Introduction.....	98
5.6.2	Loads .....	99
5.6.3	Geometric Data (Fig. 5.10, 5.11) .....	100
5.6.4	Rod Forces from a Horizontal Force $F = 1$ .....	103
5.6.5	Rod Forces from $H$ , $F1$ and $F2$ .....	104
5.6.6	Optimization Process .....	104
5.6.7	Formulae for Cross-Sectional Areas of Governing Rods.....	104
5.6.8	Formulae for Volume $V$ and Cost $K$ of the Truss in the Function of $\beta$ .....	105
5.6.9	Search for $\beta_{opt}$ for $V_{min}$ and $K_{min}$ .....	106
5.6.10	Selection of Available Profiles .....	107
5.6.11	Optimum Mass of the Tower .....	107
5.6.12	Mass Comparison with the Tower Published by Rao (1995).....	107
<b>6</b>	<b>Frames .....</b>	<b>109</b>
6.1	Minimum Cost Seismic Design of a Welded Steel Portal Frame with X-Bracing .....	110
6.1.1	Absorbed Energy of CHS and SHS Braces Cyclically Loaded in Tension-Compression .....	110
6.1.2	Seismic Design of a Portal Frame.....	116
6.1.2.1	Calculation of the Seismic Force.....	116
6.1.2.2	Normal Forces and Bending Moments in Vertical Frames (Fig. 6.6) .....	118
6.1.2.3	Geometric Characteristics of the Square Hollow Section (Fig. 6.7) .....	119
6.1.2.4	Calculation of the Elastic Sway.....	120
6.1.2.5	Constraint on Sway Limitation .....	121
6.1.2.6	Local Buckling Constraints .....	123
6.1.2.7	Stress Constraint for the Columns .....	123
6.1.2.8	Stress Constraint for the Beams.....	124
6.1.2.9	Investigation of the Joint of the Beam and Brace .....	125
6.1.2.10	The Cost Function.....	126
6.1.2.11	Optimization and Results.....	127
6.1.2.12	Conclusions .....	128
6.2	Seismic Design of a V-Braced 3D Multi-storey Steel Frame.....	129
6.2.1	Introduction.....	129
6.2.2	Main Dimensions of the Given Frame .....	130
6.2.3	Loads .....	131
6.2.3.1	Vertical Loads .....	131

6.2.3.2	Seismic Load .....	131
6.2.4	Design of CHS V-Bracings.....	132
6.2.4.1	Constraint on Tensile Stress .....	132
6.2.4.2	Constraint on Overall Buckling.....	133
6.2.4.3	Constraint on Strut Slenderness for Seismic Zone .....	133
6.2.4.4	Constraint on Energy Absorption Capacity .....	133
6.2.4.5	Design Results .....	134
6.2.5	Design of Beams.....	135
6.2.6	Design of Columns .....	137
6.2.7	Design of Joints .....	139
6.2.7.1	Beam-to-Column Connections .....	139
6.2.7.2	Joints of Braces.....	140
6.2.8	Conclusions.....	141
<b>7</b>	<b>Stiffened Plates.....</b>	<b>143</b>
7.1	Minimum Cost Design of an Orthogonally Stiffened Welded Steel Plate with a Deflection Constraint.....	144
7.1.1	Introduction.....	144
7.1.2	Residual Welding Deflection from Longitudinal Welds of a Straight Beam .....	145
7.1.3	Residual Welding Curvatures in an Orthogonally Stiffened Plate .....	147
7.1.4	The Grid Effect.....	148
7.1.5	Assembly Desk of Square Symmetry with 4-4 Stiffeners.....	150
7.1.5.1	Solution of the Gridwork from Shrinkage of Welds (Fig. 7.4).....	150
7.1.5.2	Solution of the Gridwork from the Uniformly Distributed Normal Load (Fig. 7.5).....	152
7.1.6	Minimum Cost Design of the Assembly Desk with 4-4 Stiffeners Considering the Grid-Effect .....	153
7.1.6.1	Stress Constraint.....	153
7.1.6.2	Deflection Constraint.....	154
7.1.6.3	Cost Function.....	155
7.1.6.4	Results of Optimization.....	156
7.1.7	Minimum Cost Design of the Assembly Desk without Grid Effect .....	156
7.1.7.1	Stress Constraint.....	156
7.1.7.2	Deflection Constraint.....	157
7.1.7.3	Cost Function.....	158
7.1.7.4	Results of Optimization.....	158
7.1.8	Conclusions.....	159
7.2	Minimum Cost Design of a Welded Stiffened Steel Sectorial Plate .....	159
7.2.1	Introduction.....	160
7.2.2	Non-equidistant Tangential Stiffening .....	160
7.2.2.1	Calculation of Stiffener Distances ( $x_{0i}$ ) .....	160
7.2.2.2	Design of Stiffeners .....	162

7.2.2.3	Cost Calculation for a Sectorial Stiffened Plate Element.....	164
7.2.3	Equidistant Tangential Stiffening with Stepwise Varying Base Plate Thickness .....	167
7.2.3.1	Design of Base Plate Thicknesses .....	167
7.2.3.2	Design of Stiffeners .....	167
7.2.3.3	Cost Calculation .....	168
7.2.4	Equidistant Tangential Stiffening Combined with Radial Stiffeners.....	170
7.2.5	Cost of the Unstiffened Plate .....	172
7.2.6	Conclusions.....	173
7.3	Optimum Design of Welded Stiffened Plate Structure for a Fixed Storage Tank Roof .....	174
7.3.1	Introduction.....	174
7.3.2	Loads .....	175
7.3.3	Numerical Data (Fig. 7.11).....	175
7.3.4	Design of Sectorial Stiffened Deck Plate Elements.....	176
7.3.4.1	Cost Calculation for a Sectorial Stiffened Plate Element.....	177
7.3.5	Design of Radial Beams .....	179
7.3.6	Cost of a Radial Beam .....	180
7.3.7	Additional Cost.....	180
7.3.8	Optimization Results.....	181
7.3.9	Conclusions.....	181
7.4	A Circular Floor Constructed from Welded Stiffened Steel Sectorial Plates .....	182
7.4.1	Introduction.....	182
7.4.2	Problem Formulation .....	183
7.4.3	Solution Strategy for the Three Optimization Phases .....	183
7.4.4	Minimum Cost Design of a Sectorial Plate.....	183
7.4.5	Optimum Design of Radial Beams .....	188
7.4.6	Optimum Number of Sectorial Plates .....	190
7.4.7	Cost Comparison with an Unstiffened Thick-Base-Plate Version.....	191
7.4.8	Conclusions.....	193
7.5	Minimum Cost Design of a Cellular Plate Loaded by Uniaxial Compression.....	193
7.5.1	Introduction.....	194
7.5.2	The Basic Formulae of Cellular Plates .....	194
7.5.3	The Overall Buckling Constraint .....	195
7.5.4	The Cost Function.....	198
7.5.5	The Optimum Design Data and Results.....	199
7.5.6	Conclusions.....	200
7.6	Minimum Cost Design of a Square Box Column with Walls Constructed from Cellular Plates with RHS Stiffeners .....	200
7.6.1	Introduction .....	201

7.6.2	Characteristics of Cellular Plates .....	202
7.6.3	Minimum Cost Design of the Square Box Column .....	203
7.6.3.1	Constraint on Overall Buckling of a Cellular Plate Wall (Fig. 7.21) .....	203
7.6.3.2	Constraint on Horizontal Displacement of the Column Top.....	205
7.6.3.3	Numerical Data (Fig. 7.20).....	205
7.6.3.4	Cost Function.....	205
7.6.3.5	Optimization and Results.....	208
7.6.4	Conclusions.....	208
<b>8</b>	<b>Cylindrical and Conical Shells.....</b>	<b>211</b>
8.1	Minimum Cost Design for Various Diameters of a Ring-Stiffened Cylindrical Shell Loaded by External Pressure.....	212
8.1.1	Introduction.....	212
8.1.2	Characteristics of the Optimization Problem .....	213
8.1.3	Constraint on Shell Buckling .....	213
8.1.4	Constraint on Ring-Stiffener Buckling .....	214
8.1.5	The Cost Function.....	215
8.1.6	Results of the Optimization .....	216
8.1.7	Conclusions.....	218
8.2	Cost Comparison of Optimized Unstiffened Cylindrical and Conical Shells for a Cantilever Column Loaded by Axial Compression and Bending .....	218
8.2.1	Introduction.....	218
8.2.2	Constraint on Conical Shell Buckling.....	219
8.2.3	The Cost Function.....	221
8.2.4	Numerical Data and Results .....	222
8.2.5	Conclusions.....	223
8.3	Conical Shell with Non-equidistant Ring-Stiffening Loaded by External Pressure.....	223
8.3.1	Introduction.....	223
8.3.2	Design of Shell Segment Lengths.....	224
8.3.3	Design of a Ring-Stiffener for Each Shell Segment .....	225
8.3.4	The Cost Function.....	227
8.3.5	Numerical Data .....	228
8.3.6	Results of the Optimization .....	228
8.3.7	Conclusions.....	229
	<b>Appendix A-D .....</b>	<b>231</b>
	<b>References .....</b>	<b>251</b>
	<b>Subject Index .....</b>	<b>263</b>

## About the Authors

**Dr. József Farkas** is a professor emeritus of metal structures at the University of Miskolc, Hungary. He graduated in 1950 at the Faculty of Civil Engineering of the Technical University of Budapest. He has been an assistant professor of the University of Miskolc since 1950, an associate professor since 1966, a university professor since 1975, professor emeritus since 1998. His scientific degrees are candidate of technical science 1966, doctor of technical science 1978. His research field is the optimum design of metal structures, residual welding stresses and distortions, tubular structures, stiffened plates, vibration damping of sandwich structures. He has written expert opinions for many industrial problems, especially on storage tanks, cranes, welded press frames and other metal structures. He is the author of a university textbook about metal structures, a book in English “Optimum Design of Metal Structures” (Ellis Horwood, Chichester 1984), the first author of three books in English “Analysis and Optimum Design of Metal Structures” (Balkema, Rotterdam-Brookfield 1997), “Economic Design of Metal Structures” (Millpress, Rotterdam 2003), “Design and optimization of metal structures” (Horwood, Chichester 2008) and about 270 scientific articles in journals and conference proceedings. He is a Hungarian delegate of the International Institute of Welding (IIW), member of the International Society for Structural and Multidisciplinary Optimization (ISSMO) and a honorary member of the Hungarian Scientific Society of Mechanical Engineers (GTE). He is doctor honoris causa of the University of Miskolc.

**Dr. Károly Jármai** is a professor at the Faculty of Mechanical Engineering at the University of Miskolc, where he graduated as a mechanical engineer and received his doctorate (dr.univ.) in 1979. He teaches design of steel structures, welded structures, composite structures and optimization in Hungarian and in the English language for foreign students. His research interests include structural optimization, mathematical programming techniques and expert systems. Dr. Jármai wrote his C.Sc. (Ph.D.) dissertation at the Hungarian Academy of Science in 1988, became a European Engineer (Eur. Ing. FEANI, Paris) in 1990 and did his habilitation (dr.habil.) at Miskolc in 1995. Having successfully defended his doctor of technical science thesis (D.Sc.) in 1995, he subsequently received awards from the Engineering for Peace Foundation in 1997 and a scholarship as Széchenyi professor between the years 1997-2000. He is the co-author (with Farkas) of three books in English *Analysis and Optimum Design of Metal Structures*, *Economic Design of Metal Structures*, *Design and optimization of metal structures* and two monographs in Hungarian, and has published over 430



professional papers, lecture notes, textbook chapters and conference papers. He is a founding member of ISSMO (International Society for Structural and Multidisciplinary Optimization), a Hungarian delegate, vice chairman of commission XV and a subcommission chairman XV-F of IIW (International Institute of Welding). He has held several leading positions in GTE (Hungarian Scientific Society of Mechanical Engineers) and has been the president of this society at the University of Miskolc since 1991. He was a visiting researcher at Chalmers University of Technology in Sweden in 1991, visiting professor at Osaka University in 1996-97, at the National University of Singapore in 1998 and at the University of Pretoria several times between 2000-2005

# List of Symbols

$a$	Spacing of ribs [mm]
$a_g$	Ground acceleration
$a_w$	Weld dimension [mm]
$A$	Cross-sectional area [mm <sup>2</sup> ]
$A_m$	Surface area of a member per unit length [mm <sup>2</sup> ]
$A_p$	Area of the inner surface of the fire protection material per unit length of the member [mm <sup>2</sup> ]
$A_p/V$	Section factor for steel members insulated by fire protection material [1/mm]
$A_r$	Cross-sectional area of a ring-stiffener [mm <sup>2</sup> ]
$A_T$	Thermal impulse due to welding [mm]
$b$	Side length, plate width, beams spacing [mm]
$B$	Bending stiffness
$B_x, B_y$	Bending stiffnesses [Nmm <sup>2</sup> ]
$c$	Specific heat
$c_a$	Temperature dependant specific heat of steel [J/kgK]
$c_p$	Temperature independent specific heat of the fire protection material [J/kgK]
$c_x, c_y, c_{fx}, c_{fy}, c_w$	Factors for bent stiffened plates
$C$	Curvature [1/mm]
$C$	Parameter
$C_w$	Welding time parameter
$d$	Diameter [mm]
$d_r$	Interstorey drift
$D$	Diameter [mm]
$D$	Plate bending stiffness
$d_p$	Thickness of fire protection material
$e$	Truss joint eccentricity [mm]
$E$	Modulus of elasticity [GPa]
$E_a$	Modulus of elasticity of steel on normal temperature [GPa]
$E_{a,\theta}$	Modulus of elasticity of steel on elevated temperature $\theta_a$ [GPa]
$E_{d,fi}$	Design effect of actions in the fire situation
$f$	Eigenfrequency [Hz]
$f_{max}$	Maximum deflection [mm]
$f_{p,\theta}$	Proportional limit for steel at elevated temperature $\theta_a$

$f_{f,\theta}$	Effective yield strength of steel at elevated temperature
$\theta_a$	
$f_y$	Yield stress [MPa]
$F$	Force [N]
$g$	Truss joint gap [mm]
$G$	Shear modulus [GPa]
$h$	Truss height [mm]
$\dot{h}_{net,d}$	Net heat flux per unit area [W/ m <sup>2</sup> ]
$H$	Plate torsional stiffness [Nmm <sup>2</sup> ]
$H$	Horizontal component force
$H_F$	Horizontal force
$I_x, I_y$	Moments of inertia [mm <sup>4</sup> ]
$I_w$	Arc current [A]
$I_t$	Torsional constant [mm <sup>4</sup> ]
$I_\omega$	Warping constant [mm <sup>6</sup> ]
$k$	Cost factor
$k_\theta$	Relative value of a strength or deformation property of steel at elevated temperature $\theta_a$
$K$	Effective length factor
$K$	Cost [\$]
$l$	Length at 20 °C [mm]
$L$	Length, span length [mm]
$m$	Mass [kg]
$M$	Bending moment [Nmm]
$n$	Number of ribs
$n$	Parameter
$N$	Normal force [N]
$p, q$	Distributed load intensity [N/mm]
$q$	Seismic behaviour factor
$q_x, q_y$	Specific shear forces
$Q$	Shear force [N]
$Q_T$	Heat input of welding [J/mm]
$r$	Radius of gyration [mm]
$R$	Shell radius [mm]
$s$	Normal force due to $X=1$
$s_e$	Effective plate width
$S$	Surface [mm <sup>2</sup> ]
$S$	Tubular member force
$S_x, S_y$	Static moments [mm <sup>3</sup> ]
$S_j$	Rotational stiffness of a beam-to-column connection
$S_d$	Seismic design spectrum
$t$	Thickness [mm]
$t$	Time in fire exposure [sec]
$T$	Time [s]
$T$	Axial force

$U$	Arc voltage [V]
$v_w$	Welding speed of travel [mm/s]
$V$	Volume [mm <sup>3</sup> ]
$w$	Deflection [mm]
$w_i$	Weighting coefficients
$W_x, W_y$	Section moduli [mm <sup>3</sup> ]
$X$	Unknown force
$Z$	Factor
$\alpha$	Angle of inclination
$\alpha$	Factor for buckling strength
$\alpha$	Parameter
$\alpha_0$	Thermal expansion coefficient
$\beta$	Web slenderness ratio
$\beta$	Seismic low bound factor
$\beta$	Parameter
$\gamma=d/2t$	Tubular truss parameter
$\gamma_{M1}$	Partial safety factor
$\gamma_{Mf}$	Fatigue safety factor
$\delta$	Local buckling factor
$\Delta t$	The time interval at fire calculation [sec]
$\varepsilon = \sqrt{235 / f_y}$	Modifying factors for steels
$\varepsilon_x, \varepsilon_y$	Specific strains
$\eta$	Heat efficiency of a welding technology
$\eta$	Column imperfection factor
$\eta_{fi}$	Reduction factor for design load level in the fire situation
$\eta_G$	Distance of gravity center [mm]
$\kappa$	Number of assembled structural elements
$\kappa$	Adaptation factor at fire resistance
$\Theta_d$	Fabrication difficulty factor
$\lambda$	Seismic correction factor
$\lambda$	Slenderness
$\lambda$	Thermal conductivity
$\lambda_p$	Thermal conductivity of the fire protection system [W/mK]
$\bar{\lambda}$	Reduced slenderness
$\mu$	Penalty parameter
$\mu_0$	Degree of utilisation at time $t = 0$
$\nu$	Poisson ratio
$\rho$	Material density [kg/m <sup>3</sup> ]
$\rho_a$	Unit mass of steel [kg/m <sup>3</sup> ]
$\rho_p$	Unit mass of the fire protection material [kg/m <sup>3</sup> ]
$\theta$	Angle of inclination

$\theta$	Temperature [°C]
$\theta_{a,t}$	Steel temperature at time $t$ [°C]
$\theta_{g,t}$	Ambient gas temperature at time $t$ [°C]
$\Theta_B$	Parameter
$\sigma$	Normal stress [MPa]
$\sigma_{cr}$	Critical buckling stress
$\sigma_{adm}$	Admissible stress [MPa]
$\tau$	Shear stress [MPa]
$\tau_{adm}$	Admissible shear stress [MPa]
$\varphi$	Number of rib spacings
$\varphi$	Angle of inclination
$\Phi$	Buckling parameter
$\chi$	Flexural buckling factor
$\psi$	Stress ratio
$\omega=H/a$	Geometric characteristic of a parallel-chord truss
$\Delta F$	Pulsating force range [N]
$\Delta\theta_{g,t}$	Increase of the ambient gas temperature during the time interval $\Delta t$ [K]
$\Delta\sigma, \Delta\tau$	Stress range [MPa]

# Abbreviations

CHS	Circular hollow section
DE	Differential evolution
EC3	Eurocode 3
EC8	Eurocode 8
ECCS	European Convention for Constructional Steelwork
FCAW	Flux Cored Arc Welding
FCAW-MC	Metal Cored Arc Welding
FRP	Fiber reinforced plastic
GA	Genetic algorithm
GMAW-C	Gas Metal Arc Welding with CO <sub>2</sub>
GMAW-M	Gas Metal Arc Welding with Mixed Gas
GTAW	Gas Tungsten Arc Welding
IIW	International Institute of Welding
PSO	Particle swarm optimization
RHS	Rectangular hollow section
SHS	Square hollow section
SAW	Submerged Arc Welding
SMAW	Shielded Metal Arc Welding
SMAW HR	Shielded Metal Arc Welding High Recovery
SSFCAW (ISW)	Self Shielded Flux Cored Arc Welding

# Chapter 1

## Experiences with the Optimum Design of Steel Structures

A brief history of the structural optimization is given. The developed system of minimum cost design is described. In 1970's a school has been found for structural optimization in the University of Miskolc. The advantages and disadvantages are compared for the design by routine and those of optimum design. The problem of interaction of two instabilities is treated with the conclusion that the optimum design is safe when the used stability constraints take into account the effect of initial imperfections and residual stresses. Some own results are detailed about the optimum design for different structural types such as compressed and bent columns, stiffened plates as well as wind turbine towers. A literature survey is given for optimum design of trusses, frames and industrial applications.

### 1.1 Introduction

In 1960 Professor Lucien Schmit jr. (University of California Los Angeles) defined the structural synthesis as a mathematical constrained function minimization problem (Schmit, 1960)

$$f(x) \rightarrow \min, x = \{x_1, x_2, \dots, x_n\}$$
$$\text{subject to } g_j(x) \leq 0, j = 1 \dots p$$

and he and his co-workers developed an effective optimum design system for aero- and astronautical structures.

Later Schmit (Schmit 1984) emphasized that the cost should be considered as an objective function instead of weight. In aircraft design the main aspect has been to minimize the weight, but the cost savings are also very important mainly for other industrial applications. From this time the author's aim was to formulate a realistic cost function for welded structures.

In 1960 the author designed a series of roofs for vertical storage tanks for fluids covered by a soil layer. The roofs were constructed from welded stiffened plates (Fig. 1.1) (Farkas 1962). At this time Farkas began his research of structural optimization of welded structures.

## 1.2 Foundation of the School for Structural Optimization at the University of Miskolc

In 1970-s Moe and Kavlie have optimized ship structures and during my trip to Trondheim I have obtained from Mr. Kavlie the Fortran program of the SUMT optimization method. My doctorand Imre Tímár has applied it for optimum design of sandwich plates. His doctoral dissertation has been the first application of computerized optimum design in Hungary (Tímár 1977).

Farkas has defended his dissertation for the academic degree “doctor of technical science” with title “Optimum design of metal structures” in 1978, which has been published as a book in 1984 (Farkas 1984).

This was followed by a series of dissertations written by K. Jármai, L. Szabó, F.J. Szabó, Gy. Kovács, Z. Virág, L. Kota, R. Dúl and others in the structural optimization school in the University of Miskolc.

The authors take part in the work of the International Institute of Welding (IIW). They have founded a subcommission IIW XV-F “Design, fabrication and economy of welded structures” its chairman is K. Jármai. They have written a lot of scientific documents and published more than 25 articles in the IIW journal “Welding in the World”.

They are also founding members of the International Society of Structural and Multidisciplinary Optimization (ISSMO) and published more articles in its journal SMO. In 2010 a course for engineers is organized by K. Jármai in the University of Miskolc to obtain the title “International Welded Structure Designer”. The structural optimization has been an important part in these lectures.

Farkas and Jármai have collected their research results in three books (Farkas and Jármai 1997, 2003, 2008.)

## 1.3 Derivation of the Structural Optimization System

It is possible to derive the structural optimization system of welded structures from the design of welded stiffened plates, since the design of this structural model contains all the important engineering aspects to be included in such a design system.

- (1) Stiffened plates can buckle and the variable load can cause fatigue cracks in stress concentration points. In the design these phenomena should be taken into account formulating *design constraints* to guarantee the *safe load-carrying capacity* of a structure.
- (2) In the production of stiffened plates different welding technologies can be used and each welding method has a defined thickness domain, thus, limitation of thicknesses should be formulated. The shrinkage of welds can cause residual stresses and distortions, which should be limited for quality assurance of welded structures. Thus, *fabrication constraints* should be formulated to guarantee the *manufacturability* of a structure.



- (3) In the design of stiffened plates the question how to determine the *optimum number of stiffeners* arises. To achieve a minimum mass structure many thin ribs should be used, but these results in a very expensive structure, since the cost of welding is high. To minimize the cost, fewer and thicker stiffeners should be used. This optimization problem can be solved by the formulation of a *mass or cost function* and by the *minimization* of this objective function considering the design and fabrication constraints. For these constrained function minimization problems effective *mathematical methods* should be used.

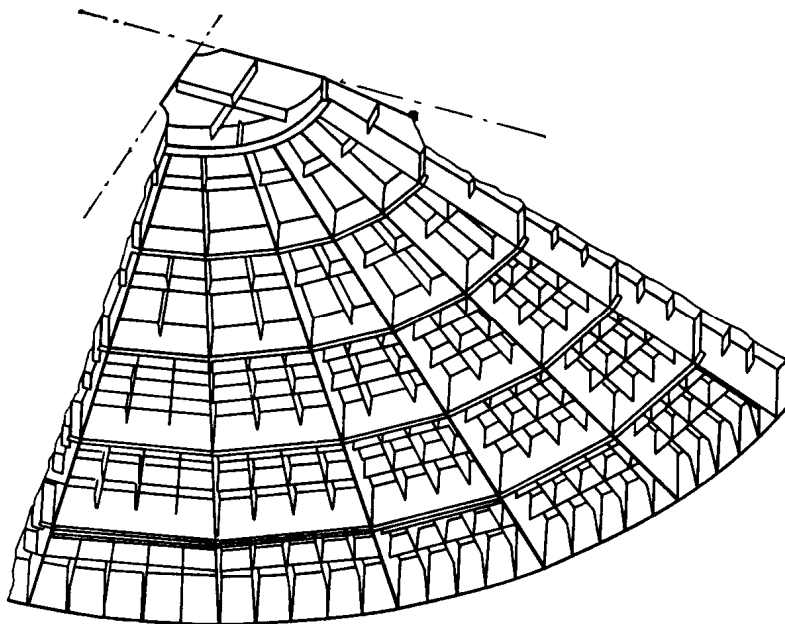


**Fig. 1.1** Part of the roof of a storage tank constructed from welded stiffened plates

The above derived structural optimization system has four main components: *design constraints, fabrication constraints, cost function and mathematical methods*. This system can fulfil all the important engineering requirements: safety and manufacturability is guaranteed by design and fabrication constraints, economy is achieved by minimizing the cost function.

This derivation illustrates the fact that *our structural optimization system is based on realistic phenomena and requirements*, which arise in modern design processes.

Optimization means a search for better solutions, which fulfil the requirements better. For a modern load-carrying engineering structure the main requirements are as follows: load-carrying capacity (safety), manufacturability and economy.

These requirements can be fulfilled by a structural synthesis system, in which a cost function is minimized considering constraints on design and manufacturability.

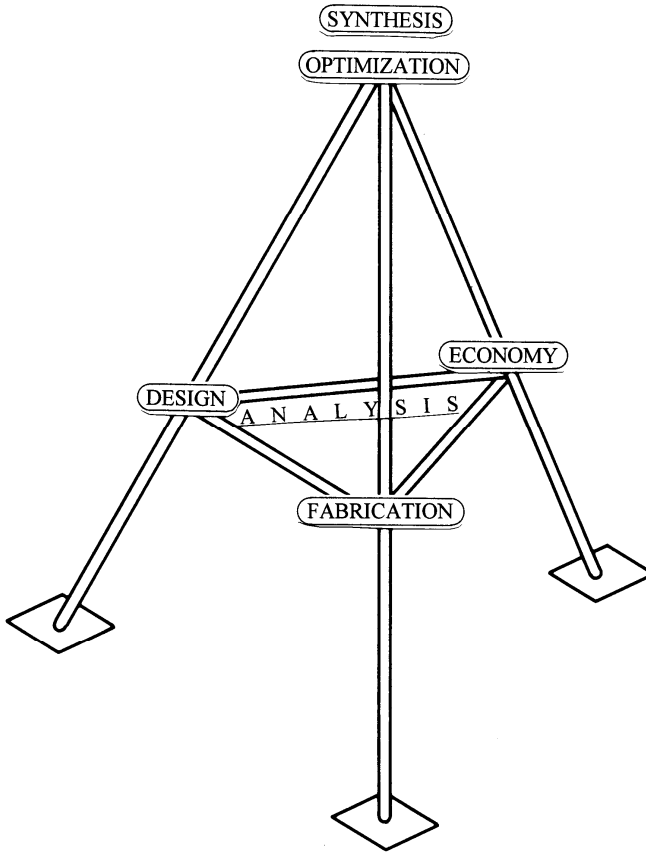


**Fig.1.2** A structural optimization system

This system can be symbolized by a simple spatial structure as shown in Fig. 1.2. This symbol also shows two important aspects: (1) when a requirement is missing, then the system does not work well, does not give better solutions; (2) close cooperation (harmony) should be realized between these main aspects, since they affect each other to a significant extent. Structural optimization is a general system, which can synthesize all the important engineering aspects.

At the analytical level the structural characteristics of the type of structure investigated should be analyzed as follows: loads, materials, geometry, boundary conditions, profiles, topology, fabrication, joints, transport, erection, maintenance, costs. Those variables whose changing will result in better solutions should be selected. A cost function and constraints on design and fabrication should be mathematically formulated in the function of variables.

At the level of synthesis the cost function should be minimized using effective mathematical methods for the constrained function minimization. Comparing the

optimum solutions designers can select the most suitable one. This comparison can result in significant mass and cost savings in the design stage.

Our aim is to show designers and manufacturers that it is worth using optimum design processes to achieve significant cost savings in the design stage. Cost savings can be achieved by various means. We dealt with the cost savings by means of changes in structural characteristics, which influence the cost function.

Fabrication constraints are the limitations of initial imperfections caused by welding, since the shrinkage of welds can cause residual stresses and distortions, which should be limited in order to achieve quality assurance of welded structures.

The developed cost function includes cost of material and fabrication. The later contains the assembly, in the case of shells the cost of forming the plate elements into shell parts, in the case of tubular structures the cutting and grinding of bar ends, welding, additional welding costs and painting. The cost of transportation and erection is neglected, since their influence on structural characteristics is little.

Our aim is to bridge the gap between the optimization theory and fabrication practice. It is very important to include fabrication aspects into design constraints and to consider also fabrication costs in the cost function.

During a stay in Japan in 1999, colleagues in the Ehime University (Matsuyama city) have organized for us a trip to Ube. We have presented lectures for engineers of the Steel Structures Factory in this large industrial area. After Farkas's presentation, an engineer has had a question how to optimize a large complicate bridge structures.

The answer was as follows: a cost function should be defined using industrial cost data, design constraints should be formulated according to valid design rules, and an effective mathematical optimization method should be used. After this visit Farkas has formulated a further aspect: the most important structural characteristics should be selected, and the minimum cost solution can be achieved by changing these characteristics.

## **1.4 Advantages and Disadvantages of Two Different Design Methods**

### ***1.4.1 Design by Routine***

The designer takes a structure by routine and checks it for fulfilling of constraints.

Advantages

- (a) Special mathematical methods are not needed,
- (b) Tables, diagrams can be used without any continuous functions,
- (c) The time-consuming investigation of many structural versions is not necessary.

#### Disadvantages

- (a) design without any goals, objective functions,
- (b) the fulfilling of the design constraints can only be reached approximately,
- (c) a minimum mass or cost is not reached,
- (d) it is impossible to develop new, innovative structural types.

### ***1.4.2 Optimum Design***

In the optimum design a structural version is sought, which fulfils the design and fabrication constraints and minimizes the cost function.

#### Advantages

- (a) clear and exact formulation of design problems (goals and constraints),
- (b) possibility to include all the important engineering aspects,
- (c) treats the fabrication aspects and cost function,
- (d) possibility to achieve significant cost savings in design stage,
- (e) possibility to give designers aspects for innovative, competitive structures,
- (f) possibility to give a realistic basis for comparison of different structural versions,
- (g) possibility to show the most important structural characteristics to be varied.

#### Disadvantages

- (a) most of problems can be treated only numerically, therefore general conclusions cannot be drawn,
- (b) in order to use continuous functions the results of experiments published in tabulated or graphic form as well as the cross-sectional characteristics of fabricated series of profiles should be formulated by approximate functions,
- (c) special mathematical methods should be used,
- (d) difficulty to obtain realistic cost data from industry,
- (e) difficulty to treat coupled instabilities (more active constraints),
- (f) cost savings is significant in serial production, but this can be realized not very often,
- (g) remuneration of designers is not proportional to cost savings, but rather to total cost.

## **1.5 The Problem of the Interaction of Two Instabilities**

Thompson and Hunt (1974) stated that in the case of two active instability constraints the optimization can result in unsafe design, since the interaction of instabilities can decrease the strength significantly due to unavoidable imperfections.

Rondal and Maquoi (1981) have shown that this decrease in strength is much more smaller in the case when the practical stability formulae take into account the effect of initial imperfections and residual stresses. Thus, it is no danger of unsafe optimum design in the case of more active stability constraints. In practice some problems can occur with possible interaction of two different failure modes, e.g. interaction of overall buckling and fatigue. In the absence of experimental results it is suggested to use an additional safety factor of 1.2 between the two constraints.

## 1.6 Detailed Results for Different Structural Types

### 1.6.1 *Compressed and Bent Columns Constructed from Stiffened Shell or from Square Box Walls of Stiffened Plates*

The vertical load  $N_F = 34000$  kN, , the horizontal force  $H_F = 0.1N_F$ , the yield stress  $f_y = 355$  MPa,  $R = 1850$  mm,  $L = a_0 = 15$  m.

It is possible to compare the costs of structural versions of the column with the same height, loads and constraints on stress and displacement as follows.

- (1) The stringer-stiffened circular shell (Fig. 1.3a) with a radius of 1850 mm has the minimum cost of  $K = 70571$  (unstiffened  $K = \$92100$ ),
- (2) The square box structure composed from orthogonally stiffened plates (Fig. 1.3b) with an optimized width of  $b_0 = 4500$  mm has the minimum cost of  $K = \$76990$ ,
- (3) The cellular box structure (Fig. 1.3c) loaded by a slightly different compression force (30000 instead of 34000 kN) with an optimized width of  $b_0 = 4700$  mm has the minimum cost of  $K = \$60430$ .

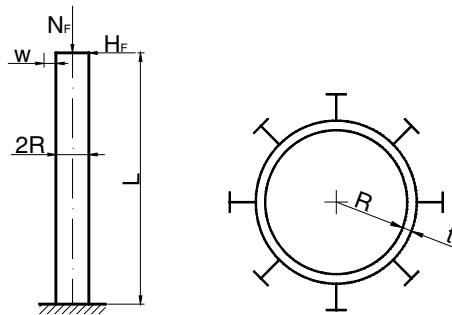


**Fig. 1.3a** A cantilever cylindrical circular stringer stiffened shell column loaded by compression and bending

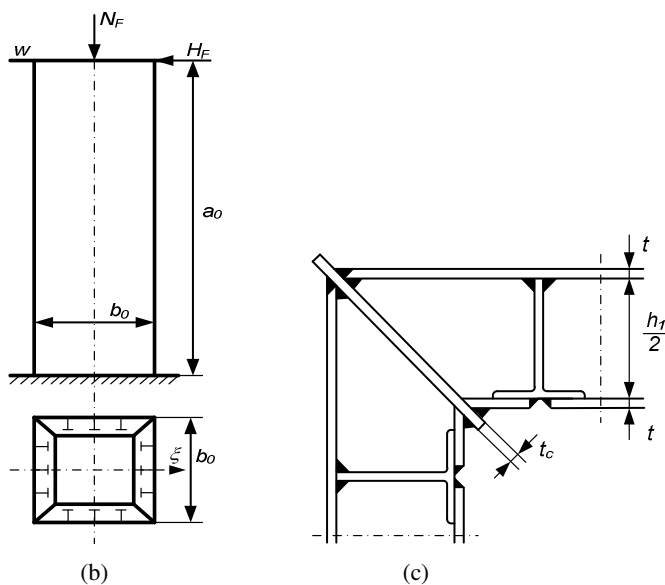


**Fig. 1.3b** A welded cantilever square box column with walls of stiffened plates loaded by compression and bending, 1.3c Corner construction with cellular plates

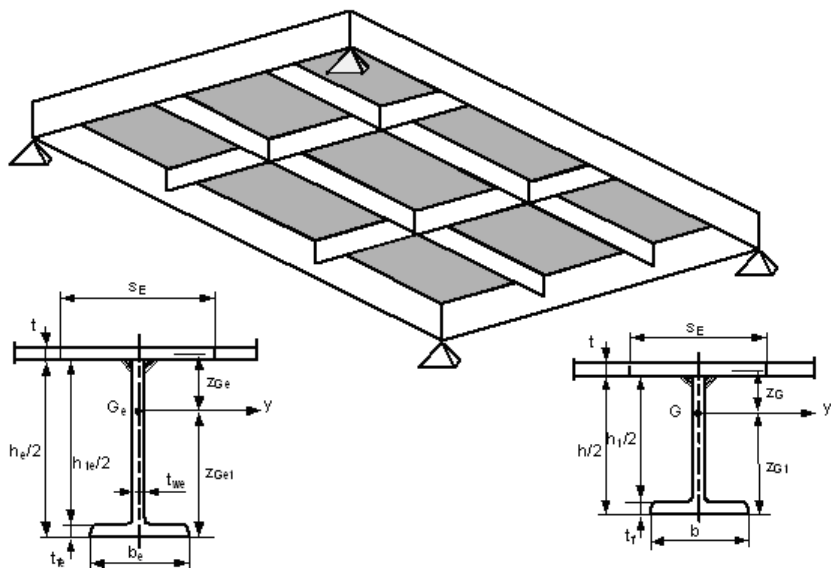


**Fig. 1.4a** Square plate supported at four corners stiffened orthogonally on one side by halved rolled I section stiffeners, the edge and internal stiffeners have different cross-section

Details can be found in the following studies:

Farkas J, Jármai K (2005), Farkas J, Jármai K (2008a), Farkas J, Jármai K (2008b).

### ***1.6.2 Stiffened or Cellular Plate Supported at Four Corners Subject to a Uniformly Distributed Normal Load (Fig.1.4)***

The edge plate length 18 m, factored load intensity  $0.0015 \text{ N/mm}^2$ , yield stress 355 MPa.

Comparing the two structural versions it can be concluded that the cellular plate is competitive to the plate stiffened one side, since the costs are nearly the same (106800 compared to \$ 106100 for cellular plate) and the cellular construction has some advantages over the stiffened one.

Details can be found in the following studies:

Farkas J, Jármai K, Snyman JA (2010), Farkas J, Jármai K (2008c).

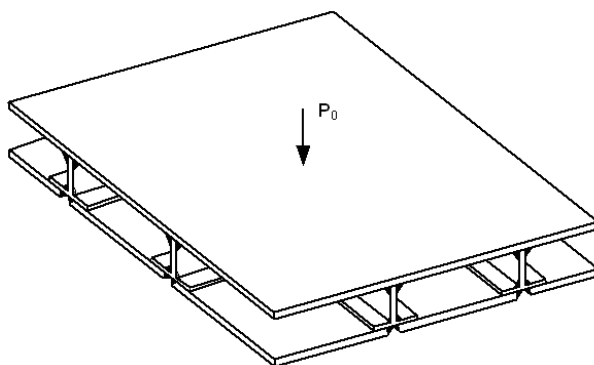


**Fig. 1.4b** A cellular plate with halved rolled I section stiffeners

### ***1.6.3 A Wind Turbine Tower Constructed as a Shell or Tubular Truss Structure***

The cost comparison is applied to two structural versions of a wind turbine tower. The tower is 45 m high, loaded on the top by a factored vertical force of 950 kN (self weight of the nacelle), a bending moment of 997 kNm and a horizontal force of 282 kN from the turbine operation. The tower width is limited to 2.5 m due to the rotating turbine blades of length 27 m. Both the shell and the truss structure are constructed from 3 parts each of 15 length with stepwise increasing widths. The 3 shell parts are joined by bolted connections.

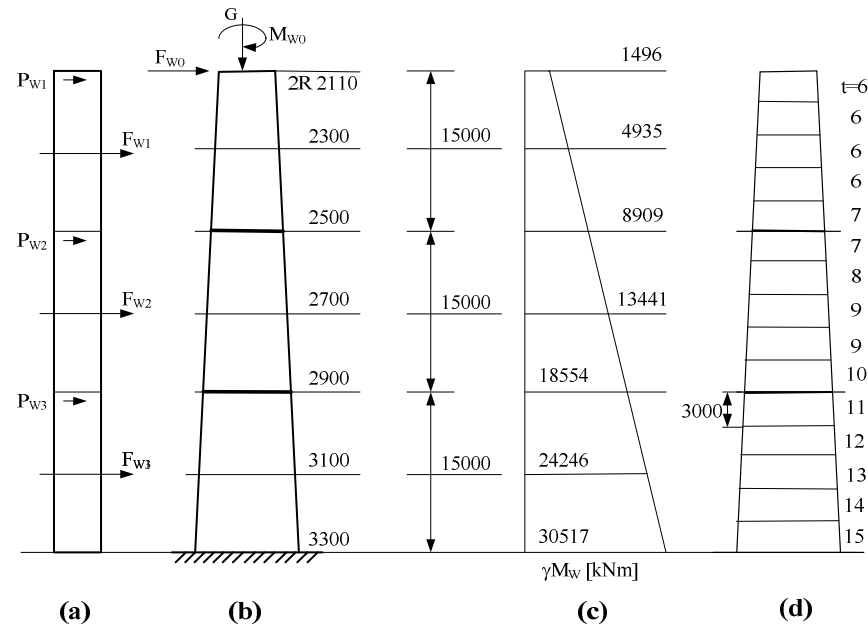


**Fig. 1.5** A wind turbine tower constructed as a ring-stiffened circular slightly conical shell. (a) wind loads, (b) diameters of the shell, (c) bending moments, (d) shell thicknesses.

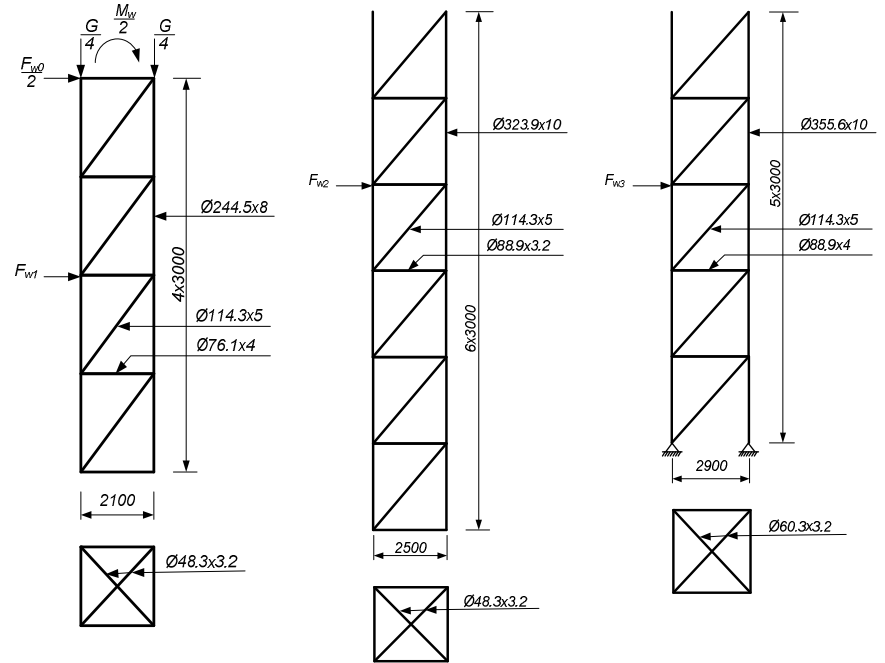


**Fig. 1.6** A wind turbine tower constructed as a tubular truss



The comparison of the two structural versions shows that the tubular truss has smaller mass (17533 compared to 30518 kg), smaller surface to be painted and is much cheaper than the shell structure (51161 compared to \$85628). This difference is caused by the much lower mass and surface of the tubular truss version.

Details can be found in the following studies:

Farkas J, Jármai K (2006), Uys PE, Farkas J, Jármai K, van Tonder F (2007), Farkas J, Jármai K (2008).

## **1.7 Survey of Selected Literature of the Optimum Design of Steel Structures**

In order to show the wide range of application of the optimum design of steel structures only some journal articles are mentioned here as follows.

### ***1.7.1 Truss Structures***

Detailed survey can be found in Chapter 5, Table 5.1.

### ***1.7.2 Building Frames***

Ali NBH, Sellami M, Cutting-Decelle AF, Mangin JC (2009) Multi-stage production cost optimization of semi-rigid steel frames using genetic algorithms. *Eng. Struct.* 31: 2766-2778

Cabrero JM, Bayo E (2005) Development of practical design methods for steel structures with semi-rigid connections. *Eng. Struct.* 27: 1125-1137

Jármai K, Farkas J, Kurobane Y (2006) Optimum seismic design of a multistorey steel frame. *Eng. Struct.* 28: No.7. June, 1038-1048

Kameshki ES, Saka MP (2003) Genetic algorithm based optimum design of nonlinear planar steel frames with various semi-rigid connections. *J. Constr. Steel Res.* 59: 109-134

Moghaddam H, Hajirasouliha I, Doostan A (2005) Optimum seismic design of concentrically braced frames: concepts and design procedures. *J. Constr. Steel Res.* 61: 2, 151-166

Simões LMC (1996) Optimization of frames with semi-rigid connections. *Comput. Struct.* 60: 4, 531-539

### ***1.7.3 Industrial Applications***

*Bridge:* Durfee RH (1987) Design of a triangular cross-section bridge truss. *J. Struct. Eng. Proc. Am Soc Civ Eng* 113: 2399-2414

*Silo:* Farkas J, Jármai K (1997) Welded steel silos. In Farkas J, Jármai K *Analysis and optimum design of metal structures*. Rotterdam-Brookfield, Balkema, 285-298

*Bunker:* Farkas J, Jármai K (2003) Bunkers constructed from welded stiffened plates. In: Farkas J, Jármai K *Economic design of metal structures*. Rotterdam, Millpress, 295-309

*Oil pipeline:* Farkas J, Jármai K (2006) Optimum strengthening of a column-supported oil pipeline by a tubular truss. *J Constr. Steel Res.* 62: No.1-2. 116-120

*Wind turbine tower:* Farkas J, Jármai K (2006) Cost comparison of a tubular truss and a ring-stiffened shell structure for a wind turbine tower. In: *Tubular Structures XI. Proc. 11th Int. Symposium and IIW Int. Conf. on Tubular Structures*, Québec City, Canada, 2006. Eds Packer JA and Willibald S, Taylor and Francis, London etc. 341-349

*Welded beam:* Ferscha F (1987) Querschnittsoptimierung biegesteifer, geschweisster Stahlstabtragwerke. *Stahlbau* 56: 313-318

*Ship:* Hart ChG, Vlahopoulos N (2010) An integrated multidisciplinary particle swarm optimization approach to conceptual ship design. *Struct. Multidisc. Optim.* 41: 481-494

*Communication tower:* Jasim NA, Galeb ACh (2002) Optimum design of square free-standing communication towers. *J. Constr. Steel Res.* 58: 413-425

*Offshore tower:* Jármai K, Snyman JA, Farkas J (2006) Minimum cost design of a welded orthogonally stiffened cylindrical shell. *Comput. Struct.* 84: No.12. 787-797

*Storage tank roof:* Jármai K, Farkas J (2008) Optimum design of welded stiffened plate structure for a fixed storage tank roof. In: *Safety and reliability of welded components in energy and processing industry. Proc. of the IIW Internat. Conference Graz Austria* Eds Mayr P, Posch G, Cerjak H. Graz Univ. of Technology. 137-142

*Offshore tower:* Karadeniz H, Togan V, Vrouwenvelder T (2009) An integrated reliability-based design optimization of offshore towers. *Reliab. Eng. System Safety* 94: 1510-1516

*Ship:* Kavlie D, Moe J (1971) Automated design of frame structures. *J. Struct.Div. Proc. Am Soc Civ Eng* 97: 33-62

*Cable-stayed bridge:* Negrão JHO, Simões LMC (1994) Three-dimensional nonlinear optimization of cable-stayed bridges. In: *Topping, B.H.V., Papadrakakis, M. (eds) Advances in Structural Optimization*. Edinburgh, Civil-Comp. Press, 203-213

*Transmission line tower:* Rao GV (1995) Optimum designs for transmission line towers. *Comput. Struct.* 57: 1, 81-92

*Bridge:* Taniwaki K (1997) Total optimal synthesis method for frame structures dealing with shape, sizing, material variables and prestressing. Doctor dissertation, Mastuyama, Ehime University, Japan

*Wind turbine tower:* Uys PE, Farkas J, Jármai K, van Tonder F (2007) Optimisation of a steel tower for a wind turbine structure. *Eng. Struct.* 29: 1337-1342

## 1.8 Conclusions

Structural optimization is a very useful system for the modern innovative design of steel structures. It can consider all the important engineering aspects and serves for realistic comparison of structural versions. The comparison of the design by routine with the optimum design shows that both methods have advantages and disadvantages, but the optimum design is superior for its systematic character.

In the stability constraints the effect of initial imperfections and residual stresses should be taken into account to avoid the strength decrease by coupled instabilities. Therefore the classic results for overall and local buckling strength should be modified as it is taken in Eurocodes.

In the structural optimization the fabrication and economic aspects play an important role, thus, the fabrication constraints and cost calculation should be involved in the design process.

Optimization and comparison of realistic numerical structural models can give useful aspects for designers to select the best, competitive versions. Such comparisons are illustrated by solved problems of compressed and bent columns stiffened plates as well as shell vs truss.

# Chapter 2

## Newer Mathematical Methods in Structural Optimization

### 2.1 Introduction

Structural optimization means finding the best solution while considering several design constraints. The optimization can be topology, shape and size optimization. Our activity is related mainly to sizing optimization. These constraints can be the behaviour of the structure, like the stresses, fatigue, deformations, stability, eigenfrequency, damping, etc. These constraints are usually highly nonlinear, so to find the optimum it is not an easy task. It is as important to have a reliable optimization technique. There are many optimization algorithms available. Non of the algorithm is superior. All of them can have benefits and disadvantages.

In our practice on structural optimization we have used several techniques in the last decades. We have published them in our books and gave several examples as engineering applications (Farkas 1984, Farkas & Jármai 1997, 2003, 2008). Most of the techniques were modified to be a good engineering tool in this work.

For single objective optimization there are a great number of methods available as it was described in Farkas & Jármai (1997, 2003, 2008). Mathematical programming methods without derivatives like: Complex (Box 1965), Flexible Tolerance (Himmelblau 1971) and Hillclimb (Rosenbrock 1960). Methods with first derivatives such as: Sequential Unconstrained Minimization Technique (*SUMT*) (Fiacco & McCormick 1968), Davidon-Fletcher-Powell (Rao 1984), etc. Methods with second derivatives such as: Newton (Mordecai 2003), Sequential Quadratic Programming, *SQP* (Fan et al. 1988), the Feasible SQP (Zhou & Tits 1996). There are also other classes of techniques like Optimality Criteria methods (*OC*) (Rozvany 1997), or the combinatorial discrete methods like Backtrack (Golomb & Baumert (1965), Annamalai 1970), the entropy-based method (Simões & Negrão 2000) (Farkas et al. 2005).

In the last three decades some new techniques appeared e.g. the evolutionary techniques, like Genetic Algorithm, *GA* by Goldberg (1989), the Differential Evolution, *DE* method of Storn & Price (1995), the Ant Colony Technique (Dorigo et al. 1999), the Particle Swarm Optimization, *PSO* by Kennedy & Eberhart (1995), Millonas (1994) and the Artificial Immune System, *AIS*

(Farmer et al. (1986), de Castro & Timmis (2001), Dasgupta (1999), the Firefly algorithm (Yang 2008). The leap-frog technique with the analogue of potential energy minimum (Snyman 1983, 2005), have also been developed.

Multicriteria optimization is used when more objectives are important to find the compromise solution (Osyczka 1984, 1992, Koski 1994, Wei and Leung 2011).

The general formulation of a single-criterion non-linear programming problem is the following:

$$\text{minimize } f(x) \quad x_1, x_2, \dots, x_N, \quad (2.1)$$

$$\text{subject to } g_j(x) \leq 0, \quad j = 1, 2, \dots, P, \quad (2.2)$$

$$h_i(x) = 0 \quad i = P+1, \dots, P+M, \quad (2.3)$$

$f(x)$  is a multivariable non-linear function,  $g_j(x)$  and  $h_i(x)$  are non-linear inequality and equality constraints, respectively.

## 2.2 Firefly Algorithm

Firefly algorithm is one of the newest evolutionary optimization algorithms, and is inspired by the flashing behaviour of fireflies. Each firefly movement is based on absorption of the other one's flash. The primary purpose for a firefly's flash is to act as a signal system to attract other fireflies. Yang X.S. (2008, 2012) formulated this firefly algorithm by assuming:

- One firefly will be attracted by all other fireflies;
- Attractiveness is proportional to their brightness (it is associated with the objective function), and for any two fireflies, the less brighter one will be attracted by the brighter one and thus moves toward it. Brightness can be proportional to the distance between fireflies and to the passing time;
- If there are no fireflies brighter than a given firefly, it will move randomly.

The single fireflies represent a solution of the problem, just like particles at PSO, or the chromosomes at the genetic algorithm. The goodness of the individuals is evaluated with penalty functions.

The core of the algorithm is as follows:

- Generate a random solution set,  $x = \{x_1, x_2, \dots, x_k\}$
- Compute intensity for each solution member,  $I = \{I_1, I_2, \dots, I_k\}$
- Moves each firefly towards other brighter fireflies, and if there is no other brighter firefly, move it randomly.
- Update the solution set.
- Terminate if a termination criterion is fulfilled otherwise go back to step 2.

From elementary physics it is clear that the intensity of light is inversely proportional to the square of the distance, say  $d$ , from the source. Furthermore when light passes through a medium with light absorption coefficient of  $\alpha$  the light intensity,  $I$  varies with distance  $d$  as given below:

$$I(r) = I_0 e^{-\alpha d} \quad (2.4)$$

where  $I_0$  is the intensity at the source point.

These can be combined as

$$I(r) = I_0 e^{-\alpha d^2} \quad (2.5)$$

However, to compute  $1/(1 + \alpha d^2)$  is easier than computing  $e^{-\alpha d^2}$

Hence the intensity can be calculated using

$$I(r) = \frac{I_0}{1 + \alpha d^2} \quad (2.6)$$

Similarly, the attractiveness of a firefly can be defined as follows (Tilahun and Ong 2012):

$$A(r) = \frac{A_0}{1 + \lambda r^2} \quad (2.7)$$

where  $A_0$  is the attractiveness at  $d = 0$ .

If a firefly located at point  $\mathbf{x}' = \{x'_1, x'_2, \dots, x'_n\}$  is brighter than another firefly located at point  $\mathbf{x} = \{x_1, x_2, \dots, x_n\}$ , the firefly located at  $\mathbf{x}$  will move towards  $\mathbf{x}'$ . The location update of the firefly located at  $\mathbf{x}$  will be done as follows:

$$\mathbf{x} = \mathbf{x} + A_0 e^{-\alpha d^2} (\mathbf{x}' - \mathbf{x}) + \mathbf{r} \quad (2.8)$$

The last term is a randomization one with  $\mathbf{r}$  vector of random numbers, whereas the second term is due to the attraction of  $\mathbf{x}$  towards  $\mathbf{x}'$ . For practical uses  $A_0$  can be taken as one,  $A_0 = 1$ .

Unlike deterministic solution methods, metaheuristic algorithms (like Firefly) are not affected by the behaviour of the optimization problem. This makes the algorithm to be used widely in different fields.

We have used Firefly to find the solution of the supplier selection (Kota, Jármai 2013). The problem is realized through the discretization of the firefly algorithm.

In the next step the light intensity is evaluated to all the fireflies. The light intensity is a sum of the target function and the penalty values.

Firefly 1	$x_1$	$x_2$	$x_3$	$x_d$
Firefly 2	$x_1$	$x_2$	$x_3$	$x_d$
.	.	.	.	.
Firefly $n$	$x_1$	$x_2$	$x_3$	$x_d$

**Fig. 2.1** Population, data structure of the fireflies

### The Penalty Functions

The penalty value under the minimum ordering quantity:

$$B^{min} = \sum_{j=1}^d (x_j^{min} - x_j)^2 \mid \text{if } x_j < x_j^{min} \quad (2.9)$$

where:

- $d$ : is the number of the suppliers,
- $x_j^{min}$ : is the minimum quantity can be ordered from the supplier  $j$ .

The penalty value above the maximum quantity:

$$B^{max} = \sum_{j=1}^d (x_j - x_j^{max})^2 \mid \text{if } x_j > x_j^{max} \quad (2.10)$$

where:

- $d$ : is the number of suppliers,
- $x_j^{max}$ : is the maximum quantity can be ordered from the supplier  $j$ .

The light intensity of an individual is:

$$I = C + B^{min} + B^{max} \quad (2.11)$$

In the next phase the individuals move towards the brighter individuals. The brightest individual moves randomly.

The definition of the movement is really simple in a continuous state space but in a discrete state space the movement and the distance function have to be defined.

The determination of the distance of the individuals is performed by the following function:

$$D(F1, F2) = \sum_{j=1}^d \text{abs}(x_j^{F1} - x_j^{F2}) \quad (2.12)$$

where:

- $F1$ : firefly 1, the first operand of the distance function, ,
- $F2$ : firefly 2, the second operand of the distance function,
- $x_j^{F1}$ : the ordering quantity from the supplier  $j$  at the first firefly,
- $x_j^{F2}$ : the ordering quantity from the supplier  $j$  at the second firefly.

The movement of the individuals is the discretized variant of the continuous movement function (Kota, Jármai 2013).

Because the sum of the ordering quantities is a given constant value which must not altered in either way, so only even variances can happen among the ordering quantities. So, if a given quantity is differ then an another quantity have to differ at alternate sign.

In the next step the light intensity is evaluated to all the fireflies. The light intensity is a sum of the target function) and the penalty values.

The Firefly algorithm was suitable for the optimization of systems. In some cases it trapped to a local minimum, but the problem was very complex, when we increased the number of elements up to 1000.

## 2.3 Particle Swarm Optimization Algorithm

### 2.3.1 *The PSO Algorithm*

Programs that work very well in optimizing convex functions very often perform poorly when the problem has multiple local minima or maxima. They are often caught or trapped in the local minima/maxima. Several methods have been developed to escape from being caught in such local optima.

The particle swarm optimization (PSO) is a parallel evolutionary computation technique developed by Kennedy and Eberhart (1995) based on the social behaviour metaphor. A standard textbook on PSO, treating both the social and computational paradigms, is Yang (2012). The PSO algorithm is initialized with a population of random candidate solutions, conceptualized as particles. Each particle is assigned a randomized velocity and is iteratively moved through the problem space. It is attracted towards the location of the best fitness achieved so far by the particle itself and by the location of the best fitness achieved so far across the whole population (global version of the algorithm).

Additionally, each member learns from the others, typically from the best performer among them. Every individual of the swarm is considered as a particle in a multidimensional space that has a position and a velocity. These particles fly through hyperspace and remember the best position that they have seen. Members of a swarm communicate good positions to each other and adjust their own position and velocity based on these good positions. The Particle Swarm method of optimization testifies the success of bounded rationality and decentralized decision making in reaching at the global optima. It has been used successfully to optimize extremely difficult multimodal functions.

*PSO* shares many similarities with evolutionary computation techniques such as Genetic Algorithms (*GA*). The system is initialized with a population of random solutions and searches for optima by updating generations. However, unlike *GA*, *PSO* has no evolution operators such as crossover and mutation. In *PSO*, the potential solutions, called particles, fly through the problem space by following the current optimum particles.

Each particle keeps track of its coordinates in the problem space which are associated with the best solution (fitness) it has achieved so far. (The fitness value is also stored.) This value is called *pbest*. Another "best" value that is tracked by the particle swarm optimizer is the best value, obtained so far by any particle in the neighbours of the particle. This location is called *lbest*. when a particle takes all the population as its topological neighbours, the best value is a global best and is called *gbest*.



The particle swarm optimization concept consists of, at each time step, changing the velocity of (accelerating) each particle toward its *pbest* and *lbest* locations (local version of *PSO*). Acceleration is weighted by a random term, with separate random numbers being generated for acceleration toward *pbest* and *lbest* locations.

In past several years, *PSO* has been successfully applied in many research and application areas. It is demonstrated that *PSO* gets better results in a faster, cheaper way compared with other methods.

One reason that *PSO* is attractive is that there are few parameters to adjust. One version, with slight variations, works well in a wide variety of applications. Particle swarm optimization has been used for approaches that can be used across a wide range of applications, as well as for specific applications focused on a specific requirement.

The method is derivative free, constrained problems can simply be accommodated using penalty functions.

*PSO* was successfully applied to the optimum shape and size design of structures by Fourie and Groenwold (2000). They reintroduced an operator, namely craziness, together with the use of dynamic varying maximum velocities and inertia.

*The pseudo code of the procedure can be written as follows:*

I) *For each particle:*

Initialize particle

II) *Do:*

a) *For each particle:*

1) Calculate fitness value

2) If the fitness value is better than the best fitness value (*pbest*) in history

3) Set current value as the new *pbest*

*End*

b) *For each particle:*

1) Find in the particle neighbourhood, the particle with the best fitness

2) Calculate particle velocity according to the velocity equation (2.13)

3) Apply the velocity constriction

4) Update particle position according to the position equation (2.14)

5) Apply the position constriction

*End*

*While* maximum iterations or minimum error criteria is not attained.

A more precise and detailed description of the particular *PSO* algorithm, as applied to penalty function formulation and used in this study now follows.

Initialise a random population (swarm) of  $M$  particles (swarm members), by assigning an initial random position  $\mathbf{x}_i^0$  (candidate solution), as well as a random initial velocity  $\mathbf{v}_i^0$ , to each particle  $i$ ,  $i=1,2,\dots,M$ . Then compute simultaneous trajectories, one for each particle, by performing the following steps.

- 1) At instant  $k$ , compute the fitness of each individual particle  $i$  at discrete point  $\mathbf{x}_i^k$ , by evaluating  $F(\mathbf{x}_i^k)$ . With reference to the minimization of (2.1), the lower the value of  $F(\mathbf{x}_i^k)$ , the greater the particle's fitness.
- 2) For  $i=1,2,\dots,M$ :
  - if  $F(\mathbf{x}_i^k) \leq F_i^b$  then set  $F_i^b = F(\mathbf{x}_i^k)$  and  $\mathbf{p}_i^b = \mathbf{x}_i^k$  {best point on trajectory  $i$ }
  - if  $F(\mathbf{x}_i^k) \leq F^g$  then set  $F^g = F(\mathbf{x}_i^k)$  and  $\mathbf{g}^b = \mathbf{x}_i^k$  {best global point}
- 3) If  $F^g < F_{before}^g$  then set  $N = 1$ , else set  $N = N + 1$ .
- 4) If  $N > N_{max}$  or  $k > k_{max}$  then STOP and set  $\mathbf{x}^* = \mathbf{g}^b$ ; else continue.
- 5) Compute new velocities and positions for instant  $k+1$ , using the rule:
  - for  $i=1,2,\dots,M$ :

$$\mathbf{v}_i^{k+1} := \mathbf{v}_i^k + c_1 r_1 (\mathbf{p}_i^b - \mathbf{x}_i^k) + c_2 r_2 (\mathbf{g}^b - \mathbf{x}_i^k), \quad (2.13)$$

$$\mathbf{x}_i^{k+1} := \mathbf{x}_i^k + \mathbf{v}_i^{k+1} t, \quad (2.14)$$

where  $r_1$  and  $r_2$  are independently generated random numbers in the interval  $[0,1]$ , and  $c_1, c_2$  are parameters with appropriately chosen values.

- 6) Set  $k = k + 1$  and  $F_{before}^g = F^g$ ; go to step 2.

PSO was applied to solve several structural optimization problems: cost minimization of an orthogonally stiffened welded steel plate (Farkas et al. 2007a), ring-stiffened conical shell (Farkas et al. 2007b), optimization of a wind turbine tower structure (Uys et al. 2007), optimization of a stiffened shell (Farkas et al. 2007c), optimization of cellular plate (Jármai, Farkas 2012).

### 2.3.2 Modification of PSO Algorithm with Gradient Estimation

As previously mentioned, several variants of the PSO algorithm have been developed to improve the effectiveness of the technique. One of the solutions is to establish multiple groups of particles instead of one group. Then the local best results in each group compared and the best result of the best group gives the solution. At this case the communication is interpreted not only between the individual particles, but between the groups, so that for individual particles in the speed and position changes not only the position of the local best of the group, but the best results of all the groups taken into consideration.

Another modification is known as crazy bird. This variant is uses randomly selected particles and these particles are flying into a random direction, so that the group does not tear out particles towards the hoped  $g_{best}$  position, which differs from current  $g_{best}$  direction. It helps finding global minimum if the number of crazy bird is kept small.

The aforementioned procedures effectiveness has a random nature. We do not know that how many groups for the particles to send into random direction to get a better result than using the standard algorithm.

At the standard algorithm there is no other information about the objective function which is computed. But in many cases, depending on the individual characteristics of the problem, it would be useful to have local knowledge, since such information may make the procedure to be more efficient. One such information is the local gradient, which as we have only discrete points of samples, can be estimated. The finite-difference-based solution is a fast and efficient solution for the gradient estimation for discrete data. Each finite difference scheme is based on the Taylor-row. At the differentiable function it is assumed that the one-dimensional function  $f(\mathbf{x})$  can be written in the following way:

$$f(x_0 + h) \approx f(x_0) + \frac{f'(x_0)}{1!}h + \frac{f''(x_0)}{2!}h^2 + \dots = \sum_{n=0}^{\infty} \frac{f^{(n)}(x_0)}{n!}h^n \quad (2.15)$$

In this case we can stop at the second member of the formula as follows:

$$f(x_0 + h) \approx f(x_0) + \frac{f'(x_0)}{1!}h \quad (2.16)$$

Expressed as the derivative of the following formula applies:

$$f'(x_0) \approx \frac{f(x_0 + h) - f(x_0)}{h} \quad (2.17)$$

This formula is called in the literature as forward difference estimate.

Then, if instead of  $f(x_0 + h)$  we use  $f(x_0 - h)$  in the equation, we get the following result:

$$f'(x_0) \approx \frac{f(x_0) - f(x_0 - h)}{h} \quad (2.18)$$

This formula in the literature is called as backward difference. As mentioned these estimates are simple and easily calculated, but its drawback that it is less accurate. More complex gradient estimations are available in the literature, but their calculation is more time consuming than the above described procedures and require more than two sampling points.

During the movement of a particle up to a given moment, the points of the earlier function values can be used to estimate gradients in this point. We have implemented the algorithm using backward difference method since it was easier to implement. The gradients of the completed algorithm is used to adjust the speed of the particles, thus the particles move faster in one interval the feasible domain and move slower on the other interval. Each particle position and velocity data are stored, also the number of consecutive points where positive gradients have been found. In case when this value exceeds a pre-defined constant, than the velocity of the particle is increased. In case a negative gradient is found, or it is not interpreted by the gradient, the speed is reset to the default value.

If a particle goes through on high number consecutive sample points, where the gradient is positive, it means that the particle during this time did not pass through the local extreme values, or the global ones, so we can accelerate the speed of the particle to have less iterations to reach the extremum. The efficiency of the method is shown at several test examples.




### 2.3.3 Comparing the Standard PSO and the Modified PSO (GPSO)

We have compared these two methods using our previously proposed set of functions (the definitions of the used composition test functions are in the above example). It is hard to create a summary which contains a lot of information and can be easily read and understood in the same time. There are a lot of articles which use different statistical indexes to propose their results.

In our test we run the two algorithms one hundred times for each 2D test function with two hundred particles and we calculate the average number of iterations (in one iteration there are two hundred function evaluations), the average of the distances between the numerical and theoretical solutions, the best solution (the distance is minimal)  $\pi$ , the worst solution, and the standard deviation of the distances between the numerical and theoretical solutions.

From the Table 2.1 and 2.2 we can conclude that the GPSO algorithm have found solutions within less iterations in the most cases than the standard algorithm. The comparisons show, that the application of gradient information makes the procedure more efficient, without great additional time consuming calculations.

**Table 2.1** Test functions

Name	Definition	optimum
 De Jong	$f(x) = -\sum_{i=1}^n x_i^2$	$\mathbf{x}^*=(0,0,0,...,0),$ $f(\mathbf{x}^*)=0$
 Rosenbrock	$f(x) = -\sum_{i=1}^{n-1} [100(x_{i+1} - x_i)^2 + (x_i - 1)^2]$	$-2.048 \leq x_i \leq 2.048$ $\mathbf{x}^*=(1,1,1,...,1)$ $f(\mathbf{x}^*)=0$
 Rastrigin	$f(x) = -(10n + \sum_{i=1}^n ((x_i)^2 - 10\cos(2\pi x_i)))$	$-5.12 \leq x_i \leq 5.12$ $\mathbf{x}^*=(0,0,0,...,0)$ $f(\mathbf{x}^*)=0$

**Table 2.2** Result of the test functions using standard PSO and GPSO

Function name	Method	Avg of iterations	Avg of distances	Best	Worst	Std dev.
De Jong	PSO	271.44	0.00012	241	307	0.00015
	GPSO	169.66	0.00019	148	184	0.00027
Rosenbrock	PSO	256.13	0.00122	134	303	0.00605
	GPSO	171.62	0.00032	124	230	0.00284
Rastrigin	PSO	157.85	0.31868	86	295	0.30559
	GPSO	122.96	0.33681	70	309	0.22001

## 2.4 The IOSO Technique

### 2.4.1 Main Features of IOSO Technology

IOSO Technology (Indirect Optimization on Self-Organization) is based on the response surface technology. That is why our strategy differs significantly from the well-known approaches to optimization. Our strategy has higher efficiency and provides wider range of capabilities than standard algorithms. The main advantage one can get from using the IOSO Technology is ability to solve very complex optimization tasks.

Unlike common response surface technology algorithms, IOSO algorithms are specifically developed for solving optimization problems. They are accurate in predicting the direction towards the optimum. We can approximate objective functions with complex topology (including the ones with local optima) using minimal number of points in the experiment plan, particularly including the case when the number of points is less than the number of design variables. For example, we start solution of the optimization problem with 140 design variables using only 40 points.

Each iteration of IOSO algorithm consists of two steps. The first step is the creation of an analytical approximation of objective function(s) and constrained parameters. The second step is the optimization of these approximation functions. Multi-objective optimization problem solution is based on the use of approximation functions for individual objectives and constraints.

The distinctive feature of IOSO multi-objective algorithm is an extremely low number of trial points to initialize the search procedure (typically 30 to 50 values of the objective function for the optimization problems with nearly 100 design variables). During the IOSO operation, the information concerning the behaviour of the objective function in the vicinity of the Pareto set is stored, and the response function is made more accurate only for this search area.

The main benefits of IOSO algorithm are its outstanding reliability in avoiding local minima and its computational speed.

### 2.4.2 Testing of the Method

Unfortunately, currently there are no common tests for multiobjective optimization methods. To estimate the efficiency of our method we solved many optimization problems where we used well-known optimization test functions as individual objectives in the multiobjective formulation. We made sure that the extrema of the single objectives did not coincide with each other. The following parameters were used as a measure of efficiency of our method:

- Precision of finding the extremes of the individual objectives;
- Average precision according to Pareto set (Fig. 2.1);
- How uniform the solutions were distributed in the space of objectives.

The results obtained showed the high efficiency of the method for solving various types of problems (Fig. 2.2).

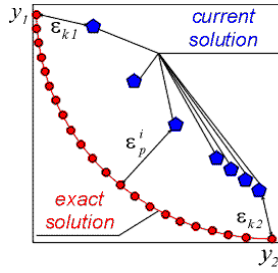


**Fig. 2.1** A set of Pareto optima in the design space

Effectiveness indicators are as follows:

The accuracy of determination of the extrema of a particular criteria

$$\varepsilon_k = (|\tilde{y}_{1best} - y_{1best}| + |\tilde{y}_{2best} - y_{2best}|) / 2 \quad (2.19)$$

The average accuracy of Pareto set

$$\varepsilon_p = \frac{1}{n_p} \sum_{i=1}^{n_p} \sqrt{(\tilde{y}_1^i - \tilde{y}_1^{Ci})^2 + ((\tilde{y}_2^i - \tilde{y}_2^{Ci}))^2} \quad (2.20)$$

The indicator of Pareto points uniformity in design space

$$u_p = \frac{1}{n_p - 1} \sum_{i=1}^{n_p-1} \left( \frac{\sqrt{(\tilde{y}_1^{i+1} - \tilde{y}_1^i)^2 + ((\tilde{y}_2^{i+1} - \tilde{y}_2^i))^2}}{R} - 1 \right) \quad (2.21)$$

where

$$R = \frac{1}{n_p - 1} \sum_{i=1}^{n_p-1} \sqrt{(\tilde{y}_1^{i+1} - \tilde{y}_1^i)^2 + ((\tilde{y}_2^{i+1} - \tilde{y}_2^i))^2} \quad (2.22)$$

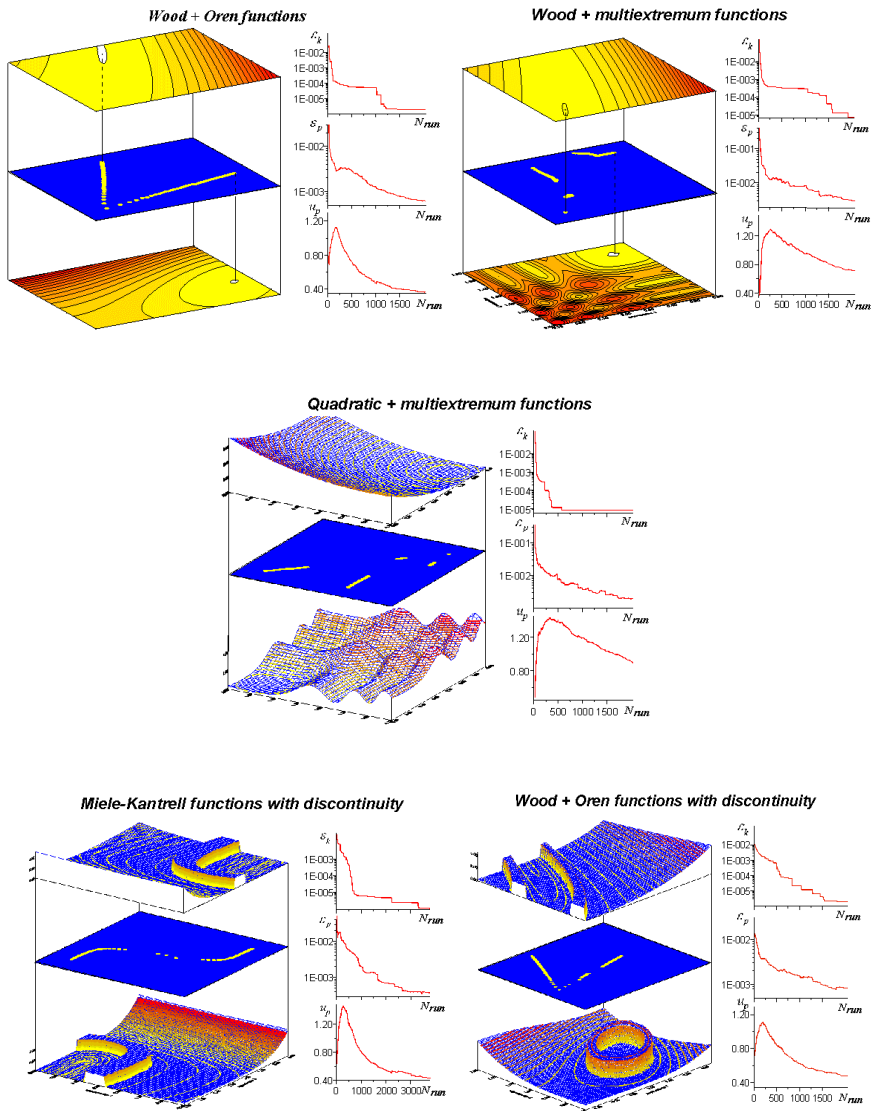


**Fig. 2.2** Some test functions

Most of the real-life engineering optimization problems require simultaneous optimization of more than one objective function. In these cases, it is often impossible that the same values of design parameters will lead to the optimal values for all goals. Hence, to ensure a satisfactory design some trade-off between the objectives is necessary. For this purpose we use the multiobjective approach to optimize the overall efficiency (Egorov 1998, Egorov et al. 1997, Egorov & Kretinin 1992, Dulikravich et al. 1999).

IOSO can be easily integrated with different applications for engineering analysis both in-house and commercial, such as NASTRAN, ANSYS, StarCD, FineDesign, Fluent etc.

### ***2.4.3 Novelty and Distinctive Features of IOSO***

- multiobjective optimization for large-dimensionality problems (up to 100 independent design variables and up to 100 constraints), which allows to reach the increase of efficiency by 2 - 7 times higher than that of middle-dimensionality optimization tasks (20-40 design variables);
- low expenditures for optimal solution search (reduction of the number of analysis code direct calls up to 20 times in comparison with traditional approaches and genetic algorithms (GA), depending on the complexity and dimensionality of the task);
- full automatic optimization technology algorithms with easy to use procedure of task setting;
- the possibility to solve multidisciplinary optimization problems;
- multiobjective optimization for stochastic problems (up to 100 independent design variables), having complex topology of objective and the large number of constraints. Now it is well-known that many methods are capable of solving the tasks having up to 10 - 20 variables, and it is not known the analogues to IOSO optimizer that is designed for large-dimensional multiobjective tasks (100 independent design variables and 20 objectives); solving all classes of optimization problems including stochastic, multiextreme and having non-differential peculiarities.

We have used IOSO for the optimization of cellular plates (Jármai, Farkas 2012).



# Chapter 3

## Cost Calculations

### 3.1 Introduction

This Chapter describes the importance of cost calculations when we optimize a structure. These cost calculations are founded on material costs and those fabrication costs, which have direct effect on the sizes, dimensions or shape of the structure. The cost function includes the cost of material, assembly, welding as well as surface preparation, painting and cutting, edge grinding, forming the shell and is formulated according to the fabrication sequence. Other costs, like amortization, investment, transportation, maintenance are not considered here. Sometimes we can predict the cost of design and inspection, but usually they are proportional to the weight of the structure. Cost and production time data come from different companies from all over the world. When we compare the same design at different countries, we should consider the differences between labour costs. It has the most impact on the structure, if the technology is the same. This Chapter describes the new cost calculations of the different technologies, considering some newer technologies like laser, plasma, waterjet, etc. These costs are the objective functions in structural optimization.

When we consider the interaction of design and fabrication technology, we should not forget about the cost as the third important characteristic of the structure. These three together help us to find the best solution.

### 3.2 The Cost Function

The cost function of a real structure may include the cost of material, assembly, the different fabrication costs such as welding, surface preparation, painting and cutting, edge grinding, forming the geometry, etc. There are some researches, which have been done in this field like Klansek & Kravanja (2006a,b), Jalkanen (2007), Tímár et al. (2003), Farkas & Jármai (1997,2003,2008), Bader (2002), Happio (2012). For composites the calculation is very different and there are some good information available on the internet (Catalog 2012, Cost studio 2012).

### 3.2.1 The Cost of Materials

$$K_M = k_M \rho V, \quad (3.1)$$

For steel the specific material cost can be  $k_M=1.0-1.3$  \$/kg, for aluminium  $k_M= 3.0-3.5$  \$/kg, for stainless steel  $k_M = 6.0-7.1$  \$/kg, for glass fibre 20-30 \$/m<sup>2</sup> depending on the thickness.

$K_M$  [kg] is the fabrication cost,  $k_M$  [\$/kg] is the corresponding material cost factor,  $V$  [mm<sup>3</sup>] is the volume of the structure,  $\rho$  is the density of the material. For steel it is  $7.85 \times 10^{-6}$  kg/mm<sup>3</sup>, for aluminium  $2.7 \times 10^{-6}$  kg/mm<sup>3</sup>, for stainless steel  $7.78 \times 10^{-6}$  kg/mm<sup>3</sup>, for glass fibre  $2.5 \times 10^{-6}$  kg/mm<sup>3</sup>. If several different materials are used, then it is possible to use different material cost factors simultaneously in Eq. (3.1).

### 3.2.2 The Fabrication Cost in General

$$K_f = k_f \sum_i T_i, \quad (3.2)$$

where  $K_f$  [\$] is the fabrication cost,  $k_f$  [\$/min] is the corresponding fabrication cost factor,  $T_i$  [min] are production times. It is assumed that the value of  $k_f$  is constant for a given manufacturer. If not, it is possible to apply different fabrication cost factors simultaneously in Eq. (3.2).

#### 3.2.2.1 Fabrication Times for Welding

The main times related to welding are as follows: preparation, assembly, tacking, time of welding, changing the electrode, deslagging and chipping.

*Calculation of the times of preparation, assembly and tacking*

The times of preparation, assembly and tacking can be calculated with an approximation formula as follows

$$T_{w1} = C_1 \Theta_{dw} \sqrt{\kappa \rho V}, \quad (3.3)$$

where  $C_1$  is a parameter depending on the welding technology (usually equal to 1),  $\Theta_{dw}$  is a difficulty factor,  $\kappa$  is the number of structural elements to be assembled. The difficulty factor expresses the complexity of the structure. Difficulty factor values depend on the kind of structure (planar, spatial), the kind of members (flat, tubular). The range of values proposed is between 1-4 (Farkas & Jármai 1997).

*Calculation of Real Welding Time*

Real welding time can be calculated on the following way

$$T_{w2} = \sum_i C_{2i} a_{wi}^2 L_{wi}, \quad (3.4)$$

where  $a_{wi}$  is weld size,  $L_{wi}$  is weld length,  $C_{2i}$  is constant for different welding technologies.  $C_2$  contains not only the differences between welding technologies but the time differences between positional (vertical, overhead) and normal welding in downhand position as well. The equations for different welding technologies can be found in the Farkas, Jármai (2008).

#### *Calculation of Additional Fabrication Actions Time*

There are some additional fabrication actions to be considered such as changing the electrode, deslagging and chipping. The approximation of this time is as follows

$$T_{w3} = 0.3 \sum C_{2i} a_{wi}^n L_{wi} \cdot \quad (3.5)$$

**Table 3.1** Welding times  $T_{w2}$  (min/mm) in the function of weld size  $a_w$  (mm) for longitudinal fillet welds, downhand position

Welding technology	$a_w$ [mm]	$10^3 T_{w2} = 10^3 C_2 a_w^2$
SMAW	0-15	$0.7889 a_w^2$
SMAW HR	0-15	$0.5390 a_w^2$
GMAW-C	0-15	$0.3394 a_w^2$
GMAW-M	0-15	$0.3258 a_w^2$
FCAW	0-15	$0.2302 a_w^2$
FCAW-MC	0-15	$0.4520 a_w^2$
SSFCAW ( ISW )	0-15	$0.2090 a_w^2$
SAW	0-15	$0.2349 a_w^2$

It is proportional to  $T_{w2}$ . It is the 30% of it. The two time elements are as follows:

$$T_{w2} + T_{w3} = 1.3 \sum C_{2i} a_{wi}^n L_{wi} \cdot \quad (3.6)$$

The welding time for ½ V, V, K and X weldings are as follows for the different technologies:

SMAW = Shielded Metal Arc Welding, SMAW HR = Shielded Metal Arc Welding High Recovery, GMAW-CO<sub>2</sub> = Gas Metal Arc Welding with CO<sub>2</sub> , GMAW-Mix = Gas Metal Arc Welding with Mixed Gas, FCAW = Flux Cored Arc Welding, FCAW-MC = Metal Cored Arc Welding, SSFCAW (ISW) = Self Shielded Flux Cored Arc Welding, SAW = Submerged Arc Welding, GTAW = Gas Tungsten Arc Welding.

**Table 3.2** Welding times  $T_{w2}$  (min/mm) in the function of weld size  $a_w$  (mm) for longitudinal 1/2 V and V butt welds downhand position

Welding technology	$a_w$ [mm]	1/2 V butt welds		V butt welds	
		$10^3 T_{w2} = 10^3 C_2 a_w^2$		$10^3 T_{w2} = 10^3 C_2 a_w^2$	
SMAW	4-6 6-15	$3.13a_w$	$0.5214a_w^2$	$2.7a_w$	$0.45a_w^2$
SMAW HR	4-6 6-15	$2.14a_w$	$0.3567a_w^2$	$1.8462a_w$	$0.3077a_w^2$
GMAW-C	4-15	$0.2245a_w^2$		$0.1939a_w^2$	
GMAW-M	4-15	$0.2157a_w^2$		$0.1861a_w^2$	
FCAW	4-15	$0.1520a_w^2$		$0.1311a_w^2$	
FCAW-MC	4-15	$0.2993a_w^2$		$0.2582a_w^2$	
SSFCAW (ISW)	4-15	$0.1384a_w^2$		$0.1194a_w^2$	
SAW	4-15	$0.1559a_w^2$		$0.1346a_w^2$	

**Table 3.3** Welding times  $T_{w2}$  (min/mm) in the function of weld size  $a_w$  (mm) for longitudinal K and X butt welds downhand position in the form  $T_{w2} = \sum_i C_{2i} a_{wi}^n L_{wi}$ 

Welding technology	$a_w$ [mm]	K butt welds	X butt welds
		$10^3 T_{w2} = 10^3 C_2 a_w^n$	$10^3 T_{w2} = 10^3 C_2 a_w^n$
SMAW	10-40	$0.3539a_w^{1.93}$	$0.3451a_w^{1.9}$
SMAW HR	10-40	$0.2419a_w^{1.93}$	$0.2363a_w^{1.9}$
GMAW-CO <sub>2</sub>	10-40	$0.1520a_w^{1.94}$	$0.1496a_w^{1.9}$
GMAW-Mix	10-40	$0.1462a_w^{1.94}$	$0.1433a_w^{1.9}$
FCAW	10-40	$0.1032a_w^{1.94}$	$0.1013a_w^{1.9}$
FCAW-MC	10-40	$0.2030a_w^{1.94}$	$0.1987a_w^{1.9}$
SSFCAW (ISW)	10-40	$0.0937a_w^{1.94}$	$0.0924a_w^{1.9}$
SAW	10-40	$0.1053a_w^{1.94}$	$0.1033a_w^{1.9}$

### 3.2.2.2 Thermal and Waterjet Cutting

The four most commonly used non-contact methods of metal cutting are oxy-fuel gas, plasma, laser, and abrasive waterjet. The first three cutting processes are thermal in nature, while the waterjet method cuts by abrasive erosion. These four processes are primarily used to make precision external and interior cuts on flat sheet and plate material.

### *Plate Cutting and Edge Grinding Times*

Oxy-fuel gas cutting, usually with acetylene gas, was once the only method of thermal cutting. The oxy-fuel torch has a pre-heating flame that heats either the iron or carbon steels to its "kindling temperature" of around 480° C. Then, a stream of pure oxygen is introduced causing the rapid combustion reaction between the steel and the oxygen. The resulting molten material, or slag, is blown through the metal by the stream of cutting oxygen, providing a relatively smooth and regular cut.

The calculation of the times of arc-spot welding, fabrication times of post-welding treatments, time for flattening plates, surface preparation time, painting times also can be found in Farkas, Jármai (2008).

### *Laser Welding*

The spectrum of laser welding extends from heat conduction welding to deep-penetration welding, a keyhole process in which aspect ratios of up to 10:1 are attained. High power densities permit a concentrated energy input, achieving high welding speeds as well as significantly reduced heat influence and distortion. Compared with arc welding, it allows a much wider range of materials to be welded, and material thicknesses of up to approximately 20 mm can be welded in one pass.

When compared to other welding processes, laser welding has some similar as well as some unique characteristics like GTAW (Gas Tungsten Arc Welding), laser welding is a fusion process performed under inert cover gas, where filler material is most times not added. Like electron beam welding, Laser welding is a high energy density beam process, where energy is targeted directly on the workpiece. Laser differs from both GTAW and EB (electron beam) welding in that it does not require that the workpiece complete an electrical circuit. And since electron beam welding must be performed inside a vacuum chamber, laser welding can almost always offer a cost advantage over EB in both tooling and production pricing.

One of the largest advantages that pulsed laser welding offers is the minimal amount of heat that is added during processing. The repeated "pulsing" of the beam allows cooling between each "spot" weld, resulting in a very small "heat affected zone". This makes laser welding ideal for thin sections or products that require welding near electronics or glass-to-metal seals. Low heat input, combined with an optical (not electrical) process, also means greater flexibility in tooling design and materials. The speed of laser welding of steel plates can be seen on Fig. 3.1ab, the value of welding speed [m/min] and time/unit length [min/m] in the function of plate thickness  $t$  [mm].

$$S = 1/\ln T = 1/(a + bt^{2.5}) \text{ [mm/min]} \quad (3.7)$$

$$a = -0.05918578241974762$$

$$b = -0.02448968345282072$$

where  $S$  is the welding speed [mm/min],  $T$  is time [min],  $t$  is thickness [mm].

### Thermal and Waterjet Cutting

The four most commonly used non-contact methods of metal cutting are oxy-fuel gas, plasma, laser, and abrasive waterjet. The first three cutting processes are thermal in nature, while the waterjet method cuts by abrasive erosion. These four processes are primarily used to make precision external and interior cuts on flat sheet and plate material.

The cutting and edge grinding can be made by different technologies, like Acetylene, Stabilized gasmix and Propane with normal and high speed.

The cutting cost function can be formulated using in the function of the thickness ( $t$  [mm]) and cutting length ( $L_c$  [mm]). Parameters are given in Farkas, Jármai (2008):

$$T_{CP} = \sum_i C_{CPi} t_i^n L_{ci} , \quad (3.8)$$

where  $t_i$  the thickness in [mm],  $L_{ci}$  is the cutting length in [mm]. The value of  $n$  comes from curve fitting calculations.

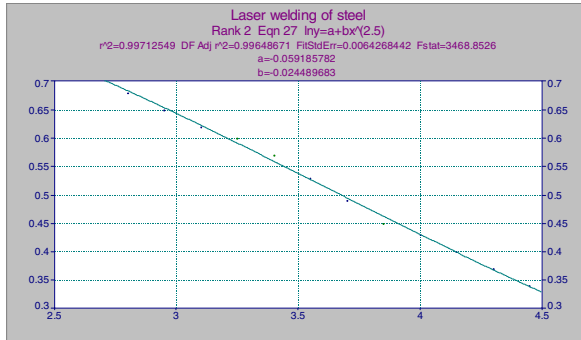


**Fig. 3.1a** Laser welding speed  $S$  [m/min] in the function of plate thickness  $t$  [mm]

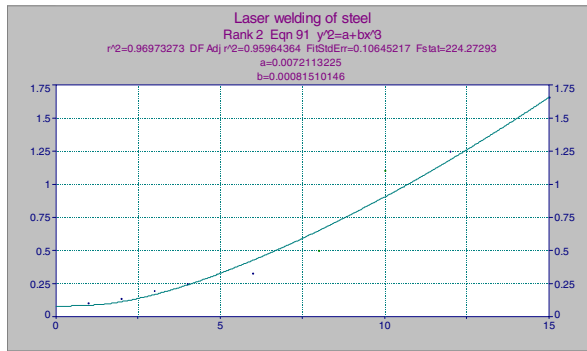


**Fig. 3.1b** Laser welding time/unit length [min/m] in the function of plate thickness  $t$  [mm]

**Table 3.4** Cutting time of plates,  $T_{CP}$  (min/mm) in the function of weld size  $a_w$  (mm) for longitudinal fillet welds and T-, V-, 1/2 V butt welds

Cutting technology	Thickness $t$ [mm]	$10^3 T_{CP} = 10^3 C_{CP} t^n$
Acetylene ( normal speed )	2-15	$1.1388t^{0.25}$
Acetylene ( high speed )	2-15	$0.9561t^{0.25}$
Stabilized gasmix ( normal speed )	2-15	$1.1906t^{0.25}$
Stabilized gasmix ( high speed )	2-15	$1.0858t^{0.23}$
Propane ( normal speed )	2-15	$1.2941t^{0.24}$
Propane ( high speed )	2-15	$1.1051t^{0.25}$

**Table 3.5** Cutting time of plates for 1 mm length,  $T_{CP}$  (min/mm) in the function of weld size  $a_w$  (mm) for fillet longitudinal X- and K butt welds

Cutting technology	Thickness $t$ [mm]	$10^3 T_{CP} = 10^3 C_{CP} t^n$
Acetylene ( normal speed )	10-40	$0.8529t^{0.36}$
Acetylene ( high speed )	10-40	$0.6911t^{0.38}$
Stabilized gasmix ( normal speed )	10-40	$0.8991t^{0.36}$
Stabilized gasmix ( high speed )	10-40	$0.6415t^{0.44}$
Propane ( normal speed )	10-40	$0.9565t^{0.36}$
Propane ( high speed )	10-40	$0.7870t^{0.38}$

The thermal processes and the oxy-fuel gas process in particular share two disadvantages. First, heat changes the structure of metal in a "heat-affected zones" adjacent to the cut. This may degrade some metallurgical qualities at the cut's edge, requiring pre-treatment or trimming. Secondly, tolerances may be less accurate than a machined cut, except for laser cutting.

*Laser Cutting of Steel (Fig. 3.2) and Aluminium (Fig. 3.3)*

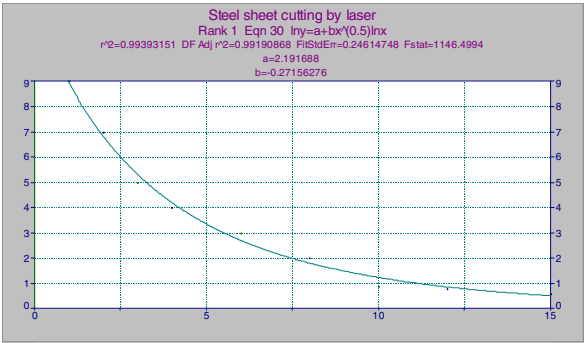


**Fig. 3.2** Steel sheet cutting speed by laser [m/min]

Laser cutting is a fairly new technology that allows metals and some non metallic materials to be cut with extreme precision if required. The laser beam is typically 0.2 mm in diameter with a power of 1-2 kW. At laser cutting process, a beam of high-density light energy is focused through a tiny hole of the nozzle. When this beam strikes the surface of the work piece, the material of the work piece is cut immediately. Lasers work best on materials such as carbon and stainless steels. Metals such as aluminium and copper alloys are more difficult to cut by laser due to their ability to reflect the laser light as well as absorb and conduct heat. The distribution of the application of laser in different manufacturing processes can be seen on Fig. 3.4. Laser cutting is the largest application.

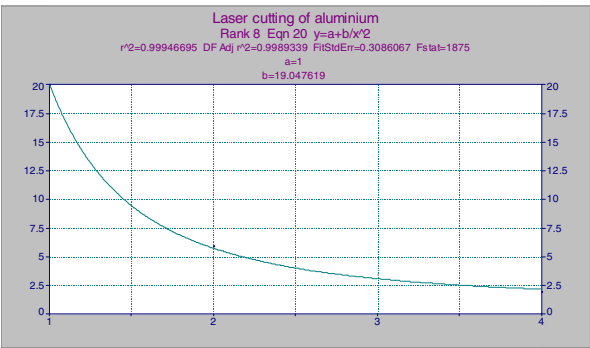


**Fig. 3.3** Aluminium sheet cutting speed by laser [m/min]



*Laser cutting of steel sheets*

$$S=1/\ln T=1/(a+bt^{0.5}\ln t) \text{ [min/mm]}$$

$a= 2.191688010897978$

$b= -0.2715627600304911$

*Laser cutting of aluminium sheets*

$$S= 1/T=1/(a+b/t^2)\text{[min/mm]}$$

$a= 1$

$b= 19.04761904761905$

(3.9)

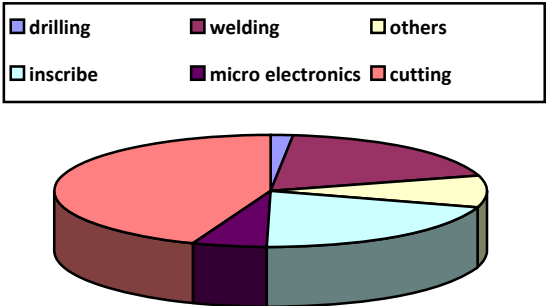


Fig. 3.4 Distribution of the application of laser in different manufacturing processes

*Waterjet Cutting of Steel (Fig. 3.5) and Stainless Steel (Fig. 3.6)*

A water jet cutter is capable of cutting a wide variety of materials using a very high-pressure jet of water, or a mixture of water and an abrasive substance.

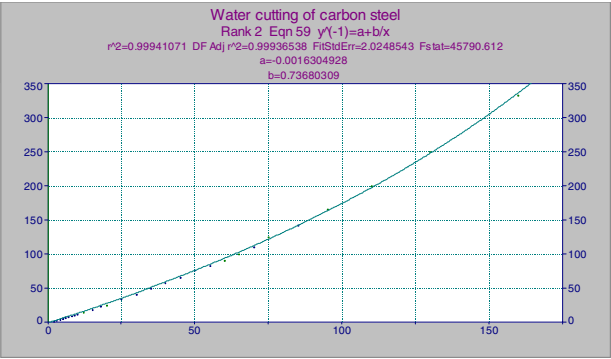


Fig. 3.5 Waterjet cutting of steel sheet cutting [min/m]

*Waterjet cutting, carbon steel 3500 bar*

$$S= 1/T=a+b/t \text{ [m/min]}$$

$a= -0.001630492750216705$

$b= 0.7368030917264656$

*Waterjet cutting stainless steel pressure 3500 bar*

$$S=1/T^{0.5}=1/(a+bt^{0.5})\text{[m/min]}$$

$a= -1.231333913075542$

$b= 1.405960445076508$

(3.10)

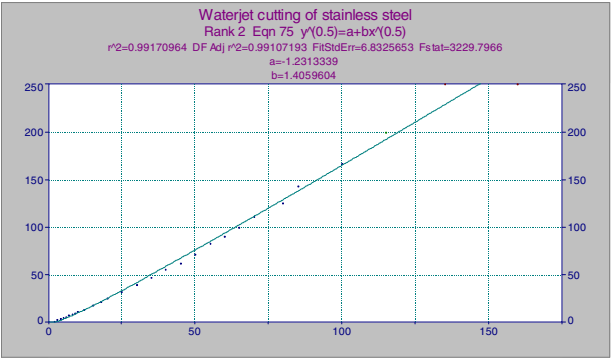


**Fig. 3.6** Waterjet cutting of stainless steel sheet cutting [min/m]

*Plasma Cutting of Steel (Fig. 3.7) and Stainless Steel (Fig. 3.8)*

Plasma cutting uses an extremely high temperature, high velocity stream of ionized gas to cut the metal. Plasma temperatures range from about 5500 °C to 28,000 °C. Depending upon the material to be plasma cut, the gases used include: standard compressed shop air, oxygen, argon and hydrogen, or nitrogen and hydrogen. Gas shielding is accomplished with air, water, or carbon dioxide.

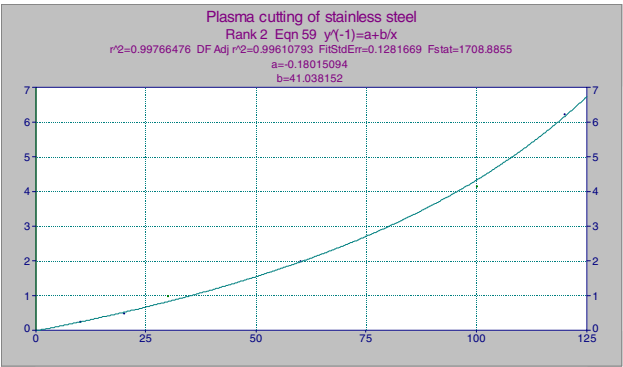


**Fig. 3.7** Plasma cutting of stainless steel [min/m]

Plasma cutting requires a torch, a power supply, and an arc-starting circuit. The plasma cutting power supply is a constant-current DC power source. A high frequency AC starting circuit ionizes the gas to make it conductive. When gas is fed to the torch, part of the gas is ionized by the high-voltage arc starter between the electrode, or cathode, in the torch, and the torch tip. When the power supply's

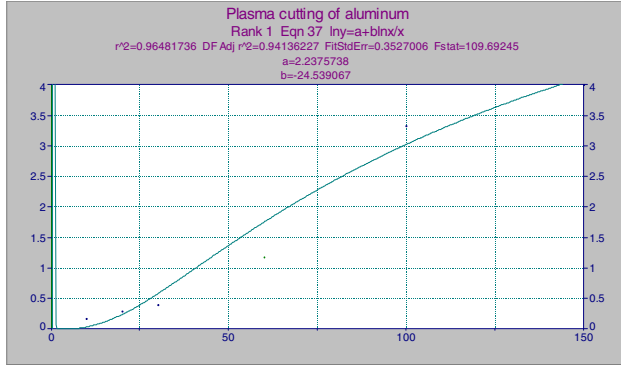


**Fig. 3.8** Plasma cutting of aluminium [min/m]

small DC current meets this high voltage gas, it creates a pilot arc. This pilot arc leaves the torch tip as a plasma jet and becomes the path for the main plasma arc. Once the pilot arc contacts the metal's surface, or anode, the main arc forms. The pilot arc then shuts off, and the cutting torch begins operation.

<p><i>Plasma cutting of stainless steel</i></p> <p><math>S=1/T=a+b/t</math> [m/min]</p> <p><math>a= -0.1801509431963638</math></p> <p><math>b= 41.03815214608195</math></p>	<p><i>Plasma cutting of aluminium</i></p> <p><math>S=1/\ln T=1/(a+b/t^{0.5})</math> [m/min]</p> <p><math>a= 2.97536641707248</math></p> <p><math>b= -18.8936784318449</math></p>
---	--

(3.11)

### 3.2.2.3 Time for Flattening Plates

$$T_{FP} = \Theta_{df} \left( a_e + b_e t^3 + \frac{1}{a_e t^4} \right) A_p, \quad (3.12)$$

where  $a_e=9.2 \times 10^{-4}$  min/mm<sup>2</sup>,  $b_e= 4.15 \times 10^{-7}$  min/mm<sup>5</sup>,  $\Theta_{df}$  is the difficulty parameter ( $\Theta_{df} = 1, 2$  or  $3$ ). The difficulty parameter depends on the form of the plate.

### 3.2.2.4 Surface Preparation Time

The surface preparation means the surface cleaning, sand spraying, etc. The surface cleaning time can be defined in the function of the surface area ( $A_s$  [mm<sup>2</sup>]) as follows:

$$T_{SP} = \Theta_{ds} a_{sp} A_s, \quad (3.13)$$

where  $a_{sp} = 3 \times 10^{-6}$  min/mm<sup>2</sup>,  $\Theta_{ds}$  is a difficulty parameter.

### 3.2.2.5 Painting Time

The painting means making the ground- and the topcoat. The painting time can be given in the function of the surface area ( $A_s$  [mm<sup>2</sup>]) as follows:

$$T_P = \Theta_{dp} (a_{gc} + a_{tc}) A_s, \quad (3.14)$$

where  $a_{gc} = 3 \times 10^{-6}$  min/mm<sup>2</sup>,  $a_{tc} = 4.15 \times 10^{-6}$  min/mm<sup>2</sup>,  $\Theta_{dp}$  is a difficulty factor,  $\Theta_{dp}=1,2$  or 3 for horizontal, vertical or overhead painting. Tizani et al. (1996) proposed a value for painting  $14.4 \times 10^{-6}$  \$/mm<sup>2</sup>. For more complicated structures we use  $k_p = 2 \times 14.4 \times 10^{-6}$  \$/mm<sup>2</sup>.

### 3.2.2.6 Times of Hand Cutting and Machine Grinding of Strut Ends

At tubular structures a main part of the total cost is the cost of hand cutting and machine grinding of strut ends. We use the following formula (Farkas & Jármai 2008).

Glijnis (1999) proposed a formula for one strut end in the case of oxyfuel cutting on CNC machine as follows:

$$K_{CG}(\$) = \frac{2.5\pi d_i}{(350 - 2t_i) 0.3 \sin \varphi_i}, \quad (3.15)$$

where 350 mm/min is the cutting speed, 0.3 is the efficiency factor,  $d_i$  and  $t_i$  are in mm,  $\varphi_i$  is the inclination angle of a diagonal brace.

### 3.2.2.7 Cost of Intumescent Painting

Intumescent paintings are getting more and more popular, because they look attractive, does not have a bad effect on slim steel structure view, but the painting is relatively expensive

$$K_{pi} = (k_p + k_{pi}) A_p, \quad (3.16)$$

where the specific painting cost  $k_p = 14$  \$/m<sup>2</sup>, means the normal painting in two layers (ground and top coat). The additional intumescent painting cost depends on its thickness. The thickness is proportional to the protection time. The cost is  $k_{pi} = 20$  \$/m<sup>2</sup>, for R30, half hour, or  $k_{pi} = 60$  \$/m<sup>2</sup> for R60, one hour protection.  $A_p$  is the full covered surface.

## 3.2.3 Total Cost Function

The total cost function can be formulated by adding the previous cost functions together (depending on the structure some can be zero).

$$\frac{K}{k_m} = \rho V + \frac{k_f}{k_m} (T_{w1} + T_{w2} + T_{w3} + T_{FP} + T_{SP} + T_P + T_{CG} + \dots) + \frac{K_{pi}}{k_m} + \dots + \quad (3.17)$$

Taking  $k_m = 0.5-1.5$  \$/kg,  $k_f = 0-1$  \$/min. The  $k_f/k_m$  ratio varies between 0 - 2 kg/min. If  $k_f/k_m = 0$ , then we get the mass minimum. If  $k_f/k_m = 2.0$  it means a very high labour cost (Japan, USA),  $k_f/k_m = 1.5$  and 1.0 means a West European labour cost,  $k_f/k_m = 0.5$  means the labour cost of developing countries. Even if the production rate is similar for these cases, the difference between costs due to the different labour costs is significant.

### 3.3 Conclusion

In this Chapter the cost calculation of different welding, cutting, painting, etc. technologies have been described. These cost calculations are founded on material costs and those fabrication costs, which have direct effect on the sizes, dimensions or shape of the structure. The calculated times for different newer technologies like laser, plasma, waterjet, etc. have been included also. These costs are the objective functions in structural optimization.

When we consider the interaction of design and technology, we should not forget the cost of the structure as the third leg of the system. These three together help us to find the best solution. These cost calculations are founded on material costs and those fabrication costs, which have direct effect on the sizes, dimensions or shape of the structure. Cost and production time data come from different companies from all over the world. When we compare the same design at different countries, we should consider the differences between labour costs. It has the greatest impact on the structure sizes, when the technology is the same.

# Chapter 4

## Beams and Columns

### 4.1 Comparison of Minimum Volume and Minimum Cost Design of a Welded Box Beam

#### Abstract

The present study shows the difference between structures optimized for minimum volume and minimum cost. The cost function contents the cost of material, assembly, welding and painting. A simply supported welded box section beam is investigated. The design constraints are as follows: limitation of the maximum stress from the maximum bending moment, limitation of plate slendernesses to avoid local buckling of flange and web. The minimization of the volume and cost results in different beam sizes, but the cost difference between the two optima is small.

#### 4.1.1 Introduction

In structural optimization researchers use volume as objective function. In order to design economic and competitive structures a cost function should be formulated and minimized. A cost calculation method is developed mainly for welded structures (Farkas and Jármai 1997, 2003, 2008). The cost function contents the cost of material, assembly, welding and painting. This function contents the main structural parameters to be optimized as the main cross-sectional dimensions as well as dimension and length of welds. Since the welding cost is proportional to the square of weld size, this size should be minimized to achieve economic structures.

The symmetrical plated unstiffened box cross-section of the beam has four variable dimensions and four longitudinal fillet welds. Since the cross-section is constant for the whole beam, in the minimum volume design it is sufficient to optimize the cross-section area. For the minimum cost design the whole beam should be investigated.

The minimum cross-section area design results in relatively simple closed formulae. Since the cost function is a more complicated non-linear one, the minimum cost design needs mathematical methods.

In a numerical problem it is shown that the optimal cross-sectional dimensions are different for minimum cross-sectional area and minimum cost, but the difference in total costs of these optima is not high. Thus, using the minimum volume design instead of minimum cost design can be allowed.

To find the optima the truss height is varied stepwise and a MathCAD algorithm is used to calculate the corresponding values.

### 4.1.2 Minimum Cross-Sectional Area Design

The symmetrical plated unstiffened box cross-section of the beam has four variable dimensions ( $h$ ,  $t_w$ ,  $b$ ,  $t_f$ ) and four longitudinal fillet welds (Fig.4.1). Since the cross-section is constant for the whole beam, in the minimum volume design it is sufficient to optimize the cross-section area. For the minimum cost design the whole beam should be investigated.

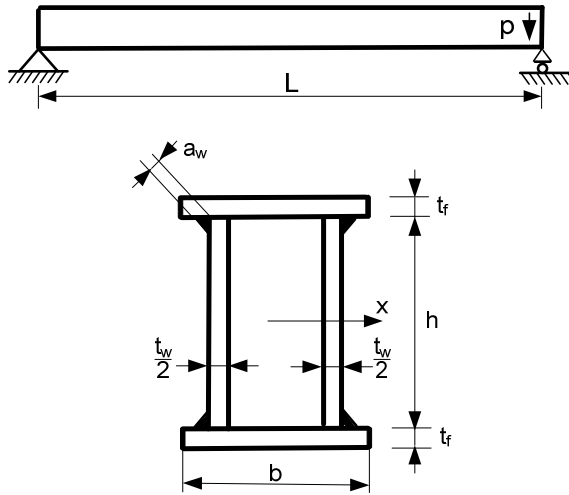


**Fig. 4.1** A simply supported welded box beam

The formulation of the optimum design of a box beam is as follows: find the optimum values of the dimensions  $h$ ,  $t_w$ ,  $b$ ,  $t_f$  to minimize the whole cross-section area

$$A = ht_w + 2bt_f \quad (4.1)$$

and fulfil the following constraints:

(a) stress constraint

$$\sigma_{max} = \frac{M}{W_x} \leq f_{y1} \quad \text{or} \quad W_x \geq \frac{M}{f_{y1}} = W_0 \quad (4.2)$$

$$I_x = \frac{h^3 t_w}{6} + 2bt_f \left( \frac{h}{2} \right)^2; W_x = \frac{I}{h/2} = \frac{h^2 t_w}{3} + bt_f h \quad (4.3)$$

The bending moment is expressed as

$$M = p_s L^2 / 8, \quad (4.4)$$

the self mass of the beam is also taken into account, so

$$p_s = 1.5p + 1.1\rho_1 A, \quad \rho_1 = 7.85 \times 10^{-5} \text{ N/mm}^3. \quad (4.5)$$

(b) constraint on local buckling of webs

$$\frac{h}{t_w/2} \leq \frac{1}{\beta}; \text{ or } t_w \geq 2\beta h \quad (4.6)$$

where

$$1/\beta = 69\varepsilon; \varepsilon = \sqrt{\frac{235}{f_y}} \quad (4.7)$$

(c) constraint for local buckling of compressed upper flange

$$\frac{b}{t_f} \leq \frac{1}{\delta} = 42\varepsilon, \quad \text{or } t_f \geq \delta b \quad (4.8)$$

Considering the local buckling constraint as active the stress constraint can be written as

$$W = \frac{\beta h^3}{3} + bt_f h \geq W_0 \quad (4.9)$$

substituting  $bt_f$  from Eq. (4.9) into Eq. (4.1) one obtains

$$A = \frac{2W_0}{h} + \frac{4\beta h^2}{3} \quad (4.10)$$

From the condition

$$\frac{dA}{dh} = 0 \quad (4.11)$$

one obtains the optimum value of  $h$  from the stress constraint

$$h_\sigma = \sqrt[3]{\frac{3W_0}{4\beta}} \quad (4.12)$$

This formula gives an approximate value for  $h_{opt}$ , since the effect of self mass in  $M_{max}$  is neglected.



### 4.1.3 Minimum Cost Design

It is important for cost to define the required fillet weld size. We take it in function of the web thickness

$$a_w = 0.3t_w/2 = 0.3\beta h \quad (4.13)$$

but  $a_{wmin} = 3$  mm.

The cost function contains the cost of material, assembly, welding and painting:

$$K = K_M + K_W + K_P \quad (4.14)$$

$$K_M = k_M \rho A L, \rho = 7.85 \times 10^{-6} \text{ kg/mm}^3, k_M = 1 \text{ \$/kg} \quad (4.15)$$

Welding cost for 4 fillet welds of GMAW-C (Gas metal arc welding with CO<sub>2</sub>) (Farkas and Jármai 2003, 2008)

$$K_w = k_w \left( C_1 \Theta_c \sqrt{\kappa \rho V} + 1.3 C_w a_w^2 L_w \right), k_w = 1.0 \text{ \$/min} : C_1 = 1.0 \text{ min/kg}^{0.5} \quad (4.16)$$

The factor of complexity of assembly is  $\Theta_c = 2$ , number of assembled parts is  $\kappa = 4$ , welding coefficient  $C_w = 0.3394 \times 10^{-3}$ , length of welds  $L_w = 4L$ .

Painting cost

$$K_p = k_p S, k_p = 28.8 \times 10^{-6} \text{ \$/mm}^2, S = 4bL \quad (4.17)$$

### 4.1.4 Numerical Data and Results

$p = 90$  N/mm,  $L = 15$  m,  $f_y = 235$  MPa. The required section modulus is according to Eq. (4.2)  $W_0 = 1841 \times 10^4 \text{ mm}^3$ , the effect of self mass is very small.

The approximate formula Eq. (4.12) gives  $h_{opt} = 972$  mm.

In the optimization process  $h$  is selected and changed stepwise. For each  $h$  a suitable  $b$  is sought to satisfy the stress constraint. The obtained volume and cost value are given in Table 4.1.

It can be seen that the optimum values of  $h$  are different, for minimum volume  $h_{opt} = 990$  mm, and for minimum cost  $h_{opt} = 920$  mm, but the difference of cost between these optima is only  $100(8940 - 8892)/8940 = 0.5\%$ . The difference between the optima is caused by the different fillet weld sizes. To decrease the welding cost the weld size should be decreased, but this decrease causes decrease in  $t_w/2$  and  $h$ , since  $a_w$  depends on  $t_w/2$  and  $t_w/2$  depends on  $h$ .

**Table 4.1** Results of the optimization process. The optima are marked by bold letters.  $W_x$  in mm<sup>3</sup>.

$h$ mm	$b$ mm	$W_x \times 10^{-4}$	$A$ mm <sup>2</sup>	$t_w/2$ mm	$a_w$ mm	$K_M$ \$	$K_W$ \$	$K_P$ \$	$K$ \$
1000	756	1844	56200	14.5	4.35	6618	826	1517	8961
995	759	1844	56130	14.4	4.33	6609	820	1515	8945
<b>990</b>	<b>763</b>	<b>1841</b>	<b>56130</b>	14.3	4.30	6609	816	1515	8940
985	767	1841	56140	14.2	4.28	6610	811	1514	8935
980	771	1842	56140	14.2	4.26	6611	806	1513	8930
--	--	--	--	--	--	--	--	--	--
940	802	1841	56240	13.6	4.09	6622	768	1505	8895
930	810	1842	56310	13.5	4.04	6631	758	1503	8893
<b>920</b>	<b>818</b>	<b>1842</b>	56400	<b>13.3</b>	<b>4.00</b>	<b>6641</b>	<b>749</b>	<b>1502</b>	<b>8892</b>
910	826	1842	56490	13.2	3.96	6652	741	1500	8893
900	834	1843	56600	13.0	3.91	6665	732	1498	8895

## 4.2 Minimum Cost Design for Fire Resistance of a Welded Box Column and a Welded Box Beam

### Abstract

The optimum design is applied to cost minimization of two types of welded steel structures in fire. Both unprotected and protected structures are investigated. The compressed rod of welded square box cross-section is designed to overall and local buckling. The bent beam of welded box section should fulfil the stress, deflection and local buckling constraints. The cost function contents the cost of material, assembly, welding, painting and fire protection. In the unprotected case the critical temperature method is used with formulae given in Eurocode 3. In both structures the protected structure is cheaper than the unprotected one. This difference is caused by the significant difference in thicknesses.

### 4.2.1 Introduction

Requirements for modern load-carrying structures are the safety, fitness for production and economy. In the optimum design procedure the safety and fitness for production are guaranteed by fulfilling of design and fabrication constraints, and the economy is achieved by minimization of a cost function.

It is possible to design a lot of structural versions. The most suitable version can be selected by cost comparison. For the purpose of economic design of welded steel structures a relatively simple cost calculation method is developed (Farkas and Jármai 1997, 2003, 2008). The cost function consists of cost of material, assembly, welding and painting.

Since the fire resistance of steel structures needs protection, the cost of various protection methods is also calculated using numerical data from industry.

The search for better solutions is performed by change of structural characteristics such as material, type of structure, profiles, main dimensions, fabrication technology, connections.

In general, the optimum design needs the solution of a constrained minimization of one or more objective nonlinear multivariable functions. Therefore the problems can only be treated numerically and the results are valid not generally. In spite of this, when the numerical data of problems are selected as near as possible to industrial application, the results are very useful for designers to find the most economic and competitive structural versions.

In our research work we have worked out a lot of numerical problems of various metal structures. Our aim is to show how to apply the economic design for fire-resistant welded steel structures. The catastrophic damages and failures show that steel structures are very sensitive to high temperatures. Therefore special design rules have been elaborated in relevant Eurocodes (Eurocode 1, Part 1-2, 2005, Eurocode 3 Part 1-2, 2005, Eurocode 3, Part 1.1, 2005), which are applied in the study.

Two numerical problems are solved as follows:

- (1) a centrally compressed rod of welded square box cross-section,
- (2) a welded box beam loaded in bending and shear.

Costs of unprotected and protected versions are compared to each other. Since only optimized versions can be compared, the both versions are optimized for minimum cost.

A lot of articles have been published on fire-resistant design of steel structures. Studies of Franssen et al. (1995), Vila Real et al. (2005) and Choi et al. (2002) can be mentioned.

### 4.2.2 The Critical Temperature Method

Figure 4.2 shows the temperature versus time for fire gas and for a steel structure. The gas temperature can be calculated as

$$\Theta_g = 20 + 345 \log \left( \frac{8T}{60} + 1 \right) \quad (4.18)$$

where  $T$  is the time in *sec*.

The temperature of steel structure in a time interval is given by

$$\Delta\Theta_a = \frac{A_m}{V} \frac{h_{netd}}{c_a \rho_m} \Delta T \quad (4.19)$$

where  $c_a$  is the specific heat of steel,

$$c_a = 425 + 7.73 \times 10^{-1} \Theta_a - 1.69 \times 10^{-3} \Theta_a^2 + 2.22 \times 10^{-6} \Theta_a^3 \quad (4.20)$$

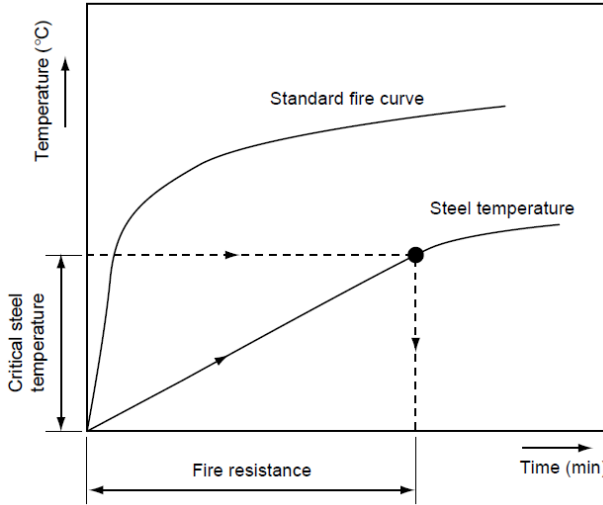


**Fig. 4.2** Critical temperature in the function of time

$\rho_m$  is the unit mass of steel,  $A_m/V$  is for rods of constant cross-section the ratio of perimeter/cross-section area, for a square box section

$$A_m/V = 1/t \quad (4.21)$$

The design value of the net heat flux per unit area is

$$h_{netd} = h_{netc} + h_{netr} \quad (4.22)$$

where the net convection heat flux is

$$h_{netc} = 25(\Theta_g - \Theta_a) \quad (4.23)$$

and the net radiative heat flux is

$$h_{netr} = 0.8 \times 5.67 \times 10^{-8} \left[ (\Theta_g + 273)^4 - (\Theta_a + 273)^4 \right] \quad (4.24)$$

$5.67 \times 10^{-8}$  is the Boltzmann constant.

The critical temperature is given by

$$\Theta_{cr} = 39.19 \ln \left( \frac{1}{0.9674 \mu_0^{3.833}} - 1 \right) + 482 \quad (4.25)$$

where

$$\mu_0 = N_{fi}/N_0 \quad (4.26)$$

is the utilization factor,  $N_{fi}$  and  $N_0$  are the limiting compression forces in the case of fire and for ambient temperature, respectively.

The fire resistance time  $R$  corresponding to the critical temperature can be obtained by step-by-step using Eqs. (4.18)-(4.26). Since until  $600^\circ\text{C}$  the parameters in Eq. (4.19). can be approximated by three linear intervals, we use intervals of

$$\Theta_{a1} = \Theta_{cr} / 3, \Theta_{a2} = 2\Theta_{cr} / 3, \Theta_{a3} = \Theta_{cr} \quad (4.27)$$

In this case the final  $R = \sum R_i$  is calculated by three iterations using a MathCAD algorithm

$$\Delta R_i = \frac{\Theta_{ai} c_{ai} \rho_m}{6 \times 10^4 h_{netdi}}, i = 1, 2, 3 \quad (4.28)$$

### 4.2.3 A Centrally Compressed Column with Pinned Ends of Welded Square Box Cross-Section

The design value of the net heat flux per unit area is

$$h_{netd} = h_{netc} + h_{netr} \quad (4.29)$$

where the net convection heat flux is

$$h_{netc} = 25(\Theta_g - \Theta_a) \quad (4.30)$$

and the net radiative heat flux is

$$h_{netr} = 0.8 \times 5.67 \times 10^{-8} \left[ (\Theta_g + 273)^4 - (\Theta_a + 273)^4 \right] \quad (4.31)$$

$5.67 \times 10^{-8}$  is the Boltzmann constant.

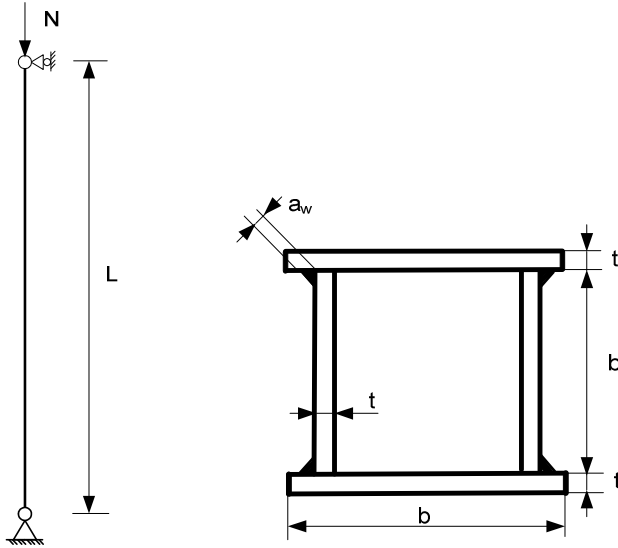


Fig. 4.3 Compressed column of welded square box section

### 4.2.3.1 Overall Buckling Constraint for Ambient Temperature

$$N \leq N_0 \quad (4.32)$$

$$N_0 = \chi_f^f A \quad (4.33)$$

the buckling factor

$$\chi = \frac{1}{\phi + \sqrt{\phi^2 - \bar{\lambda}^2}}, \phi = \frac{1}{2} \left[ 1 + \alpha (\bar{\lambda} - 0.2) + \bar{\lambda}^2 \right] \quad (4.34)$$

where

$$\bar{\lambda} = \frac{\lambda}{\lambda_E}, \lambda = \frac{L}{r}, r = \sqrt{\frac{I}{A}}, \lambda_E = \pi \sqrt{\frac{E}{f_y}} \quad (4.35)$$

In the case of a square box section

$$A = 4bt \quad (4.36)$$

$$I = \frac{2b^3t}{3} + \frac{bt^3}{6} \quad (4.37)$$

For fire design  $\alpha = 0.49$ .

### 4.2.3.2 Overall Buckling Constraint in Fire

$$N \leq N_{fi,t} \quad (4.38)$$

$$N_{fi,t} = \chi_{fi} A k_{y\Theta i} f_y / \gamma_{Mfi} \quad (4.39)$$

$$\gamma_{Mfi} = 1$$

$$\chi_{fi} = \frac{1}{\phi_{\Theta} + \sqrt{\phi_{\Theta}^2 - \bar{\lambda}_{\Theta}^2}}, \phi_{\Theta} = \frac{1}{2} \left( 1 + \alpha \bar{\lambda}_{\Theta} + \bar{\lambda}_{\Theta}^2 \right) \quad (4.40)$$

$$\alpha = 0.65 \sqrt{\frac{235}{f_y}}, \bar{\lambda}_{\Theta} = \bar{\lambda} \sqrt{\frac{k_{y\Theta i}}{k_{E\Theta i}}} \quad (4.41)$$

Factors of  $k_{y\Theta i}$  and  $k_{E\Theta i}$  can be approximated by linear intervals of

$$k_{y\Theta 0} = 1 \quad \text{if } 20^\circ\text{C} < \Theta_a < 400^\circ\text{C} \quad (4.42)$$

$$k_{y\theta 1} = \frac{500 - \theta_a}{100} 0.22 + 0.78 \quad \text{if } 400^\circ\text{C} < \theta_a < 500^\circ\text{C} \quad (4.43)$$

$$k_{y\theta 2} = \frac{600 - \theta_a}{100} 0.31 + 0.47 \quad \text{if } 500^\circ\text{C} < \theta_a < 600^\circ\text{C} \quad (4.44)$$

and

$$k_{E\theta 0} = 1 \quad \text{if } 20^\circ\text{C} < \theta_a < 100^\circ\text{C} \quad (4.45)$$

$$k_{E\theta 1} = \frac{500 - \theta_a}{400} 0.4 + 0.6 \quad \text{if } 100^\circ\text{C} < \theta_a < 500^\circ\text{C} \quad (4.46)$$

$$k_{E\theta 2} = \frac{600 - \theta_a}{100} 0.29 + 0.31 \quad \text{if } 500^\circ\text{C} < \theta_a < 600^\circ\text{C} \quad (4.47)$$

#### 4.2.3.3 Local Buckling Constraint

For ambient temperature

$$b/t \leq 42\varepsilon, \varepsilon = \sqrt{235/f_y} \quad (4.48)$$

For fire Eurocode 3 proposed a decreased value of

$$b/t \leq 0.8 \times 42\varepsilon = 33.6\varepsilon \quad (4.49)$$

According to the experiments of Knobloch (2008)

$$b/t \leq 0.6 \times 42\varepsilon = 25.2\varepsilon \quad (4.50)$$

#### 4.2.3.4 Cost Function

Material cost

$$K_m = k_m \rho V, V = AL, k_m = 1.0\$/kg \quad (4.51)$$

Welding cost for 4 fillet welds of GMAW-C (Gas metal arc welding with CO<sub>2</sub>)

$$K_w = k_w \left( C_1 \theta_c \sqrt{\kappa \rho V} + 1.3 C_w a_w^2 L_w \right), k_w = 1.0\$/\text{min} : C_l = 1.0 \text{ min/kg}^{0.5} \quad (4.52)$$

The factor of complexity of assembly is  $\theta_c = 2$ , number of assembled parts is  $\kappa = 4$ , fillet weld size  $a_w = 0.3t$ , welding coefficient  $C_w = 0.3394 \times 10^{-3}$ , length of welds  $L_w = 4L$ .

Painting cost

$$K_p = k_p S, k_p = 28.8 \times 10^{-6} \$/\text{mm}^2, S = 4bL \quad (4.53)$$

Total cost

$$K = K_m + K_w + K_p \quad (4.54)$$

#### 4.2.3.5 Numerical Data and Results

Centric compression force for fire  $N = 10^7$  [N]. This load is calculated from the actual ones using a reduction factor  $\eta_{fi}$ . Rod length  $L = 6$  m. Yield stress of steel  $f_y = 235$  MPa.

The optimization is performed by a systematic search using a MathCAD algorithm. Results are given in Tables 4.2 and 4.3.

**Table 4.2** Results for the unprotected structure for a fire resistance time  $R = 30$  min. Optimum is marked by bold letters.

$b$ mm	$t$ mm	$10^{-3}A$	$K$ \$	$\Theta_{cr}$ °C	$R$ min	$10^{-7}N_{fi,T}$ [N]
500	38	76.00	5541	556	31.2	1.013
500	37	74.00	5372	551	30.2	0.977
<b>510</b>	<b>37</b>	<b>75.48</b>	<b>5451</b>	<b>555</b>	<b>30.5</b>	<b>1.003</b>
520	36	74.88	5359	554	29.9	0.856
530	35	74.20	5265	553	29.4	0.857

**Table 4.3** Results for protected structure for fire resistance time  $R = 60$  min. Optimum is marked by bold letters.  $K$  is the cost according to Eq. (4.51) without the cost of protection. The result in the last row does not fulfil the local buckling constraint.

$b$ mm	$t$ mm	$10^{-3}A$	$K$ \$	$10^{-7}N_{fi,T}$ [N]	$b/t$
630	20	50.40	3385	1.012	31.5
<b>660</b>	<b>19</b>	<b>50.16</b>	<b>3357</b>	<b>1.014</b>	<b>34.7</b>
700	18	50.40	3361	1.028	38.9
720	17	48.96	3271	1.003	42.4

#### 4.2.3.6 Cost Including Protection

The following approximate cost data are from Hungarian industry.

##### (a) Intumescent paint “Polylack”

Cost factor  $k_{p1} = 60$  \$/m<sup>2</sup>, superficies :  $S = 4 \times 0.66 \times 6 = 15.84$  m<sup>2</sup>

$K_{p1} = k_{p1}S = 950$  \$

$K_1 = K - K_p + K_{p1} = 3357 - 456 + 950 = 3851$  \$

Cost without protection  $K = 5451$  \$, thus, the cost savings is 29%.

##### (b) Fire resistant plasterboard “Rigips” of thickness 12.5 mm

Cost factor  $k_{p2} = 5.0$  \$/m<sup>2</sup>,  $K_{p2} = k_{p2}S = 79.0$  \$, labour cost  $K_L = 70$  \$

$K_2 = 3357 - 456 + 79 + 70 = 3050$  \$

Cost without protection  $K = 5451$  \$, thus, the cost savings is 44%.



#### 4.2.4 A Simply Supported Uniformly Loaded Welded Box Beam

Optimum design of this structure is treated for four cases as follows: unprotected and protected beam with stress or deflection constraint. In Equations the following subscripts are used: unprotected stress constraint  $\sigma$ , unprotected deflection constraint  $w$ , protected stress constraint  $\sigma_1$ , protected deflection constraint  $w_1$ .

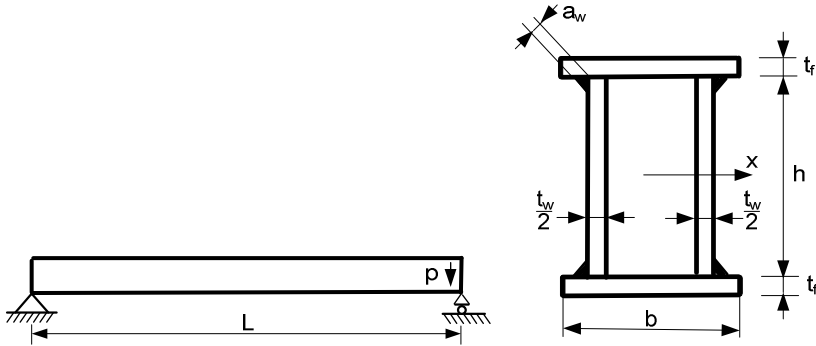


Fig. 4.4 A simply supported welded box beam

##### 4.2.4.1 Optimum Design

It is sufficient to solve the optimization problem for minimum cross-section area instead of minimum cost, since the welding cost of four longitudinal fillet welds does not have significant effect on the optimum beam dimensions.

The formulation of the optimum design of a box beam is as follows: find the optimum values of the dimensions  $h$ ,  $t_w$ ,  $b$ ,  $t_f$  to minimize the whole cross-section area  $A$ . As it is derived in Section 4.1.2 one obtains the optimum value of  $h$  from the stress constraint.

$$h_{\sigma} = \sqrt[3]{\frac{3W_0}{4\beta}} \quad (4.55)$$

In fire conditions the constraint on local buckling of webs

$$\frac{h}{t_w/2} \leq \frac{1}{\beta}; \text{ or } t_w \geq 2\beta h \quad (4.56)$$

where

$$1/\beta = 69\varepsilon; 1/\beta_{fi} = 69\varepsilon\alpha_{fi}, \varepsilon = \sqrt{\frac{235}{f_y}} \quad (4.57)$$

For unprotected beam  $\alpha_{fi} = 0.6$ , for protected one  $\alpha_{fi} = 1$ .

The constraint for local buckling of compressed upper flange

$$\frac{b}{t_f} \leq \frac{1}{\delta} = 42\varepsilon, \frac{1}{\delta_{fi}} = 42\varepsilon\alpha_{fi}, \quad \alpha_{fi} = 0.6 \quad \text{or} \quad t_f \geq \delta b \quad (4.58)$$

The deflection constraint

$$w_{\max} = \frac{C_w}{I} \leq w_{adm} = \frac{L}{\phi}; \quad C_w = \frac{5p_d L^4}{384E}; \quad \phi = 300 \quad (4.59)$$

or

$$I \geq I_0 = \frac{5p_w L^4}{384Ew_{adm}}$$

**Table 4.4** Characteristics of optimum box sections

Stress constraint	Deflection constraint
$h_\sigma = \sqrt[3]{0.75W_0 / \beta}$	$h_w = \sqrt[4]{3I_0 / \beta}$
$t_{w\sigma} / 2 = \beta h_\sigma$	$t_{ww} / 2 = \beta h_w$
$A_\sigma = 4\beta h_\sigma^2 = \sqrt[3]{36\beta W_0^2}$	$A_w = 8\beta h_w^2 / 3 = \sqrt[4]{64\beta I_0 / 3}$
$b_\sigma = h_\sigma \sqrt{\beta / \delta}$	$b_w = h_w \sqrt{\beta / (3\delta)}$
$t_{f\sigma} = \delta b_\sigma$	$t_{fw} = \delta b_w$
$I_{x\sigma} = 2\beta h_\sigma^4 / 3$	$I_{xw} = \beta h_w^4 / 3$
$W_{x\sigma} = 4\beta h_\sigma^3$	$W_{xw} = 2\beta h_w^3 / 3$

From deflection constraint

$$h_w = \sqrt[4]{\frac{3I_0}{\beta}}; I_0 = \frac{\phi C_w}{L} \quad (4.60)$$

The advantage of this optimization method is that the other characteristics of the optimum cross-section can be expressed by  $h_\sigma$  or  $h_w$ . These characteristics are summarized in Table 4.4.

*Numerical data*

$$p = 90 \text{ N/mm}, \quad L = 15 \text{ m}, \quad f_y = 235 \text{ MPa}, \quad f_{yI} = f_y / 1.1 = 213.6 \text{ MPa}.$$

#### 4.2.4.2 Optimum Design of Unprotected Beam with Stress Constraint

Factored load in ambient temperature

$$p_\sigma = 1.5p + 1.1\rho_1 A_\sigma \quad (4.61)$$

Factored load in fire

$$p_{\sigma fi} = 1.5p + 1.1\rho_1 A_{\sigma fi}; A_{\sigma fi} = 4\beta_{fi} h_{\sigma}^2 \quad (4.62)$$

Bending moment for fire

$$M_{fi} = p_{\sigma fi} L^2 / 8 \quad (4.63)$$

Bending moment capacity in ambient temperature

$$M_0 = W_{x\sigma} f_{y1} \quad (4.64)$$

The utilization factor

$$\mu_0 = \frac{M_{fi}}{M_0} \quad (4.65)$$

The ratio of perimeter/cross-section area for a box beam

$$\frac{A_m}{V} = \frac{2(h_{\sigma} + b_{\sigma})}{A_{\sigma}} = \frac{1 + \sqrt{\frac{\beta}{\delta}}}{2\beta_{fi} h_{\sigma}} = \frac{61.41\epsilon\alpha_{fi}}{h_{\sigma}} \quad (4.66)$$

The search for the optimum  $h_{\sigma}$  is performed according to section 4.2.2 using the critical temperature method. The result for fire resistance time  $R = 30$  min is  $h_{\sigma} = 1230$  mm. The other data for the beam are given in Table 4.5.

The maximum stress

$$\sigma_{\max \sigma} = \frac{M_{fi}}{W_{x\sigma}} \quad (4.67)$$

The maximum deflection

$$w_{\max \sigma} = \frac{5p_{\sigma fi} L^4}{384k_{E\Theta} EI_{x\sigma}} \quad (4.68)$$

where  $k_{E\Theta}$  is calculated according to Eq. (4.47),

$$p_{\sigma fi} = p + \rho_1 A_{\sigma} \quad (4.69)$$

For the cost calculation Eqs. (4.51)-(4.54) are used with the following changes:

$$V_{\sigma} = A_{\sigma} L; S_{\sigma} = 2L(h_{\sigma} + b_{\sigma}), \quad a_{w\sigma} = 0.3 \frac{t_{w\sigma}}{2} \quad (4.70)$$

The costs are calculated similar to Eqs. (4.51, 4.52, 4.53) with the following differences:

$$K_m = k_m \rho V_{\sigma}, \quad K_p = k_p S_{\sigma} \quad (4.71)$$

#### 4.2.4.3 Optimum Design of the Protected Beam with Stress Constraint

The optimization is performed using Table 4.4. thus, subscripts of  $\sigma l$  are used. The optimum height of the beam is  $h_{\sigma l} = 990$  mm.

$$\sigma_{\max \sigma l} = \frac{p_{\sigma l} L^2}{8W_{x\sigma l}}; p_{\sigma l} = 1.5p + 1.1\rho_1 A_{\sigma l} \quad (4.72)$$

$$w_{\max \sigma l} = \frac{5p_{w\sigma l} L^4}{384EI_{x\sigma l}}; p_{w\sigma l} = p + \rho_1 A_{\sigma l} \quad (4.73)$$

The costs are calculated similar to section 4.2.3.6.

It should be mentioned that the self mass of the protection can be neglected. (The specific mass of plasterboard protection Rigips of thickness 12.5 mm is 10.5 kg/m<sup>2</sup>, and that of an intumescent painting of thickness 2 mm is 3.5 kg/m<sup>2</sup>.)

The results are given in Table 4.5.

Results in Table 4.5 show that the protected beam is much more cheaper than the unprotected one. The protection with plasterboard Rigips is cheaper than the Polyack painting.

#### 4.2.4.4 Optimum Design of Unprotected Beam with Deflection Constraint

Formulae in the right side column of Table 4.4 with subscript  $w$  are used. Eqs. (4.61)-(4.64) are used with subscript  $w$  instead of  $\sigma$ . Eq. (4.65) is changed to

**Table 4.5** Results for unprotected and protected beams with stress constraint. Dimensions in mm, stresses in MPa, costs in \$.

Unprotected	Protected
$h_{\sigma} = 1230$	$h_{\sigma l} = 990$
$b_{\sigma} = 960$	$b_{\sigma l} = 775$
$t_{w\sigma} = 60$	$t_{w\sigma l} = 30$
$t_{f\sigma} = 38$	$t_{f\sigma l} = 19$
$\sigma_{\max \sigma} = 69$	$\sigma_{\max \sigma l} = 202$
$w_{\max \sigma} = 22$	$w_{\max \sigma l} = 31$
$K_m = 17280$	$K_{ml} = 6965$
$K_w = 2670$	$K_{wl} = 870$
$K_p = 1892$	$K_{pro} = 3177, K_{pro l} = 476$
$K = 21840$	$K_l = 11010, K_2 = 8311$

$$\mu_0 = \frac{p_{wfi}}{p_w} = \frac{E_{fi} I_{0fi}}{EI_0} = \frac{k_{E\Theta} (600^0)}{\beta_1} = \frac{0.31}{0.6} = 0.517 \quad (4.74)$$

Eq. (4.66) is changed to

$$\frac{A_m}{V} = \frac{2(h_w + b_w)}{A_w} = \frac{3 \left( 1 + \sqrt{\frac{\beta}{3\delta}} \right)}{\beta h_w} = \frac{75.06 \varepsilon \alpha_{fi}}{h_w} \quad (4.75)$$

The critical temperature according to Eq. (4.25) is  $579^{\circ}\text{C}$ .

The optimum design procedure according to section 4.2.2 for fire resistant time  $R = 30$  min results in  $h_{wopt} = 1500$  mm.

In Eqs. (4.67)-(4.71) the subscripts  $F$  are changed to  $w$ .

The optimum beam dimensions and characteristics are summarized in Table 4.6.

#### 4.2.4.5 Optimum Design of the Protected Beam with Deflection Constraint

The optimization is performed using Table 4.4. Thus, subscripts  $wI$  are used. The optimum height of the beam is  $h_{wI} = 1050$  mm. In Eqs. (4.72) and (4.73) subscripts  $FI$  are changed to  $wI$ .

Results are given in Table 4.6.

**Table 4.6** Results for unprotected and protected beams with deflection constraint. Dimensions in mm, stresses in MPa, costs in \$.

Unprotected	Protected
$h_w = 1500$	$h_{wI} = 1050$
$b_w = 680$	$b_{wI} = 475$
$t_{ww} = 74$	$t_{wwI} = 32$
$t_{fw} = 27$	$t_{fwI} = 19$
$\sigma_{maxw} = 75$	$\sigma_{maxwI} = 255$
$w_{maxw} = 21$	$w_{maxwI} = 37$
$K_m = 17390$	
$K_w = 3789$	
$K_p = 1884$	
$K = 23070$	

It can be seen that the protected beam does not fulfil the stress constraint ( $255 > 213$  MPa), thus the costs are not calculated for this case.

Comparison of Tables 4.5 and 4.6 shows that the deflection constraint results in a more expensive beam than that with the stress constraint.

### 4.2.5 Conclusions

A compressed rod of welded square box cross-section is designed for overall and local buckling. In the case of a simply supported beam of welded box section loaded by bending and shear the stress, deflection and local buckling constraints are considered.

In the optimization procedure the systematic search method is used with MathCAD program. In the case of bent box beam the optimum dimensions are derived by an analytical method.

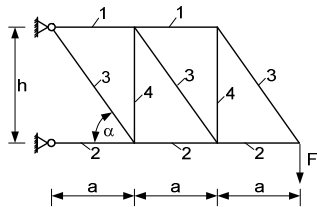
The cost function contents the cost of material, assembly, painting and fire protection. Two types of protection are considered: intumescent painting Polylock and plasterboard Rigips.

The fire resistance time is 30 min for unprotected and 60 min for protected structures. The critical temperature method is suitable for the design using formulae given by Eurocode 3.

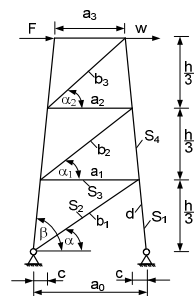
In the case of bent beam the structure for stress constraint is cheaper than that for deflection constraint.

In both structures the protected ones are much more cheaper than the unprotected ones. This difference is caused by the significant difference of section thicknesses.

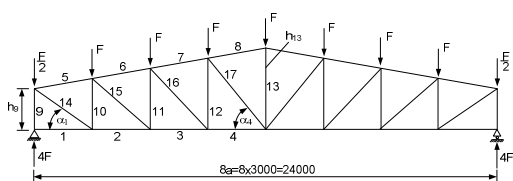
# Chapter 5 Tubular Trusses



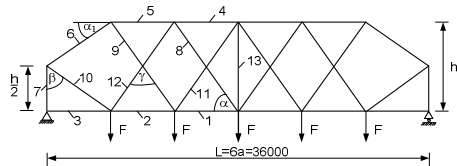
Section 5.2



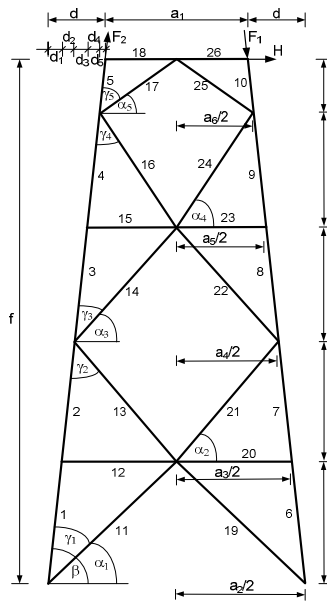
Section 5.3



Section 5.4



Section 5.5



Section 5.6

## 5.1 Survey of Selected Literature

In order to illustrate the literature of the optimum design of trusses, the characteristics of some articles are summarized in Table 5.1.

**Table 5.1** Literature survey of selected journal articles about the optimization of trusses

Author	Examples	Math. method	Material	Buckling calculation	Cross-section	Constraint
Gil (2001)	non-parallel chords	conjugates gradient	steel	EC3		stress and geometric
Tong (2001)	10-,25-bar	combinatorial	alum.			stress and frequency
Makris (2002)	3-,10-,25-, 60-and 132-bar	strain-energy-density	alum.	No buckling		displacement
Hasancebi (2002)	224-bar 3D pyramid, simply supported	simulated annealing	steel	AISC	CHS, W-section	layout optimization
Kripakaran (2007)	10-,18-, 21-bar	new algorithm	steel, alum.	AASHTO Euler	CHS	minimum Cost
Lamberti (2008)	18-bar cantilever, 25-bar 3D, 45-72-and 200-bar	simulated annealing	steel, alum.	Euler		stress, nodal displacement
Silih (2008)	non-parallel chords	MINLP	Steel	EC3	CHS	minimum mass or cost
Kaveh (2009)	10-,25-,120-200-, and 244-bar Tower	PSO, ACO, HS	steel, alum.	AISC		stress, nodal displacements
Jármai (2004)	Simply supported, parallel chords, 5, 8 spacing	Leap-frog, dynamic-Q	Steel	EC3	CHS	optimum height, effect of loads, min. volume

*Abbreviations:* AISC American Institute of Steel Construction, CHS Circular Hollow Section, AASHTO American Assoc. of State and Highway Transportation Officials, EC3 Eurocode 3 (EN 1993-1-1: 1992), W – American wide flange beam, PSO particle swarm optimizer, ACO ant colony strategy, HS harmony search, MINLP mixed-integer nonlinear programming, alum – aluminium.

*Remarks:*

- (1) In trusses the compression members should be designed against overall buckling. The use of Euler-formula gives unsafe design, since it does not take into account the effect of initial imperfections and residual stresses. Therefore buckling formulae of Eurocode 3 or another up-to-date improved buckling formulae should be used.
- (2) The type of the investigated cross section should be given, since it has been shown (Farkas and Jármai 1997) that the cross-sectional form affects the optima significantly.



## 5.2 Comparison of Minimum Volume and Minimum Cost Design of a Welded Tubular Truss

### Abstract

The present study shows the difference between structures optimized for minimum volume and minimum cost. The cost function contains the cost of material, assembly, welding and painting. A cantilever tubular truss with parallel chords is investigated. The compression rods are designed against overall buckling so that the required cross-sectional areas are calculated with approximate closed formulae. In the cost function also the cost of cutting and edge grinding of the circular hollow section rod ends is included. The heights of the truss corresponding to minimum volume and cost are different, but the cost difference between the two optima is not high.

### 5.2.1 Introduction

In structural optimization researchers use volume as objective function. In order to design economic and competitive structures a cost function should be formulated and minimized. The cost function contains the cost of material, assembly, welding and painting. This function contains the main structural parameters to be optimized as the main cross-sectional dimensions as well as dimension and length of welds. Since the welding cost is proportional to the square of weld size, this size should be minimized to achieve economic structures.

The N-type planar truss (Fig. 5.1) is welded from circular hollow section (CHS) rods. Four different CHS profiles are applied for upper and lower chord, for diagonal and vertical braces. The rods are welded together by fillet welds without gusset plates. The constraint of overall and local buckling of compression rods as well as the stress constraint for tension rods are considered.

In cost function the material, cutting and grinding of rod ends, assembly, welding and painting cost is considered. To find the optima the truss height is varied stepwise and a MathCAD algorithm is used to calculate the corresponding values.

A numerical problem shows that the rod profiles are different for minimum volume and minimum cost, but the cost difference between the two optima is small.

### 5.2.2 Minimum Volume Design

The rods of the cantilever truss of parallel chords (Fig.5.1) are divided to four groups of the same cross-section area:

Group 1: Tension rods of the upper chord in which the maximum rod force is

$$S_1 = 2aF / h \quad (5.1)$$

with a required cross-sectional parameters

$$A_1 = S_1 / f_{y1}, f_{y1} = f_y / 1.1, D_1 = \sqrt{A_1 \delta / \pi}, t_1 = D_1 / \delta \quad (5.2)$$

$f_y$  is the steel yield stress,  $\delta = D/t$  is the circular hollow section slenderness, we use here the limiting slenderness of  $\delta = 50$ , prescribed by Wardenier et al. (1991). Note that the available profiles have generally smaller slenderness.

Group 2: Compression rods of the lower chord in which the maximum force is

$$S_2 = 2aF / h \quad (5.3)$$

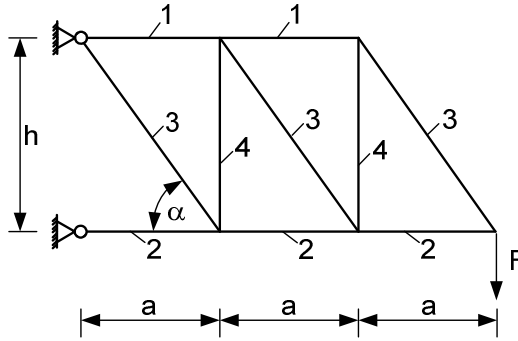


**Fig. 5.1** A cantilever truss of parallel chords

These rods should be designed against overall buckling. The required cross-sectional area cannot be expressed explicitly using the complicate verification formula of Eurocode 3 (2002), therefore we use here the approximate formulae of the Japan Railroad Association (Hasegawa and Abo 1985)

$$\frac{S}{A} \leq \chi f_{y1} \quad (5.4)$$

$$\chi = 1 \quad \text{for} \quad \bar{\lambda} \leq 0.2 \quad (5.5a)$$

$$\chi = 1.109 - 0.545 \bar{\lambda} \quad \text{for} \quad 0.2 \leq \bar{\lambda} \leq 1 \quad (5.5b)$$

$$\chi = \frac{1}{0.773 + \bar{\lambda}^2} \quad \text{for} \quad \bar{\lambda} \geq 1 \quad (5.5c)$$

$$\bar{\lambda} = \frac{\lambda}{\lambda_E}, \lambda = \frac{kL}{r}, r = \sqrt{\frac{I_x}{A}}, \lambda_E = \pi \sqrt{\frac{E}{f_y}} \quad (5.6)$$

For rods of circular hollow section (CHS) with a symbol of  $\delta = D/t$

$$A = \frac{\pi D^2}{\delta}, I_x = \frac{\pi D^4}{8\delta} \quad (5.7)$$

In order to design rods of CHS we introduce notations

$$\vartheta = \frac{100D}{L}, c = \frac{100k\sqrt{8}}{\lambda_E}, \nu = \frac{10^4 S \delta}{L^2 \pi f_{y1}} \quad (5.8)$$

with these notations

$$\bar{\lambda} = \frac{c}{\vartheta} \quad (5.9)$$

and one obtains closed formulae

for  $0.2\vartheta \leq c \leq \vartheta$

$$\vartheta = 0.24572c \left( 1 + \sqrt{1 + \frac{14.93475\nu}{c^2}} \right) \quad (5.10a)$$

for  $\vartheta \leq c$

$$\vartheta = \left[ 0.3865\nu \left( 1 + \sqrt{1 + \frac{6.69424c^2}{\nu}} \right) \right]^{1/2} \quad (5.10b)$$

Knowing  $\vartheta$  the cross-sectional parameters are

$$D = \frac{\vartheta L}{100}, t = \frac{D}{\delta}, A = \frac{\pi D^2}{\delta} \quad (5.11)$$

For the rods of group 2

$$k = 0.9, L = a, \delta = 50, S = S_2. \quad (5.12)$$

$k$  is the effective buckling length factor, according to Rondal et al. (1992) for chords 0.9 and for bracings 0.75,  $L$  is the rod length between joints.

Group 3: tension braces with rod force of

$$S_3 = F \sqrt{\left(\frac{a}{h}\right)^2 + 1} \quad (5.13)$$

and cross-sectional area

$$A_3 = \frac{S_3}{f_{y1}}, D_3 = \sqrt{\frac{A_3 \delta}{\pi}}, t_3 = \frac{D_3}{\delta} \quad (5.14)$$

Group 4: compression braces with rod force of

$$S_4 = F, \quad (5.15)$$

$$k = 0.75, L = h, \delta = 50, S = S_4 \quad (5.16)$$

The structural volume of the truss is given by

$$V = 2aA_1 + 3aA_2 + 3A_3 \sqrt{a^2 + h^2} + 2hA_4 \quad (5.17)$$

Using this formula one can optimize the truss height  $h$  for minimum volume.

### 5.2.3 Minimum Cost Design

The cost function contents material, cutting and grinding of CHS rod ends, assembly and welding as well as painting cost.

The material cost is defined by

$$K_M = k_M \rho V, k_M = 1.0 \text{ \$/kg} \quad (5.18)$$

The cost of cutting and edge grinding of CHS rod ends (Farkas and Jármai 2003, 2008)

$$K_{CG} (\$) = \frac{2.5\pi D}{(350 - 2t)0.3 \sin \alpha} \quad (5.19)$$

where 350mm/min is the cutting speed, 0.3 is the efficiency factor,  $D$  and  $t$  are in mm,  $\alpha$  is the inclination angle of diagonal braces, in our case

$$\sin \alpha = \frac{h}{\sqrt{a^2 + h^2}} \quad (5.20)$$

In the case of our truss

$$K_{CG} = \Theta_{CG} 2.5\pi \left[ \frac{4D_4}{(350 - 2t_4)0.3} + \frac{6D_3}{(350 - 2t_3)0.3 \sin \alpha} \right], \Theta_{CG} = 3 \quad (5.21)$$

The general formula for the welding cost is as follows

$$K_w = k_w \left( C_l \Theta \sqrt{\kappa \rho V} + 1.3 \sum_i C_{wi} a_{wi}^n C_{pi} L_{wi} \right) \quad (5.22)$$

where  $k_w$  [\$/min] is the welding cost factor,  $C_l$  is the factor for the assembly usually taken as  $C_l = 1 \text{ min/kg}^{0.5}$ ,  $\Theta$  is the factor expressing the complexity of assembly, the first member calculates the time of the assembly,  $\kappa$  is the number of structural parts to be assembled,  $\rho V$  is the mass of the assembled structure, the second member estimates the time of welding,  $C_w$  and  $n$  are the constants given for the specified welding technology and weld type.

Furthermore  $C_{pi}$  is the factor for the welding position (download 1, vertical 2, overhead 3),  $L_w$  is the weld length, the multiplier 1.3 takes into account the additional welding times (deslagging, chipping, changing the electrode).

The cost of assembly and welding using SMAW (shielded metal arc welding) fillet welds is given according to Eq. (5.22) by

$$K_w = k_w \left[ \Theta \sqrt{\kappa \rho V} + 1.3 \times 0.7889 \times 10^{-3} \left( 4\pi D_4 t_4^2 + \frac{6\pi D_3 t_3^2}{\sin \alpha} \right) \right] \quad (5.23)$$

$$k_w = 1.0 \text{ $/min}, \quad \kappa = 7.$$

The cost of painting is calculated as

$$K_p = k_p S_p, k_p = 28.8 \times 10^{-6} \quad (5.24)$$

The superficies to be painted is

$$S_p = 2a\pi D_1 + 3a\pi D_2 + 2h\pi D_4 + 3\pi D_3 \sqrt{a^2 + h^2} \quad (5.25)$$

The total cost is given by

$$K = K_M + K_{CG} + K_w + K_p \quad (5.26)$$

### 5.2.4 Numerical Data and Results

$$F = 600 \text{ kN}, a = 5000, f_y = 355 \text{ MPa}, E = 2.1 \times 10^5 \text{ MPa}.$$

In order to find the optimum  $h$  for minimum volume and minimum cost,  $h$  is changed stepwise and for each  $h$  the required diameters and thicknesses as well as the volume and cost are calculated using a MathCAD algorithm. The calculation results are given in Table 5.2.

**Table 5.2** Volume and costs in function of  $h$ . The optima are marked by bold letters. Dimensions in mm, volume in  $\text{mm}^3$  and costs in \$.

$h$	$D_1 \times t_1$	$D_2 \times t_2$	$D_3 \times t_3$	$D_4 \times t_4$	$V$	$K_{CG}$	$K_W$	$K_P$	$K$
8500	187x3.7	262x5.2	185x3.5	231x4.6	2075	441	509	1376	3956
8000	192x3.8	268x5.4	185x3.7	227x4.6	2049	437	512	1345	3903
7500	198x4.0	275x5.5	189x3.8	222x4.4	2034	436	517	1317	3866
<b>7000</b>	<b>206x4.1</b>	<b>283x5.7</b>	<b>191x3.8</b>	<b>218x4.4</b>	<b>2031</b>	436	523	1292	3845
<b>6500</b>	<b>213x4.3</b>	<b>292x5.8</b>	<b>193x3.7</b>	<b>214x4.3</b>	2042	<b>438</b>	<b>532</b>	<b>1271</b>	<b>3844</b>
6000	222x4.4	302x6.0	196x3.9	209x4.2	2069	443	544	1255	3867
5500	232x4.6	314x6.3	200x4.0	205x4.1	2117	451	561	1243	3918

It should be mentioned that the CHS dimensions are not fabricated (available) profiles, we have not used them, since it is impossible to show the difference between optima with available profiles. It can be seen that the truss height is different for minimum volume and minimum cost, but the difference between the corresponding costs is very small. Thus, the minimum volume design can be used with a good approximation.

### 5.2.5 Conclusions

In order to show the difference between the minimum volume and minimum cost designs a simple structure is optimized for both minima. The results show that the structural dimensions are different, but the difference in corresponding costs is small.

It should be mentioned that the difference in costs depends on the amount of fabrication cost. In our two cases this amount is not very large, but in more complicated structures it can be larger.

## 5.3 Optimum Design of Tubular Trusses for Displacement Constraint

### Abstract

The developed method is applied to truss columns of parallel and non-parallel chords. The cantilever columns are loaded on the top by a horizontal concentrated force and the horizontal displacement of the top is limited. In the case of the parallel-chord-truss the distance of the chords is optimized. In the case of non-parallel chords the slope angle of chords is optimized for minimum structural volume. The comparison of the two optimized trusses shows that the truss with non-parallel chords has smaller volume.

### 5.3.1 Introduction

Using formulae for volume and for displacement of a truss structure a method is worked out to calculate the optimum circular hollow sections (CHS) and the optimum geometry of a truss. These cross-sections are larger than those required to prevent overall buckling of rods. The cross section of compressed rods are optimized for overall buckling using the formulae of Eurocode 3 and a special Mathcad algorithm.

The developed method is applied to truss columns of parallel and non-parallel chords. The cantilever columns are loaded on the top by a horizontal concentrated force and the horizontal displacement of the top is limited. In the case of the parallel-chord-truss the distance of the chords is optimized. In the case of non-parallel chords the slope angle of chords is optimized for minimum structural volume. The comparison of the two optimized trusses shows that the truss with non-parallel chords has smaller volume.

Tubular trusses should fulfil in several cases not only the overall buckling constraints but also displacement prescriptions. In the present study it is shown that, in the case of a strict displacement constraint the required cross-sectional areas and the truss geometry can be optimized. The objective function is the structural volume, but later it is possible to consider also the cost function.

### 5.3.2 The Displacement Constraint

The displacement constraint is formulated as

$$w = \sum \frac{S_i s_i L_i}{EA_i} \leq w_0 \quad (5.27)$$

where  $E$  is the elastic modulus,  $S_i$  is the force acting in a rod,  $s_i$  is the rod force for  $F = 1$ ,  $L_i$  is the rod length,  $A_i$  is the cross-sectional area,  $w_0$  is the allowable displacement.

### 5.3.3 Design for Overall Buckling

The used method is given in Section 5.2.2 Eqs. (5.4 – 5.11).

In the case of very long struts with small compressive force, the limitation of the strut slenderness can be governing. From the limitation of

$$\lambda = KL / r \leq \lambda_{\max} \quad (5.28)$$

the required radius of gyration is

$$r \geq KL / \lambda_{\max} . \quad (5.29)$$

According to BS 5400 (1982)  $\lambda_{\max} = 180$ .

### 5.3.4 A Truss Column with Parallel Chords (Fig. 5.2)

The numbers show that only three different cross-sectional areas are considered for only three different rod forces. In the calculation these three cross-sectional areas are taken into account with different multipliers as

$$A_i = \mu_i A \quad (5.30)$$

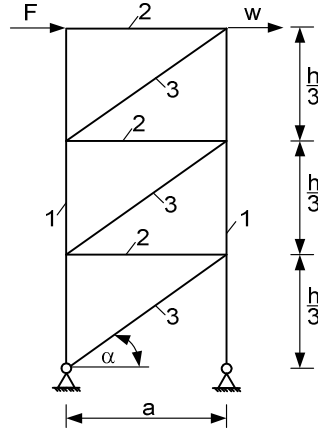


**Fig. 5.2** A tubular truss with parallel chords

so the displacement constraint is given by

$$w = \frac{1}{EA} \sum_i \frac{S_i s_i L_i}{\mu_i} \leq w_0 \quad (5.31)$$

from which one obtains

$$A \geq \frac{1}{E w_0} \sum_i \frac{S_i s_i L_i}{\mu_i} \quad (5.32)$$

The structural volume is calculated as

$$V = \sum_i A_i L_i = \frac{1}{E w_0} \sum_i \frac{S_i s_i L_i}{\mu_i} \sum_i \mu_i L_i \quad (5.33)$$

Using a notation

$$\omega = \tan \alpha = \frac{h}{3a} \quad (5.34)$$

the rod forces are

$$S_1 = 3F\omega, S_2 = F, S_3 = F\sqrt{\omega^2 + 1} \quad (5.35)$$



and the rod lengths are

$$L_1 = \frac{h}{3}, L_2 = \frac{h}{3\omega}, L_3 = \frac{h}{3\omega} \sqrt{\omega^2 + 1} \quad (5.36)$$

Using these formulae one obtains

$$w = \frac{Fh v_2}{EA}, A = \frac{Fh v_2}{E w_0}, V = A h v_1 = \frac{F h^2 v_1 v_2}{E w_0} \quad (5.37)$$

where

$$v_1 = 2\mu_1 + \frac{\mu_2}{\omega} + \frac{\mu_3}{\omega} \sqrt{\omega^2 + 1} \quad (5.38)$$

and

$$v_2 = \frac{2\omega^2}{\mu_1} + \frac{1}{\mu_2 \omega} + \frac{(\omega^2 + 1)^{3/2}}{\mu_3 \omega} \quad (5.39)$$

In the optimum design  $\omega_{opt}$  is sought, which minimizes the structural volume or the value of

$$V_I = v_1 v_2. \quad (5.40)$$

The values of  $\mu_i$  are selected as  $\mu_1 = 1, \mu_2 = \mu_3 = 0.8$  taking into account the fabrication of tubular joints. With these values the search results in

$$\omega_{opt} = 0.85, \alpha = 40^\circ \quad (5.41)$$

The details of the systematic search are given in Table 5.3.

**Table 5.3** Details of the systematic search

$\omega$	$V_I = v_1 v_2$
0.70	28.289
0.75	26.606
0.80	26.215.
<b>0.85</b>	<b>26.061</b>
0.90	26.106
0.95	26.318
1.00	26.676

#### *Numerical example*

$F = 100000$  N,  $h = 12000$ ,  $f_y = 355$  MPa,  $E = 2.1 \times 10^5$  MPa,  $w_0 = 12$  mm.  
 $A_1 = 2971$ ,  $A_2 = A_3 = 2377$  mm<sup>2</sup>.

It should be noted that another values of  $\mu_2$  and  $\mu_3$  give larger values of  $V_I$ .

The rod forces for the displacement constraint ( $S_i$ ) and for overall buckling constraint ( $1.5S_i$ ), lengths ( $L_i$ ), factors of the buckling length ( $K$ ), the required CHS profiles and their cross-sectional areas are given in Table 5.4.

**Table 5.4** Data for the optimal truss with parallel chords

Forces	$S_i$ [kN]	$L_i$ [mm]	$K$	CHS	$A$ [mm <sup>2</sup> ]	$r$ [mm]
$S_1$	255.0	--	--	163.3x6	3060	57.4
$1.5S_1$	382.5	4000	0.9	139.7x5	2120	47.7
$S_2$	100.0	--	--	139.7x6	2520	47.3
$1.5S_2$	150.0	4706	0.75	101.6x3.6	1110	34.7
$S_3$	131.2	--	--	139.7x6	2520	47.3
$1.5S_3$	196.8	6176	0.75	114.3x5	1720	38.7

It can be seen that for all rods  $A(\text{displacement}) > A(\text{buckling})$ . The actual structural volume for the optimal truss is  $V = 1.557 \times 10^8 \text{ mm}^3$ . The values of  $r$  show that the profiles for displacement constraint fulfil the overall buckling constraint as well.

### 5.3.5 A Truss Column with Non-parallel Chords (Fig. 5.3)

In order to show the savings in structural volume obtainable by using non-parallel chords instead of parallel ones, a tubular truss column with non-parallel chords is investigated. The column height, the horizontal force and the allowable horizontal displacement are the same as in Section 5.3.4.

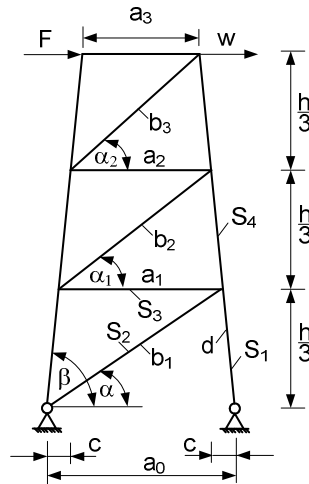


**Fig. 5.3** A tubular truss with non-parallel chords

Introducing notations

$$\omega = \tan \alpha, \vartheta = \tan \beta \quad (5.42)$$

the geometric data of the truss are as follows:

$$c = \frac{h}{3\vartheta}, a_0 = a_3 + 6c, a_1 = a_3 + 4c, a_2 = a_3 + 2c \quad (5.43)$$

Since in the systematic search the values of  $a_3$  and  $\omega$  are varied, all data are given in function of these variables.

$$\omega = \frac{h}{3(a_0 - c)} = \frac{h}{3(a_3 + 5c)} \quad (5.44)$$

from which

$$\vartheta = \frac{1}{\frac{1}{5\omega} - \frac{3a_3}{5h}} \quad (5.45)$$

$$d = \sqrt{\left(\frac{h}{3}\right)^2 + c^2}, b_1 = \sqrt{\left(\frac{h}{3}\right)^2 + (a_0 - c)^2} \quad (5.46)$$

$$b_2 = \sqrt{\left(\frac{h}{3}\right)^2 + (a_1 - c)^2}, b_3 = \sqrt{\left(\frac{h}{3}\right)^2 + (a_2 - c)^2} \quad (5.47)$$

The rod forces are as follows

$$S_1 = \frac{3Fd}{a_0}, S_4 = \frac{2Fd}{a_1}, S_2 = (S_1 - S_4) \frac{b_1}{d} \quad (5.48)$$

$$S_3 = (S_1 - S_4) \frac{a_0}{d} \quad (5.49)$$

It is supposed that the force in all chords is  $S_I$ , the force in all diagonals is  $S_2$ , the force in the upper horizontal rod is  $F$ , in other horizontals is  $S_3$ .

Similar to the formulae used in Section 5.3.4

$$v_1 = \frac{6\mu_1 d}{h} + \frac{\mu_2(b_1 + b_2 + b_3)}{h} + \frac{\mu_3(a_1 + a_2 + a_3)}{h} \quad (5.50)$$

$$v_2 = \frac{6S_1 s_1 d}{Fh\mu_1} + \frac{S_2 s_2(b_1 + b_2 + b_3)}{Fh\mu_2} + \frac{S_3 s_3(a_1 + a_2)}{Fh\mu_3} + \frac{a_3}{h\mu_3} \quad (5.51)$$

Fabrication constraints are also introduced to guarantee the minimum angle  $30^0$  ( $\tan 30^0 = 0.577$ ) between the rods.

$$\psi = \tan(\beta - \alpha) = \frac{\vartheta - \omega}{1 + \vartheta\omega} \geq 0.577 \quad (5.52)$$

$$\psi_1 = \tan(\beta - \alpha_1) = \frac{\vartheta - \frac{h}{3(a_1 - c)}}{1 + \frac{\vartheta h}{3(a_1 - c)}} \geq 0.577 \quad (5.53)$$

$$\psi_2 = \tan(\beta - \alpha_2) = \frac{\vartheta - \frac{h}{3(a_2 - c)}}{1 + \frac{\vartheta h}{3(a_2 - c)}} \geq 0.577 \quad (5.54)$$

$$\psi_3 = \tan \alpha_1 = \frac{h}{3(a_1 - c)} \geq 0.577 \quad (5.55)$$

$$\psi_4 = \tan \alpha_2 = \frac{h}{3(a_2 - c)} \geq 0.577 \quad (5.56)$$

#### Numerical example

$F = 100000$  N,  $h = 12000$ ,  $f_y = 355$  MPa,  $E = 2.1 \times 10^5$  MPa,  $w_0 = 12$  mm.

In the optimization process the optimum values of  $a_3$  and  $\omega$  are sought which minimize  $V_I = v_I v_2$ . The details of the search are given in Table 5.5.

**Table 5.5** Search details

$a_3$ [mm]	$\omega_{min}$	$V_I = v_I v_2$
3400	0.43	19.238
3300	0.43	18.974
3200	0.42	18.258
<b>3100</b>	<b>0.42</b>	<b>18.015</b>
3000	0.45	19.157
2900	0.48	20.398

$\omega$ -values smaller than  $\omega_{min}$  do not fulfil the constraints of  $\psi_i \geq 0.577$ .

The optimum is given by bold letters.  $\omega = 0.42$  ( $\alpha = 22.8^0$ ),  $\vartheta = 72.2^0$ ,  $a_0 = 10810$  mm.

$A_I = 2311$ ,  $A_2 = A_3 = 1848$  mm<sup>2</sup>.

The rod forces for the displacement constraint ( $S_i$ ) and for overall buckling constraint ( $1.5S_i$ ), lengths ( $L_i$ ), factors of the buckling length ( $K$ ), the required CHS profiles and their cross-sectional areas are given in Table 5.6.

**Table 5.6** Data for the optimal truss with non-parallel chords. \*Prescription for max. slenderness  $\lambda=180$  is governing.

Forces	$S_i$ [kN]	$L_i$ [mm]	$K$	CHS	$A$ [mm <sup>2</sup> ]	$R$ [mm]
$S_I$	119.4	4171	--	168.3x4.5	2320	57.9
$1.5S_I$	179.1	4171	0.9	168.3x4.5	2320	57.9
$S_2$	40.4	10130	--	139.7x4.0	1710*	48.0
$1.5S_2$	60.7	10130	0.75	139.7x4.0	1710*	48.0
$S_3$	41.8	8239	--	114.3x6.0	2040*	38.3
$1.5S_3$	62.8	$a_I=8239$	0.75	101.6x3.6	1110	34.7
$1.5S_3$	150.0	$a_3=3100$	0.75	101.6x3.6	1110	34.7

It can be seen that for all rods  $A(\text{displacement}) \geq A(\text{buckling})$ . The actual structural volume for the optimal truss is  $V = 1.347 \times 10^8 \text{ mm}^3$ .

The comparison of the trusses with parallel and non-parallel chords shows that the structural volume of the truss with non-parallel chords is 12% smaller than that of truss with parallel chords, i.e. the second version is more economic.

## 5.4 Volume and Cost Minimization of a Tubular Truss with Non-parallel Chords in the Case of a Displacement-Constraint

### Abstract

The minimum volume and cost of a simply supported planar truss with N-type bracing is optimized. The lower chord of the truss is horizontal, but the symmetric upper chord parts are non-parallel and their inclination angle as well as the cross-sectional areas of CHS (circular hollow section) rods are optimized. For the calculation of required cross-sectional area of compression struts closed formulae are used as a good approximation of Eurocode 3 buckling curve. A special method is developed for the minimum volume design considering the deflection constraint. In the case of a strong displacement constraint the cross-sectional areas required for the allowed deflection are larger than those required for stress and buckling constraints. The cost function includes the cost of material, cutting and grinding of CHS strut ends, assembly, welding and painting. Special mathematical methods are used to find the optima in the case of a numerical problem.

### 5.4.1 Introduction

The aim of the present study is to show the minimum volume and cost optima of a truss and solve the optimum design problem subject to a strong displacement

constraint. In the case of stress constraints the tension rods are designed for yield stress by using a safety factor for loading and the compression rods are designed for overall buckling. In the case of a strong displacement constraint the required cross-sectional areas are larger than those required for stress constraints.

In the optimum design process of a truss the optimal value of the cross-sectional areas of struts and the geometric characteristics of the truss are sought which minimize an objective function and fulfil the design and fabrication constraints. The objective function can be the volume (weight) or cost, the design constraints are the limitation of stress and displacement, the fabrication constraints ease the manufacturing (welding) process.

In the case of an active displacement constraint a special method is developed to calculate the required cross-sectional areas and the truss geometry.

It is shown that the non-parallel chords are more economic than the beam with parallel chords. Thus, in our case the angle of the upper chord (unknowns  $h_9$  and  $h_{13}$  in Fig. 5.4) is optimized.

Another problem is the grouping of rods having the same cross-sectional area. The design of all the rods having different cross-sectional areas can cause difficulties in fabrication, but the design of all the rods with the same cross-sectional area would be uneconomic. Thus, the economy depends on grouping of rods. In our case four groups are used.

For the minimization of the structural volume or cost, minimization of the cross-sectional areas of rods is needed. The cross-sectional area of compression rods cannot be calculated from the Eurocode 3 buckling formulae. Therefore approximate formulae of Japan Road Association are used. Stress and buckling constraints are calculated using factored forces, whilst the deflection is calculated with forces without a safety factor.

In order to obtain comparable optima the required cross-sectional areas are not rounded to available profiles and the most economic  $\delta = D/t = 50$  slenderness (diameter/thickness) of CHS is used.

The limitation of the angle between CHS struts (minimum  $30^\circ$ ) is taken into account as a fabrication constraint. Another fabrication constraint is that the diameters of the chords should be larger than those of verticals and diagonals of the bracing.

The effect of self mass is neglected in this comparative study.

#### ***5.4.2 Minimum Volume Design of the Tubular Truss with Non-parallel Chords***

Relatively simple formulae can be derived for trusses to minimize the structural volume and fulfil a displacement constraint.

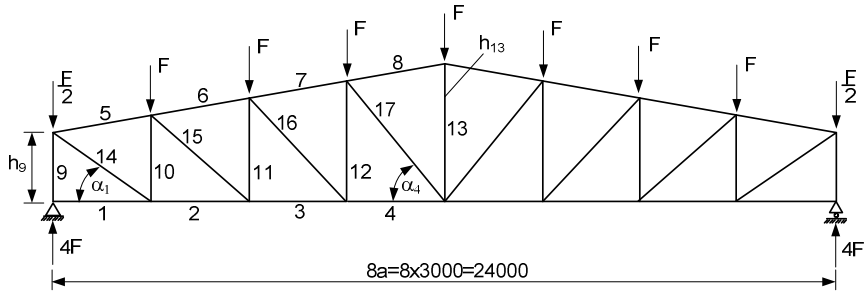


**Fig. 5.4** The simply supported truss with non-parallel chords

The truss rods are divided into  $n$ -groups having the same cross-sectional areas ( $A_i$ ), so

$$A_i = \mu_i A, i = 1 \dots n, \quad (5.57)$$

where  $\mu_i$  are multipliers and the displacement constraint is given by

$$w = \frac{1}{EA} \sum_i \frac{S_i s_i L_i}{\mu_i} \leq w_0, \quad (5.58)$$

where  $E$  is the elastic modulus,  $S_i$  is the rod force,  $s_i$  is the rod force from the unit force acting at the midspan,  $L_i$  is the rod length,  $w_0$  is the admissible deflection.

From Eq. (5.58) one obtains

$$A \geq \frac{1}{E w_0} \sum_i \frac{S_i s_i L_i}{\mu_i}. \quad (5.59)$$

The structural volume is calculated as

$$V = \sum_i A_i L_i = \frac{1}{E w_0} \sum_i \mu_i L_i \sum_i \frac{S_i s_i L_i}{\mu_i} = \frac{v_1 v_2}{E w_0}, \quad (5.60)$$

where

$$v_1 = \sum_i \mu_i L_i, \quad v_2 = \sum_i \frac{S_i s_i L_i}{\mu_i}. \quad (5.61)$$

In the minimum volume design the truss geometry is sought, which minimizes

$$V_1 = v_1 v_2. \quad (5.62)$$

In the case of the simply supported truss shown in Figure 5.4 the spacing is constant, the non-parallel upper chord is determined by variable heights  $h_9$  and  $h_{13}$ . The truss is subject to a set of vertical static forces  $F$  acting on the upper nodes. The displacement of the central lower node is prescribed. It is supposed that all the truss nodes are restrained against transverse deformation.

The variables to be optimized are the heights  $h_9$  and  $h_{13}$  as well as the cross sectional areas of rods ( $A$  and  $\mu_i$ ).

The calculations show that, in the case of a strong displacement constraint the necessary rod cross-sectional areas are so large that the stress constraints on tension and overall buckling are fulfilled. In spite of this fact these constraints should be checked.

To facilitate the welding of nodes for tubular trusses a geometric fabrication constraint should be considered that the minimal angle between rods should be equal or greater than  $30^\circ$ , in our case (Figure 5.4)

$$\tan \alpha_1 = \frac{h_9}{a} \geq \tan 30^\circ, \quad (5.63)$$

from which

$$h_9 \geq a \tan 30^\circ = 1732 \text{ mm}, \quad (5.64)$$

and

$$\tan \alpha_4 \leq 60^\circ = \frac{\pi}{3}. \quad (5.65)$$

In our case these constraints are always active.

**Table 5.7** Characteristics of rods in the lower chord,  $L_i = a$

$i$	$S_i$	$s_i$
1	0	0
	$3.5Fa/h_{10}$	$0.5a/h_{10}$
3	$6Fa/h_{11}$	$a/h_{11}$
4	$7.5Fa/h_{12}$	$1.5a/h_{12}$

The rod forces and lengths ( $S_i$ ,  $s_i$ ,  $L_i$ ) are expressed in function of  $h_9$  and the inclination angle of the upper chords  $\alpha$ .

$$\tan \alpha = \frac{h_{13} - h_9}{4a}, \cos \alpha = \frac{1}{\sqrt{(\tan \alpha)^2 + 1}}, \sin \alpha = \sqrt{1 - (\cos \alpha)^2}. \quad (5.66)$$

The formulae for  $S_i$ ,  $s_i$  and  $L_i$  are given in Tables 5.7, 5.8, 5.9 and 5.10.



**Table 5.8** Characteristics of rods in the upper chord

$i$	$S_i$	$s_i$	$L_i$
5	$\frac{3.5Fa}{h_{10} \cos \alpha}$	$\frac{0.5a}{h_{10} \cos \alpha}$	$\frac{a}{\cos \alpha}$
6	$\frac{6Fa}{h_{11} \cos \alpha}$	$\frac{a}{h_{11} \cos \alpha}$	$\frac{a}{\cos \alpha}$
7	$\frac{7.5Fa}{h_{12} \cos \alpha}$	$\frac{1.5a}{h_{12} \cos \alpha}$	$\frac{a}{\cos \alpha}$
8	$\frac{8Fa}{h_{13} \cos \alpha}$	$\frac{2a}{h_{13} \cos \alpha}$	$\frac{a}{\cos \alpha}$

**Table 5.9** Characteristics of verticals

$i$	$S_i$	$s_i$	$L_i$
9	$4F$	$0.5$	$h_9$
10	$-3.5F + S_5 \sin \alpha$	$-0.5 + s_5 \sin \alpha$	$h_{10} = h_9 + a \tan \alpha$
11	$-2.5F + S_6 \sin \alpha$	$-0.5 + s_6 \sin \alpha$	$h_{11} = h_9 + 2a \tan \alpha$
12	$-1.5F + S_7 \sin \alpha$	$-0.5 + s_7 \sin \alpha$	$h_{12} = h_9 + 3a \tan \alpha$
13	$-F + 2S_8 \sin \alpha$	$2s_8 \sin \alpha$	$h_{13}$

**Table 5.10** Characteristics of diagonals

$i$	$S_i$	$s_i$	$L_i$
14	$S_5 L_{14} \cos \alpha / a$	$s_5 L_{14} \cos \alpha / a$	$\sqrt{h_9^2 + a^2}$
15	$(2.5F - S_6 \sin \alpha) L_{15} / h_{10}$	$(0.5 - s_6 \sin \alpha) L_{15} / h_{10}$	$\sqrt{h_{10}^2 + a^2}$
16	$(1.5F - S_7 \sin \alpha) L_{16} / h_{11}$	$(0.5 - s_7 \sin \alpha) L_{16} / h_{11}$	$\sqrt{h_{11}^2 + a^2}$
17	$(0.5F - S_8 \sin \alpha) L_{17} / h_{12}$	$(0.5 - s_8 \sin \alpha) L_{17} / h_{12}$	$\sqrt{h_{12}^2 + a^2}$

The rods are divided into four groups having the same cross-section): lower chord (1,2,3,4), upper chord (5,6,7,8), verticals (9,10,11,12,13) and diagonals (14,15,16,17).

In order to facilitate the fabrication, the lower and upper chords have the same cross-section ( $\mu_1 = \mu_2 = 1$ ) and the optimal values of  $\mu_3$  (multiplier for verticals) and  $\mu_4$  (multiplier for diagonals) are sought, which should be smaller than  $\mu_1$ .

The components of  $V_1 = v_1 v_2$  to be minimized are as follows.

$$v_1 = 8(a + L_7) + 2\mu_3 \sum_{i=9}^{12} h_i + \mu_3 h_{13} + 2\mu_4 \sum_{i=14}^{17} L_i, \quad (5.67)$$

$$v_2 = 2a \sum_{i=2}^4 S_i s_i + 2L_7 \sum_{i=5}^8 S_i s_i + \frac{2}{\mu_3} \sum_{i=9}^{12} S_i s_i h_i + \frac{S_{13} s_{13} h_{13}}{\mu_3} + \frac{2}{\mu_4} \sum_{i=14}^{17} S_i s_i L_i \quad (5.68)$$

With the optimum values of  $h_9$ ,  $h_{13}$ ,  $\mu_3$  and  $\mu_4$

$$A_1 = A_2 = \frac{v_{2opt}}{Ew_{adm}}, \quad A_3 = \mu_{3opt} A_1, \quad A_4 = \mu_{4opt} A_1 \quad (5.69)$$

The minimum structural volume is

$$V_{min} = v_1 A_1. \quad (5.70)$$

For a circular hollow section (CHS of diameter  $D$  and thickness  $t$ )

$$A = \pi D t = \pi D^2 / \delta, \quad \delta = D / t, \quad (5.71)$$

from which

$$D = \sqrt{\frac{A \delta}{\pi}}, \quad t = \frac{D}{\delta}. \quad (5.72)$$

In the design we should use the maximum value of  $\delta$ , but it is limited to 50 (Wardenier et al. 1991). In the case of available CHS profiles according to (EN 10210-2, 2006)  $\delta$  is varied between 10-50. In order to obtain realistic optima in all cases the optimum  $\delta = 50$  is used.

### 5.4.3 Check of the Compression Rods for Overall Buckling

The used method is described in Section 5.2.2 Eqs. (5.4-5.11) and Eqs. (5.28-5.29).

For the check of overall buckling the following constraint should be fulfilled for all compression rods

$$A_i \geq \frac{\pi D_i}{\delta}, \quad (5.73)$$

where  $A_i$  is the optimum cross-sectional area for displacement constraint and  $D_i$  is the required diameter from overall buckling calculation.

### 5.4.4 The Cost Function

The cost function contains the cost of material, cutting and grinding of CHS strut ends, assembly, welding and painting.

The cost of material is given by

$$K_M = k_M \rho V_2, \quad (5.74)$$

where an average specific cost of  $k_M = 1.0$  \$/kg is considered,  $\rho = 7.85 \times 10^{-6}$  kg/mm<sup>3</sup> for steel.  $V_2$  is the actual structural volume (see Eq. 5.81).

The cost of cutting and grinding of CHS strut ends is calculated with a formula proposed by Glijnis (Farkas & Jármai 2003)

$$K_{CG} (\$) = k_F \Theta_{CG} \frac{2.5\pi D}{(350 - 2t)0.3 \sin \alpha}, \quad (5.75)$$

where  $k_F = 1.0$  \$/min is the specific fabrication cost,  $\Theta_{CG} = 3$  is a factor for work complexity, 350 mm/min is the cutting speed, 0.3 is the efficiency factor, diameter  $D$  and thickness  $t$  are in mm,  $\alpha$  is the inclination angle of diagonal braces.

In our case for verticals

$$K_{CG} = \Theta_{CG} 2.5\pi 9D_3 \frac{1 + \frac{1}{\cos \alpha}}{(350 - 2t_3)0.3}. \quad (5.76)$$

For diagonals at the lower strut ends

$$K_{CG1} = \Theta_{CG} 2.5\pi 2D_4 \frac{\sum_{i=1}^4 \frac{1}{\cos \alpha_i}}{(350 - 2t_4)0.3}, \quad (5.77)$$

where

$$\tan \alpha_1 = h_9 / a, \quad \tan \alpha_2 = h_{10} / a, \quad \tan \alpha_3 = h_{11} / a, \quad \tan \alpha_4 = h_{12} / a \quad (5.78)$$

For diagonals at the upper strut ends

$$K_{CG2} = \Theta_{CG} 2.5\pi 2D_4 \frac{\sum_{i=1}^4 \frac{1}{\cos \beta_i}}{(350 - 2t_4)0.3}, \quad (5.78)$$

where

$$\beta_i = 90^\circ - \alpha - \alpha_i, \quad i = 1, 2, 3, 4. \quad (5.79)$$

For welding costs  $k_w = 1.0$  \$/min,  $\Theta = 3$ .

The cost of assembly and welding using SMAW (shielded metal arc welding) fillet welds is given by for verticals

$$K_W = k_W \left[ \Theta \sqrt{21\rho V_2} + 1.3 \times 0.7889 \times 10^{-3} \times 9\pi D_3 \left( 1 + \frac{1}{\cos \alpha} \right) t_3^2 \right], \quad (5.80)$$

$$V_2 = 8aA_1 + 8L_7A_2 + 2A_3 \sum_{i=9}^{12} h_i + A_3 h_{13} + 2A_4 \sum_{i=14}^{17} L_i. \quad (5.81)$$

For diagonals at the lower strut ends

$$K_{W1} = 1.3 \times 0.7889 \times 10^{-3} \times 2\pi D_4 t_4^2 \sum_{i=1}^4 \frac{1}{\cos \alpha_i}. \quad (5.82)$$

For diagonals at the upper strut ends

$$K_{w1} = 1.3 \times 0.7889 \times 10^{-3} \times 2\pi D_4 t_4^2 \sum_{i=1}^4 \frac{1}{\cos \beta_i}. \quad (5.83)$$

The cost of painting is calculated as

$$K_p = k_p S_p, k_p = 28.8 \times 10^{-6} \text{ \$/mm}^2. \quad (5.84)$$

The superficies to be painted is

$$S_p = 8\pi D_1 + 8L_7\pi D_2 + 2\pi D_3 \sum_{i=9}^{12} h_i + \pi D_3 h_{13} + 2\pi D_4 \sum_{i=14}^{17} L_i. \quad (5.85)$$

The total cost is given by

$$K = K_M + K_{CG} + K_{CG1} + K_{CG2} + K_W + K_{w1} + K_{w2} + K_P. \quad (5.86)$$

### 5.4.5 Numerical Data

Loads for displacement calculation (without safety factor)  $F = 120000$  N, for stress and buckling constraints  $F_0 = 1.5F = 180000$  N (safety factor of 1.5). Yield stress of steel  $f_y = 355$  MPa, elastic modulus  $E = 2.1 \times 10^5$  MPa, span length  $L = 24$  m, allowable displacement at the middle of the span  $w_0 = 32$  mm  $= L/750$ .

### 5.4.6 The Optimization Process

Calculate the optimum values of  $h_9$ ,  $h_{13}$ ,  $\mu_3$  and  $\mu_4$  to obtain  $V_{\min}$  or  $K_{\min}$  and fulfil the constraints on displacement, on minimum angle  $\alpha_1$  [Eq. (5.64)], on maximum angle  $\alpha_4$  [Eq. (5.65)] as well as on stress and overall buckling.

The ranges of unknowns are as follows:  $1732 < h_9 < 5000$  mm,  $4000 < h_{13} < 8000$  mm and  $h_9 < h_{13}$ ,  $0.5 < \mu_3 < 1$ ,  $0.5 < \mu_4 < 1$ .

In the case of minimum volume design Eqs. (5.69) and (5.70) give the results and Eq. (5.73) should be fulfilled. In the case of minimum cost Eq. (5.86) should be minimized, for which Eqs. (5.67), (5.68), (5.69), (5.72) and (5.81) should be used.

### 5.4.7 Results of the Optimization

The fabrication constraints [Eq. (5.63) and (5.64)] determine the optimal pair of unknowns  $h_9$  and  $h_{13}$  as follows: for a given  $h_9$  a value of  $h_{13}$  smaller than  $h_{13\text{opt}}$  gives larger  $v_1 v_2$ , larger does not fulfill the fabrication constraint Eq. (5.64). Table 5.11 shows the max  $h_{13}$  in function of  $h_9$ .

**Table 5.11** Maximum  $h_{13}$  values in function of  $h_9$ . Values in mm.

$h_9$	1750	1850	1950	2000	2100	2200	2300
$h_{13\text{opt}}$	6340	6310	6280	6260	6220	6190	6160

Furthermore the calculations show that the best value for  $\mu_3$  and  $\mu_4$  is 0.6, since the value of 0.5 gives cross-sections which do not fulfill the buckling constraints. Thus, the remaining unknown  $h_9$  can be optimized using the MathCAD program. Table 5.12 gives the volume and cost in function of  $h_9$ . The optimum  $h_9$  minimizes the product  $v_1 v_2$  (fulfilling the deflection constraint) and also  $V$  and  $K$ .

Table 5.12 shows that the following optima are determined: in the case of  $\mu_3 = \mu_4 = 0.6$ ,  $h_{9opt} = 1950$ ,  $h_{13opt} = 6280$ ,  $v_1 v_{2min} = 2.321 \times 10^{15}$ ,  $V_{min} = 3.454 \times 10^8 \text{ mm}^3$ ,  $K_{min} = \$7825$ ,  $A_1 = A_2 = 3708$ ,  $A_3 = A_4 = 2225 \text{ mm}^2$ . Table 5.12 shows that the sensitivity of  $V$  and  $K$  is small.

The cross-sectional areas required for stress and buckling constraints are as follows:  $A_1 = A_2 = 2195$ ,  $A_3 = 2084$ ,  $A_4 = 2094 \text{ mm}^2$ . It can be seen that the cross-sectional areas determined for a strong displacement constraint are larger than those required for stress or buckling constraints.

In addition the calculation results for  $\mu_3 = 0.7$  and  $\mu_4 = 0.5$  are given.

**Table 5.12** Volume and cost in the function of  $h_9$ ,  $h$  in mm. Optima are marked with bold letters.

$h_9$	$h_{13}$	$v_1 v_2 \times 10^{-15}$	$V \times 10^{-8} \text{ mm}^3$	$K \$$
1750	6390	2.331	3.469	7854
1850	6310	2.324	3.459	7830
<b>1950</b>	<b>6280</b>	<b>2.321</b>	<b>3.454</b>	<b>7825</b>
2000	6260	2.322	3.456	7829
2100	6220	2.327	3.463	7843

**Table 5.13** Results in the case of  $\mu_3 = 0.7$  and  $\mu_4 = 0.5$ . Optimum is marked by bold letters.

$h_9$	$h_{13}$	$v_1 v_2 \times 10^{-15}$
1750	6390	2.335
1850	6310	2.329
<b>1950</b>	<b>6280</b>	<b>2.326</b>
2000	6260	2.328
2100	6220	2.334

Another optimum values for  $h_9 = 1950 \text{ mm}$ :  $A_1 = A_2 = 3728$ ,  $A_3 = 2610$ ,  $A_4 = 1864 \text{ mm}^2$ .  $V = 3.462 \times 10^8 \text{ mm}^3$ ,  $K = \$7818$ . Since  $A_4 = 2094 \text{ mm}^2$  is necessary for buckling constraint, the value of  $\mu_4 = 0.5$  is too small and  $\mu_4 = 0.6$  should be used.

For comparison the optimum data for the truss of parallel chords:  $h_{9opt} = h_{13opt} = 5000 \text{ mm}$ ,  $V_{min} = 5.852 \times 10^8 \text{ mm}^3$ .  $K_{min} = \$11350$ . It can be seen that the truss of non-parallel chords is much more economic than the truss of parallel chords.

#### 5.4.8 Check of Strength of a Tubular Joint

After the optimization the optimal cross-sections should be replaced by available profiles according to EN 10291-2 and the joints should be checked for strength according to new IIW rules (Static design 2009). To illustrate this procedure a tubular joint of the truss optimized for strength is shown in Figure 5.5.

The related rod forces are as follows:  $S_3 = 787.4$  kN (tension),  $S_{12} = 11.1$  kN (tension),  $S_{15} = 233.4$  kN (tension), governing for diagonals, also for rod 16, for which  $S_{16} = 13820$  N compression.

The available CHS profiles for the optimized truss are as follows: chords:  $\varnothing 273.0 \times 5$  mm, verticals and diagonals:  $\varnothing 139.7 \times 6$  mm.

According to Figure 5.5 the joint is designed an overlap K-joint, with the eccentricity of  $e = 0.25 \times 273 = 68$  mm, the overlap is  $Ov = 100q/p = 100 \times 34.3/161.6 = 21.2\%$ .

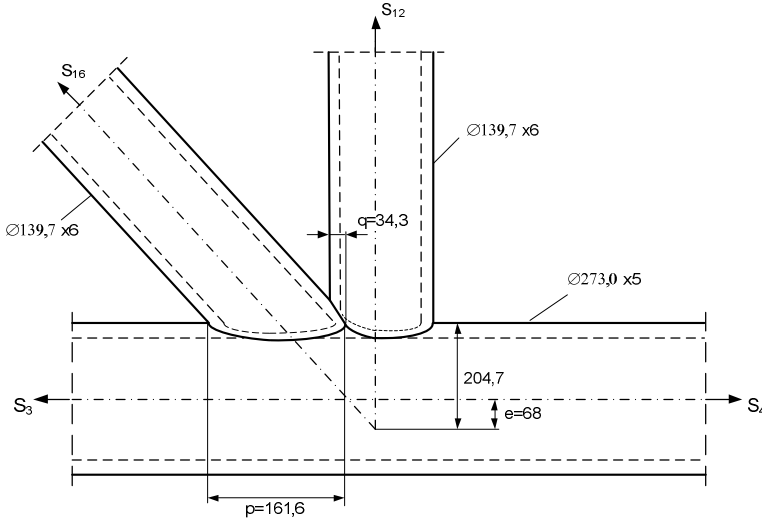


**Fig. 5.5** The overlapped tubular joint

(a) Check of local yielding of overlapping brace

$$N^* = f_y t_i L_{b,eff},$$

$$L_{b,eff} = \frac{\pi}{4} (2d_i + d_{ei} + d_{e.ov} - 4t_i),$$

$$d_{ei} = \frac{12}{d_0/t_0} \frac{t_0}{t_i} d_i \leq d_i.$$

Indices: for overlapping brace i, for overlapped brace j

$$d_{e.ov} = \frac{12}{d_j/t_j} \frac{t_j}{t_i} d_i \leq d_i.$$

In our case  $d_0 = 273, d_i = d_j = 139.7, t_i = t_j = 6, t_0 = 5$

$$d_{ei} = 25.6, d_{eov} = 72, L_{b,eff} = 277.2 .$$

$$N^* = 355 \times 6 \times 277.2 = 5900533 > 233400 \text{ N, OK.}$$

(b) *Check of local chord member yielding*

$$\left( \frac{N_0}{N_{pl,0}} \right)^{1.7} \leq 1, \quad N_{pl,0} \geq N_0, \quad N_{pl,0} = A f_y,$$

$$N_{pl,0} = 3781 \times 355 = 1342255 > 787400 \text{ N, OK.}$$

(c) *Check of brace shear*

$$N_i \cos \theta_i + N_j \cos \theta_j \leq N_s^*$$

$$N_s^* = \frac{\pi}{4} \left( 0.58 f_{ui} \frac{100 - Ov}{100} \frac{2d_i + d_{ei}}{\sin \theta_i} t_i + 0.58 f_{ui} \frac{2d_j + d_{ej}}{\sin \theta_j} t_j \right).$$

In our case

$$Ov = 21.2, f_{ui} = 510, d_{ei} = d_{ej} = 25.6, d_i = d_j = 139.7, t_i = t_j = 6,$$

$$S_{15} \cos \theta_j = 116700 < N_s^* = 833513 \text{ N, OK.}$$

## 5.4.9 Conclusions

The optimization problem to be solved is the following: find the optimal geometry and cross-sectional areas of rods which minimize the structural volume or cost for a simply supported tubular truss with non-parallel chords for a strong displacement constraint.

For the solution of this problem a developed calculation method is used. Besides the displacement constraint the rods are checked for tension stress and overall buckling. It is shown that, in the case of a strong displacement constraint the cross-sectional areas are larger than those required for constraints on stress and buckling.

The fabrication (welding) constraints on minimal angle between tubular rods ( $30^\circ$ ) have been also active. In the calculation of overall buckling the Eurocode 3 formulae are approximated by formulae of Japan Road Association enabling the explicit expression of the necessary cross-sectional area.

Special formulae are used for the cost calculation. The cost function expresses the cost of material, cutting and grinding of the tubular (CHS) rod ends, assembly, welding and painting. It is shown that, in this case, the structural optima for minimum volume and minimum cost are the same. Check of strength of a tubular joint shows that the chords and braces of available CHS profiles fulfil the requirements.

## **5.5 Minimum Cost Design and Comparison of Tubular Trusses with N- and Cross-(Rhombic)-Bracing**

### **Abstract**

Two similar simply supported optimized tubular trusses with parallel chords and N- and rhombic-type bracing are compared to each other. In the optimization process the truss height and cross-sectional areas of circular hollow section (CHS) struts are sought which minimize the structural volume or cost and fulfil the stress and buckling or deflection constraint. The required cross-sectional area of compression rods are calculated using closed formulae to approximate the Eurocode 3 buckling curve. A special method is developed for the optimization of trusses in the case of a deflection constraint. The cost function includes the cost of material, cutting and grinding of CHS strut ends, assembly, welding and painting. The comparison shows that the rhombic-type truss is more advantageous than the N-type one, since its structural volume and cost is smaller.

### **5.5.1 Introduction**

It is useful for designers to compare different structural types to achieve development of competitive structures. For the realistic comparison the different structural types should be optimized. The optimization can be performed according to different aspects. In the present study the volume (mass) and cost serve as objective function to be minimized and the stress, buckling and deflection constraints are considered as main requirements.

Trusses of parallel chords can be constructed using different bracings, such as K-, N- and cross-type ones. The aim of the present study is to compare trusses with N- and cross-type trusses. Cross-(rhombic)-type trusses are often used, but their advantages are not investigated. Adeli and Balasubramanyan (1988) have optimized X- (Pratt) type trusses. Simos et al. (2008) have compared N- and X-type trusses regarding their resistance against progressive failure.

For the struts of trusses the hollow sections are the most economic profiles because of their large buckling resistance. Optimum design of tubular trusses are treated in books (Farkas 1984, Farkas and Jármai 1997, 2003, 2008) The speciality of tubular trusses is the geometric constraint, which prescribes the minimum angle between rods to enable the welding of joints.



Compression rods should be designed against overall buckling. In order to minimize the structural volume, it is necessary to have explicit formulae for the cross-sectional areas. Since the buckling formulae of Eurocode 3 are too complicate, approximate expressions are used for hollow section rods.

In the case of optimum design considering the deflection constraint a special method is used developed by the authors. This method enables to calculate the cross-sectional areas required for a prescribed deflection.

In the cost function the costs of material, cutting and grinding of circular hollow section strut ends, assembly, welding and painting are taken into account.

The effect of self mass in this comparative study is neglected.

These problems are complicated, thus only numerical studies can be performed, but the conclusions can be useful for designers.

### 5.5.2 The Optimization Process

The optimum design procedure for both structural versions can be summarized as follows.

- (a) Formulation of the problem: find the optimum height of the simply supported truss with parallel chords, which minimizes the structural volume and cost as well as fulfil the constraints on stress, stability, geometry and deflection.
- (b) Selection of design variables: the truss height  $h$  and (in steps k1-k6) the factors  $\mu_i$  determining the ratio between the cross-sectional areas of rod groups.
- (c) Determination of rod forces in function of  $h$ .
- (d) Formulation of constraints on stress, overall and local buckling of tubular rods, on deflection of the mid-span point and on geometry (angle between rods  $\alpha_i \geq 30^\circ$ ).
- (e) Creation of the formulae for cross-sectional areas  $A_i$  required for tension and compression rods.
- (f) Creation of the formulae for structural volume and cost in function of  $h$  and the cross-sectional areas.
- (g) Search the optimum  $h$  and  $A_i$  for minimum volume and cost using a mathematical constrained function minimization method.
- (k) In order to fulfil the deflection constraint the following steps are needed:
  - (k1) Determination of rod forces from the unique force acting on the mid-span in function of  $h$ .
  - (k2) Selection of rod groups of equal cross-sectional area based on required  $A_i$  (step (e)).
  - (k3) Creation of the formulae for  $v_1$  and  $v_2$  (see below).
  - (k4) Search the optimal values for  $h$  and  $\mu_i$  to minimize  $V_I = v_1 v_2$  and fulfil the constraint on geometry using a mathematical method.
  - (k5) Calculation of the required cross-sectional areas  $A = v_2 / (E w_{adm})$  and  $A_i = \mu_i A$ ,  $w_{adm}$  is the admissible deflection.
  - (k6) Determination of the final  $A_i$ , which are larger from those obtained in steps (g) and (k5).

### 5.5.3 Optimum Design of an N-Type Planar Tubular Truss

#### 5.5.3.1 Optimum Height and Cross-Sectional Areas for Stress and Overall Buckling Constraints

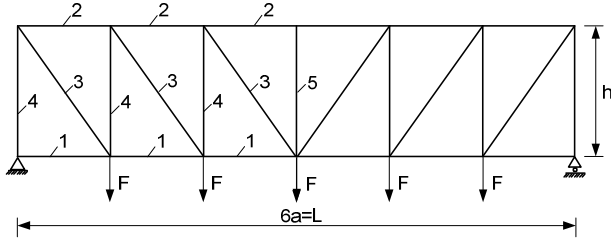


Fig. 5.6 N-type truss with parallel chords, numbering of rod groups

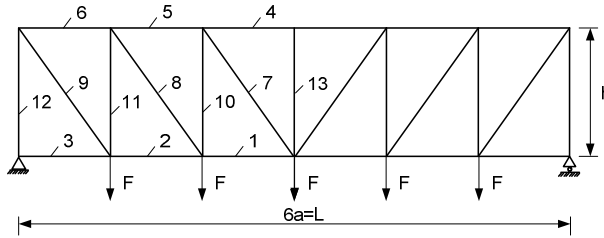


Fig.5.7 Numbering of rods in Fig.5.6

As it can be seen on Fig. 5.6, cross-sectional area is the same for all the tension rods of the lower chord (marked by 1), for all the compression rods of the upper chord (mark 2), all the diagonals (3) and verticals (4).

Rod groups of equal cross-sectional areas:

Chords: 1-2-3-4-5-6 (governing  $A_4$ ), diagonals 7-8-9 ( $A_9$ ), columns 10-11-12 ( $A_{12}$ ), central column 13 ( $A_{13}$ )

(1) tension rods of the lower chord in which the maximum rod force is

$$S_1 = 4aF / h \quad (5.87)$$

with a required cross-sectional parameters

$$A_1 = S_1 / f_{y1}, \quad f_{y1} = f_y / 1.1, \quad D_1 = \sqrt{A_1 \delta / \pi}, \quad t_1 = D_1 / \delta \quad (5.88)$$

$f_y$  is the steel yield stress,  $\delta = D/t$  is the circular hollow section slenderness, we use here the limiting slenderness of  $\delta = 50$ , prescribed by Wardenier et al. (1991). Note that the available profiles have generally smaller slenderness.

(2) compression rods of the lower chord in which the maximum force is

$$S_2 = 4.5aF / h \quad (5.89)$$

These rods should be designed against overall buckling. The calculation of the required cross-sectional area is described in Section 5.2.1 by Eqs. (5.4)-(5.11).

In order to obtain comparable optima the calculated rod diameters and thicknesses are not modified according to fabricated available profiles.

Using notation  $b = \sqrt{a^2 + h^2}$

the rod forces for rods 3 (compression) and 4 (tension) are as follows:

$$S_3 = 2.5bF / h, \quad S_4 = 2.5F \quad (5.90)$$

Since the middle vertical rod is loaded only by a secondary force, its cross-sectional area, diameter and thickness are taken as

$$A_5 = 0.5A_4, \quad D_5 = \sqrt{A_5 \delta / \pi}, \quad t_5 = D_5 / \delta \quad (5.91)$$

The volume of the truss is given by

$$V = (A_1 + A_2)L + 6A_3b + 6A_4h + A_5h \quad (5.92)$$

The cost function contents the cost of material, cutting and grinding of CHS strut ends, assembly, welding and painting.

The cost of material is given by

$$K_M = k_M \rho V \quad (5.93)$$

where an average specific cost of  $k_M = 1.0$  \$/kg is considered,  $\rho = 7.85 \times 10^{-6}$  kg/mm<sup>3</sup> for steel.

The cost of cutting and grinding of CHS strut ends is calculated with a formula proposed by Glijnis (1999)

$$K_{CG} (\$) = k_F \Theta_{CG} \frac{2.5\pi D}{(350 - 2t)0.3 \sin \alpha} \quad (5.94)$$

where  $k_F = 1.0$  \$/min is the specific fabrication cost,  $\Theta_{CG} = 3$  is a factor for work complexity, 350mm/min is the cutting speed, 0.3 is the efficiency factor, diameter  $D$  and thickness  $t$  are in mm,  $\alpha$  is the inclination angle of diagonal braces, in our case

$$\sin \alpha = \frac{h}{\sqrt{a^2 + h^2}} \quad (5.95)$$

In our case the KCG formula should be multiplied for diagonals (3) and verticals (4) by 12, for vertical (5) by 2.

The cost of assembly and welding using SMAW (shielded metal arc welding) fillet welds is given by

$$K_w = k_w \left[ \Theta \sqrt{\kappa p V} + 1.3 \times 0.7889 \times 10^{-3} \left( 12\pi D_4 t_4^2 + \frac{12\pi D_3 t_3^2}{\sin \alpha} + 2\pi D_5 t_5^2 \right) \right] \quad (5.95)$$

In our case  $k_w = 1.0$  \$/min,  $\kappa = 15$ ,  $\Theta = 3$ ,

The cost of painting is calculated as

$$K_p = k_p S_p, k_p = 28.8 \times 10^{-6} \text{ $/mm}^2. \quad (5.96)$$

The superficies to be painted is

$$S_p = L\pi D_1 + L\pi D_2 + 6h\pi D_4 + 6\pi D_3 b + h\pi D_5 \quad (5.97)$$

The total cost is given by

$$K = K_M + K_{CG} + K_w + K_p \quad (5.98)$$

*Numerical data:* factored forces  $F = 500$  kN,  $a = 6$  mm  $f_y = 355$  MPa,  $E = 2.1 \times 10^5$  MPa.

The search for optimum  $h$  is performed by using a MathCAD and a PSO algorithm (Farkas and Jármai 2003). The results are given in Table 5.14.

**Table 5.14** Volume and cost in function of  $h$ . Optima are marked by bold letters.

$h$ mm	$V \times 10^{-8} \text{ mm}^3$	$K$ \$
7100	10.58	17040
7200	10.57	17033
7300	10.56	<b>17031</b>
7400	10.5546	17032
7500	10.5517	17040
7600	<b>10.5506</b>	17040
7700	10.5524	17050
7800	10.56	17070

It can be seen that  $h_{opt} = 7600$  mm for  $V_{min}$  and  $h_{opt} = 7300$  mm for  $K_{min}$ . It can be seen that  $h_{opt} = 7400$ -7700 mm for  $V_{min}$  and  $h_{opt} = 7200$ -7400 mm for  $K_{min}$ . This means that the optima for volume and for cost are different. Note that the change in volume and in cost in the optimum domain is very small.

The cross-sectional areas for  $h = 7400$  mm are as follows:  $A_4 = 7185$ ,  $A_9 = 4986$ ,  $A_{12} = 5342$ ,  $A_{13} = 2155 \text{ mm}^2$ .

### 5.5.3.2 Optimum Height and Cross-Sectional Areas for Deflection Constraint

The used method is described in Section 5.4.3 by Eqs. (5.57)-(5.62).

In our case the deflection is calculated with forces without safety factor 1.5, thus  $F = 333333$  N. The effect of self mass is neglected.

$$v_1 = 2L + 6\mu_4 h + 6\mu_3 b + \mu_5 h \quad (5.99)$$

$$v_2 = S_1 s_1 L + S_2 s_2 L + \frac{6S_3 s_3 b}{\mu_3} + \frac{6S_4 s_4 h}{\mu_4} \quad (5.100)$$

$$s_1 = a/h, s_2 = 1.5a/h, s_3 = 0.5b/h, s_4 = 0.5 \quad (5.101)$$

The values of  $\mu_i$  are selected as  $\mu_1 = \mu_2 = 1$ ,  $\mu_3 = \mu_4 = 0.75$ ,  $\mu_5 = 0.4$  taking into account the fabrication of tubular joints. The results of the search are given in Table 5.15.

**Table 5.15** Search for  $h_{\text{opt}}$  in the case of a deflection constraint. Optimum is marked by bold letters.

$h$ mm	$V_I \times 10^{-15} \text{ mm}^3$
8900	6.588
9000	6.584
<b>9100</b>	<b>6.582</b>
<b>9200</b>	<b>6.582</b>
9300	6.584
9400	6.587

For an allowed deflection of  $w_0 = L/1500 = 24$  mm the required cross-sectional areas are as follows:  $A_4 = 7975$ ,  $A_9 = 0.75 \times 7975 = 5981$ ,  $A_{13} = 0.4 \times 7975 = 3190 \text{ mm}^2$ .

It can be seen that the cross-sectional areas required for the allowed deflection are larger than those required for stress and buckling constraints.

The corresponding structural volume and cost for these cross-sectional areas is  $V = 1.321 \times 10^9 \text{ mm}^3$  and  $K = \$20410$ .

### 5.5.4 Optimum Design of a Rhombic-Type Planar Tubular Truss

#### 5.5.4.1 Optimum Height and Cross-Sectional Areas for Stress and Overall Buckling Constraints

According to Fig. 5.8, four rod groups of equal cross-sectional area are selected as follows: chords marked by 1,2,3, 4,5,6,7 tension diagonals 8,9,10, compression diagonals 11,12, column 13.

(1) tension rods of the lower chord in which the maximum rod force is

$$S_1 = 4.25aF/h \quad (5.102)$$

with a required cross-sectional parameters

$$A_1 = S_1 / f_{y1}, \quad f_{y1} = f_y / 1.1, \quad D_1 = \sqrt{A_1 \delta / \pi}, \quad t_1 = D_1 / \delta \quad (5.103)$$

- (2) compression rods of the upper chord (cross-sectional area  $A_2$ ) in which the maximum force is

$$S_4 = 4.25aF / h \quad (5.104)$$

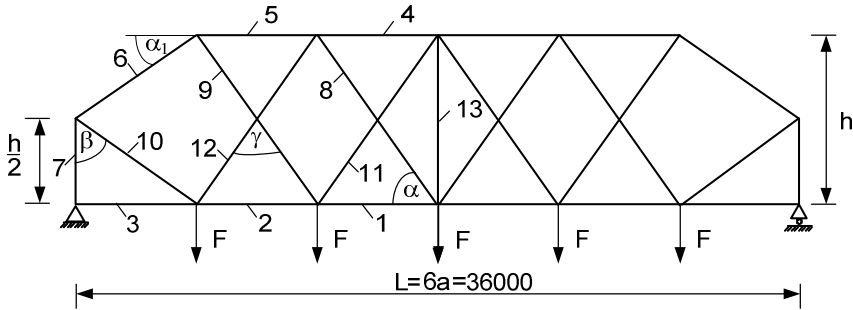


**Fig. 5.8** Rhombic-type truss with parallel chords

- (3) tension diagonals (cross-sectional area  $A_3$ ) with rod force

$$S_9 = 1.25qF / h, \quad q = \sqrt{h^2 + a^2} \quad (5.105)$$

- (4) compression diagonals (cross-sectional area  $A_4$ ) with rod force

$$S_{11} = 0.25qF / h \quad (5.106)$$

According to Eurocode 3, Part 3-1 (2006) the effective buckling length of these diagonals is  $0.5q$ .

Tension column (cross-sectional area  $A_5$ ) with rod force

$$S_{13} = 0.5F \quad (5.107)$$

The structural volume is given by

$$V = 3aA_1 + (2a + q_1 + h/2)A_2 + (2q + q_1)A_3 + 2qA_4 + hA_5 \quad (5.108)$$

The cost function contents the cost of material, cutting and grinding of CHS strut ends, assembly, welding and painting.

The cost of material is given by Eq. (5.93), the cost of cutting and grinding of CHS strut ends is calculated with a formula Eq.(5.94).

In our case the diagonals (11,12) should be interrupted in the middle of rods. Thus

$$K_{CG1} = \Theta_{CG} \frac{2.5\pi}{0.3} \left[ \frac{8D_{10}}{(350-t_{10})\sin\alpha} + \frac{2D_4}{(350-t_4)\sin\alpha_1} + \frac{2D_4}{(350-t_4)\sin\beta} \right] + K_{CG2} + K_{CG3} \quad (5.109)$$

$$\sin \alpha = h/q, \quad \tan \alpha_1 = h/2a, \quad \sin \beta = a/q_1, \quad q_1 = \sqrt{\frac{h^2}{4} + a^2} \quad (5.110)$$

$$K_{CG2} = \Theta \frac{2.5\pi}{0.3} \left[ \frac{4D_4}{(350-t_4)} + \frac{2D_{10}}{(350-t_{10})\sin \alpha_1} + \frac{2D_{10}}{(350-t_{10})\sin \beta} \right] \quad (5.111)$$

$$K_{CG3} = \Theta_{CG} \frac{2.5\pi}{0.3} \left[ \frac{8D_{11}}{(350-t_{11})\sin \alpha} + \frac{8D_{11}}{(350-t_{11})\sin \gamma} + \frac{8D_{13}}{350-t_{13}} \right] \quad (5.112)$$

The cost of assembly and welding using SMAW (shielded metal arc welding) fillet welds is given by

$$K_w = \Theta \sqrt{\kappa p V} + 1.3 \times 0.7889 \times 10^{-3} \pi (T_1 + T_2 + T_3) \quad (5.113)$$

$$T_1 = \frac{8D_{10}t_{10}^2}{\sin \alpha} + \frac{2D_4t_4^2}{\sin \alpha_1} + \frac{2D_4t_4^2}{\sin \beta} \quad (5.113a)$$

$$T_2 = 2D_4t_4^2 + \frac{2D_{10}t_{10}^2}{\sin \alpha_1} + \frac{2D_{10}t_{10}^2}{\sin \beta} \quad (5.113b)$$

$$T_3 = \frac{8D_{11}t_{11}^2}{\sin \alpha} + \frac{8D_{11}t_{11}^2}{\sin \gamma} + 2D_{13}t_{13}^2 \quad (5.113c)$$

$k_w = 1.0$  \$/min,  $\kappa = 21$ .

The cost of painting is calculated with Eq.(5.96). The superficies to be painted is

$$S_p = \pi (10aD_4 + 4qD_{10} + 4qD_{11} + 2q_1D_4 + 2qD_{10} + hD_{13}) \quad (5.114)$$

The total cost is given by

$$K = K_M + K_{CG} + K_{CG1} + K_{CG2} + K_w + K_p \quad (5.115)$$

In the optimization process a fabrication constraint should be taken into account, namely the prescription for tubular truss nodes that the angle between rods should be larger than  $30^\circ$  to guarantee the easy welding of nodes. In our case this constraint is formulated as

$$\alpha \leq 30^\circ \quad (5.116)$$

The search for optimum  $h$  is performed by using a MathCAD and the PSO algorithm (Farkas and Jármai 2003). The results are given in Table 5.16.

**Table 5.16** Volume and cost in function of  $h$ . Optima are marked by bold letters.

$h$ mm	$V \times 10^{-8}$ mm <sup>3</sup>	$K \times 10^{-4}$ \$	$(90-\alpha)^0$
9000	7.294	1.414	56.3
10000	7.048	1.378	59.0
10300	6.991	1.370	59.8
<b>10400</b>	<b>6.973</b>	<b>1.368</b>	<b>60.0</b>
10500	6.957	1.366	60.2
11000	6.883	1.357	61.4

#### 5.5.4.2 Check of a Truss Joint with Available Tubular Profiles

After the optimization the optimal cross-sections should be replaced by available profiles according to EN 10291-2 and the joints should be checked for strength according to new IIW rules (Static design 2009). To illustrate this procedure a tubular joint of the rhombic braced truss optimized for strength is shown in Fig. 5.9.

The related rod forces are as follows:  $S_4 = 4.25Fq/h = 1226$  kN (compression),  $S_8 = 0.25Fq/h = 144$  kN,  $S_9 = 721.6$  kN,  $S_{10} = 954.3$  kN (tension),  $S_{11} = S_{12} = 144$  kN (compression),  $S_{13} = 250$  kN (tension).

The available CHS profiles for the rhombic truss optimized for strength are as follows:

Chords 1,2,3,4,5,6,7:  $\emptyset 244.5 \times 8$ ,

Tension diagonals: 8:  $\emptyset 139.7 \times 10$ , 9:  $\emptyset 168.3 \times 5$ , 10:  $\emptyset 168.3 \times 6$ ,

Compression diagonals 11,12:  $\emptyset 114.3 \times 4$ ,

Column 13:  $\emptyset 88.9 \times 3$ .

According to Fig. 5.9 the joint is designed a K-joint with gap, with the eccentricity of  $e = 0.25d_4 = 61$  mm the gap is  $g = 65$  mm.

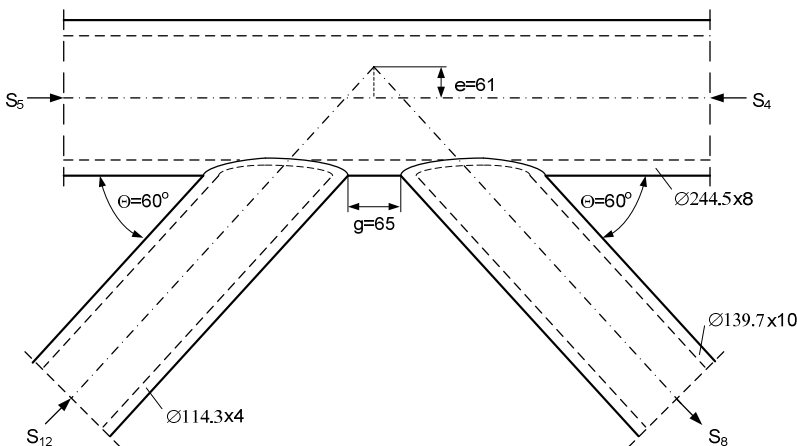


**Fig. 5.9** Truss joint with available tubular profiles



Check of rod 8 for chord plastification:

$$N^* = Q_u Q_f \frac{f_{y0} t_0^2}{\sin \theta}$$

$$Q_u = 1.65(1 + 8\beta^{0.6})\gamma^{0.3} \left[ 1 + \frac{1}{1.2 + (g/d_0)^{1.6}} \right]$$

$$\beta = d_8 / d_4 = 0.5714, \gamma = d_4 / (2t_4) = 15.28$$

$$Q_f = (1 - |n|)^{C_1}, n = N_0 / N_{p0} = S_4 / (A_4 f_{y0}) = 1.226 \times 10^6 / (5940 \times 355) = 0.5814$$

With values of  $C_1 = 0.25, Q_f = 0.8044, \theta = 60^\circ, Q_u = 18.3917$

$$N^* = 388 > 144 \text{ kN, OK.}$$

Check of rod 12 is similarly  $N^* = 306 > 144 \text{ kN, OK.}$

Check of rod 8 for chord punching shear:

$$N^* = 0.58 f_y \pi d_8 t_4 \frac{1 + \sin \theta}{2 \sin^2 \theta} = 735 > 144 \text{ kN, OK.}$$

#### 5.5.4.3 Optimum Height and Cross-Sectional Areas for Deflection Constraint

As it has been described in Section 5.4.3 the structural volume is calculated as

$$V = \sum_i A_i L_i = A \sum_i \mu_i L_i = A v_1 \quad (5.117)$$

$$V = \sum_i A_i L_i = \frac{1}{EA} \sum_i \frac{S_i s_i L_i}{\mu_i} \sum_i \mu_i L_i = \frac{v_1 v_2}{E w_0} \quad (5.118)$$

In the optimum design  $h_{opt}$  is sought, which minimizes the structural volume or the value of

$$V_l = v_1 v_2. \quad (5.119)$$

$\mu$ -factors are taken considering the cross-sectional areas corresponding to the average  $h_{opt} = 10400 \text{ mm}$  as follows:  $A_4 = 5201, A_{10} = 2957, A_{11} = 1073, A_{13} = 773 \text{ mm}^2$ , thus,  $\mu_1 = \mu_2 = 1, \mu_3 = 0.6, \mu_4 = 0.2, \mu_5 = 0.15$ .

The other rod forces are as follows:

$$S_2 = 2.75aF/h = S_5, \quad S_6 = 2.5Fq_1/h, \quad S_7 = 2.5F, \quad S_8 = S_{11} = 0.25Fq/h = S_{12} \quad (5.120a)$$

$$S_9 = 1.25Fq/h, \quad S_{10} = 2.5Fq_1/h \quad (5.120b)$$

$$s_1 = 1.25a/h = s_4, \quad s_2 = 0.75a/h = s_5, \quad s_3 = 0, \quad s_7 = 0.5 \quad (5.121a)$$

$$s_8 = s_9 = 0.25q/h, \quad s_6 = -0.5q_1/h, \quad s_{10} = 0.25q_1/h, \quad s_{11} = s_{12} = -0.25q/h, \quad s_{13} = 0.5 \quad (5.121b)$$

$$v_1 = 5 + q_1 + \frac{h}{2} + \mu_3(q_1 + 2q) + \mu_4 2q + \mu_5 h \quad (5.122)$$

$$v_{21} = (S_1 s_1 + S_2 s_2 + S_4 s_4 + S_5 s_5)a + S_6 s_6 q_1 + S_7 s_7 h/2 \quad (5.123a)$$

$$v_{22} = \frac{(S_8 s_8 + S_9 s_9)q + S_{10} s_{10} q_1}{\mu_3} \quad (5.123b)$$

$$v_{23} = \frac{(S_{11} s_{11} + S_{12} s_{12})q}{\mu_4} + \frac{S_{13} s_{13} h}{\mu_5} \quad (5.123c)$$

$$v_2 = v_{21} + v_{22} + v_{23} \quad (5.124)$$

$$s_1 = 1.25a/h = s_4, \quad s_2 = 0.75a/h = s_5, \quad s_3 = 0, \quad s_7 = 0.5 \quad (5.125a)$$

$$s_8 = s_9 = 0.25q/h, \quad s_6 = -0.5q_1/h, \quad s_{10} = 0.25q_1/h, \quad s_{11} = s_{12} = -0.25q/h, \quad s_{13} = 0.5 \quad (5.125b)$$

The results of the search are given in Table 5.17.

**Table 5.17** Search for  $h_{\text{opt}}$  in the case of a deflection constraint. Optimum is marked by bold letters.

$h$ mm	$V_I \times 10^{-16}$ mm <sup>3</sup>	$(90-\alpha)^0$
10200	1.924	59.5
10300	1.922	59.8
<b>10400</b>	<b>1.921</b>	<b>60.0</b>
10500	1.920	60.2

It can be seen that  $V_I$  decreases with the increase of  $h$ , but the inclination angle of diagonals shall be smaller than  $30^0$ , therefore  $h_{\text{opt}} = 10400$  mm.

For  $h = 10400$  mm truss height for a force  $F = 333$  kN the deflection is  $w = 35$ mm. To allowed deflection of 24 mm correspond the following cross-sectional areas:  $A_4 = 5549 > 5201$ ,  $A_{10} = 3329 > 2957$ ,  $A_{11} = 1110 > 1073$ ,  $A_{13} = 832 > 773$  mm<sup>2</sup>.

The corresponding structural volume and cost for these cross-sectional areas is  $V = 7.535 \times 10^8$  mm<sup>3</sup> and  $K = \$14500$ .

### 5.5.5 Comparison of the Two Bracing Types

The data for the comparison are summarized in Tables 5.18 and 5.19.

The volume and cost minima are smaller for rhombic-type truss both in the case of stress and deflection constraint. In the case of stress constraint this difference is  $100(10.55-6.973)/10.55 = 34\%$  in volume and 20% in cost. In the case of deflection constraint this difference is 37% in volume and 29% in cost.

**Table 5.18** Comparison of the minima of the volume and cost for stress and buckling constraints

Truss type	Stress and buckling constraints, $F = 500$ kN	Deflection constraint $F = 333$ kN
N	$h_{\text{opt}} = 7400$ mm $V = 10.55 \times 10^8$ , $K = \$17030$	$h_{\text{opt}} = 9100$ mm $V = 13.21 \times 10^8$ , $K = \$20410$
rhombic	$h_{\text{opt}} = 10400$ mm $V = 6.973 \times 10^8$ , $K = \$13680$	$h_{\text{opt}} = 10400$ mm $V = 7.535 \times 10^8$ , $K = \$14500$

**Table 5.19** Cost components in Table 5. 18 (in \$)

	$K_M$	$K_{CG}$	$K_W$	$K_P$	$K$
N-type	8285	1889	1903	4955	17030
Rhombic	5474	1969	1507	3902	13680

The analysis of cost components (Table 5.19) shows that the material, welding and painting cost for rhombic-type truss is smaller, the cutting and grinding cost is larger than that for N-type truss.

It can be concluded that, in this numerical problem, the rhombic-type truss is more advantageous than the N-type one. The greatest difference occurs in volumes for deflection constraint.

### 5.5.6 Conclusions

A comparison is carried out for a numerical problem of simply supported trusses with parallel chords with the same number of joint spacing and with the same loading.

The comparison of the optimized versions of planar N- and rhombic-type tubular trusses shows that the rhombic-type truss has smaller volume and cost in the case of stress and deflection constraint.

In the case of stress constraint the compression rods are designed against overall buckling using an approximate buckling curve instead of the Eurocode 3 curve. In the case of the deflection constraint a special method is worked out to obtain the required cross-sectional areas of struts. These areas are always larger than those required for overall buckling.

Stress and buckling constraints are calculated using factored forces, the deflection is calculated with forces without a safety factor. To obtain comparable optima the required cross-sectional areas are not rounded to available profiles and the most economic  $\delta = D/t = 50$  slenderness of CHS is used.

Special fabrication constraints are taken into account that the diameters of chords should be larger than those of bracing and the angle between rods should be larger than  $30^\circ$  to ease the welding of the nodes.

The cost function includes the cost of material, cutting and grinding of CHS rod ends, assembly and welding as well as painting. In the case of rhombic-type truss the compression diagonals should be interrupted in the middle joints and additive costs of cutting and grinding as well as assembly and welding are taken into account. Despite of these additive costs the rhombic-type truss has smaller volume and total cost than the N-type one.

The calculations also show that the optimum truss height and cross-sectional areas are approximately the same for minimum volume and minimum cost. Thus, the cost for minimum volume is a good approximation for the minimum cost.

## 5.6 Optimum Design of a Transmission Line Tower Constructed from Welded Tubular Truss

### Abstract

The aim of this study is to show the advantages of trusses constructed from circular hollow section (CHS) rods with welded nodes. Another aim is to solve the following optimization problem: determine the slope angle (sprawling) of the four main rods of the truss tower and the cross-sectional areas of rods, which minimize the structural volume or cost and fulfil the design and fabrication constraints. Design constraints relate to the tensile stress and overall buckling strength of rods. Fabrication constraints prescribe the minimum angle between CHS rods to ease the welding of nodes. For the numerical optimization process a tower of 45 m height is selected and the loads are determined according to the rules of the Hungarian Standard for transmission lines.

### 5.6.1 Introduction

The trusses of transmission line towers are usually constructed from rods of angle profile with bolted connections, as it is used by Rao (1995) and Silva et al (2005). These rods have a poor overall buckling strength. The aim of this study is to show the advantages of trusses constructed from circular hollow section (CHS) rods with welded nodes. Taniwaki and Ohkubo (2004) have used CHS rods, they have considered special Japanese problems of seismic-design and cost of land as well as special mathematical methods.

Another aim is to solve the following optimization problem: determine the slope angle (sprawling) of the four main rods of the truss tower and the cross-sectional areas of rods, which minimize the structural volume or cost and fulfil the design and fabrication constraints.

Design constraints relate to the tensile stress and overall buckling strength of rods. Fabrication constraints prescribe the minimum angle between CHS rods to ease the welding of nodes.

For the numerical optimization process a tower of 45 m height is selected and the loads are determined according to the rules of the Hungarian Standard for transmission lines MSZ 151 (2000, 1988). The cost function contents the cost of material, cutting and grinding of the ends of CHS rods, assembly, welding and painting.

More groups of rods having the same cross-sectional area are selected. Approximate formulae are used instead of overall buckling formulae of Eurocode 3, which allow for expressing the cross-sectional area of compressed rods explicitly.

To obtain comparable optima the required cross-sectional areas are not rounded to available profiles.

### 5.6.2 Loads

The tower has two main parts. The upper part solves for the fixing of conductors. The whole height of the tower is 45 m, the height of the upper part is 21 m. The present study treats the optimum design of the lower part with the height of 24 m. The loads acting from the upper part are calculated according to the MSZ 151 (1988, 2000). The governing load combination is as follows: in the one side of the tower the whole tension and on the other side the half of the tension of conductors + rime without wind load.

The distance of towers: 400 m.

Weight of two lightning conductors:  $2 \times 712 \times 0.4 \times 9.81 = 5587 \text{ N}$ .

Weight of 12 electric conductors:  $12 \times 1935 \times 0.4 \times 9.81 = 91115 \text{ N}$ .

Weight of the upper part of the tower: approximately 40 kN.

Additional load according to the Hungarian standard MSZ 151-1 (2000) the weight of rime is

$$z = 3.25 + 0.25d, \text{ where } d \text{ is the wire-diameter.}$$

For the lightning conductors with  $d = 16 \text{ mm}$   $z = 7.25 \text{ N/m}$ , for electric conductors with  $d = 31.05$   $z = 11.025 \text{ N/m}$ . For 400 m distance it is 2900 N and 4405 N, respectively.

Vertical load from the upper part of the tower is multiplied by a safety factor of 1.1:

$$V = 1.1(91.115 + 5.5587 + 40) + 12 \times 4.405 + 2 \times 2.9 = 209.03 \text{ kN}$$

The allowable tensile stress of a 95/55 steel lightning conductor is  $140 \text{ N/mm}^2$  and that of a 500/66 aluminium electric conductor is  $85 \text{ N/mm}^2$ .

The tensile force of a lightning conductor is

$$(96.5 + 56.3)140 = 21392N$$

and that of an electric conductor

$$(504.7 + 65.4)85 = 48458N .$$

The governing load combination is the half of the tensile force of conductors.

The horizontal force acting on the top of the lower part of the tower:

$$H_0 = (2 \times 21.392 + 12 \times 48.4585)0.5 = 312.143 \text{ kN}$$

and the bending moment from the tensile forces

$$M = 21.392 \times 21.8 + 2 \times 48.4585(16.4 + 8.2) = 2850.5 \text{ kNm}.$$

It is supposed that the tower is square symmetric in plane.

Vertical loads acting on the half lower part of the tower (width of the tower  $a_1 = 3.7 \text{ m}$ ) (Fig. 5.10):

$$F_{10} = \frac{209.03}{4} + \frac{2850.5}{2 \times 3.7} = 437.46 \text{ kN} \quad (5.126)$$

$$F_{20} = \frac{2850.5}{2 \times 3.7} - \frac{209.03}{4} = 332.94 \text{ kN} \quad (5.127)$$

Loads acting on the inclined tower plane (Fig. 5.11)

$$F_1 = 437.46\Theta / \Omega, F_2 = 332.94\Theta / \Omega \quad (5.128)$$

$$H = \frac{H_0}{2} - \frac{437.46 + 332.94}{\Omega} = 156.07 - \frac{770.4}{\Omega} \quad (5.129)$$

### 5.6.3 Geometric Data (Fig. 5.10, 5.11)

Factors for the transformation of loads from vertical to inclined plane:

$$\Omega = \sqrt{\theta^2 - 1}, \Theta = \sqrt{\theta^2 + 1}, \text{ where } \theta = \tan \beta \quad (5.130)$$

$$c = L \frac{\Theta}{\Omega}, d = \frac{L}{\Omega}, f = \theta l \quad (5.131)$$

$$h_1 = 6000f / L, h_2 = 7000f / L, h_3 = 4500f / L, h_4 = 4500f / L, h_5 = 2000f / L \quad (5.132)$$



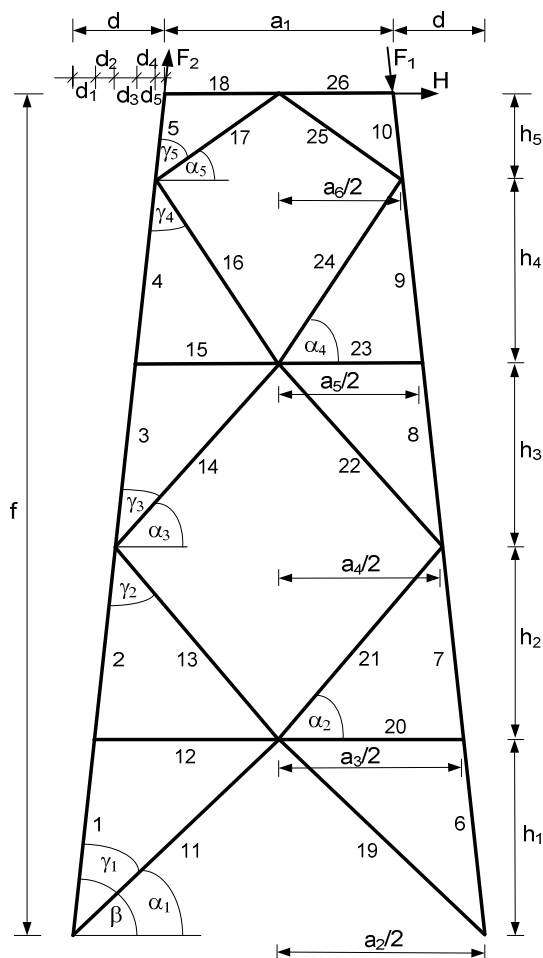


**Fig.5.11** The trussed inclined plan of the bottom part

Rod lengths:

$$L_i = h_i c / f, i = 1 \dots 5, \quad (5.141)$$

$$L_6 = L_1, L_7 = L_2, L_8 = L_3, L_9 = L_4, L_{10} = L_5 \quad (5.142)$$

$$L_{11} = L_{19} = \sqrt{h_1^2 + \frac{a_2^2}{4}}, L_{12} = L_{20} = \frac{a_3}{2}, L_{13} = L_{21} = \sqrt{h_2^2 + \frac{a_4^2}{4}} \quad (5.143)$$



$$L_{14} = L_{22} = \sqrt{h_3^2 + \frac{a_4^2}{4}}, L_{15} = L_{23} = \frac{a_5}{2}, L_{16} = L_{24} = \sqrt{h_4^2 + \frac{a_6^2}{4}} \quad (5.144)$$

$$L_{17} = L_{25} = \sqrt{h_5^2 + \frac{a_6^2}{4}}, L_{18} = L_{26} = \frac{a_6}{2} \quad (5.145)$$

#### 5.6.4 Rod Forces from a Horizontal Force $F = 1$

$$S_{17} = F \frac{L_{17}}{a_6}, S_{25} = -S_{17} \quad (5.146)$$

$$S_4 = \frac{F(h_4 + h_5)}{a_5 \sin \beta} \quad (5.147)$$

$$S_{16} = \frac{S_{17} \cos \alpha_5 - S_4 \cos \beta}{\cos \alpha_4}, S_{24} = -S_{16} \quad (5.148)$$

$$S_9 = -S_4 \quad (5.149)$$

$$S_{14} = S_{16} \frac{a_6 L_{14}}{L_{16} a_4}, S_{22} = -S_{14} \quad (5.150)$$

$$S_{13} = -S_{14} \frac{\theta \cos \alpha_3 - \sin \alpha_3}{\theta \cos \alpha_2 + \sin \alpha_2}, S_{21} = -S_{13} \quad (5.151)$$

$$S_{11} = S_{13} \frac{a_4 L_{11}}{L_{13} a_2}, S_{19} = -S_{11} \quad (5.152)$$

$$S_2 = \frac{F(h_2 + h_3 + h_4 + h_5)}{a_3 \sin \beta} \quad (5.153)$$

$$\sin \beta = \frac{\theta}{\sqrt{\theta^2 + 1}}, S_7 = -S_2 \quad (5.154)$$

### 5.6.5 Rod Forces from $H$ , $F_1$ and $F_2$

$$H = 156070 - \frac{770400}{\Omega}, F_1 = 437460 \frac{\Theta}{\Omega} \quad (5.155)$$

$$F_2 = 332940 \frac{\Theta}{\Omega} \quad (5.156)$$

$$N_2 = HS_2 + F_2, N_4 = HS_4 + F_2, \quad (5.157)$$

$$N_7 = -HS_2 - F_1, N_9 = -HS_4 - F_1 \quad (5.158)$$

$$N_{11} = HS_{11}, N_{13} = HS_{13} \quad (5.159)$$

$$N_{14} = HS_{14}, N_{16} = -HS_{16} \quad (5.160)$$

$$N_{17} = HS_{17}, N_{19} = -N_{11} \quad (5.161)$$

$$N_{21} = -N_{13}, N_{22} = -N_{14} \quad (5.162)$$

$$N_{24} = -N_{16}, N_{25} = -N_{17} \quad (5.163)$$

$$N_{18} = 332940/\Omega, N_{26} = 156070 - 437460/\Omega \quad (5.164)$$

$$N_{10} = -F_1, N_5 = F_2 \quad (5.165)$$

### 5.6.6 Optimization Process

Selection of a preliminary slope angle:  $\beta_{\text{opt}} = 80^\circ$ .

Determination of rod forces for  $80^\circ$ .

Determination of rod groups having the same cross-sectional area on the basis of rod forces. The selected rod groups are as follows:

- (a) lower chords 1-2-6-7, governing rod: 7,
- (b) upper chords: 3-4-5-8-9-10, governing rod: 9,
- (c) braces 11-13-14-16-19-21-22-24-18-26 governing rod: 11,
- (d) upper braces 17-25 governing rod: 17.

### 5.6.7 Formulae for Cross-Sectional Areas of Governing Rods

The calculation method is described in Section 5.2.2 by Eqs. (5.4)-(5.11).

In the case of very long struts with small compressive force, the limitation of the strut slenderness can be governing. From the limitation of

$$\lambda = KL/r \leq \lambda_{\text{max}} \quad (5.166)$$

the required radius of gyration is

$$r \geq KL / \lambda_{\max} . \quad (5.167)$$

According to BS 5400 (1983)  $\lambda_{\max} = 180$ .

### 5.6.8 *Formulae for Volume V and Cost K of the Truss in the Function of $\beta$*

$$V = 2A_7(L_6 + L_7) + 2A_9(2L_9 + L_5) + V_1 \quad (5.168a)$$

$$V_1 = 2A_{11}(L_{11} + L_{21} + L_{14} + L_{16} + L_{18}) + 2A_{17}L_{17} \quad (5.168b)$$

The cost function contents the cost of material, cutting and grinding of CHS strut ends, assembly, welding and painting.

The cost of material is given by

$$K_M = k_M \rho V \quad (5.169)$$

where an average specific cost of  $k_M = 1.0$  \$/kg is considered,  $\rho = 7.85 \times 10^{-6}$  kg/mm<sup>3</sup> for steel.

The cost of cutting and grinding of CHS strut ends is calculated with a formula proposed by Glijnis (1999)

$$K_{CG} (\$) = k_F \Theta_{CG} \frac{2.5\pi D}{(350 - 2t)0.3 \sin \alpha} \quad (5.170)$$

where  $k_F = 1.0$  \$/min is the specific fabrication cost,  $\Theta_{CG} = 3$  is a factor for work complexity, 350 mm/min is the cutting speed, 0.3 is the efficiency factor, diameter  $D$  and thickness  $t$  are in mm,  $\alpha$  is the inclination angle of diagonal braces.

In our case

$$K_{CG} = \frac{5k_F \Theta_{CG} \pi}{0.3} (G_1 + G_2 + G_3) \quad (5.171a)$$

$$G_1 = \frac{D_{11}}{350 - t_{11}} \left[ \sum_{i=1}^4 \left( \frac{1}{\sin \alpha_i} + \frac{1}{\sin \gamma_i} \right) \right] \quad (5.171b)$$

$$G_2 = \frac{D_{11}}{350 - t_{11}} \frac{1}{\sin \beta} \quad (5.171c)$$

$$G_3 = \frac{D_{17}}{350 - t_{17}} \left( \frac{1}{\sin \alpha_5} + \frac{1}{\sin \gamma_5} \right) \quad (5.171d)$$

In our case  $k_F = 1.0$  \$/min,  $\Theta = 3$ ,

$$K_W = k_F \left[ \Theta \sqrt{\kappa \rho V} + 1.3 \times 0.7889 \times 10^{-3} (T_1 + T_2 + T_3) \right] \quad (5.172a)$$

$$T_1 = 2D_{11} t_{11}^2 \left[ \sum_{i=1}^4 \left( \frac{1}{\sin \alpha_i} + \frac{1}{\sin \gamma_i} \right) \right] \quad (5.172b)$$

$$T_2 = \frac{2D_{11} t_{11}^2}{\sin \beta} \quad (5.172c)$$

$$T_3 = 2D_{17} t_{17}^2 \left( \frac{1}{\sin \alpha_5} + \frac{1}{\sin \gamma_5} \right) \quad (5.172d)$$

$$\kappa = 15$$

The cost of painting is calculated as

$$K_p = k_p S_p, k_p = 28.8 \times 10^{-6} \text{ $/mm}^2. \quad (5.173)$$

The superficies to be painted is

$$S_p = S_{p1} + S_{p2} + S_{p3} \quad (5.174a)$$

$$S_{p1} = 2\pi D_7 (L_1 + L_2) + 2\pi D_9 (L_3 + L_4 + L_5) \quad (5.174b)$$

$$S_{p2} = 2\pi D_{11} (L_{11} + L_{13} + L_{14} + L_{16} + L_{18}) \quad (5.174c)$$

$$S_{p3} = 2\pi D_{17} L_{17} \quad (5.174d)$$

### 5.6.9 Search for $\beta_{opt}$ for $V_{min}$ and $K_{min}$

The search is performed by using a MathCAD algorithm. The results are given in Table 5.20.

**Table 5.20** Optimum truss angle for minimum volume and cost

$\beta^0$	$\gamma_3^0$	$10^{-8} V \text{ mm}^3$	$K \text{ \$}$
79	30.3	1.902	3952
<b>80</b>	<b>29.9</b>	<b>1.874</b>	<b>3903</b>
81	29.4	1.854	3855
82	28.9	1.844	3820
83	28.4	1.845	3800
84	27.6	1.857	3796
85	26.9	1.883	3812

It can be seen that the constraint for the angles between the rods is active for angle  $\gamma_3$ , thus the optimum truss angle is  $\beta = 80^\circ$ . Disregarding the angle constraint the optimum for minimum volume would be  $82^\circ$  and for minimum cost  $84^\circ$ .

### 5.6.10 Selection of Available Profiles

Table 5.21 shows the available profiles

**Table 5.21** Selected available CHS profiles. For rod 11 the requirement of radius of inertia ( $r$ ) is governing.

Rod group	Governing rod	Required cross-sectional area mm <sup>2</sup>	Selected CHS profile	Cross-sectional area
1,2,6,7	7	3073	177.8/6	3240
3,4,5,8,9,10	9	2195	168.8/4.5	2320
11,13,14,16, 19,21,24,18,26	11	734	114.3/5	1720 ( $r=38.7>36$ )
17,25	17	254	39.7/4	373

### 5.6.11 Optimum Mass of the Tower

The volume (in mm<sup>3</sup>) an inclined side of the tower calculating with the cross-section of the selected profiles:

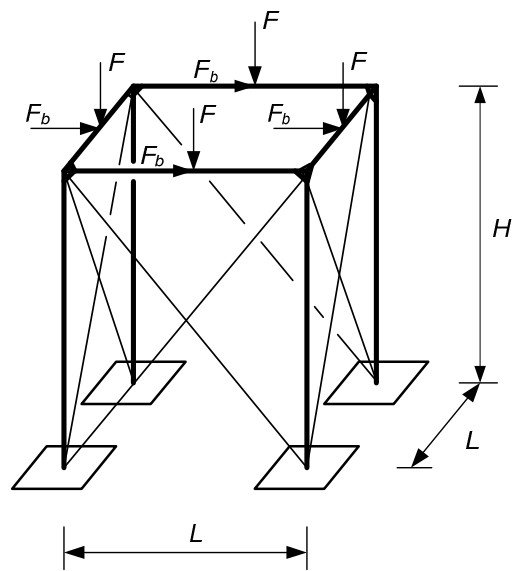
$$V = 2A_7(L_6 + L_7) + 2A_9(2L_9 + L_5) + 2A_{11}(L_{11} + L_{13} + L_{14} + L_{16} + 0.5L_{18}) + 2A_{17}L_{17} = 2.21 \times 10^8$$

The mass is  $4 \times 2.21 \times 10^8 \times 7.85 \times 10^{-6} = 6939$  kg. The additional mass of the diaphragms of CHS profile 168.8/4.5 is  $6.828 \times 2320(10150 + 6029) \times 7.85 \times 10^{-6} = 2012$  kg, together with the mass of the upper part (400 kg) the total mass of the tower is 9351 kg. The optimum clearance is  $a_2 = 12300$  mm.

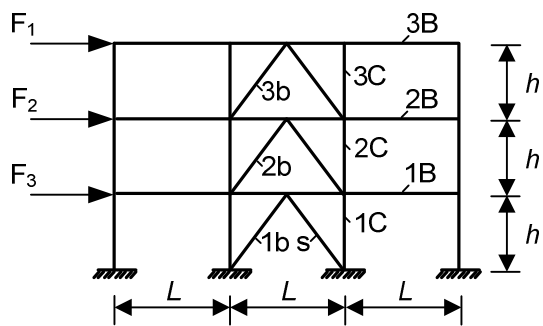
### 5.6.12 Mass Comparison with the Tower Published by Rao (1995)

Rao has optimized a 400 kV tower of high 44.3 m with lightning conductors (groundwires) of diameter 11 mm and electric conductors of diameter 31.77 mm, the ground clearance  $a_2 = 8.84$  m, rods of L-shaped angles with a bolted type construction. The total mass was 11400 kg. Since the tower of Rao is very similar to the present tower, the comparison is realistic. It can be concluded that using CHS profiles instead of angles and optimizing the clearance a saving in mass of  $(11400 - 9351)/11400 \times 100 = 18\%$  can be achieved.

# Chapter 6 Frames



Section 6.1



Section 6.2

## 6.1 Minimum Cost Seismic Design of a Welded Steel Portal Frame with X-Bracing

### Abstract

The calculation of the absorbed energy i.e. the area of the hysteretic loop for rods of circular and square hollow sections (CHS and SHS) has been worked out. The limiting points of the hysteretic loop have been determined on the basis of experimental results published in the literature.

A square symmetric portal frame with four horizontal beams and four columns, carrying a silo is designed for vertical and seismic loads. Design rules of Eurocodes 3 and 8 are used. X-bracing is applied, in which the compressive member absorbs the energy by a hysteretic cycle with overall buckling. The cost function for the braced portal frame is expressed in function of unknown dimensions of beams, columns and braces.

The beams and columns are constructed from SHS profiles. All joints are fully welded. The design constraints are formulated for beams and columns on stress, overall buckling and admissible sway for unbraced frame. This sway has two main components: the sway of the vertical frames and the deformation of the beam due to bending in horizontal plane. The constraint on slenderness of braces is also important.

### 6.1.1 Absorbed Energy of CHS and SHS Braces Cyclically Loaded in Tension-Compression

Braces play an important role in the earthquake-resistant design of frames. The efficiency of bracing is characterized by the absorbed energy which can be obtained as the area of the hysteretic loop.

Studies have shown that the first critical overall buckling strength decreases during the second and third cycle, but after a few cycles the hysteretic loop becomes stable. This degradation is caused by the Bauschinger-effect and by the effect of residual camber as explained by Popov and Black (1981). Unfortunately, these effects cannot be considered by analytical derivations, thus, the characteristics of the stable hysteretic loop will be taken from the experimental data published in the literature.

Our aim is to derive simple closed formulae for the calculation of the area of the stable hysteretic loop. The derived formulae enable designers to analyze the effect of some important parameters such as the yield stress of steel, end restraint and cross-sectional shape, and to work out aspects of optimization, i.e. the increasing of the energy-absorbing capacity of braces.

The stable hysteretic loop is shown schematically in Fig. 6.1. The characteristics obtained by experiments are summarized in Table 6.1. It can be seen that, for

$\eta$  and  $z_I$  the approximate value of 0.5 is predominantly obtained. The sum of relative axial shortenings  $x + |x_I|$  varies in range of 5 - 14. On the basis of these data we consider the values  $\eta = z_I = 0.5$  and  $x_0 = 1$ ,  $x_I = -5$ .

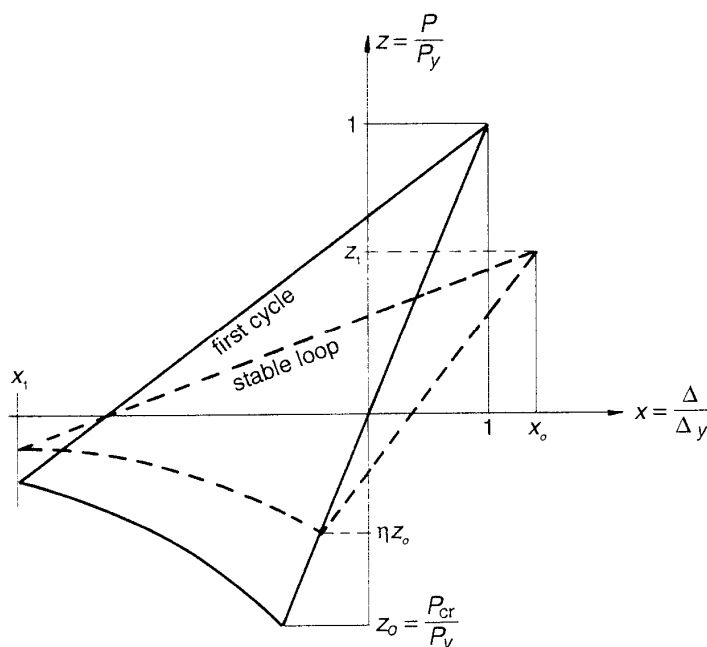


**Fig. 6.1** Characteristics of a stable hysteretic loop

**Table 6.1** Characteristics of the stable hysteretic loop according to Fig. 6.1

Reference	$x_0$	$x_I$	$\eta$	$z_I$	cross-section
Jain 1980	2	-12	0.5	1	SHS
Liu and Goel 1988	2	-10	0.5	0.5	RHS
Matsumoto 1987	2	-10	0.5	0.5	CHS
Nonaka 1977	4	-4	0.5	0.8	Solid square
Ochi 1990	1	-10	0.5	0.5	CHS
Papadrakakis 1987	1	-4	0.5	0.5	CHS
Prathuangsit 1978	1	-12	0.5	0.5	I
Shibata 1982	5	-5	0.5	0.5	I

Another important problem is the local buckling. According to many authors, e.g. Lee and Goel (1987), it is recommended to avoid local buckling. Unfortunately, one can find very few proposed values for the limiting  $D/t$  or  $b/t$  ratios,



in the case of cyclic plastic stress. For CHS Zayas et al. (1982) proposed  $(D/t)_L = 6820/f_y$  where  $f_y$  is the yield stress in MPa, thus, for yield stress of 235 and 355 MPa one obtains 29 and 20, respectively.

For SHS or RHS Liu and Goel (1988) proposed  $(b/t)_L = 14$  for  $f_y = 371$  MPa, thus, we take for 355 MPa the value of 15 and for 235 MPa  $15(355/235)^{0.5} = 19$ . Sizes of SHS and RHS sections can be found in Appendices A, B.

The limitation of the strut slenderness plays also an important role. API (1989) proposed  $KL/r < 80$ .

The relationship axial force - axial shortening  $(P - \Delta)$  (Fig. 6.2) has been derived for CHS struts by Supple and Collins (1980) using the simple plastic hinge method:

The bending moment at the middle of the rod is  $M = a_o P$ , thus  $a_o = M/P$ . The plastic axial shortening is caused by curvature, so (Fig. 6.2)

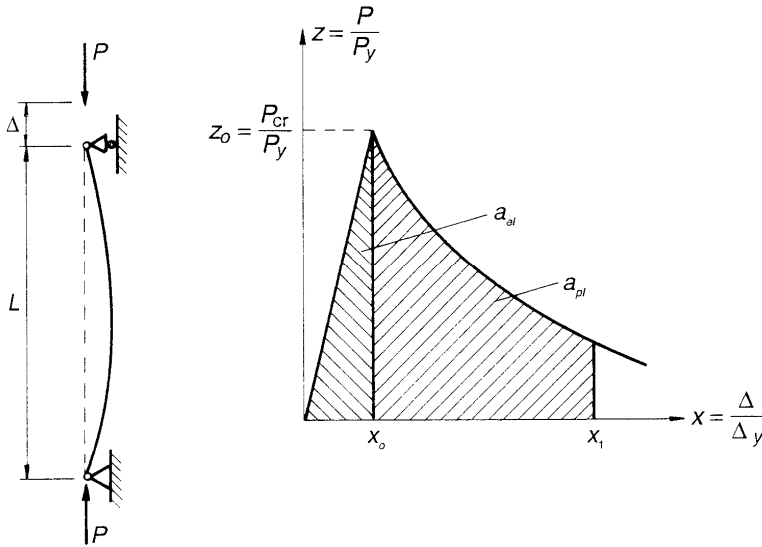


**Fig. 6.2** Post-buckling behaviour and the related specific areas

$$\Delta_{pl} = \int_0^L (ds - dx) \cong \frac{1}{2} \int_0^L \left( \frac{dy}{dx} \right)^2 dx \quad (6.1)$$

since

$$\frac{ds}{dx} = \sqrt{\left( \frac{dy}{dx} \right)^2 + 1} \approx 1 + \frac{1}{2} \left( \frac{dy}{dx} \right)^2 \quad (6.2)$$

Taking  $y = a_0 \sin(\pi x / L)$  we obtain

$$\Delta_{pl} = \frac{1}{2} \int_0^L \frac{\pi^2 a_0^2}{L^2} \cos^2\left(\frac{\pi x}{L}\right) dx = \frac{\pi^2 a_0^2}{4L} = \frac{\pi^2}{4L} \left(\frac{M}{P}\right)^2. \quad (6.3)$$

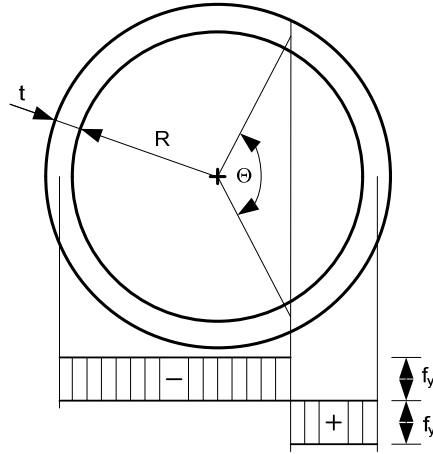


**Fig. 6.3** Plastic stress distribution

The squash load is  $P_y = 2R\pi f_y$ . The plastic stress distribution shown in Fig. 6.3 can be divided into two parts, one of them is caused by the compressive force, the second is caused by the bending moment. The plastic compressive force is

$$P = 2f_y R\pi - 2f_y R\Theta = P_y \left(1 - \frac{\Theta}{\pi}\right) \quad (6.4)$$

from which

$$\frac{\Theta}{2} = \frac{\pi}{2} - \frac{\pi P}{2P_y}. \quad (6.5)$$

The bending moment of the plastic zone is

$$M = 2 \int_0^{\Theta/2} R \cos(\varphi) (2f_y t R d\varphi) = 4f_y R^2 t \sin \frac{\Theta}{2} \quad (6.6)$$

where

$$\sin \frac{\Theta}{2} = \cos \left( \frac{\pi P}{2 P_y} \right) \quad (6.7)$$

Thus,

$$\Delta_{pl} = \frac{D^2}{4L} \left[ \frac{P_y}{P} \cos \left( \frac{\pi P}{2 P_y} \right) \right]^2 \quad (6.8)$$

and

$$\Delta = \Delta_{el} + \Delta_{pl} = \frac{PL}{AE} + \frac{\alpha D^2}{4L} \left[ \frac{P_y}{P} \cos \left( \frac{\pi P}{2 P_y} \right) \right]^2 \quad (6.9)$$

where  $\alpha$  is the end restraint factor, for pinned ends  $\alpha = 1$ , for fixed ends  $\alpha = 4$ .

Using notations  $x = \Delta / \Delta_y$ ,  $z = P / P_y$ ,  $z_0 = P_{cr} / P_y$ ,  $x_0 = \Delta_{el} / \Delta_y = P_{cr} / P_y = z_0$

Eq. (6.8) can be written in the form

$$x - x_0 = C_1 \left[ \frac{\cos^2(\pi z / 2)}{z^2} - C_2 \right];$$

$$C_1 = \frac{\alpha D^2 E}{4 L^2 f_y} : C_2 = \frac{\cos^2(\pi z_0 / 2)}{z_0^2} \quad (6.10)$$

For  $z < 0.4$  the following approximation is acceptable

$$\cos(\pi z / 2) \approx 1 - \pi^2 z^2 / 8 \quad \text{and} \quad \cos^2(\pi z / 2) \approx 1 - \pi^2 z^2 / 4 \quad (6.11)$$

and Eq.(6.10) takes the form

$$x - x_0 = C_1 \left( \frac{1}{z^2} - \frac{\pi^2}{4} - C_2 \right) \quad (6.12)$$

from which one obtains

$$z = C_1^{1/2} \left( x - x_0 + \frac{C_1 \pi^2}{4} + C_1 C_2 \right)^{-1/2} \quad (6.13)$$

The areas shown in Fig. 6.2 can be calculated as follows:

$$a_{el} = z_0^2 / 2 \quad (6.14)$$

and

$$a_{pl} = \int_{x_0}^{x_1} z dx = 2C_1^{1/2} \left[ \left( x_1 - x_0 + \frac{C_1 \pi^2}{4} + C_1 C_2 \right)^{1/2} - \left( \frac{C_1 \pi^2}{4} + C_1 C_2 \right)^{1/2} \right] \quad (6.15)$$

It is possible to derive similar formulae for SHS struts. The results are as follows.

$$A_{pl} = \frac{\alpha \pi^2}{4L} \left( \frac{M}{P} \right)^2 = \frac{\alpha \pi^2 b^2}{16L} \left( \frac{3}{4z} - z \right)^2 \quad (6.16)$$

and

$$x - x_0 = \frac{A_{pl}}{A_y} = C_3 \left( \frac{3}{4z} - z \right)^2 + C_4; \quad (6.17)$$

$$C_3 = \frac{\alpha \pi^2 b^2}{16L^2 f_y}; \quad C_4 = C_3 \left( \frac{3}{4z_0} - z_0 \right)^2$$

Expressing  $z$  from Eq. (6.17) we obtain

$$z = \frac{1}{2C_3^{1/2}} \left[ (x - x_0 + 3C_3 + C_4)^{1/2} - (x - x_0 + C_4)^{1/2} \right] \quad (6.18)$$

and the area in the post-buckling range is

$$a_{pl} = \int_{x_0}^{x_1} z dx = \frac{1}{3C_3^{1/2}} \left[ (x_1 - x_0 + 3C_3 + C_4)^{3/2} - (x_1 - x_0 + C_4)^{3/2} - (3C_3 + C_4)^{3/2} + C_4^{3/2} \right] \quad (6.19)$$

We consider the stable hysteretic loop according to Fig. 6.4. The whole specific absorbed energy as the area shown in Fig. 6.4 is

$$\sum_i a_i = a_{el} + a_{pl} + 10x_0.5/2 - 10.5z_{\min}/2 \quad (6.20)$$

For  $a_{el}$  and  $a_{pl}$  we use Eqs. (6.14), (6.15) or (6.19), but instead of  $x_0 = z_0$  we calculate with  $\eta x_0 = \eta z_0, \eta = 0.5$ .  $z_{\min}$  is calculated using Eq. (6.13) or (6.18) taking  $x=10$  and instead of  $x_0$  taking  $0.5x_0$ .

The energy absorbing capacity of a strut is

$$F_{bo} = \left( \sum_i a_i \right) f_y A \quad (6.21)$$

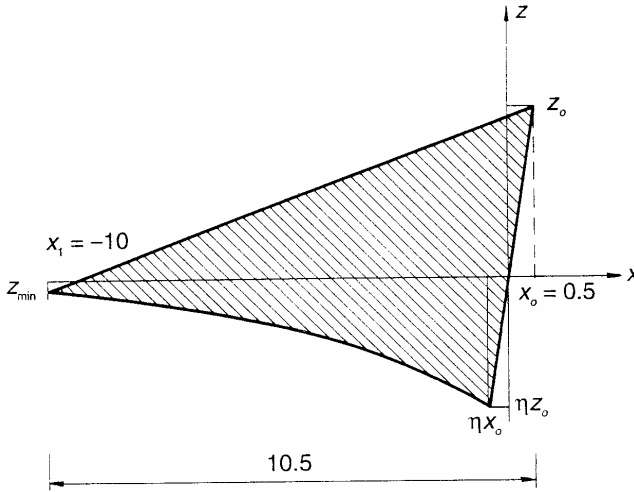


**Fig. 6.4** Area of the stable hysteretic loop

### 6.1.2 Seismic Design of a Portal Frame

Consider a square symmetrical portal frame shown in Fig. 6.5 carrying a silo. The mass of the silo is divided to four forces  $F$  acting on the middle of beams. The seismic shear forces  $F_b$  are acting also in these points.

#### 6.1.2.1 Calculation of the Seismic Force

According to Eurocode 8 (2008)

$$F_b = S_d(T_1) m \lambda, \quad (6.22)$$

where  $S_d(T_1)$  = the ordinate of the design spectrum at period  $T_1$ ,  $m$  = the silo mass,  $\lambda$  = correction factor. Values of the parameters describing the recommended Type 1 elastic response spectra are as follows: ground type C is selected,  $S = 1.15$ ,  $T_B = 0.20$ ,  $T_C = 0.60$ ,  $T_D = 2.0$ .

$T_I$  (s) is approximated by the expression:

$$T_1 = C_1 H^{0.75}, C_1 = 0.085, H = 4, T_1 = 0.24 \text{ s}, \quad (6.23)$$

$$\text{for } T_B < T_I < T_C, \quad S_d = \alpha S \frac{2.5}{q}. \quad (6.24)$$

We use the highest value applied for Japan  $\alpha = 0.40$ , the behaviour factor  $q = 5.5$ . Thus  $S_d = 0.4 \times 1.15 \times 2.5 / 5.5 = 0.2091$ , required cross-section Class 1 (plastic).

For  $T_I < 2T_C$   $\lambda = 0.85$ .

Thus, the silo mass  $m$  should be multiplied by  $0.85 \times 0.2091 = 0.1777$ . The silo mass is 1000 kN, the seismic horizontal force acting on a beam is  $F_b = 0.1777 \times 250 = 44.25$  kN.

According to Eurocode 8 (2008) the seismic action has two perpendicular components. Therefore this horizontal seismic force should be multiplied by a spatial factor. In the case of square symmetry of the structural plan, this factor is 1.3. Thus, the actual seismic force is  $F_b = 1.3 \times 44.25 = 57.52$  kN.

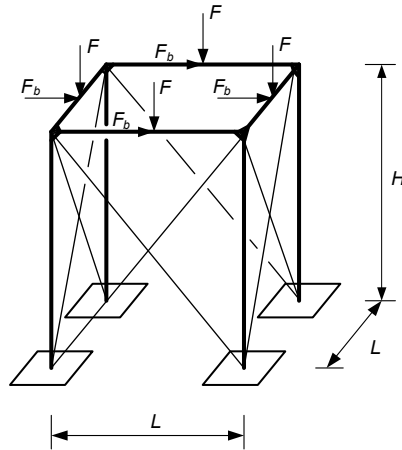


**Fig. 6.5** Supporting X-braced portal frame structure with vertical and horizontal forces

The horizontal force acting on the braced frame is

$$F_b - F_{b0} / \sqrt{2} \quad (6.25)$$

When the force calculated with Eq. (6.25) is negative then the horizontal force is 0. In this case the force acting on the brace is  $F_{br} = F_b / \sqrt{2}$ .

Load combination:  $\sum G_k + \psi_E Q_k, \psi_E = \varphi \psi_{21} = 1$ , since, for storage structures,  $\varphi = \psi_{21} = 1$ .

In order to ease the fabrication we use here equal square hollow sections (SHS) (Fig. 6.7) for beams and columns, i.e.  $A_1 = A_2, h_1 = b_1 = b_2, t = t_1 = t_2$ . Thus, the moments of inertia are also equal  $I_{z1} = I_{z2} = I_{y1} = I_{y2}$ .

### 6.1.2.2 Normal Forces and Bending Moments in Vertical Frames (Fig. 6.6)

According to Glushkov et al. (1975)

$$H_A = \frac{3M_A}{H}, \quad M_A = \frac{M_B}{2}, \quad M_B = \frac{FL}{4(k+2)},$$

$$k = \frac{I_{y2}H}{I_{y1}L}, \quad (6.26)$$

$$M_E = \frac{FL}{4} - M_B, \quad M_1 = \frac{3F_b H k}{2(6k+1)}, \quad V_{D1} = \frac{2M_1}{L}, \quad (6.27)$$

$$N_1 = F + V_{D1}, \quad H_{D1} = \frac{k+1}{k+2} F_b \quad (6.28)$$

$$M_{A1} = \frac{3k+1}{6k+1} F_b H, \quad M_{B1} = \frac{3k}{6k+1} F_b H,$$

$$H_2 = \frac{3k}{6k+1} H, \quad (6.29)$$

$$M_{Bt} = M_B + M_{B1}, \quad M_{At} = M_A + M_{A1} \quad (6.30)$$

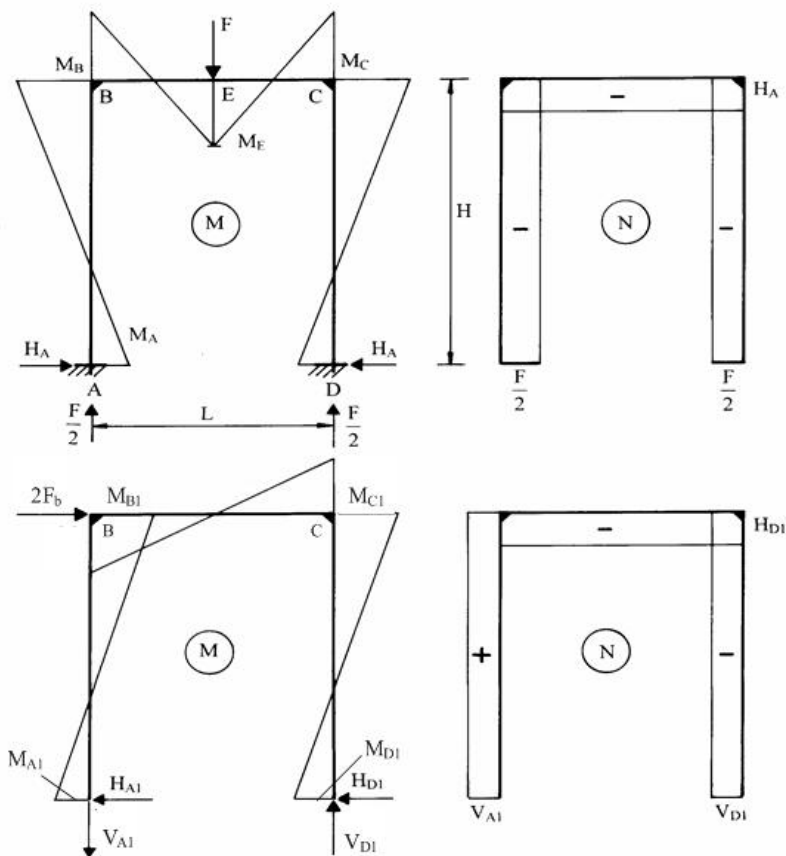


**Fig. 6.6** Diagrams for the bending moments and normal forces of a frame

### 6.1.2.3 Geometric Characteristics of the Square Hollow Section (Fig. 6.7)

Areas and moments of inertia are calculated according to DAST Richtlinie 016 (1986)

Area of the cross-section for columns and beams

$$A_I = 4t_I(b_I - t_I) \left( 1 - 0.43 \frac{2t_I}{b_I - t_I} \right) \quad (6.31)$$



moment of inertia for columns and beams

$$I_x = I_y = \left[ \frac{2(b_l - t_l)^3 t_l}{3} \right] \left( 1 - 0.86 \frac{2t_l}{b_l - t_l} \right) \quad (6.32)$$

where  $b_l = h_l$ .

section modulus for columns and beams

$$W_y = W_z = \frac{2I_y}{b_l} \quad (6.33)$$

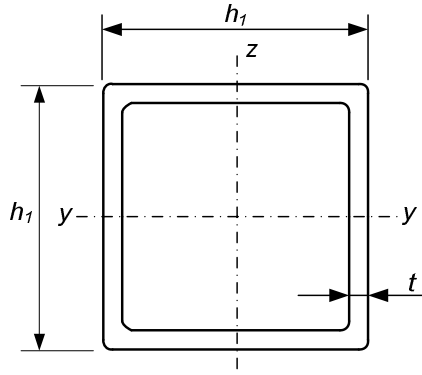


**Fig. 6.7** Dimensions of a square hollow section (SHS)

#### 6.1.2.4 Calculation of the Elastic Sway

$$u_e = u_f + u_b + u_t + u_{tl}, \quad (6.34)$$

where  $u_f$  = the sway of the frame,  $u_b$  = displacement due to bending of a beam in horizontal plane,  $u_t$  = beam displacement due to frame corner angle deformation,  $u_{tl}$  = beam displacement due to torsion.

$$u_f = \frac{2M_{A1} m_{A1} H_1}{3EI_{x1}} + \frac{2M_{B1} m_{B1} H_2}{3EI_{x1}} + \frac{M_{B1} m_{B1} L}{3EI_{x2}}, \quad (6.35)$$

where

$$M_{A1} = \frac{3k+1}{6k+1} F_b H; m_{A1} = \frac{3k+1}{6k+1} \frac{H}{2}; H_1 = \frac{3k+1}{6k+1} H, \quad (6.36)$$

$$M_{B1} = \frac{3k}{6k+1} F_b H; m_{B1} = \frac{3k}{6k+1} \frac{H}{2}; H_2 = \frac{3k}{6k+1} H; k = \frac{I_{x2} H}{I_{x1} L}, \quad (6.37)$$

The displacement  $u_b$  due to two horizontal forces  $F_b$  in the horizontal plane of the frame with rigid corners is calculated as follows. The corner bending moment  $M$  can be obtained from the equation of angular deformations (Fig. 6.8)

$$\varphi_1 = \varphi_2, \quad EI_{y2} \varphi_1 = \frac{F_b L^2}{16} - \frac{ML}{2}, \quad EI_{y2} \varphi_2 = \frac{ML}{6}. \quad (6.38)$$

Considering Eq. (6.38) one obtains

$$M = \frac{3F_b L}{32}, \quad (6.39)$$

and the displacement from  $F_b$  and  $M$

$$u_b = \frac{F_b L^3}{48EI_{y2}} - \frac{ML^2}{8EI_{y2}} = \frac{7F_b L^3}{768EI_{y2}}. \quad (6.40)$$

The displacement due to angle deformation of the beam caused by the frame corner angle deformation can be obtained from

$$u_t = \frac{1}{2EI_{y1}} (M_{A1} H_1 - M_{B1} H_2) \frac{h_1}{2} \quad (6.41)$$

Finally, the beam deformation due to torsion is

$$u_{t1} = \varphi_t \frac{h_1}{2}; \varphi_t = \frac{F_b h_1 L}{8GI_{t2}}; I_{t2} = h_1^3 t_2; u_{t1} = \frac{F_b L}{16Gh_1 t_2}. \quad (6.42)$$

### 6.1.2.5 Constraint on Sway Limitation

The allowable sway is calculated as follows. The elastic displacement for ductile non-structural elements should fulfil the following limitation

$$u_e \leq \frac{0.0075H}{\gamma_1 q \nu} = \frac{0.0075 \times 5000}{1.4 \times 4 \times 0.4} = 16.7 \text{ mm} \quad (6.43)$$

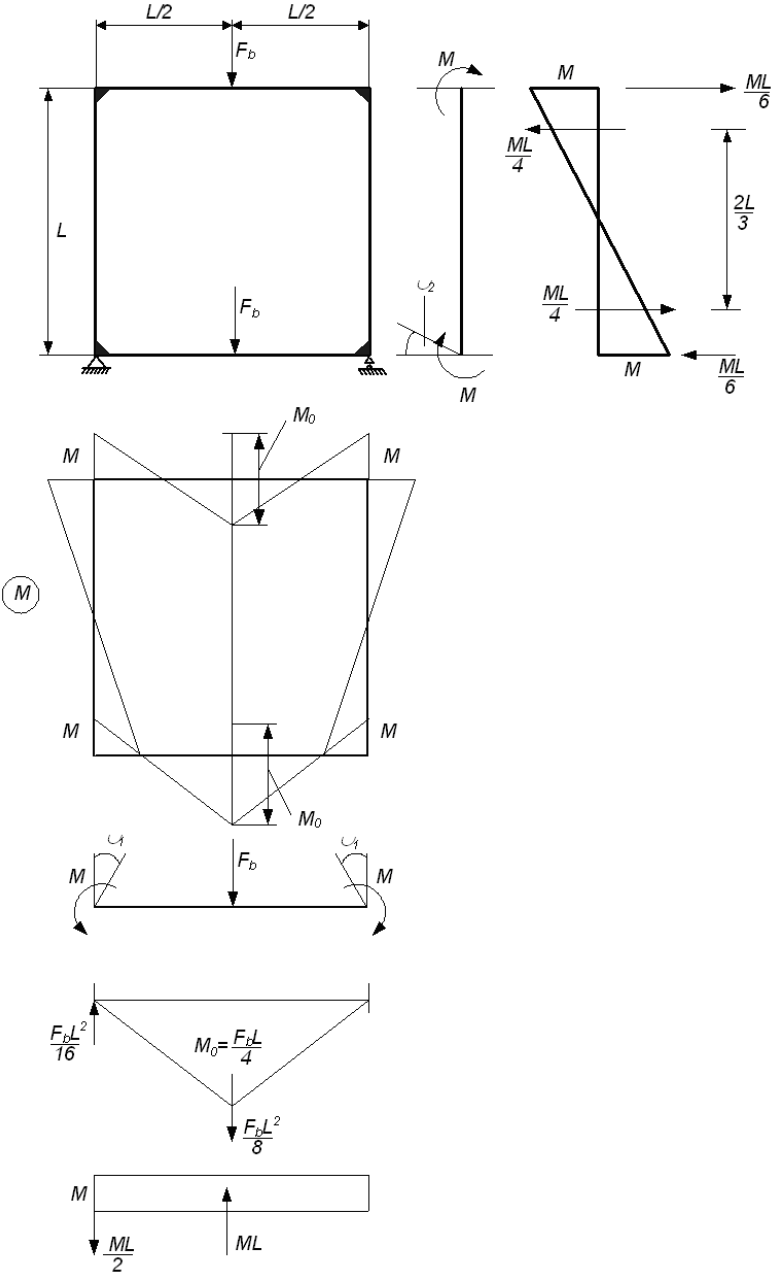


**Fig. 6.8** Bending moment diagram and calculation of angular deformations due to forces  $F_b$  in the horizontal plane

Importance class for power plants is IV. Structural height  $H = 5000$  mm. The recommended safety factor for importance class IV is  $\gamma_I = 1.4$ . The reduction factor  $\nu = 0.4$ . Behaviour factor  $q = 4$ .

### 6.1.2.6 Local Buckling Constraints

For SHS columns and beams of section class 1 (plastic) the constraint is given by:

$$\frac{h_1 - 3t_i}{t_i} = \frac{h_1}{t_i} - 3 \leq 33\varepsilon, \varepsilon = \sqrt{\frac{235}{f_y}}, i = 1, 2. \quad (6.44)$$

$$\text{For braces} \quad b/t \leq 19. \quad (6.45)$$

### 6.1.2.7 Stress Constraint for the Columns

According to Eurocode 3 (2005) the SHS section is not susceptible to torsional deformations, thus  $\chi_{LT} = 1$ ,  $k_{yx} = 0$  and the second constraint in EC3 should not be considered.

$$\frac{N_1}{\chi_{1,min} A_1 f_{y1}} + \frac{k_{yy1}(M_C + M_{B1})}{W_{y1} f_{y1}} + \frac{k_{zz1}(M_C)}{W_{z1} f_{y1}} \leq 1, \quad \text{or } C_1 \leq 1 \quad (6.46)$$

$$k_{yy1} = \min \left( C_{my1} \left( 1 + \frac{0.6 \lambda_{y1}(H_A + H_{D1})}{\chi_{y1} A_1 f_{y1}} \right), C_{my1} \left( 1 + \frac{0.6(H_A + H_{D1})}{\chi_{y1} A_1 f_{y1}} \right) \right) \quad (6.47)$$

$$C_{my1} = 0.4, \quad (6.48)$$

$$r_{y1} = \left( \frac{I_{y1}}{A_1} \right)^{0.5}; r_{z1} = \left( \frac{I_{z1}}{A_1} \right)^{0.5}; \bar{\lambda}_{y1} = \frac{K_{y1} H}{r_{y1} \lambda_E}; \quad (6.49)$$

The value of  $K_{y1}$  and  $K_{x1}$  are taken according to Eurocode 3 (2005)

$$K_{y1} = 2.19; \bar{\lambda}_{z1} = \frac{K_{z1} H}{r_{z1} \lambda_E}; K_{z1} = 0.5$$

$$\bar{\lambda}_{1,max} = \max(\bar{\lambda}_{y1}, \bar{\lambda}_{z1}), \quad (6.50)$$

$$\chi_{i.min} = \frac{1}{\phi_i + \left( \phi_i^2 - \bar{\lambda}_{i.max}^2 \right)^{0.5}}; \quad i = 1, 2,$$

$$\phi_i = 0.5 \left[ 1 + 0.34 \left( \bar{\lambda}_{i.max} - 0.2 \right) + \bar{\lambda}_{i.max}^2 \right] \quad (6.51)$$

### 6.1.2.8 Stress Constraint for the Beams

$$\frac{H_A + H_{D1}}{\chi_{2.min} A_2 f_{y1}} + \frac{k_{yy2} M_E}{W_{y2} f_{y1}} + \frac{k_{yz2} M}{W_{z2} f_{y1}} \leq 1, \quad f_{y1} = \frac{f_y}{\gamma_{M1}} \quad \text{or} \quad C_2 \leq 1 \quad (6.52)$$

The flexural buckling factor is

$$\chi_i = \frac{1}{\phi_i + \left( \phi_i^2 - \bar{\lambda}_i^2 \right)^{0.5}}; \quad \phi_i = 0.5 \left[ 1 + 0.34 \left( \bar{\lambda}_i - 0.2 \right) + \bar{\lambda}_i^2 \right], \quad (6.53)$$

$$\bar{\lambda}_{y2} = \frac{K_{y2} L}{r_{y2} \lambda_E}; \quad (6.54)$$

the effective length factor is  $K_{y2} = 0.5$ ,

$$r_{y2} = \left( \frac{I_{y2}}{A_2} \right)^{0.5}; \quad \lambda_E = \pi \left( \frac{E}{f_y} \right)^{0.5}. \quad (6.55)$$

$E$  is the elastic modulus.

$$\bar{\lambda}_{z2} = \frac{K_{z2} L}{r_{z2} \lambda_E}; \quad (6.56)$$

the effective length factor is  $K_{z2} = 0.5$ ,

$$r_{z2} = \left( \frac{I_{z2}}{A_2} \right)^{0.5}, \quad (6.57)$$

$\chi_{2,min}$  is calculated from  $\bar{\lambda}_{2,max} = \max(\bar{\lambda}_{y2}, \bar{\lambda}_{z2})$ .

$$k_{yy2} = \min \left( C_{my2} \left( 1 + \frac{0.6\lambda_{y2}(H_A + H_{D1})}{\chi_{y2}A_2f_{y1}} \right), C_{my2} \left( 1 + \frac{0.6(H_A + H_{D1})}{\chi_{y2}A_2f_{y1}} \right) \right),$$

$$C_{my2} = 0.9, \quad (6.58)$$

$$k_{zz2} = \min \left( C_{mz2} \left( 1 + \frac{0.6\lambda_{z2}(H_A + H_{D1})}{\chi_{z2}A_2f_{y1}} \right), C_{mz2} \left( 1 + \frac{0.6(H_A + H_{D1})}{\chi_{z2}A_2f_{y1}} \right) \right),$$

$$C_{mz2} = 0.4, \quad k_{yz2} = 0.8k_{yy2}. \quad (6.59)$$

### 6.1.2.9 Investigation of the Joint of the Beam and Brace

Constraint on the beam (chord) plastification

For a Y joint of SHS profiles according to Static Design Procedure (2009)

$$F_{br} \leq N^* = Q_u Q_f \frac{f_{y1} t_1^2}{\sin \theta} \quad (6.60)$$

$f_{y1}$  is the yield stress of the beam,  $t_1 = t_2$  thickness of the beam

$$Q_u = \frac{2\eta}{(1-\beta)\sin \theta} + \frac{4}{\sqrt{1-\beta}}, \eta = \beta = \frac{b}{b_1} \quad (6.61)$$

$b$  the brace width,  $b_1$  the beam width

$$Q_f = (1 - |n|)^{C_1}, C_1 = 0.6 - 0.5\beta,$$

$$|n| = \frac{N_1}{N_{1,pl}}, N_1 = H_A + H_{D1}, N_{1,pl} = f_{y1} A \quad (6.62)$$

$N_0$  is the compression force in the beam,  $A = A_2$  is the cross-section area of the beam.

Constraint on chord punching shear

$$F_{br} \leq N_1^* = \frac{0.58f_{y1}t_1}{\sin \theta} L_{b,eff}, \quad L_{b,eff} = 2b + 2b_e - 4t, \quad b_e = \frac{10}{b_1/t_1} \frac{f_{y1}t_1}{f_y t} b \quad (6.63)$$

### 6.1.2.10 The Cost Function

The cost function includes the material, fabrication and painting costs as follows

$$K = K_M + K_F + K_p, \quad K_M = k_M \rho V_1, \rho = 7.85 \times 10^{-6} \text{ kg/mm}^3, \quad (6.64)$$

$$V_I = V + V_b + V_h, \quad (6.65)$$

Volume of the frame

$$V = 4A_2H + 4A_1L. \quad (6.66)$$

Volume of X-braces

$$V_b = 8aA_b, a = \sqrt{H^2 + L^2} \quad (6.67)$$

volume of head plates

$$V_h = 4 \times 3.5 h_1^2 t_h, t_h = 8 \text{ mm}, \quad (6.68)$$

Number of assembled elements  $\kappa = 12$ , with braces 20, the welding cost factor and the difficulty factor for a spatial structure  $k_w = 1.0$  \$/min,  $\Theta = 3$ , the factors for welding position to be multiplied with welding times are as follows: downhand 1, vertical 2, overhead 3.

The welding cost

$$K_w = k_w \left[ \Theta \sqrt{\kappa \rho V_1} + 1.3(T_1 + T_2 + T_3 + T_4) \right] \quad (6.69)$$

Welding time for the connection of a SHS beam to a SHS column with 2 vertical, one overhead and one downhand single bevel (1/2V) butt SMAW weld of size  $t_1$  and length  $b_1$

$$T_1 = 8 \times 8 \times 0.5214 \times 10^{-3} b_1 t_1^2 \quad (6.70)$$

welding time for the connection of a head plate to the frame corner with overhead fillet welds of size 5 mm and length  $6h_1$  and with downhand fillet welds of length  $2h_1$

$$T_2 = 4(3 \times 6 + 2) b_1 0.7889 \times 10^{-3} 5^2 \quad (6.71)$$

Welding time for joints of braces to beams with fillet welds

$$T_3 = 8(2 + 2\sqrt{2}) \times 3b \times 0.7889 \times 10^{-3} t^2 \quad (6.72)$$

Welding time for joints of braces together

$$T_4 = 4 \times 4(3 + 1)b \times 3.13 \times 10^{-3} t \quad (6.73)$$

Painting cost

$$K_p = k_p S_p, k_p = 28.8 \times 10^{-6} \text{ \$/mm}^2 \quad (6.74)$$

The superficies to be painted

$$S_p = 16b_1(H + L) + 8ab \quad (6.75)$$

#### 6.1.2.11 Optimization and Results

Numerical data:  $E = 2.1 \times 10^5$  MPa,  $G = 0.8 \times 10^5$  MPa,  $H = L = 5000$  mm,  $F = 250$  kN,  $2F_b = 1.3 \times 88.85 = 115.50$  kN.

The suitable SHS for columns and beams are selected using a cold-formed SHS catalogue EN 10219. Since the minimum thickness is limited by the local buckling constraint (Eq.28), only that thicknesses can be used, which are larger than this limit, e.g. for  $b_l = 220$   $t_l = 6.3$ , for  $b_l = 250$   $t_l = 8$ , for  $b_l = 260$   $t_l = 8$  and for  $b_l = 300$   $t_l = 10$  mm, for  $b_l = 400$   $t_l = 12$  mm Therefore the number of SHS to be investigated is limited.

**Table 6.2** Data for some brace profiles, dimensions in mm

$b$	$t$	$b/t$	$A_b, \text{mm}^2$	$r$	$\lambda$	$F_{br}$ kN
100	6	17	2160	37.9	70	1464
90	5	18	1640	34.3	77	1037
80	5	16	1440	30.3	87	816

It should be mentioned that the values of  $F_{rb}$  are larger than the required value of 115.05 kN.

Note that the frame without braces fulfils the constraint on sway, since the sway is  $10.1 < 16.7$  mm.



**Table 6.3** Volume and cost in function of the dimensions of the frame profiles. The values of  $C_1$  and  $C_2$  show that the profile of beams and column fulfil the constraints on stress.

$F$ kN	$F_b$ kN	Beam	$C_1$	$C_2$	Braces	$V \times 10^{-8} \text{ mm}^3$	$K$ \$
250	115.05	300x16	0.869	0.979	---	6.941	11540
<b>250</b>	<b>0</b>	<b>300x10</b>	<b>0.625</b>	<b>0.933</b>	<b>90x5</b>	<b>5.549</b>	<b>9596</b>
250	0	300x10	0.625	0.933	80x5	5.435	9389
250	0	300x10	0.625	0.933	70x4	5.192	8975

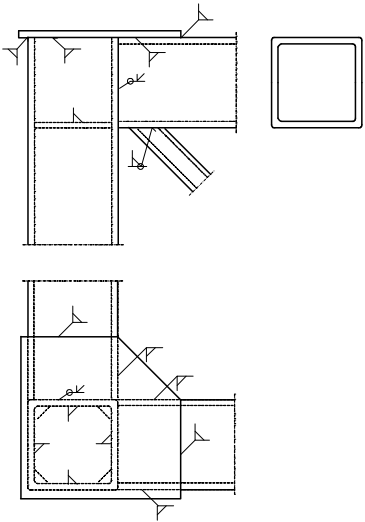


**Fig. 6.9** The welded frame corner

It can be seen that the structural volume and cost can be decreased using braces. The measure of savings depends on the brace profile. Table 6.2 shows that the profile 80x5 does not fulfil the requirement of  $\lambda \leq 80$ , thus it is recommended to use profile 90x5 (Table 6.3), for which the savings in volume is 20% and in cost 17%.

Note that the braces of profile 90x5 fulfil the constraint on chord plastification ( $N^* = 198.1 > 163.3$  kN) and on punching shear ( $N_1^* = 539.7 > 163.3$  kN), since the acting  $N_{br}$  is only 115.05 kN, although the capacity  $F_{br}$  given in Table 6.2 is larger than 115.05 kN.

**6.1.2.12 Conclusions**

The horizontal seismic forces and the allowable horizontal sway of a simple frame is calculated according to the Eurocode 8. The frame with rigid joints supports a silo, the failure of which caused by earthquake can be dangerous. The stress

constraints for columns and beams are formulated according to Eurocode 3. The frame is welded from SHS profiles. For the fabrication reasons the section width of columns and beams should be equal. Thus, the unknowns are the width and thickness of the basic frame and the braces. The minimum thicknesses are limited by the local buckling constraint for section of class 1 (plastic).

The detailed calculation of sway due to bending deformations of the frame in vertical and horizontal plane and due to the torsion of the beams is presented. The objective function is the structural volume or cost.

The optimum cross-sections are selected from a discrete series for SHS using a systematic search. Calculating the sway components it is found that the deformation due to torsion of beams and the sway from the angular deformation of frame corners can be neglected.

The governing constraints are the constraints on stress in beams and columns as well as the limitation of local and overall slendernesses of braces.

The use of braces results in significant savings in weight and cost of the whole structure.

## **6.2 Seismic Design of a V-Braced 3D Multi-storey Steel Frame**

### **Abstract**

The seismic design process is detailed for a spatial V-braced three-bay three-storey steel frame. In the case of a 3D frame the seismic forces should be multiplied by a factor prescribed in Eurocode 8. In this way the spatial frame can be regarded as a plan one. The V-bracing rods of circular hollow section (CHS) should absorb the seismic energy, but their overall buckling resistance should be smaller than the seismic rod force. The interstorey drift is so small that the braced frame can be designed as a non-sway one.

The beams of rolled UB profile are designed for normal force and bending moment, including the effect of the unbalanced force due to the buckling of braces. The columns of CHS profile are designed for compression force. The design of a bolted beam-to-column connection and a bolted joint of a brace is also treated. MathCAD algorithms are used to fulfil the design constraints.

### **6.2.1 Introduction**

The aim of the study is to show by a numerical problem the seismic design process of a spatial steel frame including the effect of concentric V-bracings. In the design of braces the energy absorbing capacity is also considered using the developed own formulae.

In the design of braces, beams and columns MathCAD algorithms are used in order to exactly fulfil the constraints, i.e. to obtain the most economic structure.

The rules of Eurocodes 3 and 8 are applied. Circular hollow sections are used for braces and columns and rolled UB profiles are applied for beams.

The design of the 3D frame is reduced to a planar one multiplying the seismic forces by a factor of 1.3. The beams and columns are designed as parts of a non-sway frame. The braces are designed to allow the overall buckling and to absorbing the seismic energy. In the design of beams the unbalanced force due to buckling of the compression brace is also considered.

The beams are subject to compression and bending and the columns are loaded by compression. In the design of beams and columns the actions due to seismic forces should be multiplied by a factor of 1.25. The design of beam-to-columns connections and the joints of braces is included.

A brief literature survey of V-braced steel frames is given as follows.

Medhekar and Kennedy (1999a,b) have investigated the seismic design of a concentrically braces single- and two-storey building using hollow section braces and W-section columns.

Mualla and Belev (2002) have shown a new friction damper device used for V-bracing.

Moghaddam et al. (2005) have treated the design of concentrically braced steel frames. The cross sections of beams and columns were unchanged during the optimization process and the braces have been designed to minimize the storey drift.

Longo et al. (2008) have designed a V-braced 3 bay 4 storey 3D building frame. HE European wide flange beam profiles have been used.

Ragni et al. (2011) have proposed analytical expressions for dissipative bracings and used them for the design of 5-bay 4- and 8-storey frames.

Roeder et al. (2011) have elaborated a simple design procedure for concentrically braced gusset plate connections considering the yield mechanism of such joints. In the appendix a detailed numerical example is given.

The design steps of the study are as follows.

1. Main dimensions of the given frame
2. Calculation of non-seismic and seismic loads
3. Design of circular hollow section (CHS) V-bracings
4. Design of rolled I-section beams
5. Design of CHS columns
6. Design of the beam-to-column connections and joints of braces

### ***6.2.2 Main Dimensions of the Given Frame***

The investigated frame is a 3D symmetric in plan, three-bay three-storey frame with V-bracings (Figure 6.10).

### 6.2.3 Loads

#### 6.2.3.1 Vertical Loads

Dead load (G): roof  $5.5 \text{ kN/m}^2$ , floors  $5.0 \text{ kN/m}^2$ , live load (Q)  $2.0 \text{ kN/m}^2$

$$G + \psi Q, \psi = \varphi \psi_2, \psi_2 = 0.3, \text{ for roof } \varphi_1 = 1, \text{ for floors } \varphi_2 = 0.5$$

Roof:  $5.5 + 0.3 \times 2 = 6.1 \text{ kN/m}^2$ , floors:  $5 + 0.15 \times 2 = 5.3 \text{ kN/m}^2$

For the whole area of  $8 \times 6 \times 6 = 288 \text{ m}^2$  and for all storeys

$$W = 6.1 \times 288 + 2 \times 5.3 \times 288 = 4809.6 \text{ kN}$$

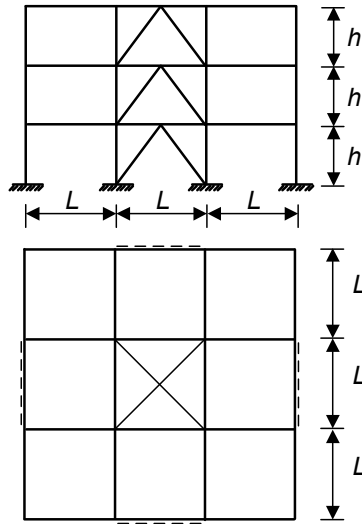


**Fig. 6.10** Elevation and ground-plan of the investigated frame. V-bracings are used in the outer plans, the central field is not loaded.  $L = 6 \text{ m}$ ,  $h = 3.6 \text{ m}$ .

#### 6.2.3.2 Seismic Load

According to Eurocode 8 (2008) the horizontal seismic force can be calculated as

$$F_b = S_d(T_1) m \lambda \quad (6.76)$$

For a centrally braced frame of height  $3 \times 3.6 = 10.8 \text{ m}$

$$T_1 = 0.050 \times 10.8^{0.75} = 0.298, q = 2.5 \quad (6.77)$$

For a subsoil of class C  $S = 1.15$ ,  $T_B = 0.2$ ,  $T_C = 0.6$ ,  $T_D = 2$ ,

For  $T_B < T_1 < T_C$ , calculating with  $a_g = 0.4 \text{ m/s}^2$

$$S_d = a_g S x 2.5 / q = 0.4 x 1.15 = 0.46 \text{ and } \lambda = 0.85 \quad (6.78)$$

$$F_b = 0.46 x 0.85 x 4809.6 = 1880 \text{ kN}$$

Distribution of the seismic force for roof and floors

$$F_i = \frac{z_i W_i}{\sum_i z_i W_i} \quad (6.79)$$

$$\sum_i z_i W_i = 3.6 x 288 (3 x 6.1 + 2 x 5.3 + 5.3) = 35458 \text{ kNm}$$

$$F_{roof} = 1880 \frac{3.6 x 3 x 6.1 x 288}{35458} = 1006 \text{ kN},$$

$$F_{floor2} = 1880 \frac{2 x 3.6 x 5.3 x 288}{35458} = 583 \text{ kN},$$

$$F_{floor1} = 1880 \frac{3.6 x 5.3 x 288}{35458} = 291 \text{ kN}$$

These horizontal seismic forces should be multiplied by 1.3 for the symmetric 3D frame and divided by 2 for a braced plane. Thus, for a braced plane the following horizontal seismic forces are acting (Figure 6.11):  $F_1 = 654$ ,  $F_2 = 379$ ,  $F_3 = 189$  kN.

## 6.2.4 Design of CHS V-Bracings

### 6.2.4.1 Constraint on Tensile Stress

$$S_b \leq A_b f_y, f_y = 235 \text{ kN} \quad (6.80)$$

where

$$S_b = F_s / L \quad (6.81)$$

is the tensile/compression force in a brace,  $F$  is the sum of horizontal seismic forces acting above the brace.

### 6.2.4.2 Constraint on Overall Buckling

$$S_{cr} = \chi A_b f_y \leq S_b, \quad \chi = \frac{1}{\phi + \sqrt{\phi^2 - \bar{\lambda}^2}} \quad (6.82)$$

since the compression brace should buckle to absorb the seismic energy.

$$\phi = 0.5 \left[ 1 + \alpha (\bar{\lambda} - 0.2) + \bar{\lambda}^2 \right], \alpha = 0.34 \quad (6.83)$$

$$\lambda = \frac{ks}{r}, s = \sqrt{h^2 + \left(\frac{L}{2}\right)^2} \quad (6.84)$$

$k = 0.7$  for 1b brace,  $k = 1$  for 2b and 3b braces.

$$\bar{\lambda} = \frac{\lambda}{\lambda_E}, \lambda_E = \pi \sqrt{\frac{E}{f_y}} \quad (6.85)$$

### 6.2.4.3 Constraint on Strut Slenderness for Seismic Zone

$$\lambda \leq 80 \quad (6.86)$$

### 6.2.4.4 Constraint on Energy Absorption Capacity

Using the formulae derived in Chapter 6.1

$$S_b \leq F_{br} = \left( \sum_i a_i \right) A_b f_y \quad (6.87)$$

$$\sum_i a_i = a_{el} + a_{pl} + 10 \frac{0.5}{2} - 10.5 \frac{z_{\min}}{2} \quad (6.88)$$

$$a_{el} = z_0^2 / 2, \quad z_0 = 0.5 \chi \quad (6.89)$$

$$a_{pl} = \int_{x_0}^{x_1} z dx = 2C_1^{1/2} \left[ \left( x_1 - x_0 + \frac{C_1 \pi^2}{4} + C_1 C_2 \right)^{1/2} - \left( \frac{C_1 \pi^2}{4} + C_1 C_2 \right)^{1/2} \right] \quad (6.90)$$

$$x_1 - x_0 = C_1 \left[ \frac{\cos^2(\pi z_0 / 2)}{z^2} - C_2 \right]; \quad C_1 = \frac{\alpha D^2 E}{4s^2 f_y}; \quad C_2 = \frac{\cos^2(\pi z_0 / 2)}{z_0^2} \quad (6.91)$$

$$\alpha = 1, z = \frac{S_b}{A_b f_y}, z_{\min} = C_1^{1/2} \left( x_1 - x_0 + \frac{C_1 \pi^2}{4} + C_1 C_2 \right)^{-1/2}, x_1 = 10 \quad (6.92)$$

The CHS dimensions are taken according to EN10210-2.

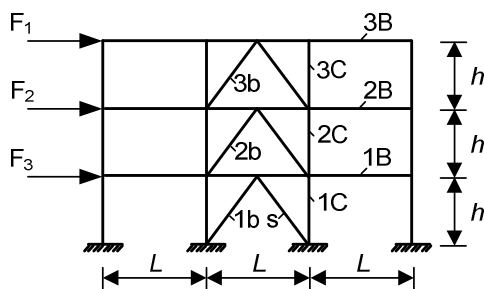


**Fig. 6.11** Horizontal seismic forces:  $F_1 = 654$ ,  $F_2 = 379$ ,  $F_3 = 189$  kN. b - braces, B - beams.

$$C - \text{columns. } s = \sqrt{h^2 + (L/2)^2}$$

#### 6.2.4.5 Design Results

Summary of the calculation results are given in Table 6.4.

**Table 6.4** Characteristics of bracings. Dimensions in mm, forces in kN.

Brace	$F$	$S_b$	$Dxt$	$A_b \text{ mm}^2$	Tension Eq. 6.80	$\lambda$ Eq. 6.86	$S_{cr}$ Eq. 6.82	$F_{br}$ Eq. 6.87
1b	1222	955	193.7x8	4670	1097	71.4	822	4647
2b	1033	807	177.8x8	4270	1003	71.4	709	3995
3b	654	511	177.8x5	2710	637	76.7	455	2558

It can be seen that the braces fulfil the constraints.  $F_{br}$  is much higher than  $F$ , since the decrease of the brace dimension is limited by the prescription of  $\lambda_{\max} = 80$ .

Let us calculate the deformation of the compressed brace 3b during the overall buckling. Using the formulae derived in the Section 6.1

$$\Delta = \Delta_{el} + \Delta_{pl} = \frac{S_{cr} s}{A_b E} + \frac{D^2}{4s} \left( \frac{S_y}{S_b} \cos \frac{\pi S_b}{2S_y} \right)^2 = \frac{455000 \times 4686}{2710 \times 2.1 \times 10^5} + \frac{177.8^2}{4 \times 4686} \left( \frac{637}{511} \cos \frac{\pi 511}{2 \times 637} \right)^2 \quad (6.93)$$

$$\Delta = 2.15 + 0.24 = 2.39 \text{ mm.}$$

The interstorey drift is the projection of the above value

$$\Delta_d = \Delta \frac{L}{2s} = 2.39 \frac{3}{4.69} = 1.53 \text{ mm.} \quad (6.94)$$

This small value of the interstorey drift shows that the braced frame can be designed as a non-sway one.

### 6.2.5 Design of Beams

Beams of UB profile are designed according to EC8 for vertical and seismic loads as members of a non-sway frame neglecting the support effect of bracings. The seismic forces are multiplied by 1.25.

Design of the beam 1B (Fig. 6.11).

$$f_y = 335 \text{ MPa}$$

Compression force is

$$N = 1.25 \times 1222 = 1528 \text{ kN}$$

Vertical load

$$p = 5.3 \times 3 = 15.9 \text{ kN/m}$$

Bending moment from vertical load as a beam built-up at the ends

$$M = pL^2/12 = 71.55 \text{ kNm} \quad (6.95)$$

According to Eurocode 8 (2008) the beam should be designed also for the unbalanced force due to the overall buckling of the compression brace. For the beams built-up at the ends

$$V = Fh/L, M_v = VL/8 \quad (6.96)$$

Stress constraint for  $N$  and  $M+M_v$  considering also the lateral torsional buckling



$$\frac{N}{\chi_y A f_y} + k_{yy} \frac{M + M_v}{\chi_{LT} W_y f_y} \leq 1 \quad (6.97)$$

$$\frac{N}{\chi_z A f_y} + k_{zy} \frac{M + M_v}{W_y f_y} \leq 1, k_{zy} = 0.8 k_{yy} \quad (6.98)$$

$$\lambda_i = \frac{L}{r_i}, \bar{\lambda}_i = \frac{\lambda_i}{\lambda_E}, i = y, z \quad (6.99)$$

$$\chi_i = \frac{1}{\phi_i + \sqrt{\phi_i^2 - \bar{\lambda}_i^2}}, \quad (6.100)$$

$$\phi_i = 0.5[1 + \alpha_i(\bar{\lambda}_i - 0.2) + \bar{\lambda}_i^2], \alpha_y = 0.21, \alpha_z = 0.34 \quad (6.101)$$

$$k_{yy} = C_{my} \left( 1 + 0.6 \bar{\lambda}_y \frac{N}{\chi_y A f_y} \right), C_{my} = 0.95 \text{ if } \bar{\lambda}_y \leq 1 \quad (6.102)$$

$$k_{yy} = C_{my} \left( 1 + 0.6 \frac{N}{\chi_y A f_y} \right) \text{ if } \bar{\lambda}_y \geq 1 \quad (6.103)$$

$$\chi_{LT} = \frac{1}{\phi_{LT} + \sqrt{\phi_{LT}^2 - 0.75 \lambda_{LT}^2}} \quad (6.104)$$

$$\phi_{LT} = 0.5[1 + \alpha_{LT}(\lambda_{LT} - 0.4) + 0.75 \lambda_{LT}^2], \alpha_{LT} = 0.49 \quad (6.105)$$

$$\lambda_{LT} = \sqrt{\frac{W_y f_y}{M_{cr}}}, M_{cr} = \frac{\pi^2 E I_z}{L^2} \sqrt{\frac{I_\omega}{I_z} + \frac{L^2 G I_t}{\pi^2 E I_z}} \quad (6.106)$$

The results are summarized in Table 6.5.

**Table 6.5** Characteristics of beams for braced fields. Stresses in MPa.

brace	$N$ (kN)	$p$ (kN/m)	$V$ (kN)	$M_V$ (kNm)	Profile UB	Stress constraints	
						Eq.(6.97)	Eq.(6.98)
1B	1528	15.9	733.2	550	610x305x149	0.806<1	0.758<1
2B	1291	15.9	621.0	466	610x229x140	0.903<1	0.952<1
3B	818	18.3	392.4	294	610x229x101	0.938<1	0.920<1

The beams fulfil the design constraints.

For the other non-braced fields, where  $M_V = 0$  the following beam dimensions can be used (Table 6.6).

**Table 6.6** Characteristics of beams for non-braced fields. Stresses in MPa.

brace	$N$ (kN)	$p$ (kN/m)	$V$ (kN)	$M_V$ (kNm)	Profile UB	Stress constraints	
						Eq.(6.97)	Eq.(6.98)
1B	1528	15.9	733.2	0	610x229x125	0.35<1,	0.89<1
2B	1291	15.9	621.0	0	610x229x113	0.35<1,	0.86<1
3B	818	18.3	392.4	0	533x210x82	0.41<1,	0.94<1

### 6.2.6 Design of Columns

Design of column 1C for overall buckling.

Compression force from horizontal seismic forces

$$N_h = 1.25 \times 1033 \frac{3.6}{6} = 775 \text{ kN}$$

Compression force from vertical loads

$$N_v = 1.1 \frac{(6.1 + 2 \times 5.3)6^2}{2} = 331 \text{ kN}$$

Total compression force

$$N = N_h + N_v = 1106 \text{ kN}$$

The effect of bending moments can be neglected, since the inertia of columns is much less than that of beams.

Self masses of beams, columns and braces as additional loads for columns are also taken into account: for column 3C 8 kN, for 2C 21 kN and for 1C 37 kN.

The columns can be designed for compression force only. The calculations show that the bending moments can be neglected, since the ratio of moments of inertia of beams and columns is very small.

Overall buckling constraint (see Section 6.2.4.2)

$$\frac{N}{A} \leq \chi_y f_y, f_y = 235 \text{ MPa} \quad (6.107)$$

For the column 1C  $k = 0.7$ , for columns 2C and 3C  $k = 1$ .

Characteristics of CHS profiles are taken from EN 10210-2. Sizes can be found in Appendix C.

Design results are given in Table 6.7.

**Table 6.7** Characteristics of CHS columns

Column	$N$ (kN)	CHS profile	$A$ (mm <sup>2</sup> )	$r$ (mm)	Constraint Eq. (6.107) (MPa)
1C	1143	219.7x8	5310	74.7	215<219
2C	737	193.7x8	4670	65.7	158<198
3C	129	114.3x3.6	1250	39.2	103<143

The column profiles fulfil the design constraints.

In order to show the economy of CHS profiles let us compare them with UC profiles. Since UC profiles are open sections, constraint on flexural-torsional buckling should also be taken into account with the following formulae (Farkas and Jármai 1997).

$$\frac{N}{A} \leq \chi_T f_y \quad (6.108)$$

$$\chi_T = \frac{1}{\phi_T + \sqrt{\phi_T^2 - \lambda_T^2}}, \quad \phi_T = 0.5[1 + \alpha_T(\lambda_T - 0.2) + \lambda_T^2], \quad \alpha_T = 0.49$$

$$\lambda_T = \sqrt{\frac{f_y}{\sigma_{Tcr}}}, \quad \sigma_{Tcr} = \frac{\pi^2 EI_\omega}{h^2 I_p} + \frac{GI_t}{I_p}, \quad I_p = I_y + I_z \quad (6.109)$$

The design results are given in Table 6.8. The overall flexural buckling constraint is checked according to formulae of Section 3.2 with respect to buckling around the axis  $z$ .

**Table 6.8** Characteristics of UC columns. Stresses in MPa.

Column	$N$ (kN)	UC profile	$A$ mm <sup>2</sup>	Constraint Eq.(6.107)	Constraint Eq.(6.108)
1C	1143	203x203x52	6628	172<195	172<190
2C	737	203x203x46	5873	125<163	125<185
3C	129	152x152x23	2925	44<122	44<166

The comparison of cross-sectional areas in Tables 6.7 and 6.8 shows the economy of CHS profiles over UC sections. Disregarding the column 3C for which the minimal UC profile is used, mass savings about 20% can be achieved by using CHS profiles.

## 6.2.7 Design of Joints

### 6.2.7.1 Beam-to-Column Connections

Let us check the bolts for 1B beam as shown in Fig. 6.12.

It is supposed that the bending moment causes forces only in the bolts of flange splices.

The shear resistance of bolts M27 of grade 10.9 (ultimate tensile strength 1000 MPa) according Eurocode 3 Part 1-8 is

$$F_R = \frac{2 \times 0.5 A f_{bu}}{\gamma_{M2}} = \frac{2 \times 0.5 \times 573 \times 1000}{1.25 \times 1000} = 458.4 \text{ kN} \quad (6.110)$$

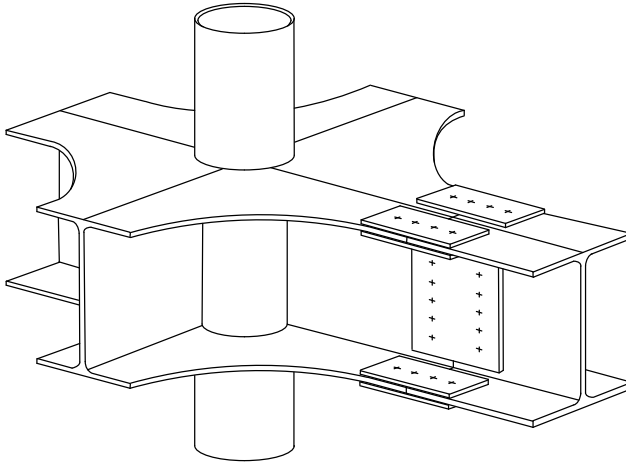


**Fig. 6.12** Beam-to-column connection

The forces in flange bolts caused by the bending moment  $M = 550 \text{ kNm}$  are

$$F_{BM} = 550000/602.6 = 912.8 \text{ kN},$$

For one bolt  $F_{BM1} = 912.8/4 = 228.2 \text{ kN}$ .

Forces in bolts from normal force  $N = 1532 \text{ kN}$   $F_{BN} = 1532/13 = 117.1 \text{ kN}$ .

Force in flange bolts from  $M$  and  $N$

$$F_f = 226.2 + 117.1 = 345.3 < 458.4 \text{ kN, OK.}$$

The shear force in the connection from  $V$  and  $p$

$$Q = \frac{V}{2} + \frac{pL}{2} = \frac{733.2}{2} + \frac{15.9 \times 6}{2} = 366.6 + 47.7 = 414.3 \text{ kN} \quad (6.111)$$

Force in one web bolt  $Q_w = 414.3/5 = 82.9 \text{ kN.}$

Shear force from  $N$   $F_{BN} = 117.1 \text{ kN.}$

Shear force from  $Q$  and  $N$  in one web bolt

$$F_w = \sqrt{82.9^2 + 117.1^2} = 143.5 < 458.4 \text{ kN, OK.}$$

The connections of rolled UB profile beams and CHS columns can be realized as shown in Fig. 6.12.

The beams are connected by bolted splices to flange and web plates welded to the columns.

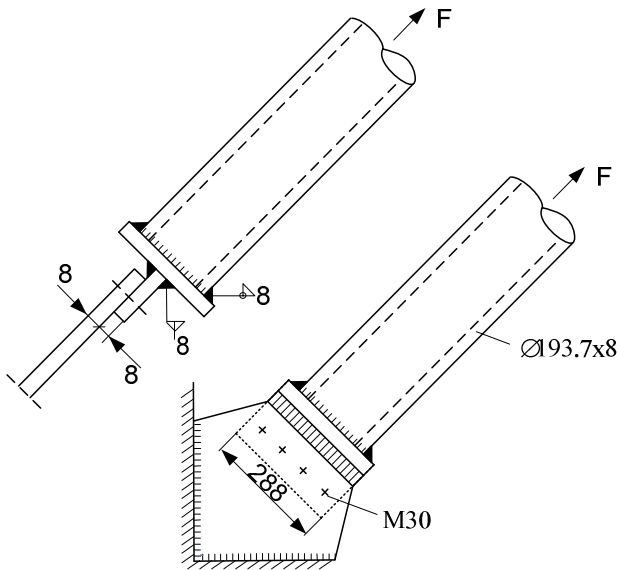


**Fig. 6.13** Bolted joint of a brace

### 6.2.7.2 Joints of Braces

The braces are connected to the columns and beams by bolted joints as shown in Fig. 6.13.

In the Fig. 6.13 the following dimensions are applied. The normal force acting in the brace 1b is  $F = 955$  kN. According to Eurocode 3 Part 1-8 (2002) the load capacity of four M30 bolts of grade 10.9 with ultimate tensile strength of  $1000 \text{ N/mm}^2$  is

$$F_v = \frac{4 \times 0.5 f_{ub} A}{\gamma_{M2}} = \frac{4 \times 0.5 \times 1000 \times 707}{1.25} = 1131 > 955 \text{ kN.} \quad (6.112)$$

The bearing resistance of 4 bolts for the plate thickness of  $t = 8$  mm is

$$F_b = \frac{1.5 f_u d t}{\gamma_{M2}} 4 = \frac{1.5 \times 1000 \times 30 \times 8 \times 4}{1.25 \times 1000} = 1152 > 955 \text{ kN} \quad (6.113)$$

The load capacity of  $a = 8$  mm size fillet welds is (for  $f_y = 235$  MPa)

$$F_w = \frac{2a288f_u}{1000\sqrt{3}\beta_w} = \frac{2 \times 8 \times 288 \times 360}{1000\sqrt{3} \times 0.8} = 1197 > 955 \text{ kN} \quad (6.114)$$

The load capacity of the  $a = 8$  mm fillet weld connecting the CHS brace

$$F_{w1} = \frac{D\pi f_u}{1000\sqrt{3}\beta_w} = \frac{193.7\pi \times 360}{1000\sqrt{3} \times 0.8} = 1265 > 955 \text{ kN.} \quad (6.115)$$

### 6.2.8 Conclusions

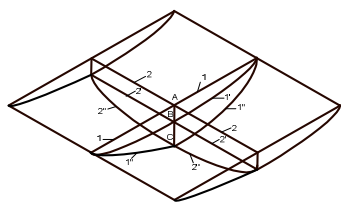
The overall buckling resistance of V-bracings should be smaller than the rod force caused by seismic forces, but the energy absorption capacity of braces should be large enough. The beams in the braced bay should be designed also for unbalanced vertical force due to buckling of compression braces. According to Eurocode 8, in the design of beams and columns the actions due to seismic forces should be multiplied by a factor of 1.25.

Since the interstorey drift of braced frame is very small, it can be designed as a non-sway one. The beams should be designed for compression force and bending moment including lateral- torsional buckling, while the columns are designed for overall buckling.

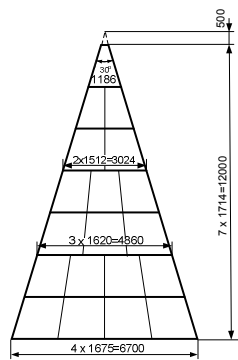
The columns are designed using also rolled UC profiles for the comparison with CHS profiles. In this case the open UC profiles should be checked against flexural-torsional buckling. The comparison shows that mass savings of about 20% can be achieved by using CHS profiles instead of UC sections.

In the design of braces, beams and columns special MathCAD algorithms are used to achieve economy due to fulfilling the design constraints as most exactly as possible.

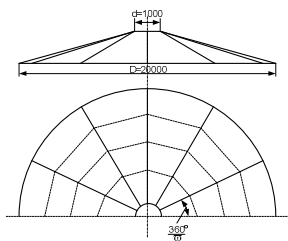
# Chapter 7 Stiffened Plates



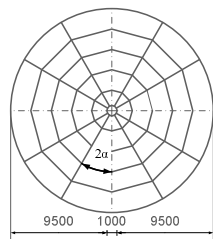
Section 7.1



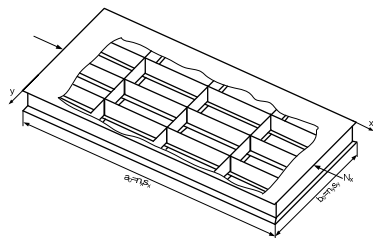
Section 7.2



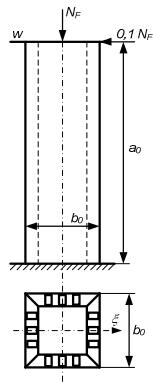
Section 7.3



Section 7.4



Section 7.5



Section 7.6

## 7.1 Minimum Cost Design of an Orthogonally Stiffened Welded Steel Plate with a Deflection Constraint

### Abstract

An assembly desk is constructed as a square plate stiffened by an orthogonal grid of ribs. The residual welding deflection is calculated applying the Okerblom's method. When the ribs are tacked to each other and to the base plate before welding, then the deflection is decreased by grid effect. The base plate thickness and the dimensions of stiffeners are optimized to minimize the cost and to fulfil the deflection constraint.. The optimization is performed with and without grid effect and it is shown that the grid effect decreases the cost significantly.

### 7.1.1 Introduction

The present study deals with the design of an assembly desk, for which the deflection constraint assures the exact operation, fitness for assembly and fabrication of structural parts. The sufficient stiffness is guaranteed by using a welded stiffened plate construction. The shrinkage of eccentric welds connecting the stiffeners to the base plate causes deflections, which should be considered in the desk design.

In the case of a square desk an orthogonal stiffening is used. The main aim of this study is to show how to calculate the residual welding deflections in the case of an orthogonally stiffened plate. We have adapted the Okerblom's calculation method worked out for longitudinal welds of a single straight beam. We apply this method for the case of orthogonal stiffenings.

An orthogonally stiffened plate can be fabricated by two different welding sequences as follows: (a) welding of continuous stiffeners in one direction to the base plate with a cost effective welding method (SAW), then welding the interrupted stiffeners in other direction using GMAW for longitudinal welds and SMAW for nodes of connecting stiffeners, (b) the whole stiffened plate is assembled by tacking of stiffeners to the base plate and to each other, then welding of longitudinal welds by GMAW and node welds by SMAW.

Since in the method (b) the nodes can transfer the bending moments, the residual deflections can be calculated as a grid structure. The Okerblom's method is used for a grid structure. It is shown that the grid-effect decreases the deflections significantly. In the case of open section stiffeners the torsionless grid calculation method is used.

The cost function for both welding sequences are formulated and minimized searching for optimum base plate thickness and stiffener dimensions, while the number of stiffeners is fixed. The more advantageous welding sequence is determined by cost comparison.



### 7.1.2 Residual Welding Deflection from Longitudinal Welds of a Straight Beam

The books of Okerblom et al. (1963), Vinokurov (1977), Masubuchi (1980) and Kuzminov (1974) give suitable calculation methods. The Okerblom's method gives relatively simple formulae, so it is adapted and applied (Farkas and Jármai 1997, 1998, 2003, 2008, Farkas 2002).

In this method it is assumed that (a) the coefficient of thermal expansion and the Young modulus are independent from the temperature, (b) the deflections are in the elastic range, the Hooke-law is valid, (c) the cross sections of the beam will be planar after deflection, (d) the cross section is uniform, (e) the beam is made of one material grade, (f) the thermal distribution is uniform along the length of the beam and steady state.

The thermal shrinkage impulse  $A_T$ , which causes the residual stresses and deformations in the structure can be calculated as

$$A_T = \frac{0.4840\alpha_o Q_T}{c_o \rho t} \ln 2 = \frac{0.3355\alpha_o Q_T}{c_o \rho t} \quad (7.1)$$

where  $Q_T = \eta_o \frac{UI_w}{v_w} = q_o A_w$ ,  $U$  arc voltage,  $I$  arc current,  $v_w$  speed of welding,  $c_o$

specific heat,  $\eta_o$  coefficient of efficiency,  $q_o$  is the specific heat for the unit welded joint area ( $\text{J/mm}^3$ ),  $A_w$  is the welded joint area. It can be seen that this formula contents all the important material and welding parameters. Thus, it can be used not only for steels but also for other materials, e.g. for aluminium-alloys.

For a mild or low alloy steels, where  $\alpha_o = 12 \times 10^{-6} [1/^\circ\text{C}]$ ,  $c_o \rho = 4.77 \times 10^{-3} [\text{J/mm}^3/^\circ\text{C}]$ , the thermal impulse is

$$A_T t [\text{mm}^2] = 0.844 \times 10^{-3} Q_T [\text{J/mm}] \quad (7.2)$$

and the basic Okerblom formulae for the strain at the centre of gravity and the curvature are as follows

$$\varepsilon_G = \frac{A_T t}{A} = -0.844 \times 10^{-3} \frac{Q_T}{A} \quad (7.3)$$

$$C = \frac{A_T t y_T}{I_x} = -0.844 \times 10^{-3} \frac{Q_T y_T}{I_x} \quad (7.4)$$

The minus sign means shrinkage. Furthermore

$$Q_T = \eta_0 \frac{UI_w}{v_w} = \eta_0 \frac{3600U[V]\rho}{\alpha_N} A_w \quad (7.5)$$

is the thermal impulse due to welding,  $A$  cross-sectional area,  $I_x$  moment of inertia of the beam cross-section,  $A_w$  cross-sectional area of the weld,  $\rho = 7.85 \times 10^{-6}$  kg/m<sup>3</sup> is the density of steel,  $\alpha_N = 8.8 \times 10^{-3}$  kg/Ah (Amper-hour) is the coefficient of penetration..

With values of  $U = 27V$ ,  $\eta_0 = 0.7$  for butt welds

$$Q_T \text{ (J/mm)} = 60.7 A_w \text{ (mm}^2\text{)}, \quad (7.6)$$

for SMAW (shielded metal arc welding) fillet welds

$$Q_T = 78.8 a_w^2 \quad (7.7)$$

and for GMAW (gas metal arc welding) of SAW (submerged arc welding) fillet welds

$$Q_T = 59.5 a_w^2. \quad (7.8)$$

$a_w$  is the fillet weld size.

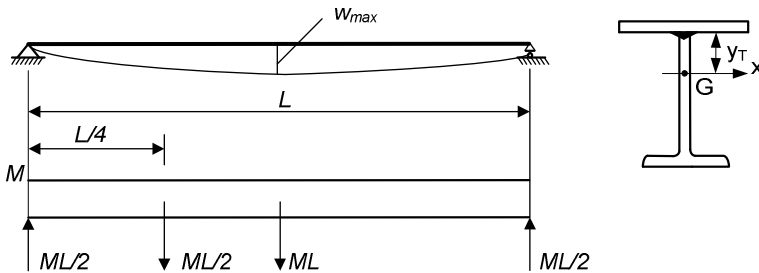


**Fig. 7.1** Calculation of the maximum deflection for a simply supported welded beam of constant cross-section

The maximum deflection due to shrinkage of a single eccentric longitudinal weld in the case of a simply supported beam of constant cross-section can be calculated using the correlation between the distributed load  $p$ , bending moment  $M$  and deflection  $w$

$$\frac{d^2 M(z)}{dz^2} = p(z) \quad (7.9)$$

and

$$\frac{d^2 w(z)}{dz^2} = \frac{M(z)}{EI_x} = C \quad (7.10)$$

i.e. the deflection can be obtained by calculating the bending moment considering the bending moment diagram as a virtual loading (Fig. 7.1)

$$w_{\max} = \frac{ML}{2EI_x} \cdot \frac{L}{4} = \frac{ML^2}{8EI_x} = \frac{CL^2}{8} \quad (7.11)$$

The longitudinal shortening is

$$\Delta L = \varepsilon_g L \quad (7.12)$$

which is important for fabrication to enable the assembly of structural components.

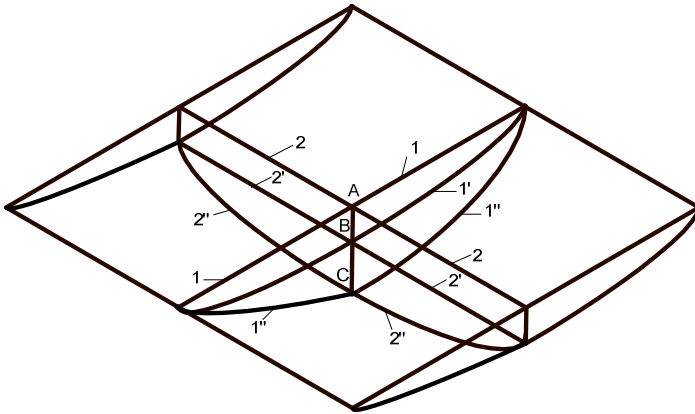


**Fig. 7.2** Deformations of a plate stiffened by two perpendicular stiffeners

### 7.1.3 Residual Welding Curvatures in an Orthogonally Stiffened Plate

Fig. 7.2 shows the deformations of a plate stiffened by two perpendicular stiffeners. First, the stiffener 1 is welded and its point A moves to point B and the stiffeners became the form of 1' and 2'. Secondly, welding of stiffener 2 causes a further curvature and the stiffeners became the form of 1'' and 2''. Thus, the curvatures are added to each other. In the case of two stiffeners in a plate of square symmetry the curvatures double. It is also the case of more stiffeners of square symmetry without grid-effect.

### 7.1.4 The Grid Effect

This effect is illustrated by an example of a rectangular plate orthogonally stiffened by one-one stiffener (Fig. 7. 3). When the stiffeners are previously tacked to the base plate and to each other, the node can transfer the bending moments and the grid-effect acts. The unknown force  $X$  acting in the node A can be calculated using the force method, i.e. from a deflection equation expressing that the deflection of two stiffeners caused by welding curvature and by force  $X$  are identical.

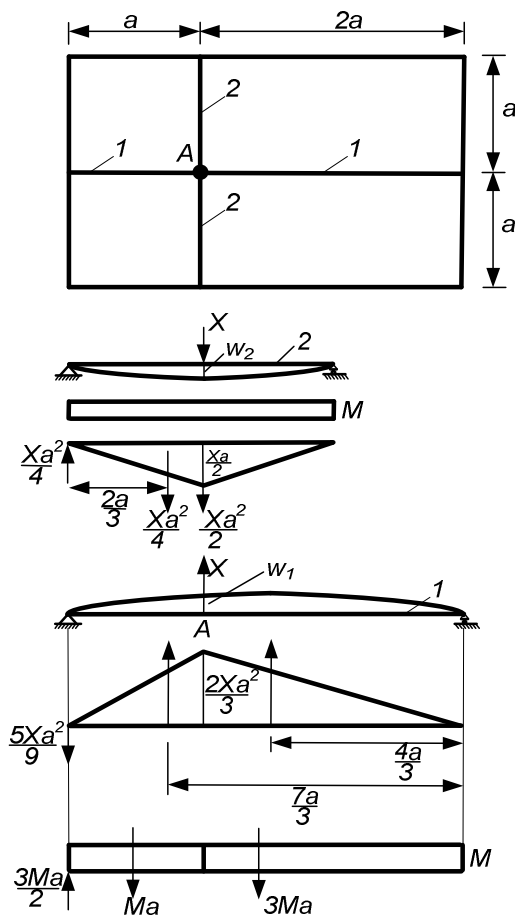


Fig. 7.3 A plate orthogonally stiffened by one-one stiffener

Using the method described in Section 2, the deflection of the stiffener 1 from the welding curvature is

$$EI_1 w_{1M} = \frac{3Ma^2}{2} - \frac{Ma^2}{2} = Ma^2; w_{1M} = C_1 a^2 \quad (7.13)$$

and from the force  $X$

$$w_{1X} = \frac{5Xa^3}{9} - \frac{Xa^3}{9} = \frac{4Xa^3}{9} \quad (7.14)$$

The deflections of the stiffener 2 are

$$w_{2M} = \frac{C_2(2a)^2}{8} = \frac{C_2 a^2}{2} \quad (7.15)$$

and

$$w_{2X} = \frac{Xa^2}{4} \frac{2a}{3} = \frac{Xa^3}{6} \quad (7.16)$$

The deflection equation can be expressed as

$$w_{1M} - w_{1X} = w_{2M} + w_{2X} \quad (7.17)$$

the unknown force from Eq (17) is

$$X = \frac{9(2C_1 - C_2)}{11} \quad (7.18)$$

and the deflection of point A considering the grid-effect

$$w_A = w_{2M} + w_{2X} = \frac{C_2 a^2}{2} + \frac{3(2C_1 - C_2)a^2}{22} = \frac{(3C_1 + 4C_2)a^2}{11} \quad (7.19)$$

and without the grid-effect

$$w_{A0} = w_{1M} + w_{2M} = (C_1 + 0.5C_2)a^2 \quad (7.20)$$

If  $C_1 = C_2 = C$

$$w_A = 0.6363Ca^2 \quad (7.21)$$

and

$$w_{A0} = 1.5Ca^2 \quad (7.22)$$

i.e. the grid-effect decreases the deflection by 57%.

### 7.1.5 Assembly Desk of Square Symmetry with 4-4 Stiffeners

We assume that the stiffeners are previously tacked to the base plate and to each other, the grid-effect acts. In the nodes of 1, 4, 6 and 7 in the Fig. 7.4 forces do not act because of symmetry, in the others the same force  $X$  acts. This force can be determined using a deflection equation. This equation expresses that, for example, the deflection of node 2 caused by the shrinkage and force  $X$  from the stiffener 1-1' and 2-8 is the same.

#### 7.1.5.1 Solution of the Gridwork from Shrinkage of Welds (Fig. 7.4)

Deflection of the stiffener 1-1' at the node 2 from the shrinkage is

$$EIw_{2M}(1-1') = \frac{ML}{2} \frac{2L}{5} - \frac{2ML}{5} \frac{L}{5} = \frac{3ML^2}{25};$$

$$w_{2M}(1-1') = \frac{3CL^2}{25} \quad (7.23)$$

and from the forces  $X$

$$w_{2X}(1-1') = \frac{3XL^2}{25} \frac{2L}{5} - \frac{2XL^2}{25} \frac{2L}{15} = \frac{14XL^3}{375} \quad (7.24)$$

Deflection of the stiffener 2-8 at the node 2 from the shrinkage

$$EIw_{2M}(2-8) = \frac{ML}{2} \frac{L}{5} - \frac{ML}{5} \frac{L}{10} = \frac{2ML^2}{25};$$

$$w_{2M}(2-8) = \frac{2CL^2}{25} \quad (7.25)$$

and from forces  $X$

$$w_{2X}(2-8) = \frac{2XL^2}{25} \frac{L}{5} - \frac{XL^2}{50} \frac{L}{15} = \frac{11XL^3}{750} \quad (7.26)$$

The deflection equation can be expressed as

$$w_{2M}(1-1') - w_{2X}(1-1') = w_{2M}(2-8) + w_{2X}(2-8) \quad (7.27)$$

The unknown force  $X$  from Eq. (26)

$$X = \frac{10C}{13L} \quad (7.28)$$

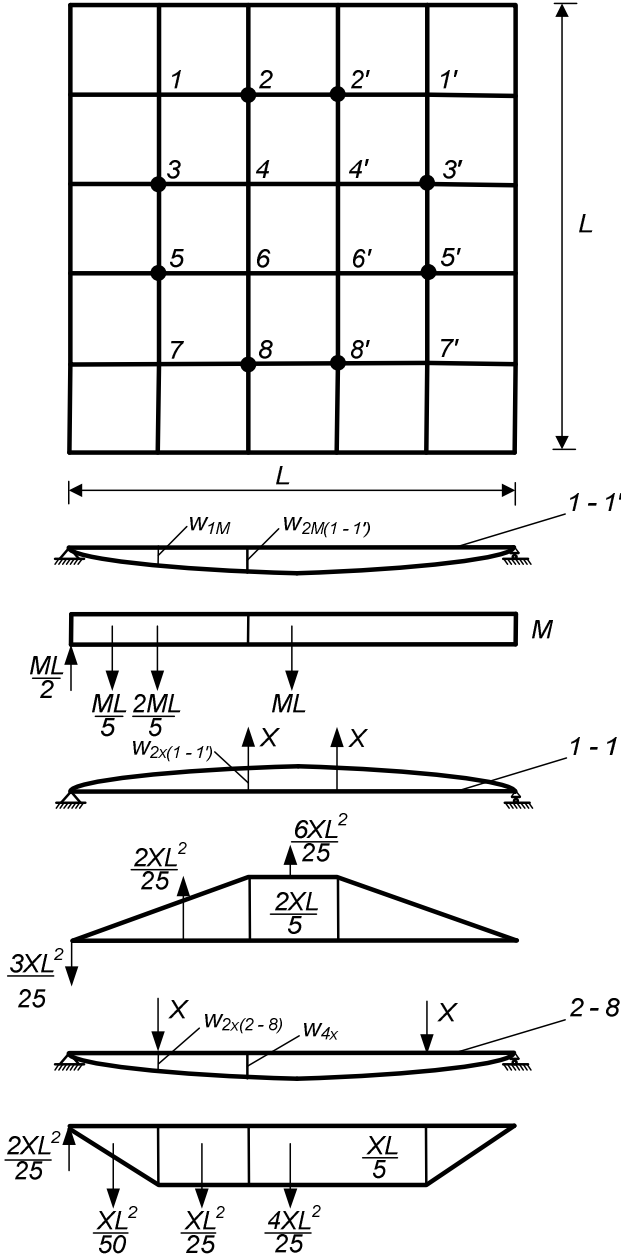


Fig. 7.4 A plate orthogonally stiffened by 4-4 stiffeners

The maximum deflection at the node 4 considering the grid-effect is

$$w_4 = w_{2M}(1-1') + w_{4X}(2-8) = \frac{3CL^2}{25} + \frac{17XL^3}{750} = \frac{134CL^2}{975} = 0.1379CL^2 \quad (7.29)$$

The deflection without the grid-effect, according to the statement detailed in Section 3, is calculated as double of the deflection of a stiffener

$$w_{40} = \frac{6CL^2}{25} = 0.24CL^2 \quad (7.30)$$

i.e. the grid-effect decreases the deflection by 42%.

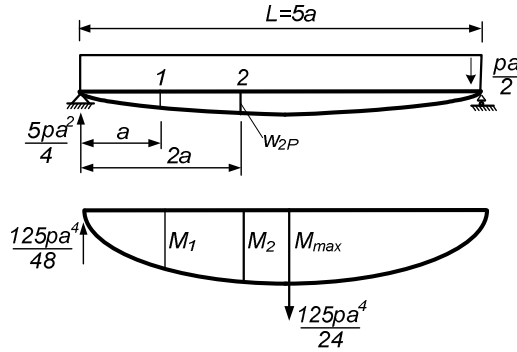


**Fig. 7.5** Bending moments from uniformly distributed normal load

### 7.1.5.2 Solution of the Gridwork from the Uniformly Distributed Normal Load (Fig. 7.5)

Since this load acts after the fabrication, the calculation considers the grid effect.

The deflection equation for the unknown force  $X_p$  is the same as in Section 7.2.5.1.

$$w_{2p}(1-1') - w_{2Xp}(1-1') = w_{2p}(2-8) + w_{2Xp}(2-8) \quad (7.31)$$

The bending moments in Fig. 7.5 are as follows:

$$M_1 = pa^3; M_2 = \frac{3}{2}pa^3 \quad (7.32)$$

The corresponding deflections are expressed as

$$EI_{xe}w_{2p}(1-1') = \frac{125}{24}pa^5 - \frac{pa^5}{3} - pa^5 = \frac{31}{8}pa^5 \quad (7.33)$$

$$EI_{xe}w_{2p}(2-8) = \frac{125}{48}pa^5 - \frac{pa^5}{48} - \frac{pa^5}{6} = \frac{29}{24}pa^5 \quad (7.34)$$



$$EI_{xe} w_{xp} (1-1') = \frac{14}{3} X_p a^3 \quad (7.35)$$

$$EI_{xe} w_{2xp} (2-8) = \frac{11}{6} X_p a^3 \quad (7.36)$$

From the deflection equation one obtains

$$X_p = \frac{16}{39} p a^2 = \frac{16}{975} p L^2 \quad (7.37)$$

The maximum bending moment at the middle of nodes 4 and 6:

$$M_{\max} = \frac{25 p a^3}{16} + X_p a = \frac{1231}{624} p a^3 = 1.9728 p a^3 \quad (7.38)$$

The maximum deflection at the node 4 is

$$w_4 = w_{2p} (1-1') + w_{4xp} (2-8) = \frac{31 p_1 a^5}{8 E I_x} + \frac{17 \times 16 p_1 a^5}{6 \times 39 E I_x} = \frac{5.0374 p_1 a^5}{E I_x} \quad (7.39)$$

where the intensity of the normal load without safety factors is

$$p_1 = p_0 + \rho_1 \frac{V}{L^2} \quad (7.40)$$

and the moment of inertia  $I_x$  is given in Section 7.1.6.2.

### 7.1.6 Minimum Cost Design of the Assembly Desk with 4-4 Stiffeners Considering the Grid-Effect

Numerical data:  $L = 6000$ ,  $a = 1200$  mm,  $p_0 = 5000$  N/m<sup>2</sup> =  $5 \times 10^{-3}$  N/mm<sup>2</sup>,  $f_y = 235$ ,  $f_{y1} = f_y/1.1$ ,  $E = 2.1 \times 10^5$  MPa

#### 7.1.6.1 Stress Constraint

The factored intensity of the uniformly distributed normal load considering also the self mass

$$p = 1.5 p_0 + 1.1 \rho_1 \frac{V}{L^2}, \quad V = L^2 t + 8 L h t_w \quad (7.41)$$

$$\sigma_{\max} = \frac{M_{\max}}{W_{xe}} \leq f_{y1} \quad (7.42)$$

$$W_{xe} = \frac{I_{xe}}{y_{Ge}} \quad (7.43)$$

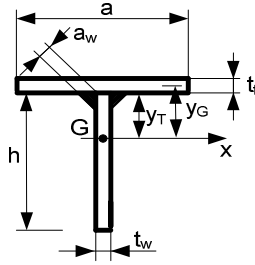


**Fig. 7.6** Dimensions of a stiffener

Cross-section area of a stiffener (Fig. 7. 6)

$$A = ht_w + at \quad (7.44)$$

The effective width of the base plate according to the DNV design rules

$$a_e = \frac{a(\lambda_p - 0.22)}{\lambda_p^2}, \quad \lambda_p = 0.525 \frac{a}{t} \sqrt{\frac{f_y}{E}} \quad (7.45)$$

Effective cross-section area is

$$A_e = ht_w + a_e t \quad (7.46)$$

The moment of inertia of the effective stiffener cross-section

$$I_{xe} = \frac{a_e t^3}{12} + a_e t y_{Ge}^2 + \frac{h^3 t_w}{12} + ht_w \left( \frac{h+t}{2} - y_{Ge} \right)^2 \quad (7.47)$$

where the distance of the gravity centre is

$$y_{Ge} = \frac{ht_w}{A_e} \frac{h+t}{2} \quad (7.48)$$

#### 7.1.6.2 Deflection Constraint

$$w_{\max} = 5.0374 \frac{p_{10} a^5}{EI_x} + 0.1379 CL^2 \leq w_{adm} = \frac{L}{1000} \quad (7.49)$$

where

$$p_{10} = p_0 + \frac{\rho_1 V}{L^2} \quad (7.50)$$

$$I_x = \frac{at^3}{12} + aty_G^2 + \frac{h^3t_w}{12} + ht_w \left( \frac{h+t}{2} - y_G \right)^2 \quad (7.51)$$

$$y_G = \frac{ht_w}{A} \frac{h+t}{2} \quad (7.52)$$

$$C = 0.844 \times 10^{-3} \frac{Q_T y_T}{I_x} \quad (7.53)$$

$$Q_T = 59.5a_w^2, \quad a_w = 0.4t_w, a_{w\min} = 3 \text{ mm} \quad (7.54)$$

$$y_T = y_G - \frac{t}{2} \quad (7.55)$$

### 7.1.6.3 Cost Function

Welding of the base plate with 3 butt welds from 4 strips (SAW) assuming that the plate thickness  $t > 15$  mm:

$$K_{w1} = k_w \left( \Theta_1 \sqrt{4\rho V_1} + 1.3 \times 0.1033 \times 10^{-3} t^{1.9} 3L \right) \quad (7.56)$$

where  $k_w = 1$  \$/min,  $\Theta_1 = 2$ ,  $V_1 = L^2 t$

Welding of the continuous and intermittent stiffeners to the base plate and the intermittent stiffeners to the continuous ones in 16 nodes:

$$K_{w4} = k_w \left( \Theta_2 \sqrt{25\rho V_3} + 1.3 \times 0.3394 \times 10^{-3} a_w^2 16L + T_1 \right) \quad (7.57)$$

$$T_1 = 1.3 \times 0.7889 \times 10^{-3} a_w^2 16 \times 4h, \quad \Theta_2 = 3 \quad (7.58)$$

$$V_3 = V_1 + 8Lht_w \quad (7.59)$$

Painting cost

$$K_P = k_P S, \quad S = 2L^2 + 16Lh \quad (7.60)$$

$$k_P = 28.8 \times 10^{-6} \text{ $/mm}^2$$

Material cost

$$K_M = k_M \rho V_3, k_M = 1 \text{ $/kg} \quad (7.61)$$

Total cost

$$K = K_M + K_{w1} + K_{w4} + K_P \quad (7.62)$$

#### 7.1.6.4 Results of Optimization

Optimization is performed using a MathCAD algorithm. Results are summarized in Table 7.1.

**Table 7.1** Results of optimization considering the grid effect. Dimensions and deflections in mm. The admissible deflection is 6 mm.

$h$	$t_w$	$t$	$w_{max}$	$K$ (\$)
240	18	23	5.95	16490
250	18	21	5.87	15850
<b>260</b>	<b>19</b>	<b>19</b>	<b>5.95</b>	<b>15670</b>
270	20	18	5.96	15920
280	20	17	5.88	15700
290	21	17	5.77	16370

The optimum is marked by bold letters. The stress constraint is passive, in the case of the optimum solution ( $h = 260$  mm)  $\sigma_{max} = 80 < 213.6$  MPa.

#### 7.1.7 Minimum Cost Design of the Assembly Desk without Grid Effect

##### 7.1.7.1 Stress Constraint

The factored intensity of the uniformly distributed normal load considering also the self mass

$$p_1 = 1.5p_0 + 1.1\rho_1 \frac{V_1}{L^2}, \quad (7.63)$$

$$V_1 = L^2 t_1 + 8Lh_1 t_{w1} \quad (7.64)$$

$$\sigma_{max1} = \frac{M_{max1}}{W_{xe1}} \leq f_{y1} \quad (7.65)$$

$$M_{max1} = 1.9728 p_1 a^3 \quad (7.66)$$

$$W_{xe1} = \frac{I_{xe1}}{y_{Ge1}} \quad (7.67)$$

Cross-section area of a stiffener

$$A_1 = h_1 t_{w1} + at_1 \quad (7.68)$$

The effective width of the base plate

$$a_{e1} = \frac{a(\lambda_{p1} - 0.22)}{\lambda_{p1}^2}, \quad \lambda_{p1} = 0.525 \frac{a}{t_1} \sqrt{\frac{f_y}{E}} \quad (7.69)$$

Effective cross-section area is

$$A_{e1} = h_1 t_{w1} + a_{e1} t_1 \quad (7.70)$$

The moment of inertia of the effective stiffener cross-section

$$I_{xe1} = \frac{a_{e1} t_1^3}{12} + a_{e1} t_1 y_{Ge1}^2 + \frac{h_1^3 t_{w1}}{12} + h_1 t_{w1} \left( \frac{h_1 + t_1}{2} - y_{Ge1} \right)^2 \quad (7.71)$$

where the distance of the gravity centre is

$$y_{Ge1} = \frac{h_1 t_{w1}}{A_{e1}} \frac{h_1 + t_1}{2} \quad (7.72)$$

#### 7.1.7.2 Deflection Constraint

$$w_{\max 1} = 5.0374 \frac{p_{11} a^5}{EI_{x1}} + 0.1379 C_1 L^2 \leq w_{adm} = \frac{L}{1000} \quad (7.73)$$

where

$$p_{11} = p_0 + \frac{\rho_1 V_1}{L^2} \quad (7.74)$$

$$I_{x1} = \frac{a t_1^3}{12} + a t_1 y_{G1}^2 + \frac{h_1^3 t_{w1}}{12} + h_1 t_{w1} \left( \frac{h_1 + t_1}{2} - y_{G1} \right)^2 \quad (7.75)$$

$$y_{G1} = \frac{h_1 t_{w1}}{A} \frac{h_1 + t_1}{2} \quad (7.76)$$

$$C_1 = 0.844 \times 10^{-3} \frac{Q_{T1} y_{T1}}{I_{x1}} \quad (7.77)$$

$$Q_{T1} = 59.5 a_{w1}^2, \quad a_{w1} = 0.4 t_{w1}, a_{w1 \min} = 3 \text{ mm} \quad (7.78)$$

$$y_{T1} = y_{G1} - \frac{t_1}{2} \quad (7.79)$$

### 7.1.7.3 Cost Function

Welding of the base plate with 3 butt welds from 4 strips (SAW) assuming that the plate thickness  $t_l > 15$  mm:

$$K_{w11} = k_w \left( \Theta_1 \sqrt{4\rho V_{11}} + 1.3 \times 0.1033 \times 10^{-3} t_1^{1.9} 3L \right) \quad (7.80)$$

where  $k_w = 1$  \$/min,  $\Theta_1 = 2$ ,  $V_{11} = L^2 t_l$ .

Welding of four continuous stiffeners with double fillet welds (SAW)

$$K_{w2} = k_w \left( \Theta_1 \sqrt{5\rho V_2} + 1.3 \times 0.2349 \times 10^{-3} a_1^2 8L \right) \quad (7.81)$$

where

$$V_2 = V_{11} + 4Lh_1 t_{w1} \quad (7.82)$$

Welding of the intermittent stiffeners with double fillet welds to the base plate and to the continuous stiffeners (GMAW-C)

$$K_{w3} = k_w \left( \Theta_2 \sqrt{21\rho V_{31}} + 1.3 \times 0.3394 \times 10^{-3} a_{w1}^2 8L + T_{11} \right) \quad (7.83)$$

$$T_{11} = 1.3 \times 0.7889 \times 10^{-3} a_{w1}^2 16 \times 4h_1 \quad (7.84)$$

$$V_{31} = V_2 + 4Lh_1 t_{w1} \quad (7.85)$$

Cost of painting

$$K_{p1} = k_p S_1, \quad S_1 = 2L^2 + 16Lh_1 \quad (7.86)$$

Material cost

$$K_{M1} = k_M \rho V_{31} \quad (7.87)$$

Total cost

$$K_1 = K_{M1} + K_{w11} + K_{w2} + K_{w3} + K_{p1} \quad (7.88)$$

### 7.1.7.4 Results of Optimization

Optimization is performed using a MathCAD algorithm. Results are summarized in Table 7.2.

**Table 7.2** Results of optimization without the grid effect. Dimensions and deflections in mm. The admissible deflection is 6 mm.

$h_I$	$t_{wI}$	$t_I$	$w_{maxI}$	$K_I$ (\$)
240	18	26	5.795	18570
245	18	25	5.88	18160
<b>250</b>	<b>18</b>	<b>24</b>	<b>5.98</b>	<b>17750</b>
255	19	24	5.94	18230
260	19	24	5.80	18310
270	20	23	6.00	18430
280	20	23	5.75	18580
290	21	23	5.77	19210

The optimum is marked by bold letters. The stress constraint is passive, in the case of the optimum solution ( $h = 250$  mm)  $\sigma_{max} = 90 < 213.6$  MPa.

### 7.1.8 Conclusions

The calculation method of residual welding deflection worked out for simple beams with longitudinal eccentric welds can be applied for orthogonally stiffened plates as well.

In the case of a plate of square symmetry orthogonally stiffened by 4-4 flat stiffeners, two fabrication sequences are investigated as follows: (a) welding of continuous welds in one direction and welding of intermittent welds in other direction, (b) assembly of the whole stiffened plate by tacking and then welding the intermittent welds. In the later sequence the grid effect decreases the residual welding deflection significantly.

It can be seen from Tables 7.1 and 7.2 that the fabrication with grid effect decreases the total cost by  $100(17750-15670)/17750 = 12\%$ .

## 7.2 Minimum Cost Design of a Welded Stiffened Steel Sectorial Plate

### Abstract

The most economic stiffening is sought for a steel sectorial plate. Stiffeners of halved rolled I-section are welded to the base plate by double fillet welds. The plate is subjected to a uniformly distributed normal load. Three stiffening types are designed as follows: (a) non-equidistant tangential stiffening with constant base plate thickness, (b) equidistant tangential stiffening with stepwise varying base plate thickness and (c) equidistant tangential stiffening with constant base plate thickness combined with radial stiffeners.

Each stiffening is designed so that the maximum stress due to bending from the factored normal load in the base plate parts should not exceed the yield stress. Positions of the non-equidistant tangential stiffeners are calculated by a special mathematical algorithm. The costs of material, assembly, welding and painting are calculated for each stiffening version and the costs are compared to each other.

The cost comparison shows that – for given numerical problem – the (b)-type stiffening is the cheapest and the (a)-type is the lightest. Type (c) needs too much welding and its cost is the highest.

### 7.2.1 Introduction

Welded stiffened plates are widely used in load-carrying structures. The best means to decrease the structural weight is to decrease the thickness of plated structures. Since the thin plates can buckle and vibrate, the best way to eliminate these disadvantages is to use stiffenings.

The present study is focused to a special plate form. Sectorial plates can be used in fixed roofs of storage tanks, circular floors or stair landings. Their special form needs special stiffenings. In this study these special stiffenings are investigated.

Three stiffening types are optimized as follows: (a) non-equidistant tangential stiffening with constant base plate thickness, (b) equidistant tangential stiffening with variable base plate thickness, (c) equidistant tangential stiffening combined with radial stiffeners. In the case of these stiffenings the optimization problem needs discrete calculation, thus, we do not use here special mathematical optimization methods, only MathCAD algorithms.

From the wide variety of stiffener forms we use here the halved rolled I-section stiffeners. Their advantage is the large selection of produced profiles and their webs need relatively small welds to connect them to the base plate.

### 7.2.2 Non-equidistant Tangential Stiffening

#### 7.2.2.1 Calculation of Stiffener Distances ( $x_{0i}$ )

These distances are determined using the condition that the maximum normal stress due to bending in each plate element between stiffeners should not be larger than the yield stress. The maximum bending moment in a deck plate element is calculated approximately for a simply supported rectangular plate according to Timoshenko and Woinowsky-Krieger (1959)

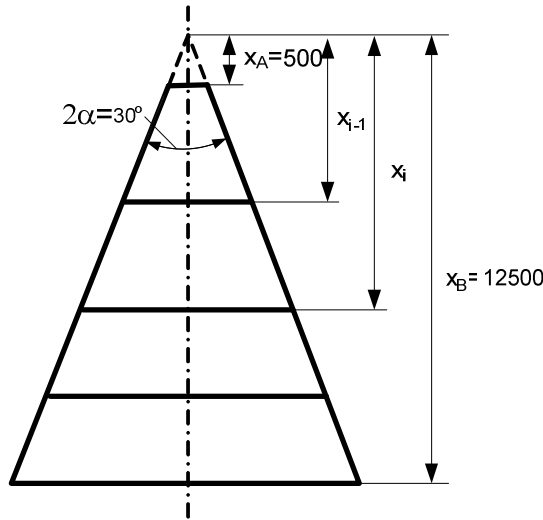
$$M_{i\max} = \beta_i p_M a_i^2 \quad (7.89)$$

where  $a_i$  is the smaller side length and  $\beta_i$  is given in function of  $b_i/a_i \geq 1$  in Table 7.3.



**Table 7.3** Bending moment factors

$b/a$	1	1.1	1.2	1.3	1.4	1.5	1.6	
$10^4\beta$	479	554	627	694	755	812	862	
$b/a$	1.7	1.8	1.9	2.0	3.0	4.0	5.0	>5
$10^4\beta$	908	948	985	1017	1189	1235	1246	1250

**Fig. 7.7** Non-equidistant tangential stiffening

To calculate the length of tangential stiffeners we introduce the factor of  $f_\omega = 2\text{tg}\alpha = 0.5359$ , since we take the half angle of the sectorial plate as  $\alpha = 15^\circ$  (Fig. 7.7).

The values of Table 7.3 are approximated by the following expressions (Fig. 7.7)

$$\beta_i = \beta_{\xi_i} \quad \text{if} \quad x_i - x_{i-1} \leq x_i f_\omega \quad \text{i.e.} \quad x_i \leq \frac{x_{i-1}}{1 - f_\omega} \quad (7.90)$$

$$\beta_i = \beta_{\eta_i} \quad \text{if} \quad x_i - x_{i-1} > x_i f_\omega \quad (7.91)$$

$$\beta_{\xi_i} = a_0 + b\xi_i + c\xi_i^2 + d\xi_i^3 + e\xi_i^4 \quad \xi_i = \frac{x_i f_\omega}{x_i - x_{i-1}} \quad (7.92)$$

$$\beta_{\eta_i} = a_0 + b\eta_i + c\eta_i^2 + d\eta_i^3 + e\eta_i^4 \quad \eta_i = \frac{x_i - x_{i-1}}{x_i f_\omega} \quad (7.93)$$

$$a_0 = -0.08022658, \quad b = 0.180443, \quad c = -0.061636, \quad d = 0.009575, \quad e = -0.00056537$$

Using Eq. (7.89) from equation

$$M_{i \max} = f_{y1} t^2 / 6 \quad (7.94)$$

one obtains

$$r_i = \sqrt{\frac{t^2 f_{y1}}{6 \beta_i p_M}} \quad (7.95)$$

$t$  is the deck plate thickness,  $f_y = 235$  MPa is the yield stress,  $f_{y1} = f_y / 1.1$ . The factored intensity of the uniformly distributed normal load is  $p_M = 1.5 \times 500 \text{ kg/m}^2 = 7.5 \times 10^{-3} \text{ N/mm}^2$ .

The sought stiffener distance is

$$x_{0i} = r_i + x_{i-1} \quad \text{if} \quad x_i \leq \frac{x_{i-1}}{1 - f_\omega} \quad (7.96)$$

$$x_{0i} = \frac{r_i}{f_\omega} \quad \text{if} \quad x_i > \frac{x_{i-1}}{1 - f_\omega} \quad (7.97)$$

The value of  $x_{0i}$  can be obtained by iteration with a MathCAD program.

It should be noted that in this calculation the transverse bending moments are neglected but the plate elements are calculated as simply supported ones and it is also neglected that their edges are partially clamped.

### 7.2.2.2 Design of Stiffeners

A stiffener is subject to a bending moment

$$M_{si \max} = p_M s_i x_i^2 f_\omega^2 / 8 \quad (7.98)$$

where  $s_i = \frac{x_{i+1} - x_{i-1}}{2}$

and the effective plate width according to design rules of Det Norske Veritas (1995)

$$s_{ei} = \left( \frac{1.8}{\beta_{0i}} - \frac{0.8}{\beta_{0i}^2} \right) s_i \quad (7.99)$$

where

$$\beta_{0i} = \frac{s_i}{t} \sqrt{\frac{f_y}{E}}, \quad \text{but} \quad \beta_{0i} \geq 1 \quad (7.100)$$

$E = 2.1 \times 10^5$  MPa is the elastic modulus.

The required section modulus is given by

$$W_{0i} = \frac{M_{si\max}}{f_{yl}} \quad (7.101)$$

The cross-sectional area of a stiffener of halved rolled I-section and the effective plate part (Fig. 7.8)

$$A_{ei} = \frac{h_{li}t_{wi}}{2} + b_it_{fi} + s_eit, \quad h_{li} = h_i - 2t_{fi} \quad (7.102)$$

The distances of the gravity centres  $G_i$

$$z_{Gi} = \frac{I}{A_{ei}} \left[ \frac{h_{li}t_{wi}}{2} \left( \frac{h_{li}}{4} + \frac{t}{2} \right) + b_it_{fi} \left( \frac{h_i + t - t_{fi}}{2} \right) \right] \quad (7.103)$$

and

$$z_{Gli} = \frac{h_i + t - t_{fi}}{2} - z_{Gi} \quad (7.104)$$

the moments of inertia

$$I_{yi} = s_eit^2z_{Gi}^2 + \frac{h_{li}^3t_{wi}}{96} + \frac{h_{li}t_{wi}}{2} \left( \frac{h_{li}}{4} + \frac{t}{2} - z_{Gi} \right)^2 + b_it_{fi} \left( \frac{h_i + t - t_{fi}}{2} - z_{Gi} \right)^2 \quad (7.105)$$

The section moduli are defined as

$$W_{yi} = I_{yi}/z_{0i} \quad (7.106)$$

where  $z_{0i}$  is the greater of  $z_{Gi}$  and  $z_{Gli}$ .

The required stiffener profile is selected from Table 7.4 to fulfil the stress constraint

$$W_{yi} \geq W_{0i} \quad (7.107)$$

**Table 7.4** UB-profiles used for halved rolled I-section stiffeners (Sales 2007)

UB profile	$h$	$b$	$t_w$	$t_f$
152x89x16	152.4	88.7	4.5	7.7
168x102x19	177.8	101.2	4.8	7.9
203x133x26	203.2	133.2	5.7	7.8
254x102x25	257.2	101.9	6.0	8.4
305x102x28	308.7	101.8	6.0	8.8
305x102x33	312.7	102.4	6.6	10.8
406x178x60	406.4	177.9	7.9	12.8

### 7.2.2.3 Cost Calculation for a Sectorial Stiffened Plate Element

The fabrication sequence has two parts:

- (a) Welding of the base plate from 8 elements using SAW (Submerged Arc Welding) butt welding. The length of the plate (12000 mm) is divided into 8 parts welded together with 7 butt welds using SAW technology. The total length of welds is

$$L_{w1} = 45500 f_{\omega} \quad (7.108)$$

The cost in the fabrication phase (a) is calculated as

$$K_{w1} = k_w \left( \Theta_1 \sqrt{8\rho V_1} + 1.3 C_{w1} t^2 L_{w1} \right) \quad (7.109)$$

where

$$k_w = 1.0 \$ / \text{min}, \Theta_1 = 2, \rho = 7.85 \times 10^{-6} \text{ kg/mm}^3, C_{w1} = 0.1559 \times 10^{-3},$$

$$V_1 = \frac{12500 + 500}{2} 12000 f_{\omega} t = 4.18 \times 10^7 t \quad (7.110)$$

- (b) Welding of stiffeners to the base plate and to two edge radial plates to complete a sectorial plate element using fillet welds:

$$K_{w2} = k_w \left( \Theta_2 \sqrt{(n_{st} + 3)\rho V_2} + \sum_i T_i + T_s \right) \quad (7.111)$$

where  $n_{st}$  is the number of stiffeners,  $\Theta_2 = 3$ ,

$$V_2 = V_1 + V_s + \sum_i V_{sti} \quad (7.112)$$

the volume of the edge radial plates is

$$V_s = 2 \times 12000 h_s t_s \quad (7.113)$$

$$h_s = 250 \text{ and } t_s = 6 \text{ mm.}$$

Volume of a stiffener is

$$V_{sti} = A_{sti} x_i f_{\omega}, A_{sti} = \frac{h_i t_{wi}}{2} + b_i t_{fi} \quad (7.114)$$

welding time for a stiffener is

$$T_i = 1.3 C_{w2} a_w^2 x_i f_{\omega} + 1.3 C_{w3} a_w^2 2(2h_{li} + 4b_i) \quad (7.115)$$

where  $C_{w2} = 0.2349 \times 10^{-3}$ ,  $C_{w3} = 0.7889 \times 10^{-3}$

constants for SAW and SMAW (Shielded Metal Arc Welding) fillet welds, respectively,

$a_w = 3$  mm, the second part is multiplied by 2, since the welding position is mainly vertical.

The time of welding of the two edge radial plates to the base deck plate is

$$T_s = 1.3C_{w3}a_w^2L_s, L_s = 2 \times 12000 \quad (7.116)$$

Material cost of a complete sectorial element is

$$K_{m1} = k_m \rho V_2, k_m = 1.0 \text{ \$/kg}. \quad (7.117)$$

The painting cost of a complete sectorial element is

$$K_{p1} = k_p S, k_p = 28.8 \times 10^{-6} \text{ \$/mm}^2, \quad (7.118)$$

$$S = S_s + \sum_i S_{sti} + 2 \times 78 \times 10^6 f_\omega \quad (7.119)$$

$$S_s = 2 \times 12000 h_s \quad (7.120)$$

$$S_{sti} = (h_{1i} + 2b_i)x_i f_\omega \quad (7.121)$$

**Table 7.5** Stiffener distances and sizes in mm for  $\alpha = 15^\circ$  and  $t = 4$  mm

$x_i$	$h$
500	-
1890	152.4
2824	152.4
3652	152.4
4451	152.4
5239	152.4
6023	152.4
6804	152.4
7585	177.8
8373	177.8
9177	203.2
10009	257.2
10839	308.7
11669	308.7
12500	

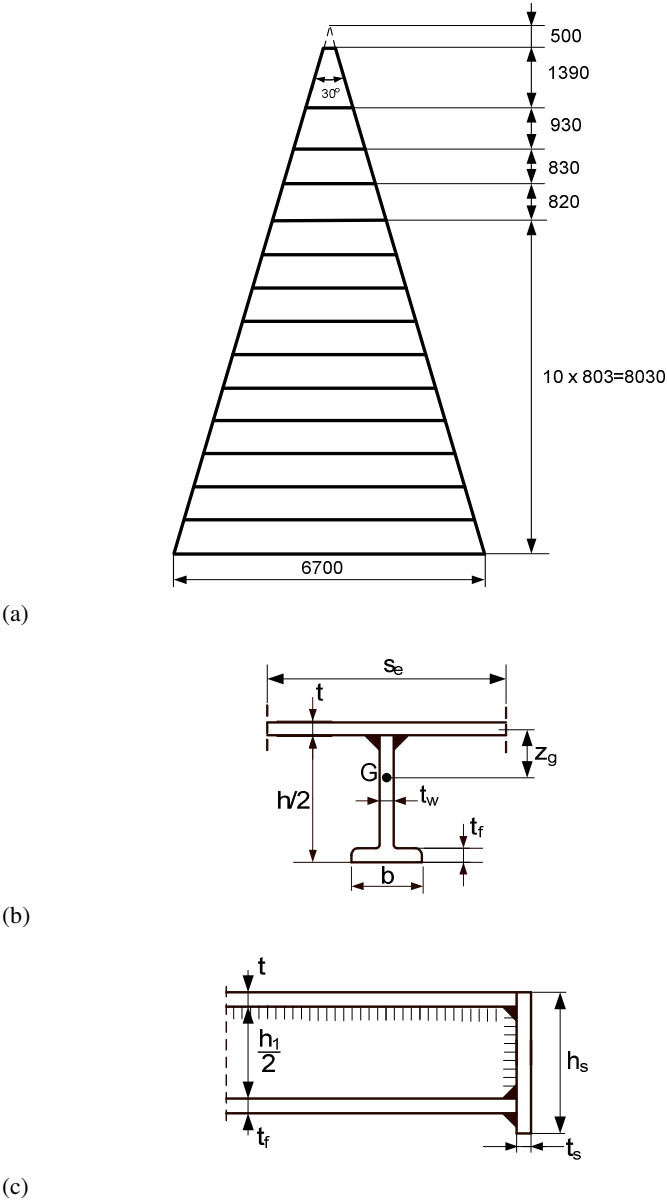


**Fig. 7.8** Non-equidistant tangential stiffening for a base plate thickness of 4 mm. (a) Stiffener positions, (b) cross-section of a stiffener of halved rolled I-section with the effective base plate width, (c) welded connection of a stiffener with the side plate of dimensions  $h_s = 250$ ,  $t_s = 6$  mm.

The total cost of a sectorial element is

$$K_s = K_{m1} + K_{w1} + K_{w2} + K_{p1} \quad (7.122)$$

Results of cost calculation for a sectorial element of  $\alpha = 15^\circ$  show that the minimum cost corresponds to the thickness of  $t = 4$  mm. (See Table 7.6.). Table 7.5 shows the calculated stiffener distances and sizes for  $\alpha = 15^\circ$  and  $t = 4$  mm.

**Table 7.6** shows the costs for different base plate thicknesses in \$

$t$ mm	$K_m$	$K_{w1}$	$K_{w2}$	$K_p$	$K$
4	2094	284	933	3125	6437
6	2588	429	713	2939	6669
8	3233	606	650	2906	7395
10	3817	818	530	2815	7980

It can be seen that the minimum material and total cost corresponds to the thickness of  $t = 4$  mm.

Fig. 7.8 shows the non-equidistant tangential stiffening for a base plate thickness of 4 mm.

### 7.2.3 *Equidistant Tangential Stiffening with Stepwise Varying Base Plate Thickness*

#### 7.2.3.1 Design of Base Plate Thicknesses

In this case the radial distance of 12000 mm is divided to  $n=4, 6$  and 8 equal parts and, using the same MathCAD algorithm the required base plate thicknesses for each part can be calculated.

#### 7.2.3.2 Design of Stiffeners

In the design of stiffeners the effective base plate width is calculated using the half parts of the corresponding neighbouring plate widths as follows: instead of Eqs. (7.99) and (7.100) we use

$$s = \frac{12000}{n} \quad (7.123)$$

$$s_{ei} = \frac{u_{ei} + u_{ei+1}}{2} \quad (7.124)$$

where

$$u_{ei} = \left( \frac{1.8}{\beta_{0i}} - \frac{0.8}{\beta_{0i}^2} \right) s \quad (7.125)$$

$$\beta_{0i} = \frac{s}{t_i} \sqrt{\frac{f_y}{E}}, \quad \text{but } \beta_{0i} \geq 1 \quad (7.126)$$

$$u_{ei+1} = \left( \frac{1.8}{\beta_{0i+1}} - \frac{0.8}{\beta_{0i+1}^2} \right) s \quad (7.127)$$

where

$$\beta_{0i+1} = \frac{s}{t_{i+1}} \sqrt{\frac{f_y}{E}}, \quad \text{but } \beta_{0i+1} \geq 1 \quad (7.128)$$

and the base plate thickness in the calculation of the cross-sectional area and section moduli of a stiffener of halved rolled I-section and the effective plate part is

$$t = \frac{t_i + t_{i+1}}{2} \quad (7.129)$$

### 7.2.3.3 Cost Calculation

*Cost for  $n = 4$*

Thicknesses for plate parts are given in Table 7.7.

**Table 7.7** Thicknesses in mm for plate parts in the case of  $n = 4$

$i$	1	2	3	4
$t_i$	8	11	14	15

The volume of the plate is

$$V_1 = \frac{s f_\omega}{2} \sum_1^4 t_i (x_{i+1} + x_i), \quad x_{i+1} = x_i + 3000 \text{ mm}, \quad s = 3000 \quad (7.130)$$

$$V_I = 5.5948 \times 10^8 \text{ mm}^3$$

The cost of welding of the base plate with butt welds from 4 parts

$$K_{w1} = \Theta_1 \sqrt{4\rho V_1} + 1.3 \times 0.1559 \times 10^{-3} f_\omega \sum_1^3 t_i^2 x_{i+1} = 577 \$ \quad (7.131)$$

*Cost for  $n = 6$*

**Table 7.8** Thicknesses for  $n = 6$

$i$	1	2	3	4	5	6
$t_i$	6	8	9	10	10	11



$$V_1 = \frac{sf_\omega}{2} \sum_1^6 t_i (x_{i+1} + x_i), x_{i+1} = x_i + 2000, s = 2000 \text{ mm} \quad (7.132)$$

$$V_I = 4.105 \times 10^8 \text{ mm}^3$$

$$K_{w1} = \Theta_1 \sqrt{6\rho V_1} + 1.3 \times 0.1559 \times 10^{-3} f_\omega \sum_1^5 t_i^2 x_{i+1} = 583 \$ \quad (7.133)$$

Cost for  $n = 8$

**Table 7.9** Thicknesses for  $n = 8$

$i$	1	2	3	4	5	6	7	8
$t_i$	5	6	7	8	8	8	8	8

$$V_1 = \frac{sf_\omega}{2} \sum_1^8 t_i (x_{i+1} + x_i), x_{i+1} = x_i + 1500, s = 1500 \quad (7.134)$$

$$V_I = 3.2355 \times 10^8 \text{ mm}^3$$

$$K_{w1} = \Theta_1 \sqrt{8\rho V_1} + 1.3 \times 0.1559 \times 10^{-3} f_\omega \sum_1^7 t_i^2 x_{i+1} = \$574 \quad (7.135)$$

Costs for welding of stiffeners to the base plate and to the side plates using double fillet welds are calculated by Eqs. (7.111-7.122).

### Summary of Results

**Table 7.10** Results for equidistant stiffenings

$n$	$K_m$	$K_{w1}$	$K_{w2}$	$K_p$	$K$
4	4794	577	472	1840	7683
6	3700	583	584	1916	6783
8	3077	574	679	1990	6320

It can be seen that the minimum cost solution for equidistant stiffening is the case of  $n = 8$ , since in this case the thicknesses are smallest.

Fig. 7.9 shows the tangential stiffening and the base plate thicknesses for  $n = 8$ . To avoid the coincidence of more welds a distance of 30 mm is proposed.

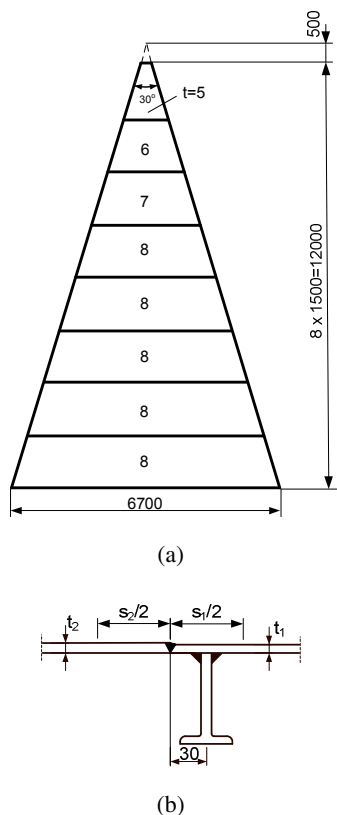


**Fig. 7.9** Equidistant tangential stiffening and the base plate thicknesses for  $n = 8$ . (a) Stiffener positions, (b) cross-section of a stiffener with the effective widths of the base plate.

### 7.2.4 Equidistant Tangential Stiffening Combined with Radial Stiffeners

The equidistant tangential stiffening and a constant base plate thickness is not an economic solution, since in this case the outermost plate part is governing for the bending stress and the other parts cannot be stressed for the allowable stress. In this case it is better to use additional radial stiffeners as well. In the case of combined stiffening the most economic solution is to design near square plate parts, since a plate of square symmetry needs the minimal thickness to be stressed by bending to allowable stress.

The maximum side dimension of a square isotropic plate with all edges built-in can be calculated using the bending moment factor of  $\beta=0.0513$  (Timoshenko and Woinowsky-Krieger 1959, p.197) similar that in Eq. (7.95)

$$a_{\max} = t \sqrt{\frac{f_{y1}}{6\beta p}} \quad (7.136)$$

Using the above data one obtains for  $t = 4, 6$  and  $8$  mm  $a_{max} = 1217, 1825$  and  $2433$  mm respectively.

The sectorial plate with combined stiffening could be designed as a grillage system, but this calculation would be very complicated. Therefore we neglect the grillage effect and design the stiffeners as simply supported beams.

The tangential stiffeners can be designed according to the method shown in section 7.2.2.1 and the radial stiffeners as simply supported beams of span length  $a_{max}$ . Calculations show that the halved rolled I-section of  $h = 152.4$  mm is suitable for all radial stiffeners.

It should be mentioned that the effect of normal load on the local plate buckling can be neglected, since – according to Paik and Thayamballi (2003) the normal load increases the buckling strength.

The results of calculation are summarized in Tables 7.11, 7.12 and 7.13. The costs are calculated for tangential and radial stiffeners separately.

**Table 7.11** Costs in \$ for base plate thickness  $t = 4$  mm

stiffening	$K_m$	$K_{w1}$	$K_{w2}$	$K_p$	$K$
tangential	2028	284	715	3179	6200
radial	233	--	1130	272	1635
Total cost	2256	284	1845	3446	7835

**Table 7.12** Costs in \$ for base plate thickness  $t = 6$  mm

Stiffening	$K_m$	$K_{w1}$	$K_{w2}$	$K_p$	$K$
Tangential	2544	429	578	3032	6583
Radial	160	--	801	186	1147
Total cost	2704	429	1379	3218	7730

**Table 7.13** Costs in \$ for base plate thickness  $t = 8$  mm

Stiffening	$K_m$	$K_{w1}$	$K_{w2}$	$K_p$	$K$
Tangential	3144	606	484	2967	7201
Radial	113	--	606	132	851
Total cost	3257	606	1090	3099	8052

It can be seen from Tables 7.11, 7.12 and 7.13 that the lowest cost corresponds to the solution  $t = 6$  mm, since in the case of  $t = 4$  mm too much (25) radial stiffeners are needed and their welding cost is very high.

Fig. 7.10 shows the combined stiffening for base plate thickness of 6 mm.

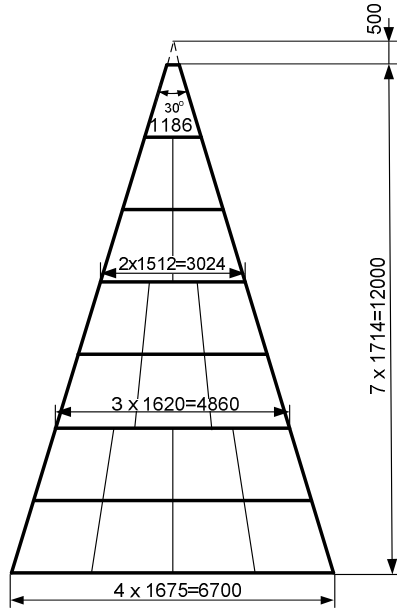


**Fig. 7.10** The combined stiffening for base plate thickness of 6 mm

### 7.2.5 Cost of the Unstiffened Plate

In order to show the economy of stiffening let us compare the costs of stiffened and unstiffened structural version. This comparison answers the question whether a thin stiffened or a thick unstiffened structural version is more economic. Such comparisons have been calculated for a lot of plates and shells (Farkas 2005). From these studies a conclusions can be drawn that, in the case of plates the stiffened thin version is always more economic, since the bending stiffness of an isotropic plate is

$$B = \frac{Et^3}{12(1-\nu^2)} \quad (7.137)$$

i.e. the thickness plays an important role in the plate strength.

In the case of the present sectorial plate we can use the data of the book (Vaynberg 1970) in which the maximum bending moment is given for the angle  $2\alpha = 28^\circ$  and for clamped edges:  $M_{max} = 5974 \text{ Nmm}$ . For simply supported edges this bending moment can approximately be taken as  $M_{maxI} = 2 \times 5974 = 11948 \text{ Nmm}$ . From the stress constraint

$$\sigma = \frac{6M_{maxI}}{t^2} \leq f_{y1} = 219.6 \text{ MPa} \quad (7.138)$$

one obtains the required plate thickness  $t = 18 \text{ mm}$ .

Using Eqs (7.109, 7.110, 7.117, 7.118, 7.119, 7.122) the material cost is  $K_m = 5906$  \$ and the total cost is  $K = 10350$  \$. This means that the cost savings achievable by stiffening is  $100(10350-6320)/10350 = 39\%$ .

### 7.2.6 Conclusions

Ten different structural solutions are designed and their costs are compared to each other. Tables 7.14, 7.15 and 7.16 summarize the material and total costs for these stiffened sectorial plates for the half angle  $\alpha = 15^\circ$ , radius  $R = 12500$  mm, factored uniformly distributed normal load of intensity  $p_M = 7.5 \times 10^{-3}$  N/mm<sup>2</sup> and yield stress  $f_y = 235$  MPa.

Comparing the costs of the different structural solutions it can be concluded that, in the present numerical problem the lowest total cost corresponds to the equidistant tangential stiffening with variable base plate thickness ( $n = 8$ ,  $K = \$6320$ ).

**Table 7.14** Material and total cost of non-equidistant tangential stiffenings with constant base plate thickness

$t$ mm	$K_m$	$K$
4	2094	6437
6	2588	6669
8	3233	7395
10	3817	7980

**Table 7.15** Material and total cost of equidistant tangential stiffening with variable base plate thickness

$n$	$K_m$	$K$
4	4794	7683
6	3700	6783
8	3077	6320

**Table 7.16** Material and total cost of equidistant tangential stiffening combined with radial stiffeners

$t$ mm	$K_m$	$K$
4	2456	7831
6	2704	7730
8	3257	8052

Similarly low total cost can be achieved by non-equidistant tangential stiffening with constant base plate thickness ( $t = 4$  mm,  $K = \$6437$ ).

The equidistant tangential stiffening combined with radial stiffeners needs much higher total cost ( $t = 6$ ,  $K = \$7730$ ).

The lowest mass (or material cost) corresponds to non-equidistant tangential stiffening with constant base plate thickness ( $t = 4$  mm,  $K_m = \$2094$ ) followed by combined stiffening ( $t = 4$  mm,  $K_m = \$2456$ ). The solution giving the lowest total cost needs larger material cost ( $n = 8$ ,  $K_m = \$3077$ ). These data show that the fabrication costs (welding and painting cost) affect significantly the total cost.

The comparison with the cost of the unstiffened sectorial plate shows that the stiffened version is much more economic than the unstiffened one.

### 7.3 Optimum Design of Welded Stiffened Plate Structure for a Fixed Storage Tank Roof

#### Abstract

The optimization problem of a welded fixed roof for a vertical storage tank is studied. The load from snow and from a 150 mm soil layer is considered. The roof is constructed from stiffened sectorial trapezoidal plate elements and radial beams. The stiffeners are of halved rolled I-section and the radial beams are constructed from rolled I-sections. To find the minimum cost solution the thickness of the base plate, the position, number and size of circumferential stiffeners, the size of radial beams as well as the number of sectors is varied. The distances of stiffeners are non-equidistant. In the cost function the cost of material, welding and painting is taken into account.

#### 7.3.1 Introduction

In 1960 the first author has designed a roof structure for a series of storage tanks. The roofs constructed from welded stiffened plate sectorial elements have been suitable for carrying the load of a 150 mm soil layer used to decrease the evaporation loss of stored liquid (kerosene).

From this time the design of stiffened plates has been the main research theme for the first author. The problem of selecting the optimal number of stiffeners led to the structural optimization and the authors have worked out a lot of studies in the field of optimum design of metal structures.

In the present study this economic design method is applied for a fixed storage tank roof constructed from stiffened plate sectorial elements and radial beams. In the optimization procedure the optimum values of the following structural characteristics are sought: number and size of radial rolled I-section-beams, the thickness and the transverse non-equidistant stiffening of the deck plate elements.

The roof is designed to carry the snow load as well as the load of 150 mm thick soil layer mentioned earlier. Since the deck plate sectorial elements are trapezoidal and the deck plate thickness should be constant, the transverse stiffening is designed as non-equidistant. The variable distance of stiffeners is calculated from the condition that the deck plate of given thickness should fulfil the bending stress constraint in each part between two stiffeners.

### 7.3.2 Loads

Snow load is calculated according to Eurocode 1 (2003)

$$s = \mu_1 C_e C_t s_k \quad (7.139)$$

$\mu_1 = 0.8, C_e = C_t = 1, s_k = 1.25 \text{ kN/m}^2$ , thus  $s = 0.8 \times 1.25 = 1.0 \text{ kN/m}^2$ .

Soil load: 150 mm thick layer of a humid light sand of bulk density  $17 \text{ kN/m}^3$

$$p_s = 0.15 \times 17 = 2.55 \text{ kN/m}^2.$$

Snow and soil together  $s + p_s = 3.55 \text{ kN/m}^2$ , multiplied by a safety factor of 1.5  
 $p_M = 5.325 \times 10^{-3} \text{ N/mm}^2$ .

Safety factor for the self mass of sectorial elements is 1.35, and for self mass of radial beams is 1.1.

### 7.3.3 Numerical Data (Fig. 7.11)

Storage tank diameter  $D = 20 \text{ m}$ , inner ring beam diameter  $d = 1.0 \text{ m}$ , roof angle  $\alpha_0 = 15^\circ$ .

Length of a radial beam  $L = 9500 / \cos 15^\circ = 9835 \text{ mm}$ . The characteristic sizes of a trapezoidal deck plate  $x_A = 618, x_B = 10353 \text{ mm}$ .  $\alpha = 180/\omega$ , where  $\omega = 10, 12, 14, 16$  is the number of sectors. The length of stiffeners is calculated for given  $\omega$ :  $y_i = x_i f_\omega$ , where  $f_\omega = 2 \tan \alpha$ .

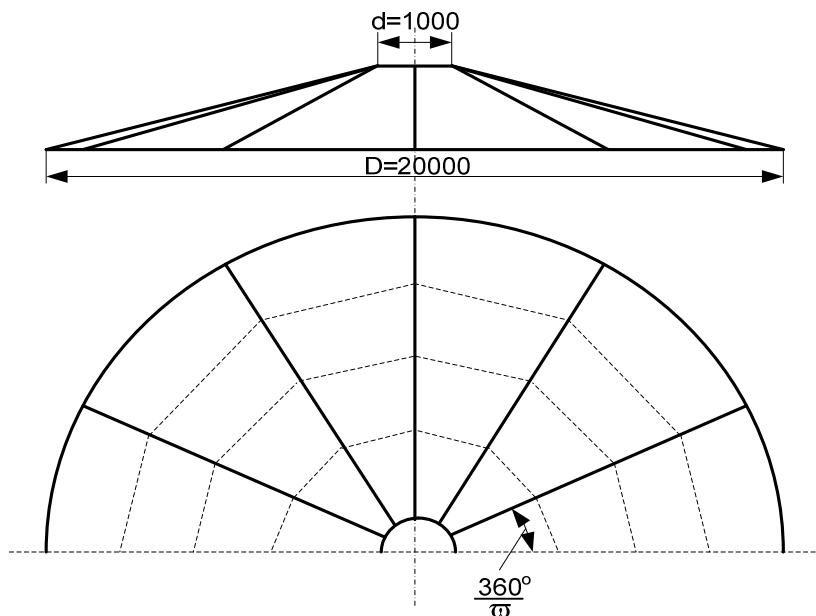
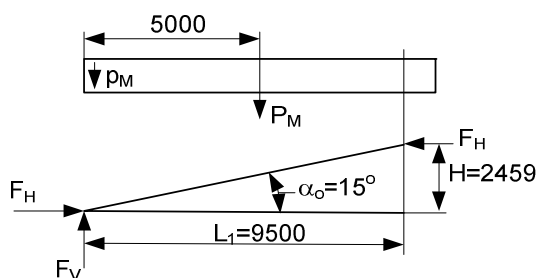


Fig. 7.11 A fixed tank roof



**Fig. 7.12** Forces from the roof load

### 7.3.4 Design of Sectorial Stiffened Deck Plate Elements

Calculation of stiffener distances ( $x_{0i}$ ) and the design of stiffeners is described in Sections 7.2.2.1. and 7.2.2.2 except of Fig.7.7 which is modified for the present case as shown in Fig. 7.13.

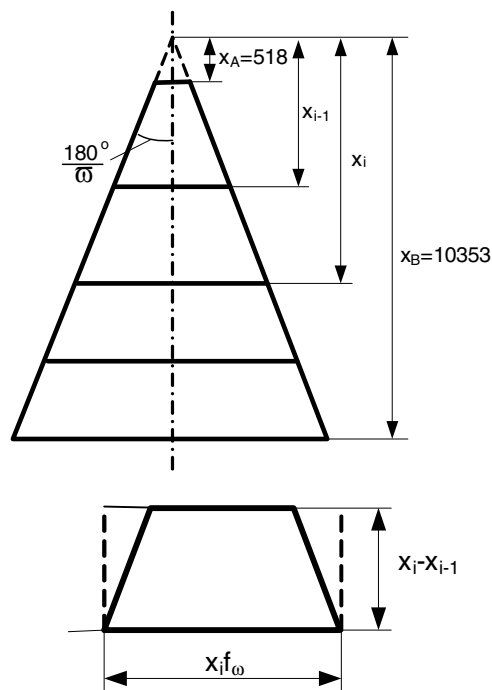


**Fig. 7.13** Stiffener distances and a part of the base plate



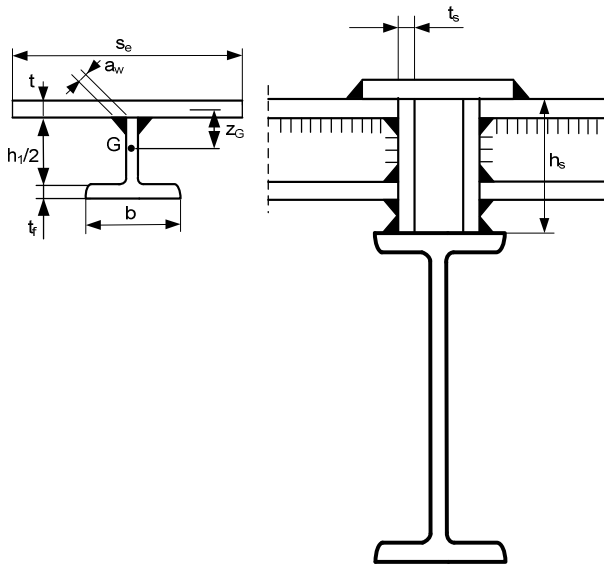


**Fig. 7.14** Cross-section of a stiffener and connection to the radial beam

#### 7.3.4.1 Cost Calculation for a Sectorial Stiffened Plate Element

The fabrication sequence has two parts:

- (a) Welding of the base plate from 7 elements using SAW (Submerged Arc Welding) butt welding. The length of the plate (9835 mm) is divided into 7 parts welded together with 6 butt welds using SAW technology. The total length of welds is

$$L_{w1} = 30783 f_w \quad (7.140)$$

and the cost is calculated as

$$K_{w1} = k_w \left( \Theta_1 \sqrt{7 \rho V_1} + 1.3 C_{w1} t^2 L_{w1} \right) \quad (7.141)$$

where

$$k_w = 1.0 \$ / \text{min}, \Theta_1 = 2, \rho = 7.85 \times 10^{-6} \text{ kg/mm}^3, C_{w1} = 0.1559 \times 10^{-3},$$

$$V_1 = \frac{10353 + 518}{2} 9835 f_w t = 53.4581 \times 10^6 f_w t \quad (7.142)$$

- (b) Welding of stiffeners to the base plate and to two edge radial plates to complete a sectorial plate element using fillet welds:

$$K_{w2} = k_w \left( \Theta_2 \sqrt{(n_{st} + 3) \rho V_2} + \sum_i T_i + T_s \right) \quad (7.143)$$

where  $n_{st}$  is the number of stiffeners,  $\Theta_2 = 3$ ,

$$V_2 = V_1 + V_s + \sum_i V_{sti} \quad (7.144)$$

the volume of the edge radial plates is

$$V_s = 2x9835h_s t_s \sqrt{1 + 0.25f_\omega^2} \quad (7.145)$$

$t_s = 6$  mm,  $h_s$  equals to the stiffener maximum height + 30 mm, volume of a stiffener is

$$V_{sti} = A_{sti} x_i f_\omega, A_{sti} = \frac{h_{li} t_{wi}}{2} + b_i t_{fi} \quad (7.146)$$

welding time for a stiffener is

$$T_i = 1.3C_{w2} a_w^2 2x_i f_\omega + 1.3C_{w3} a_w^2 2(2h_{li} + 4b_i) \quad (7.147)$$

where  $C_{w2} = 0.2349 \times 10^{-3}$ ,  $C_{w3} = 0.7889 \times 10^{-3}$

constants for SAW and SMAW (Shielded Metal Arc Welding) fillet welds, respectively,

$a_w = 3$  mm, the second part is multiplied by 2, since the welding position is mainly vertical.

The time of welding of the two edge radial plates to the base deck plate is

$$T_s = 1.3C_{w3} a_w^2 L_s, L_s = 2x9835 \sqrt{1 + 0.25f_\omega^2} \quad (7.148)$$

Material cost of a complete sectorial element is

$$K_{m1} = k_m \rho V_2, k_m = 1.0 \text{ \$/kg}. \quad (7.149)$$

The painting cost of a complete sectorial element is

$$K_{p1} = k_p S, k_p = 28.8 \times 10^{-6} \text{ \$/mm}^2, \quad (7.150)$$

$$S = S_s + \sum_i S_{sti} + 2x53.4581 \times 10^6 f_\omega \quad (7.151)$$

$$S_s = 2x9835h_s \sqrt{1 + 0.25f_\omega^2} \quad (7.152)$$

$$S_{sti} = (h_{li} + 2b_i) x_i f_\omega \quad (7.153)$$

The total cost of a sectorial element is

$$K_s = K_{m1} + K_{w1} + K_{w2} + K_{p1} \quad (7.154)$$

Results of cost calculation for a sectorial element of  $\omega = 12$  show that the minimum cost corresponds to the thickness of  $t = 4$  mm. Therefore the further calculations are performed for this thickness only. Table 7.17 shows the calculated stiffener distances and sizes for  $\omega = 12$  and  $t = 4$  mm.

**Table 7.17** Stiffener distances and sizes in mm for  $\omega = 12$  and  $t = 4$  mm

$x_i$	$h$
518	-
2197	152.4
3314	152.4
4299	152.4
5248	152.4
6184	152.4
7114	152.4
8041	152.4
8968	177.8
9600	177.8

The cost parts in \$ for this sectorial element are as follows:  $K_m = 1259$ ,  $K_{wl} = 212$ ,  $K_{w2} = 639$ ,  $K_p = 2001$ , the total cost for one element is  $K_s = 4112$ .

### 7.3.5 Design of Radial Beams

Radial beams of rolled I-section (Fig.7.14) are subject to bending and compression. The load is calculated from snow and soil load ( $p_M$ ), the mass of a sectorial element ( $q$ ) and the self mass ( $\rho_I A_r$ ):

$$p = p_M + q + \rho_I A_r, \quad q = \rho_I V_2 / L_I, \quad \rho_I = 7.85 \times 10^{-5} \text{ N/mm}^3, \quad L_I = 9500 \text{ mm.} \quad (7.155)$$

The maximum bending moment is

$$M_{r \max} = p L_1^2 / 8 \quad (7.156)$$

The compression force is

$$N_H = F_M \cos 15^\circ + F_V \sin 15^\circ \quad (7.157)$$

where

$$F_V = P_M = p L / 2, \quad L = 20000 \text{ mm}, \quad H = 9500 \times \sin 15^\circ = 2459 \text{ mm} \quad (7.158)$$

$$F_H = \frac{1}{H} \left[ F_V L_1 - P_M \left( \frac{L}{2} - \frac{d}{2} \right) \right] = 2.0333 P_M \quad (7.159)$$

Stress constraint for bending and compression according to Eurocode 3 (2002)

$$\frac{N_H}{\chi A_r f_{y1}} + k_{yy} \frac{M_{r \max}}{W_y f_{y1}} \leq 1 \quad (7.160)$$

where

$$\chi = \frac{1}{\phi + \sqrt{\phi^2 - \bar{\lambda}^2}}, \phi = 0.5 \left[ 1 + 0.21(\bar{\lambda} - 0.2) + \bar{\lambda}^2 \right] \quad (7.161)$$

$$\bar{\lambda} = \frac{10353}{r \lambda_E}, \lambda_E = \pi \sqrt{\frac{E}{f_y}} = 93.9 \quad (7.162)$$

$r$  is the radius of gyration,  $A_r$  is the cross-sectional area,

$$k_{yy} = 0.95 \left( 1 + 0.6 \bar{\lambda} \frac{N_H}{\chi A_r f_{y1}} \right) \quad (7.163)$$

The suitable rolled I-profile is selected from an Arcelor product catalogue using the British UB profiles.

### 7.3.6 Cost of a Radial Beam

Material cost

$$K_M = k_m \rho V_R, V_R A_r L_R, L_R = 9825 \text{ mm}, \quad (7.164)$$

cost of welding to the inner ringbeam and to the tank shell

$$K_W = k_w \left[ \Theta_2 \sqrt{\rho V_R} + 1.3 C_{w3} a_w^2 2x2(2h_l + 4b) \right] \quad (7.165)$$

the factor of 2 is used since the welding is mainly vertical.

Cost of painting

$$K_P = k_P (2h_l + 4b) L_R \quad (7.166)$$

Total cost of a radial beam

$$K_R = K_M + K_W + K_P \quad (7.167)$$

### 7.3.7 Additional Cost

Material, welding and painting of a deck plate of size 200x6x9825 connecting the sectorial elements as well as welding of the sectorial elements to the radial beam

$$K_A = k_m \rho V_A + 1.3 C_{w2} a_w^2 4 L_R k_w + k_p 200 L_R \quad (7.168)$$

$$V_A = 200 \times 6 L_R \quad (7.169)$$

Total cost of the whole roof structure

$$K = \omega (K_s + K_R + K_A) \quad (7.170)$$

### 7.3.8 Optimization Results

Table 7.18 and 7.19 summarize the results (masses and costs) for different values of  $\omega$  for a sector and for the whole roof.

**Table 7.18** Masses in kg and costs in \$ for a sector containing a sectorial element and a radial beam

$\omega$	$\rho V_s$	$K_s$	$\rho V_R$	$K_R$
10	1600	5046	806	1352
12	1259	4112	729	1248
14	1072	3556	588	1078
16	927	3081	588	1078

**Table 7.19** Masses in kg and costs in \$ for the whole roof

$\omega$	$\rho V_{roof}$	$K_{roof}$
10	24060	66550
12	23856	67400
14	23240	68470
16	24240	70650

It can be seen that  $\omega = 14$  and  $\omega = 10$  gives the minimum mass and minimum cost for the whole roof, respectively. It should be noted that the case of  $\omega = 8$  is unrealistic, since in that case the sectorial element has not a trapezoidal but a circular sector form, which needs also partial radial stiffeners beside of the circumferential ones and the cost increases.

### 7.3.9 Conclusions

Minimum cost design of a fixed roof of a vertical steel storage tank is worked out for a numerical model structure. Load of snow and a soil layer is considered. The roof is constructed from sectorial stiffened plate elements and radial beams.

The number of sectors is varied between 10 and 16. The sectorial elements are circumferential stiffened with halved rolled I-section stiffeners welded to the base plate. The non-equidistant distances of stiffeners are calculated so that the plate parts are equally stressed. The radial beams are constructed from rolled I-sections. The cost function contains the cost of material, welding and painting. The cost calculation shows that the minimum roof mass and cost corresponds to the number of sections of 14 and 10 respectively.

## 7.4 A Circular Floor Constructed from Welded Stiffened Steel Sectorial Plates

### Abstract

The problem of finding the most economic (minimum cost) structural version of a large diameter circular floor constructed from stiffened sectorial plate elements supported by radial beams is a threefold optimization problem:

- (a) Determination of the most economic stiffening of a sectorial plate. The cost of tangential non-equidistant stiffening for a fixed number of sectors ( $\omega=12$ ) is calculated for different base plate thicknesses ( $t = 4, 6, 8$ ). The distances of the tangential non-equidistant stiffening are determined by using an iterative algorithm. The cost of combined (tangential and radial) stiffening for different thicknesses ( $t = 4, 8$ ) is calculated. The costs of various stiffenings show that the non-equidistant tangential stiffening and the base plate thickness of 4 mm give the minimum cost solution.
- (b) Determination of the optimum dimensions of radial welded box beams for a circular floor supported at the centre.
- (c) The total costs of the floor structure calculated for different numbers of sectorial plates (8, 12 and 16) show that the number of 12 gives the minimum total cost.

### 7.4.1 Introduction

Circular plates can be applied in many steel structures such as floors, roofs, stair landings, etc. They can be constructed from sectorial plates supported by radial beams.

The sectorial (trapezoidal) plate elements can be stiffened by tangential or radial stiffeners or these stiffeners can be combined. The stiffeners can be flat, halved rolled I-section (T-shape), trapezoidal or other shapes. They are welded to the base plate by double fillet welds.

We use in the present study halved rolled I-section stiffeners and we investigate both tangential and combined stiffening.

### 7.4.2 Problem Formulation

The problem of finding the most economic (minimum cost) structural version of a large diameter circular floor constructed from stiffened sectorial plate elements supported by radial beams (Fig. 7.15) is a *threefold optimization task*: (1) determination of the most economic stiffening of a sectorial plate, (2) determination of the optimum dimensions of radial beams, (3) determination of the optimum number of sectors.

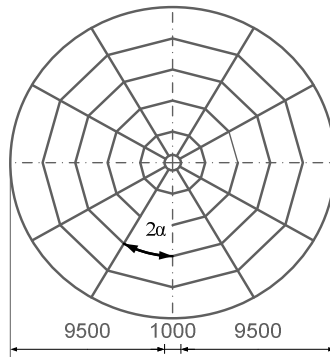


**Fig. 7.15** A large diameter circular floor with 12 tangentially stiffened sectorial plates

### 7.4.3 Solution Strategy for the Three Optimization Phases

- Calculate the cost of tangential non-equidistant stiffening for a fixed number of sectors ( $\omega=12$ ) for different base plate thicknesses ( $t = 4, 6, 8$ ), then calculate the cost for combined (tangential and radial) stiffening for different thicknesses ( $t = 4, 8$ );
- Calculate the optimum dimensions of radial welded box beams for a circular floor supported at the centre, using stress and deflection constraints;
- Cost calculation of the whole floor structure for different numbers of sectors ( $\omega = 8, 12, 16$ ).

### 7.4.4 Minimum Cost Design of a Sectorial Plate

Calculation of stiffener distances ( $x_{0i}$ ) and the design of stiffeners is described in Sections 7.2.2.1. and 7.2.2.2 except of Fig. 7.7 which is modified for the present case as shown in Fig. 7.16.

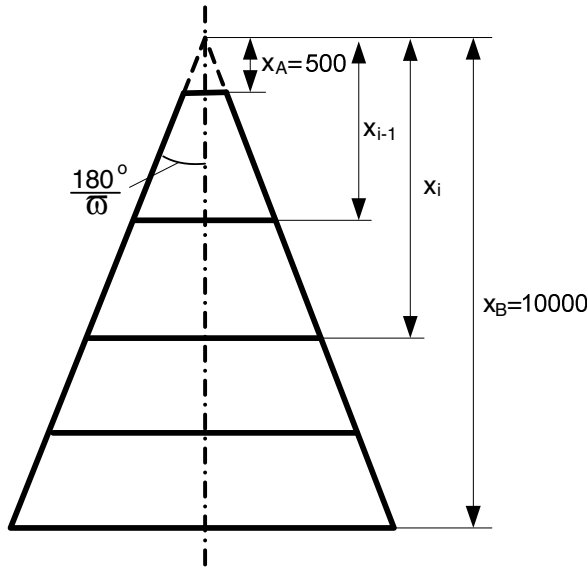


**Fig. 7.16** Non-equidistant tangential stiffening

The applied UB profiles for stiffeners are given in Table 7.4.

Cost calculation for a sectorial stiffened plate element.

The fabrication sequence has two parts:

- (a) Welding of the base plate from 6 elements using SAW (Submerged Arc Welding) butt welding. The length of the plate (9500 mm) is divided into 6 parts welded together with 5 butt welds using SAW technology. The total length of welds is

$$L_{w1} = 27500f_{\omega} \quad (7.171)$$

The cost in the fabrication phase (a) is calculated as

$$K_{w1} = k_w \left( \Theta_1 \sqrt{6\rho V_1} + 1.3C_{w1}t^2 L_{w1} \right) \quad (7.172)$$

where

$$k_w = 1.0\$/\text{min}, \Theta_1 = 2, \rho = 7.85 \times 10^{-6} \text{ kg/mm}^3, C_{w1} = 0.1559 \times 10^{-3},$$

$$V_1 = \frac{10000 + 500}{2} 9500 f_{\omega} t = 49.875 \times 10^6 f_{\omega} t \quad (7.173)$$

- (b) Welding of stiffeners to the base plate and to two edge radial plates to complete a sectorial plate element using fillet welds:



$$K_{w2} = k_w \left( \Theta_2 \sqrt{(n_{st} + 3) \rho V_2} + \sum_i T_i + T_s \right) \quad (7.174)$$

where  $n_{st}$  is the number of stiffeners,  $\Theta_2 = 3$ ,

$$V_2 = V_1 + V_s + \sum_i V_{sti} \quad (7.175)$$

the volume of the edge radial plates is

$$V_s = 2 \times 9500 h_s t_s \quad (7.176)$$

$h_s$  and  $t_s$  are the dimensions of the half radial beam web of a box section estimated preliminary and obtained by iteration taking into account the self mass of the stiffened sector.

Volume of a stiffener is

$$V_{sti} = A_{sti} x_i f_\omega, A_{sti} = \frac{h_{li} t_{wi}}{2} + b_i t_{fi} \quad (7.177)$$

welding time for a stiffener is

$$T_i = 1.3 C_{w2} a_w^2 x_i f_\omega + 1.3 C_{w3} a_w^2 2(2h_{li} + 4b_i) \quad (7.178)$$

where  $C_{w2} = 0.2349 \times 10^{-3}$ ,  $C_{w3} = 0.7889 \times 10^{-3}$

constants for SAW and SMAW (Shielded Metal Arc Welding) fillet welds, respectively,

$a_w = 3$  mm, the second part is multiplied by 2, since the welding position is mainly vertical.

The time of welding of the two edge radial plates to the base deck plate is

$$T_s = 1.3 C_{w3} a_w^2 L_s, L_s = 2 \times 9500 \quad (7.179)$$

Material cost of a complete sectorial element is

$$K_{m1} = k_m \rho V_2, k_m = 1.0 \text{ \$/kg}. \quad (7.180)$$

The painting cost of a complete sectorial element is

$$K_{p1} = k_p S, k_p = 28.8 \times 10^{-6} \text{ \$/mm}^2, \quad (7.181)$$

$$S = S_s + \sum_i S_{sti} + 2 \times 49.875 \times 10^6 f_\omega \quad (7.182)$$

$$S_s = 2 \times 9500 h_s \quad (7.183)$$

$$S_{sti} = (h_{li} + 2b_i) x_i f_\omega \quad (7.184)$$

The total cost of a sectorial element is

$$K_s = K_{m1} + K_{w1} + K_{w2} + K_{p1} \quad (7.185)$$

Results of cost calculation for a sectorial element of  $\omega = 12$  show that the minimum cost corresponds to the thickness of  $t = 4$  mm. (See Table 7.21). Therefore the further calculations are performed for this thickness only. Table 7.20 shows the calculated stiffener distances and sizes for  $\omega = 12$  and  $t = 4$  mm.

**Table 7.20** Stiffener distances and sizes in mm for  $\omega = 12$  and  $t = 4$  mm

$x_i$	500	1890	2824	3652	4451	5239	6023	6804	7585	8373	9177	1000
$h$	-	152	152	152	152	152	152	152	178	178	203	-

### Combined Tangential and Radial Stiffening

The equidistant tangential stiffening and a constant base plate thickness is not an economic solution, since in this case the outermost plate part is governing for the bending stress and the other parts cannot be stressed for the allowable stress. In this case it is better to use additional radial stiffeners as well. In the case of combined stiffening the most economic solution is to design near square plate parts, since a plate of square symmetry needs the minimal thickness to be stressed by bending to allowable stress.

The maximum side dimension of a square isotropic plate with all edges built-in can be calculated using the bending moment factor of  $\beta=0.0513$  (Timoshenko and Woinowsky-Krieger 1959, p.197) similar that in Eq. (7.157)

$$a_{\max} = t \sqrt{\frac{f_{y1}}{6\beta p}} \quad (7.186)$$

For  $f_y = 235$  MPa, factored uniformly distributed normal load of intensity  $p = 1.5 \times 500 = 750$  kg/m<sup>2</sup> =  $7.5 \times 10^{-3}$  N/mm<sup>2</sup> and thickness  $t = 4$  mm one obtains  $a_{\max} = 1217$  mm. Fig. 7.17 shows the combined stiffening with near square distances for  $t = 8$  mm.

The sectorial plate with combined stiffening could be designed as a grillage system, but this calculation would be very complicated. Therefore we neglect the grillage effect and design the stiffeners as simply supported beams. The tangential stiffeners can be designed according to the method shown in section 7.2.2.2 and the radial stiffeners as simply supported beams of span length 1187 mm.

The safety against local buckling of the base plate parts is considered by using the method of effective plate width. For the effective width there are different formulae proposed by Eurocode 3 (2002) or DNV rules (2002). We use here the formulae of DNV rules.

It should be mentioned that the effect of normal load on the local plate buckling can be neglected, since – according to Paik and Thayamballi (2003) the normal load increases the buckling strength.

The corresponding dimension of the radial stiffeners is  $h = 152.4$  mm. It should be mentioned that the required thickness of the outermost plate part without radial stiffeners would be  $t = 6.1$  mm, thus radial stiffeners should be used.

For thickness  $t = 8$  mm the maximum side length is  $a_{max} = 2570$  mm. The corresponding combined stiffening is shown is Fig. 7.17.

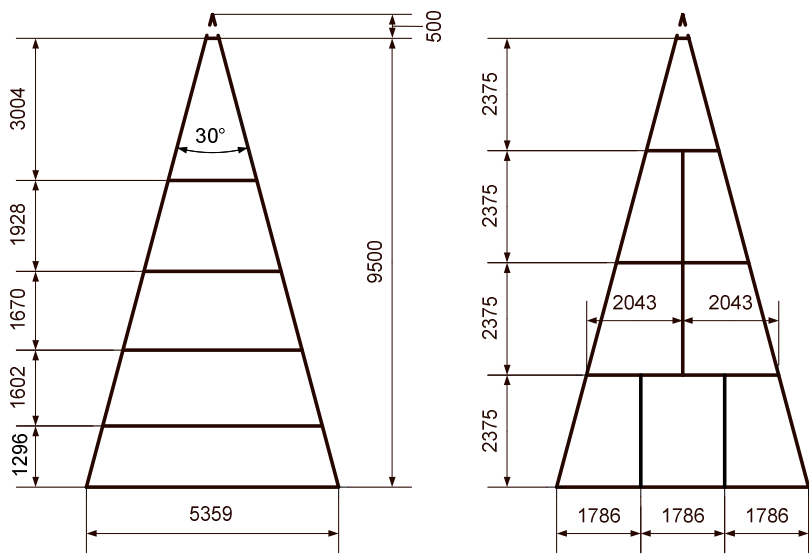


**Fig. 7.17** Non-equidistant tangential and combined stiffening in the case of  $\omega = 12$  and  $t = 8$  mm

Cost comparison of the sectors with different stiffenings.

The costs calculated for non-equidistant tangential and for the equidistant combined stiffening are summarized in Table 7.21.

**Table 7.21** Costs in \$ for a sectorial stiffened plate in the case of  $\omega = 12$ .  $K_{w3}$  is the welding cost of the radial stiffeners. The minimum cost is marked by bold letters.

Stiffening	$T$	$K_m$	$K_{w1}$	$K_{w2}$	$K_{w3}$	$K_p$	$K_s$
non-equidistant tangential	4	1594	190	558	-	2098	<b>4439</b>
	6	1940	281	482	-	2007	4710
	8	2318	392	422	-	1958	5089
combined	4	1524	190	511	722	2183	5130
	8	2277	392	341	402	1989	5402

It can be seen that the minimum cost solution is the sector with non-equidistant stiffening of thickness  $t = 4$  mm. Therefore this type of sectorial plate will be applied for other values of  $\omega$ .

### 7.4.5 Optimum Design of Radial Beams

In order to facilitate the assembly the sectorial plates have only side plates. These plates form the webs of the radial beams of welded box section. When all sectors are assembled, these side plates are connected with upper and lower flange plates (Fig. 7.18).

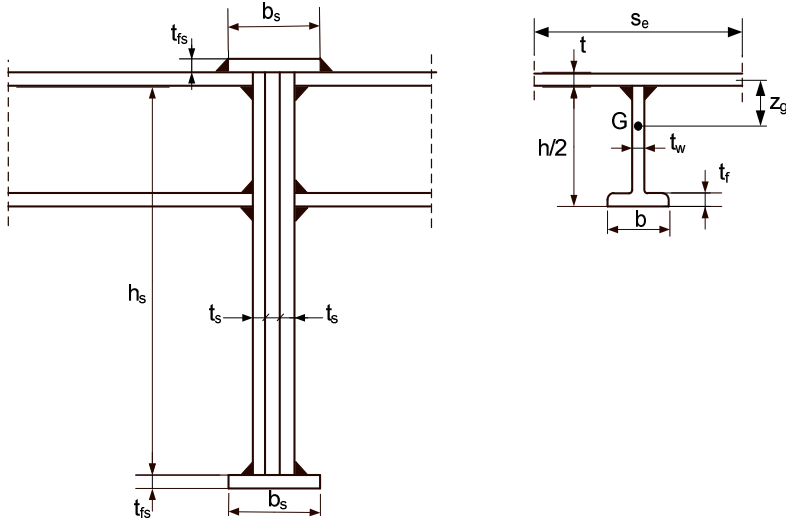


**Fig. 7.18** Radial beam of box section and the connected stiffened sectorial plates

The radial beams are designed for bending considering stress and deflection constraints. The formulation of the optimum design of a radial box beam is as follows: find the optimum values of the dimensions  $h_s$ ,  $t_s$  and the cross-section area of a flange  $A_f = b_s t_f$  to minimize the whole cross-section area

$$A = 2h_s t_s + 2A_f \quad (7.187)$$

and fulfil the following constraints:

(a) stress constraint

$$\sigma_{\max} = \frac{M}{W} \leq f_{y1} \quad \text{or} \quad W \geq \frac{M}{f_{y1}} = W_0 \quad (7.188)$$

$$I = \frac{h_s^3 t_s}{6} + 2A_f \left( \frac{h_s}{2} \right)^2; W = \frac{I}{h_s/2} = \frac{h_s^2 t_s}{3} + A_f h_s \quad (7.189)$$

The bending moment is expressed as

$$M = p_s L^2 / 8, \quad (7.190)$$

the average width of the sectorial plate is  $5000f_\omega$ , thus the intensity of the uniformly distributed normal load is  $7.5 \times 5000 f_\omega = 37.5 f_\omega$ . Furthermore the self mass of the sectorial plate is also taken into account, so

$$p_s = 37.5 f_\omega + 1.1 \left( \frac{\rho_1 V_2}{L} + 2\rho_1 A_f \right), \quad \rho_1 = 7.85 \times 10^{-5} \text{ N/mm}^3. \quad (7.191)$$

Since  $A_f$  is not known an iteration is needed.

The floor is supported at the centre by a column, thus the span length of a radial beam is  $L=9500$  mm.

(b) deflection constraint

$$w_{\max} = \frac{C_w}{I} \leq w_{adm} = \frac{L}{\phi}; \quad C_w = \frac{5p_d L^4}{384E}; \quad \phi = 300 \quad (7.192)$$

or

$$I \geq I_0 = \frac{5p_d L^4}{384Ew_{adm}} \quad (7.193)$$

For the deflection constraint the load intensity is calculated without safety factors, thus

$$p_d = 2.5 f_\omega + \frac{\rho_1 V_2}{L} + 2\rho_1 A_f \quad (7.194)$$

(c) constraint on local buckling of webs

$$\frac{h_s}{t_s} \leq \frac{1}{\beta}; \quad \text{or} \quad t_s \geq \beta h_s \quad (7.195)$$

$$\text{where} \quad 1/\beta = 69\epsilon; \quad \epsilon = \sqrt{\frac{235}{f_y}} \quad (7.196)$$

Considering the local buckling constraint as active the stress constraint can be written as

$$W = \frac{\beta h_s^3}{3} + A_f h_s \geq W_0 \quad (7.197)$$

substituting  $A_f$  from Eq. (7.187) into one obtains

$$A = \frac{2W_0}{h_s} + \frac{4\beta h_s^2}{3} \quad (7.198)$$

From the condition

$$\frac{dA}{dh_s} = 0 \quad (7.199)$$

one obtains the optimum value of  $h_s$  from the stress constraint

$$h_{s\sigma} = \sqrt[3]{\frac{3W_0}{4\beta}} \quad (7.200)$$

Similarly from deflection constraint

$$h_{sw} = \sqrt[4]{\frac{3I_0}{\beta}}; I_0 = \frac{\phi C_w}{L} \quad (7.201)$$

and

$$2A_{fw} = \sqrt{\frac{4\beta I_0}{3}} \quad (7.202)$$

The optimum dimensions of the radial beams are summarized in Table 7.22 (Fig. 7.18).

**Table 7.22** Optimum dimensions of the radial beams

$\omega$	webs $h_s \times t_s$	flanges
8	530x8	170x8
12	475x7	160x7
16	450x7	160x6

#### 7.4.6 Optimum Number of Sectorial Plates

Calculation of the total cost of the floor structure.

The additional cost of the welding of radial beam flanges with double fillet welds of size  $a_{wf}=5$  mm

$$K_{add} = k_w \left( \Theta_2 \sqrt{2\omega \rho V_{add}} + 1.3 \times 0.3394 \times 10^{-3} a_{wf}^2 L_{wf} \right) \quad (7.203)$$

where

$$V_{add} = 2A_f \omega L \quad (7.204)$$

and the weld length is

$$L_{wf} = 4\omega L \quad (7.205)$$

The additional painting cost is

$$K_{padd} = k_p 4b_s \omega L \quad (7.206)$$

The total cost is

$$K_{total} = \omega K + K_{add} + K_{padd} \quad (7.207)$$

The costs for different numbers of sectorial plates are summarized in Table 7.23.

**Table 7.23** Costs in \$ of different numbers of sectorial plates

$\omega$	$K$	$\omega K$	$K_{add}$	$K_{padd}$	$K_{total}$
8	7141	57128	3837	1488	62450
12	4567	54804	3877	2181	60790
16	3636	58176	7519	2802	66770

The corresponding masses are summarized in Table 7.24.

**Table 7.24** Masses in kg for different numbers of sectorial plates

$\omega$	$G$	$\omega G$	$G_{add}$	$G_{total}$
8	2684	21472	1623	23095
12	1604	19248	2005	21253
16	1281	20496	2290	22786

It can be seen that the optimum number of sectorial plates is 12, which gives the minimum total cost and minimum total mass of the floor.

#### 7.4.7 Cost Comparison with an Unstiffened Thick-Base-Plate Version

In order to show the cost difference between stiffened thin plate and unstiffened thick plate version we calculate the total cost for a structural version in which the sectorial plates are unstiffened and the radial beams are of rolled I-section.

Timoshenko and Woinowsky-Krieger (1959) have given formulae for bending of sectorial plates. We use the bending moment for angle of  $\pi/4$ , which corresponds to  $\omega = 8$ . The maximum bending moment is

$$M = 0.0183 p_M R^2 \quad (7.208)$$

From the stress constraint

$$\sigma_{\max} = \frac{6M}{t^2} \leq f_{y1} \quad (7.209)$$

the required thickness of an unstiffened sectorial plate is

$$t \geq \sqrt{\frac{6M}{f_{y1}}} \quad (7.210)$$

For our case  $t = 19.3$  rounded 20 mm.

The required moment of inertia of a radial beam from the deflection constraint (Eq. 7.193)

$$I_o = 43.385 \times 10^7 \text{ mm}^4.$$

In Eq. (7.193) the value of  $p_o$  should be calculated taking into account the self mass of the sectorial plate

$$V_p = \frac{R^2 \pi}{8} = 7.854 \times 10^8 \text{ mm}^3,$$

$$p_o = 25f_w + \frac{\rho_i V_p}{L} = 27.2 \text{ N/mm}.$$

We select for radial beams a rolled I-profile of UB457x191x98 with  $I = 45.73 \times 10^7 \text{ mm}^4$ .

Specific self mass of a radial beam is  $G = 98.3 \text{ kg/m}$ .

Material cost of the whole base plate

$$K_{Mplate} = k_M \rho R^2 \pi = \$49323.$$

Material cost of the radial beams is

$$K_{rad} = k_M 8GL = \$7471.$$

Cost of welding of a sectorial plate, using SAW butt welds to connect 7 plate strips, the calculated weld length is 23 m

$$K_{wplate} = k_w (2\sqrt{7 \times 49323} + 1.3 \times 0.1033 \times 20^{1.9} \times 23) = \$2090.$$

Cost of welding of the sectorial plates to the radial beams with SAW double fillet welds of size 10 mm

$$K_{wl} = k_w (2\sqrt{8 \times 49323} + 1.3 \times 0.2349 \times 10^2 \times 2 \times 8 \times 9.5) = \$5898.$$

Cost of painting

$$K_{pl} = k_p (2R^2 \pi + 8(2 \times 428 + 4 \times 192.8)) = \$21657.$$

Total cost is

$$K_{unstiff} = K_{Mplate} + K_{rad} + 8K_{wplate} + K_{wl} + K_{pl} = \$101069.$$

The cost difference between the unstiffened and stiffened circular floor structure is  $(101069 - 62210)/101069 \times 100 = 38\%$ , thus it can be concluded that the stiffening is very cost effective.



### 7.4.8 Conclusions

A large-diameter circular floor structure is optimized. This welded steel structure consists of sectorial stiffened plates and radial beams. The floor is supported by a circumferential beam or wall and a column at the centre.

The optimization procedure is a threefold process as follows: (a) optimum stiffening is sought for a trapezoid-like sectorial plate, (b) optimum dimensions of welded box radial beams are determined, (c) optimum number of sectorial plates is determined.

The optima are determined by cost comparisons. A cost calculation method is developed and applied. The cost function consists of costs of material, assembly, welding and painting.

The sectorial plates can be stiffened by non-equidistant tangential stiffeners or by a combination of equidistant tangential and radial stiffeners. The distances of non-equidistant tangential stiffeners are calculated using an algorithm, which considers the condition that all the base plate parts should be fully stressed from bending moments.

The costs of various stiffenings show that the non-equidistant tangential stiffening and the base plate thickness of 4 mm give the minimum cost solution.

The optimization of the radial beams is performed by the minimization of the cross-section area of the welded box profile with the design constraints of stress, deflection and local web buckling.

The total costs of the floor structure calculated for different numbers of sectorial plates show that the number of 12 gives the minimum total cost.

The stiffened structure is 38% cheaper than the unstiffened one, since the base plate thickness is 4 mm instead of 20 mm.

## 7.5 Minimum Cost Design of a Cellular Plate Loaded by Uniaxial Compression

### Abstract

Cellular plates are constructed from two base plates and an orthogonal grid of stiffeners welded between them. Halved rolled I-section stiffeners are used for fabrication aspects. The torsional stiffness of cells makes the plate very stiff. In the case of uniaxial compression the buckling constraint is formulated on the basis of the classic critical stress derived from the Huber's equation for orthotropic plates. The cost function contains the cost of material, assembly and welding and is formulated according to the fabrication sequence. The unknown variables are the base plate thicknesses, height of stiffeners and numbers of stiffeners in both directions. The cellular plate is lighter and cheaper than the plate stiffened on one side. The Particle Swarm Optimization and the IOSO techniques are used to find the optimum. PSO contains crazy bird and dynamic inertia reduction criteria, IOSO is based on a response surface technology.

### 7.5.1 Introduction

Cellular plates can be applied in various structures e.g. in floors and roofs of buildings, in bridges, ships, machine structures etc. Cellular plates have the following advantages over the plates stiffened on one side: (a) because of their large torsional stiffness the plate thickness can be decreased, which results in decrease of welding cost, (b) their planar surface is more suitable to corrosion protection, (c) their quasi-symmetric welds do not cause residual distortion.

In previous studies (Farkas 1985, Farkas and Jármai 2006) it has been shown that cellular plates can be calculated as isotropic ones, bending moments and deflections can be determined by using classic results of isotropic plates for various load and support types.

A large research project was performed by Williams (1969) who used a welded cellular plate model for double bottom of ships. Pettersen (1979) has worked out a detailed analysis of double-bottom plates of ships. Evans and Shanmugam (1984), Shanmugam and Evans (1984) as well as Shanmugam and Balendra (1986) have treated the analytical problems of cellular plates relating to the ship construction.

A base plate for transportation of heavy structures may be built by using an orthogonal grid welded from rolled I-beams. The lower face plate has been joined to the grid by plug welds Sahmel (1978). In the revolving frame of surface mining equipment (dragline) a platform for boom, cab, power unit and other structural parts forms an all-welded multi-cell structure Birchfield (1981). Laser welding technology has been used for welding of “Norsial” metallic sandwich plates and a corrugated sheet sandwiched between them (Haroutel 1982).

In the book Farkas and Jármai (1997) some problems can be found about cellular plates. Welded cellular plates for ships investigated in (Farkas and Jármai 2003) consist of two face sheets and some longitudinal ribs of square hollow section welded between them using arc-spot welding technology.

In the present study the load is uniaxial compression, the stiffening is constructed with longitudinal halved rolled I-section stiffeners, the material is a higher-strength steel with yield stress of 355 MPa, the fabrication technology is welding (continuous longitudinal fillet submerged arc – SAW - welds).

### 7.5.2 The Basic Formulae of Cellular Plates

The Huber's equation for the deflection  $w(x,y)$  orthotropic plates in the case of a uniaxial compression  $N_x$

$$B_x \frac{\partial^4 w}{\partial x^4} + 2H \frac{\partial^4 w}{\partial x^2 \partial y^2} + B_y \frac{\partial^4 w}{\partial y^4} + N_x \frac{\partial^2 w}{\partial x^2} = 0 \quad (7.211)$$

where

$$H = B_{xy} + B_{yx} + \frac{\nu}{2}(B_x + B_y) \quad (7.212)$$

is the torsional stiffness of an orthotropic plate,  $\nu = 0.3$  is the Poisson's ratio.

The corresponding bending and torsional stiffnesses are defined as

$$B_x = \frac{E_1 I_y}{a_y}; B_y = \frac{E_1 I_x}{a_x}; E_1 = \frac{E}{1-\nu^2} \quad (7.213)$$

$E = 2.1 \times 10^5$  MPa is the elastic modulus.

For cellular plates with the shear modulus  $G$

$$B_{xy} = \frac{GI_y}{a_y}; B_{yx} = \frac{GI_x}{a_x}; G = \frac{E}{2(1+\nu)} \quad (7.214)$$

$$H = B_{xy} + B_{yx} + \frac{\nu}{2}(B_x + B_y) = \frac{E_1}{2} \left( \frac{I_y}{a_y} + \frac{I_x}{a_x} \right)$$

The solution of Eq. (7.211) is given by

$$N_E = \frac{\pi^2}{b_0^2} \left[ B_x \left( \frac{b_0}{a_0} \right)^2 + 2H + B_y \left( \frac{a_0}{b_0} \right)^2 \right] \quad (7.215)$$

### 7.5.3 The Overall Buckling Constraint

The buckling constraint is given by

$$\frac{N_x}{n_y A_{ey}} \leq \sigma_{cr} = \frac{f_y}{\sqrt{1+\lambda^4}}, \quad \lambda = \sqrt{\frac{f_y}{\sigma_E}}, \sigma_E = \frac{N_E s_y}{A_{ey}} \quad (7.216)$$

The classic critical buckling stress  $\sigma_E$  should be decreased using the above formulae, since it does not include the effect of initial imperfections and residual welding stresses. The DNV design rules are used for this decreasing (DNV 1995).

$f_y$  is the yield stress.

$$A_{ey} = \frac{h_1 t_w}{2} + b t_f + s_{ey1} t_1 + s_{ey2} t_2 \quad (7.217)$$

$$A_{ex} = \frac{h_1 t_w}{2} + b t_f + s_{ex1} t_1 + s_{ex2} t_2 \quad (7.218)$$

$$h_1 = h - 2t_f \quad (7.219)$$

$$s_y = \frac{b_0}{n_y}, s_x = \frac{a_0}{n_x} \quad (7.220)$$

where  $n_y$  and  $n_x$  are the spacing of stiffeners in  $y$  and  $x$  directions (Fig. 7.19).

The effective widths of plate parts can be calculated according to Eurocode 3 Part 1-5 (2006) as

$$s_{ey1} = \rho_{y1} s_y, s_{ey2} = \rho_{y2} s_y, s_{ex1} = \rho_{x1} s_x, s_{ex2} = \rho_{x2} s_x \quad (7.221)$$

where

$$\rho_{y1} = \frac{\lambda_{py1} - 0.22}{\lambda_{py1}^2} \quad \text{if} \quad \lambda_{py1} = \frac{s_y}{56.8 \varepsilon_1} \geq 0.673, \quad \varepsilon = \sqrt{\frac{235}{f_y}} \quad (7.222a)$$

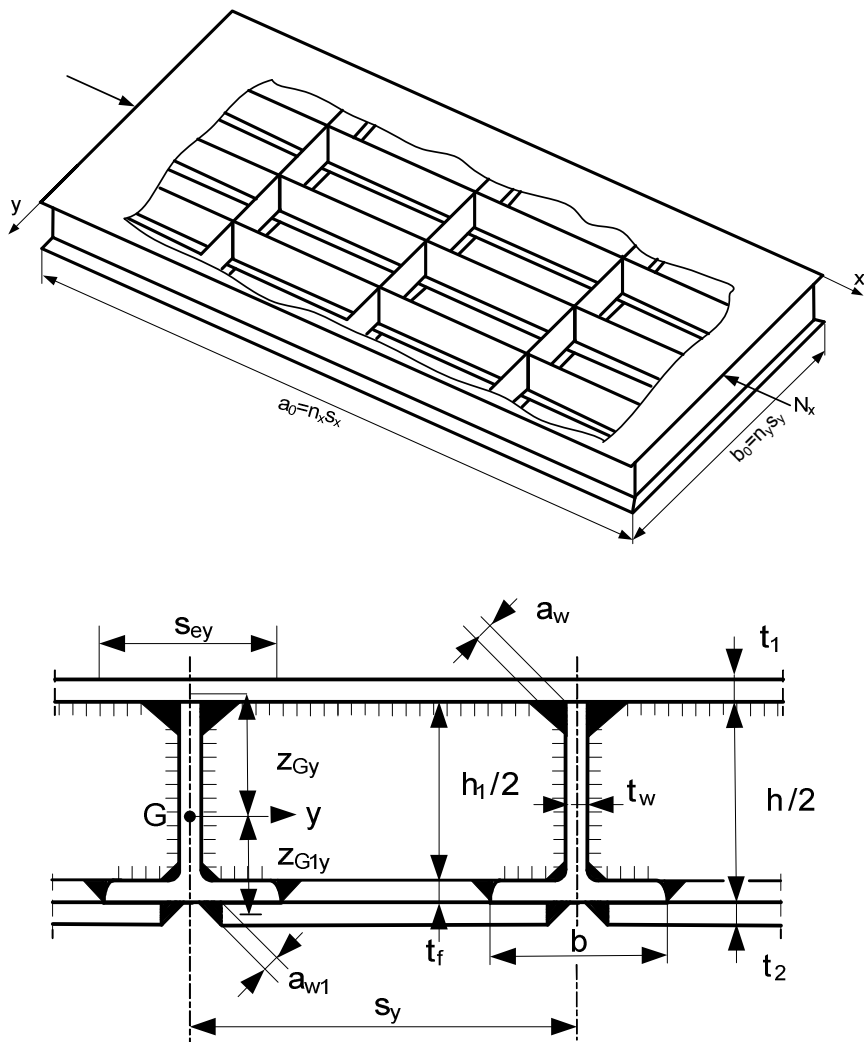


Fig. 7.19 Orthogonally stiffened cellular plate and its cross-section

$$\rho_{y1} = 1 \quad \text{if} \quad \lambda_{py1} < 0.673 \quad (7.222b)$$

$$\rho_{y2} = \frac{\lambda_{py2} - 0.22}{\lambda_{py2}^2} \quad \text{if} \quad \lambda_{py2} = \frac{s_y}{56.8\epsilon t_1} \geq 0.673 \quad (7.223a)$$

$$\rho_{y2} = 1 \quad \text{if} \quad \lambda_{py2} < 0.673 \quad (7.223b)$$

$$\rho_{x1} = \frac{\lambda_{px1} - 0.22}{\lambda_{px1}^2} \quad \text{if} \quad \lambda_{px1} = \frac{s_x}{56.8\epsilon t_2} \geq 0.673 \quad (7.224a)$$

$$\rho_{x1} = 1 \quad \text{if} \quad \lambda_{px1} < 0.673 \quad (7.224b)$$

$$\rho_{x2} = \frac{\lambda_{px2} - 0.22}{\lambda_{px2}^2} \quad \text{if} \quad \lambda_{px2} = \frac{s_x}{56.8\epsilon t_2} \geq 0.673 \quad (7.225a)$$

$$\rho_{x2} = 1 \quad \text{if} \quad \lambda_{px2} < 0.673 \quad (7.225b)$$

The distances of the gravity centres are expressed as

$$z_{Gy} = \frac{1}{A_{ey}} \left[ \frac{h_1 t_w}{2} \left( \frac{h_1}{4} + \frac{t_1}{2} \right) + b t_f \left( \frac{h_1 + t_f + t_1}{2} \right) + s_{ey2} t_2 \left( \frac{h_1 + t_f + t_1 + t_2}{2} \right) \right] \quad (7.226)$$

$$z_{Gx} = \frac{1}{A_{ex}} \left[ \frac{h_1 t_w}{2} \left( \frac{h_1}{4} + \frac{t_1}{2} \right) + b t_f \left( \frac{h_1 + t_f + t_1}{2} \right) + s_{ex2} t_2 \left( \frac{h_1 + t_f + t_1 + t_2}{2} \right) \right] \quad (7.227)$$

and the moments of inertia are given by

$$I_y = s_{ey1} t_l z_{Gy}^2 + \frac{h_l^3 t_w}{96} + \frac{h_l t_w}{2} \left( \frac{h_l}{4} + \frac{t_l}{2} - z_{Gy} \right)^2 + I_{y1} \quad (7.228a)$$

$$I_{y1} = b t_f \left( \frac{h_1 + t_f + t_1}{2} - z_{Gy} \right)^2 + s_{ey2} t_2 \left( \frac{h_1 + t_f + t_1 + t_2}{2} - z_{Gy} \right)^2 \quad (7.228b)$$

$$I_x = s_{ex1} t_l z_{Gx}^2 + \frac{h_l^3 t_w}{96} + \frac{h_l t_w}{2} \left( \frac{h_l}{4} + \frac{t_l}{2} - z_{Gx} \right)^2 + I_{x1} \quad (7.229a)$$

$$I_{x1} = b t_f \left( \frac{h_1 + t_f + t_1}{2} - z_{Gx} \right)^2 + s_{ex2} t_2 \left( \frac{h_1 + t_f + t_1 + t_2}{2} - z_{Gx} \right)^2 \quad (7.229b)$$

The fabrication constraint makes it possible to weld the fillet welds connecting the web of the stiffeners to the upper base plate

$$s_{y,x} - b \geq 300mm \quad (7.230)$$

The unknowns are as follows:  $x_1=t_1$  upper cover plate thickness,  $x_2=t_2$  lower cover plate thickness,  $x_3=h$  height of the I beam,  $x_4=n_x$  number of stiffeners in x-directions,  $x_5=n_y$  number of stiffeners in y-directions.

### 7.5.4 The Cost Function

There are relatively few papers using cost calculation (Krack et al. 2011, Pavlovic et. al. 2004, Sarma and Adeli 2002, Kravanja et al. 2008). The cost consists of the cost of material ( $K_M$ ) and welding ( $K_W$ ).

$$K_M = k_M \rho V \quad (7.231)$$

where  $k_M = 1.0$  \$/kg,  $\rho = 7.85 \times 10^{-6}$  kg/mm<sup>3</sup>,  $V$  is the volume.

The welding costs are formulated according to the fabrication sequence.

- (a) Welding the upper base plate with SAW (submerged arc welding) butt welds.

The weld length is  $L_{W1} = 3(a_0 + b_0)$ , the structural volume  $V_1 = a_0 b_0 t_1$ ,

$\Theta_1 = 2$ , number of elements  $\kappa_1 = 16$ .  $k_W = 1.0$  \$/min.

$$\text{For } t_1 \geq 15 \text{ mm } C_W a_W^n = 0.1346 \times 10^{-3} t_1^2 \quad (7.232a)$$

$$\text{and for } t_1 < 15 \text{ mm } C_W a_W^n = 0.1033 \times 10^{-3} t_1^{1.94} \quad (7.232b)$$

$$K_{W1} = k_W \left( \Theta_1 \sqrt{\kappa_1 \rho V_1} + 1.3 C_W a_W^n L_{W1} \right). \quad (7.233)$$

- (b) Welding of longitudinal stiffeners to the upper base plate with two SAW fillet welds.

$$L_{W2} = 2a_0(n_y + 1), \kappa_2 = n_y + 2, V_2 = V_1 + a_0(bt_f + h_I t_w / 2)(n_y + 1), a_W = 0.4t_w,$$

$$\Theta_2 = 3. \quad (7.234)$$

$$K_{W2} = k_W \left( \Theta_2 \sqrt{\kappa_2 \rho V_2} + 1.3 \times 0.2349 \times 10^{-3} a_W^2 L_{W2} \right). \quad (7.235)$$

- (c) Welding of transverse stiffener parts to the upper base plate and to the longitudinal stiffeners, the webs with double fillet welds (GMAW-C gas metal arc welding with CO<sub>2</sub>) and flanges with butt welds.

$$V_3 = V_2 + b_0(bt_f + h_I t_w / 2)(n_x + 1), \kappa_3 = 1 + n_y(n_x + 1),$$

$$L_{W3} = (n_x + l)(2b_0 + n_y(h_l + b)) \quad (7.236)$$

$$K_{W3} = k_W \left( \Theta_2 \sqrt{\kappa_3 \rho V_3} + 1.3 \times 0.3394 \times 10^{-3} a_W^2 L_{W3} + 1.3 C_{Wf} t_f^n L_{Wf} \right), \quad (7.237)$$

$$\text{For } t_f \geq 15 \text{ mm } C_{Wf} t_f^n = 0.1496 \times 10^{-3} t_f^{1.9029}, \quad (7.238a)$$

$$\text{for } t_f < 15 \text{ mm } C_{Wf} t_f^n = 0.1939 \times 10^{-3} t_f^2. \quad (7.238b)$$

$$L_{Wf} = 2bn_y(n_x + l) \quad (7.239)$$

(d) Welding of lower base plate elements to the flanges of stiffeners with SAW fillet welds.

$$V_4 = V_3 + a_0 b_0 t_2, \kappa_4 = 1 + n_x n_y, L_{W4} = 2(a_0 n_y + b_0 n_x), a_{W1} = 0.7t_2, \quad (7.240)$$

$$K_{W4} = k_W \left( \Theta_1 \sqrt{\kappa_4 \rho V_4} + 1.3 \times 0.2349 \times 10^{-3} a_{W1}^2 L_{W4} \right). \quad (7.241)$$

The total cost is

$$K = K_M + K_{W1} + K_{W2} + K_{W3} + K_{W4}. \quad (7.242)$$

### 7.5.5 The Optimum Design Data and Results

The unknowns are as follows:  $h, t_1, t_2, n_x, n_y$ .

*Numerical data*

$$b_0 = 8000, a_0 = 24000 \text{ mm}, N = 3 \times 10^7 \text{ [N]}, f_y = 355 \text{ MPa}, E = 2.1 \times 10^5 \text{ MPa}.$$

Ranges of variables are as follows:  $t = 4 - 40 \text{ mm}$ ,  $h = 152.4 - 910.4 \text{ mm}$ , the maximum value of  $n$  is given by the fabrication constraint (Eq. 7.230 or 7.243)

$$n_{max} = \frac{b_0}{b + 300} \quad (7.243)$$

The  $n_{max}$  values are given in the Table 7.25.

**Table 7.25**  $n_{max}$  values for rolled I-sections – dimensions in mm

$h$	353.4	403.2	454.6	533.1	607.6	683.5	762.2	840.7	910.4	1008.1
$b$	126.0	142.2	152.9	209.3	228.2	253.7	266.7	292.4	304.1	302.1
$n_{max}$	18	18	17	15	15	14	14	13	13	13

Approximate formulae have been used to determine the UB profile dimensions in the function of the height  $h$ . UB profiles are given in Appendix D.

The Particle Swarm Optimization and the IOSO techniques are used to find the optimum. PSO contains crazy bird and dynamic inertia reduction criteria, IOSO is based on a response surface technology (see Chapter 2).

Table 7.26 shows the discrete optima using PSO and IOSO techniques. The number of stiffeners in  $x$  direction is relatively small.

**Table 7.26** Optimum values for the cellular plate – dimensions in mm, cost in USD

Technique	$x_1=t_1$ [mm]	$x_2=t_2$ [mm]	$x_3=h$ [mm]	$x_4=n_x$	$x_5=n_y$	Cost [\$]	Iteration number	Number of par- ticles
<i>PSO</i>	6	5	533.1	2	12	46044	--	50
<i>PSO</i>	<b>8</b>	<b>5</b>	<b>454.6</b>	<b>2</b>	<b>13</b>	<b>44849</b>	--	500
<i>IOSO</i>	11	4	454.6	2	11	45867	211	--
<i>IOSO</i>	<b>8</b>	<b>4</b>	<b>454.6</b>	<b>2</b>	<b>14</b>	<b>43769</b>	522	--

The discrete values are found finding the continuous ones. At IOSO a parametric study is needed to do this. At PSO there is a built in calculation for this. The number of stiffeners and height of stiffeners have no conflict as it is given in Table 7.26.

### 7.5.6 Conclusions

Cellular plates are constructed from two base plates and an orthogonal grid of stiffeners welded between them. Such plates have a large torsional stiffness, which makes the plate very stiff and economic.

In the case of uniaxial compression the overall buckling constraint is derived from the Huber's equation for orthotropic plates. The local buckling of plate elements is considered by effective widths. The fabrication constraint expresses that the distance between the stiffeners should be sufficient for welding the stiffeners to the upper face plate.

The unknowns are as follows: upper and lower cover plate thickness, height of the halved rolled I-stiffeners, number of stiffeners in  $x$ - and  $y$ -directions. The cost function contains the cost of material, assembly and welding and is formulated according to the fabrication sequence.

The Particle Swarm Optimization and the IOSO techniques are used to find the optimum. The two optimizers give nearly the same solution. Both of them are very robust techniques.

## 7.6 Minimum Cost Design of a Square Box Column with Walls Constructed from Cellular Plates with RHS Stiffeners

### Abstract

Rectangular hollow sections (RHS) can advantageously applied in cellular plates as an orthogonal grid of stiffeners. Formulae are given for the overall buckling strength of a uniaxially compressed rectangular simply supported cellular plate.



This strength is much more larger than that of a plate stiffened on one side by open section ribs because of the large torsional stiffness of the cellular plate. The four walls of a square box column are constructed from cellular plates with tubular stiffeners. The cantilever column is loaded by compression and bending. In the optimization process the optimal sizes and number of RHS stiffeners in both directions as well as the deck plate thickness and the width of the box column section are sought, which minimize the cost function and fulfil the design constraints. Constraint on maximum stress and limitation of the horizontal displacement of the column top are considered. The cost function contains the cost of material, assembly, welding and painting.

### **7.6.1 Introduction**

Box beams and columns of large load-carrying capacity are widely applied in bridges, buildings, highway piers, pilons etc. Since the thickness required for an unstiffened box column can be too large, stiffened plate elements or cellular plates should be used.

Steinhardt (1975) has proposed a design method for box beams with stiffened flange plates using formulae for effective plate width. Nakai et al. (1985) have worked out empirical formulae for stiffened box stub-columns subject to combined actions of compression and bending.

Ge et al. (2000) and Usami et al. (2000) have studied the cyclic behaviour and ductility of stiffened steel box columns used as bridge piers. Longitudinal flat plate stiffeners and diaphragms as well as constant compressive axial force and cyclic lateral loading have been considered. Empirical formulae have been proposed for ultimate strength and ductility capacity.

Another papers about bridge piers can be found in a conference proceedings as follows: Yamao et al. (2004), Ohga et al. (2004) and Hirota et al. (2004).

Cellular plates have the following advantages over plates stiffened on one side: (a) their torsional stiffness contribute to the overall buckling strength significantly, therefore, their height and thicknesses can be smaller and the welding cost lower, (b) their symmetry eliminates the large residual welding distortions, which can occur due to the shrinkage of eccentric welds, (c) their plane surfaces can be better protected against corrosion.

In a study we have elaborated a minimum cost design of a cellular plate subject to uniaxial compression (Farkas and Jármai 2008). This method is used in present study for a square box column constructed from four walls of equal cellular plates.

A cantilever column is loaded by a compression force and a horizontal load, thus, it is subject to compression and bending. From this loading a compression force is calculated for two opposite plate elements, while the remaining plate elements are subject to compression and bending. Since this loading is not so dangerous for the buckling of remaining side plate elements, it is sufficient to design only the two main plate elements.

The aim of the present study is to show that the rectangular hollow section (RHS) stiffeners can be applied in welded cellular plates from which steel structures of advantageous characteristics can be constructed.

Cellular plates consist from two base plates between which a grid of stiffeners is welded (Fig. 7.20). In the case of RHS stiffeners the base plate elements are welded using square butt CJP (complete joint penetration groove) SAW (submerged arc welding) welds. Sizes of RHS sections can be found in Appendix B.

The cost function contains the cost of material, assembly, welding and painting and is formulated according to the fabrication sequence. In the material cost the cost factors for plates and RHS stiffeners are different.

In the present numerical problem the following data are given: the cantilever column height, the vertical compressive force, the horizontal force acting on column top, the steel yield strength, the factors for cost calculation. The following variables are optimized: width of the square box column section, base plate thickness, number and dimensions of the RHS stiffeners in both directions. Constraints on maximum stress and allowable horizontal displacement on the column top are considered.

### 7.6.2 Characteristics of Cellular Plates

The basic formulae for cellular plates are given in Section 7.5.2.

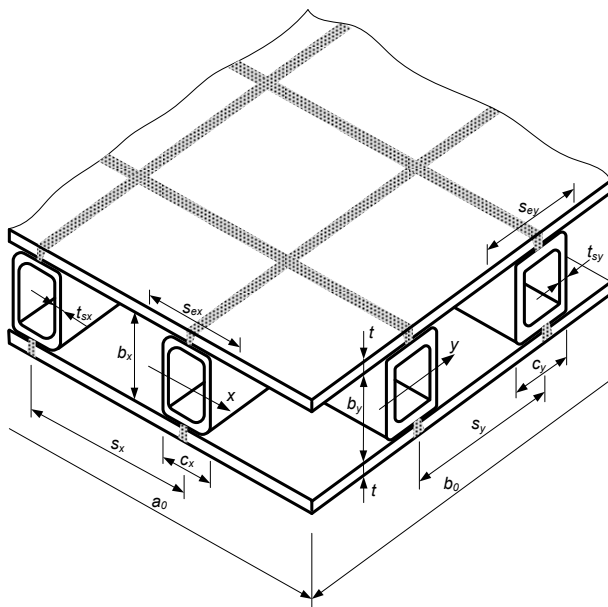


**Fig. 7.20** Cellular plate with RHS stiffeners

Effective plate widths (Eurocode 3, 2002)

$$s_{ey} = C_y s_y, s_{ex} = C_x s_x \quad (7.244)$$

where

$$s_y = b_0 / n_y, s_x = a_0 / n_x \quad (7.245)$$

$$C_y = 1 \quad \text{if } \lambda_y = \frac{s_y}{56.84t\varepsilon} < 0.673 \quad (7.246a)$$

$$C_y = \frac{\lambda_y - 0.22}{\lambda_y^2} \quad \text{if } \lambda_y \geq 0.673 \quad (7.246b)$$

$$C_x = 1 \quad \text{if } \lambda_x = \frac{s_x}{56.84t\varepsilon} < 0.673 \quad (7.247a)$$

$$C_x = \frac{\lambda_x - 0.22}{\lambda_x^2} \quad \text{if } \lambda_x \geq 0.673 \quad (7.247b)$$

$$\varepsilon = \sqrt{\frac{235}{f_y}} \quad (7.248)$$

$f_y$  is the yield stress.

Effective cross-sectional areas

$$A_{ey} = A_{RHSy} + 2s_{ey}t, A_{ex} = A_{RHSx} + 2s_{ex}t \quad (7.249)$$

Moments of inertia

$$I_y = I_{RHSy} + 2s_{ey}t \left( \frac{b_y + t}{2} \right)^2, I_x = I_{RHSx} + 2s_{ex}t \left( \frac{b_x + t}{2} \right)^2 \quad (7.250)$$

### 7.6.3 Minimum Cost Design of the Square Box Column

In the optimum design the following variables should be optimized: the column width  $b_0$ , the outer and inner base plate thickness  $t$ , dimensions and numbers of stiffeners

The buckling constraints are formulated according to the Det Norske Veritas rules (2002).

#### 7.6.3.1 Constraint on Overall Buckling of a Cellular Plate Wall (Fig. 7.21)

A cantilever column is loaded by a compression force and a horizontal load, thus, it is subject to compression and bending. From this loading a compression force is calculated for two opposite plate elements, while the remaining plate elements are subject to compression and bending. Since this loading is not so dangerous for the buckling of remaining side plate elements, it is sufficient to design only the two main plate elements.

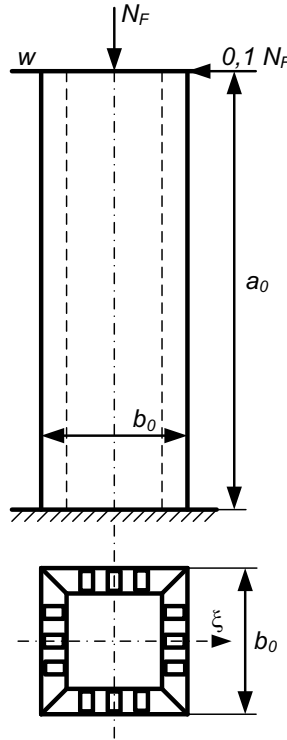


**Fig. 7.21** A cantilever column of square box cross section. The walls are constructed from cellular plates with RHS stiffeners.

$$\sigma = \frac{N_F}{4A_{ey}(n_y - 1)} + \frac{0,1N_F a_0}{W_\xi} \leq \sigma_{cr} = \frac{f_{y1}}{\sqrt{1 + \lambda^4}} \quad (7.251)$$

where

$$\sigma_E = \frac{N_E s_y}{A_{ey}} \quad (7.252)$$

$$\lambda = \sqrt{\frac{f_{y1}}{\sigma_E}}, \quad f_{y1} = \frac{f_y}{\gamma_{M1}}, \quad \gamma_{M1} = 1.1 \quad (7.253)$$

$$W_\xi = \frac{2I_\xi}{b_0} \quad (7.254)$$

$$I_{\xi} = 2I_y(n_y - 1) + 2(n_y - 1)A_{ey}\left(\frac{b_0}{2}\right)^2 + 2I_{\xi s} \quad (7.255)$$

where the moment of inertia of RHS stiffeners is given by

$$I_{\xi s} = I_{RHSz}(n_y - 1) + 2A_{ey}s_y^2n_y \frac{n_y^2 - 1}{24} \quad (7.256)$$

### 7.6.3.2 Constraint on Horizontal Displacement of the Column Top

$$w_{\max} = \frac{H_F}{\gamma_M} \frac{L^3}{3EI_{\xi}} \leq \frac{L}{\phi}, \gamma_M = 1.5, \phi = 300 - 1000 \quad (7.257)$$

### 7.6.3.3 Numerical Data (Fig. 7.20)

$a_0 = 15000$  mm,  $N_x = 3 \times 10^7$  [N], steel yield stress  $f_y = 355$  MPa, elastic modulus  $E = 2.1 \times 10^5$  MPa, shear modulus  $G = 0.81 \times 10^5$ , density  $\rho = 7.85 \times 10^{-6}$  kg/mm<sup>3</sup>, Poisson ratio  $\nu = 0.3$ .

### 7.6.3.4 Cost Function

In our problem the fabrication has two phases:

- (1) Fabrication of four cellular plates: (a) welding the grid of RHS stiffeners, (b) welding of the deck plate elements to the grid, (c) welding of the base plate elements to the grid, except the two outermost plate strips to make it possible to weld the transverse stiffeners to the corner diagonal plates.
- (2) Fabrication of the whole square box column from four cellular plates: (a) welding of the deck plates and the transverse stiffeners to the four corner diagonal plates, (b) welding the 8 outermost base plate strips to the corner plates.

The cost functions are formulated according to these fabrication phases. For each phase the number of assembled elements, the volume of the assembled structure, the characteristics of used welds (size, type, welding method and weld length) should be determined as shown in Eq. (7.258).

1a: Welding of the grid of RHS stiffeners.

Continuous  $(n_y - 1)$  stiffeners in  $x$ -direction of sizes  $b_y, c_y, t_{sy}$  (cross-section area  $A_{RHSy}$ ), intermittent  $(n_x - 1)$  ones in  $y$ -direction of sizes  $b_x, c_x, t_{sx}$  ( $A_{RHSx}$ )

Number of assembled elements  $\kappa_I = n_y - 1 + (n_x - 1)n_y = n_x n_y - 1$ .

SMAW (shielded metal arc welding) fillet welds of size  $a_w = 0.5t_{sx}$ .

Volume:  $V_1 = a_0(n_y - 1)A_{RHSy} + (n_x - 1)A_{RHSx}[b_0 - (n_y - 1)c_y]$

Weld length:  $L_{w1} = 2(b_x + c_x)2(n_x - 1)(n_y - 1)$

Welding cost:

$$K_{w1} = k_w \left( \Theta \sqrt{\kappa_1 \rho V_1} + 1.3 \times 0.7889 \times 10^{-3} a_w^2 L_{w1} \right), \quad (7.258)$$

$$\Theta = 2, \rho = 7.85 \times 10^{-6} \text{ kg/mm}^3, k_w = 1.0 \$/\text{min}.$$

1b: Welding of deck plate elements to the grid of stiffeners from above.

Special square butt CJPG (complete joint penetration groove) SAW (submerged arc welding) welds. Since their gap is of size  $t$  (plate thickness), the  $C_w$  constant relating to an I-butt weld is multiplied by 1.5.

$$\kappa_2 = n_x n_y + 1 \quad (7.259)$$

$$V_2 = V_1 + a_0 t \left[ b_0 + \sqrt{2} \left( \frac{b_y}{2} + 1 \right) \right] \quad (7.260)$$

$$L_{w2} = a_0 (n_y - 1) + b_0 (n_x - 1) \quad (7.261)$$

$$K_{w2} = k_w \left[ \Theta \sqrt{\kappa_2 \rho V_2} + 1.3 \times 1.5 (0.01066 t^2 + 1.698) 10^{-3} L_{w2} \right] \quad (7.262)$$

1c: Welding of the base plate elements to the grid from outside. The difference from 1b is that the two outermost plate strips are not welded to make it possible to weld the transverse stiffeners to the corner plates. The other difference is that one side of the plate strips second from outside are welded using SAW fillet welds of size  $a_{wl} = 0.7t$  instead of square butt welds.

$$\kappa_3 = n_x (n_y - 2) + 1 \quad (7.263)$$

$$V_3 = V_2 + a_0 (n_y - 2) s_y t, s_y = b_0 / n_y \quad (7.264)$$

Length of square butt welds:

$$L_{w3} = a_0 (n_y - 3) + s_y (n_x - 1) (n_y - 2) \quad (7.265)$$

Length of fillet welds:

$$L_{w3a} = 2a_0 \quad (7.266)$$

$$K_{w3} = k_w \left[ \Theta \sqrt{\kappa_3 \rho V_3} + 1.3 \times 1.5 (0.01066 t^2 + 1.698) 10^{-3} L_{w3} + 1.3 \times 0.2349 \times 10^{-3} a_{wl}^2 L_{w3a} \right] \quad (7.267)$$

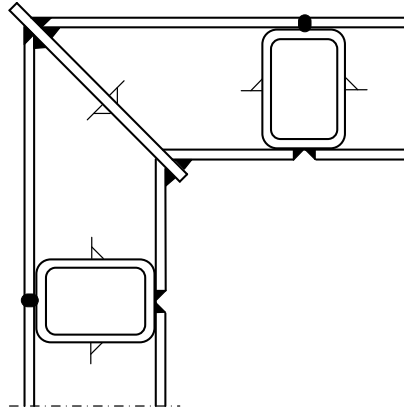


**Fig. 7.22** The corner of the square box column

2a: Welding of the whole square box column from four cellular plates using four corner diagonal plates of sizes  $a_0$ ,  $t_c$  and  $(\sqrt{2}b_y + 8t_c)$  (Fig. 7.22).

Welding of 4x2 SAW fillet welds of size  $a_{wl}$  and length of  $L_{w4} = 8a_0$  connecting the corner plates to the deck plates as well as welding of  $8(n_x-1)$  transverse stiffeners to the corner plates with SMAW fillet welds of size  $a_w$  and length of

$$L_{w4a} = 8(n_x - 1)(2\sqrt{2}b_x + 2c_x). \quad (7.268)$$

$$V_4 = 4V_3 + 4a_0t_c(\sqrt{2}b_y + 8t_c) \quad (7.269)$$

$$K_{w4} = k_w \left( \Theta_1 \sqrt{8\rho V_4} + 1.3 \times 10^{-3} a_{wl}^2 L_{w4} + 1.3 \times 10^{-3} a_w^2 L_{w4a} \right) \quad (7.270)$$

2b: Welding of the  $8n_x$  closing base plate elements to each other using square butt welds of length

$$L_{w5a} = 8(n_x - 1) \left[ s_y - \sqrt{2} \left( \frac{b_y}{2} + t \right) \right] \quad (7.271)$$

to the base plates and to the corner plates using SAW fillet welds of size  $a_{wl}$  and length  $L_{w5} = 16a_0$

$$V_5 = V_4 + 8a_0t \left[ s_y - \sqrt{2} \left( \frac{b_y}{2} + t \right) \right] \quad (7.272)$$

$$K_{w5} = k_w \left[ \Theta_1 \sqrt{(8n_x + 1)\rho V_5} + 1.3 \times 10^{-3} a_{wl}^2 L_{w5} + \dots \right]$$

$$K_{w5} = k_w \left[ \dots + 1.3 \times 1.5 (0.01066t^2 + 1.698) 10^{-3} L_{w5a} \right] \quad \Theta_1 = 3. \quad (7.273)$$

Cost of painting of the surface  $S_p$

$$K_p = k_p \Theta_p S_p, k_p = 14.4 \times 10^{-6} \text{ \$/mm}^2, \Theta_p = 2, S_p = 4a_0b_0 \quad (7.274)$$

Material cost

$$K_m = k_{mplates} \rho \left[ 8a_0b_0t + 4a_0t_c (\sqrt{2}b_y + 8t_c) \right] + 4K_{mRHS} \quad (7.275)$$

$$K_{mRHS} = k_{RHSy} a_0 A_{RHSy} (n_y - 1) \rho + k_{RHSx} A_{RHSx} [b_y - (n_y - 1)c_y] (n_x - 1) \rho \quad (7.276)$$

$$k_{mplates} = 1.0 \text{ \$/kg}, k_{mRHS} = 1.24 \text{ \$/kg}. \quad (7.277)$$

Total cost

$$K = K_m + 4(K_{w1} + K_{w2} + K_{w3}) + K_{w4} + K_{w5} + K_p \quad (7.278)$$

### 7.6.3.5 Optimization and Results

The results of the optimization are summarized in Table 7.27.

## 7.6.4 Conclusions

It is possible to compare the costs of structural versions of the column with the same height, loads ( $N_x = 34000 \text{ kN}$ ) and constraints on stress and displacement ( $\phi = 1000$ ) as follows:

- (1) The stringer-stiffened circular shell with halved rolled I-section stiffeners and with a radius of 1850 mm has the minimum cost of  $K = 70571$  (unstiffened  $K = \$92100$ ) (Farkas and Jármai 2008a),

**Table 7.27** Optimum values of the variables in function of the limited deflection in the case of continuous as well as discrete variables. Dimensions in mm, cost in \$.

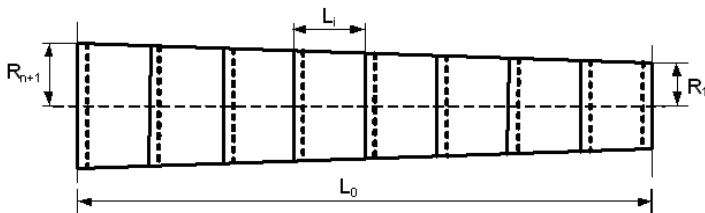
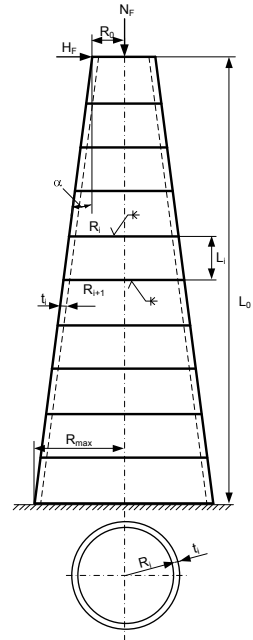
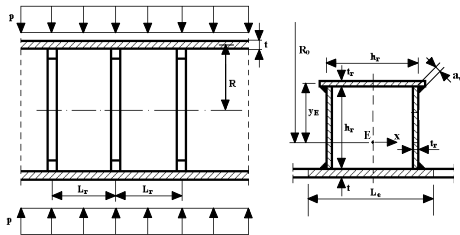
	$\phi$	$b_o$	$t$	$b_x$	$c_x$	$c_y$	$t_{bx}$	$t_{by}$	$n_x$	$n_y$	$K$
Contin.	1000	4095	8	67.2	41.4	30	17.3	10.2	16.8	2.8	61503
Discret.	1000	4100	8	70	40	30	18	12	16	2	62433
Contin.	800	3893	7	86.4	48.7	30	4.6	7.5	18	2.4	57959
Discret.	800	3900	7	90	40	30	5	8	17	2	58505
Contin.	600	3281	9.4	68.9	30.6	30	19.3	7.4	11.6	2.6	54960
Discret.	600	3300	10	60	30	30	20	8	11	2	56936
Contin.	400	3104	10	73.6	98.7	30	4.0	16.5	10.4	2.4	54549
Discret.	400	3100	10	80	90	30	5	18	10	2	55136
Contin.	200	3194	9.3	80.1	48.2	30	11.0	19.6	11.6	2.1	54424
Discret.	200	3100	10	80	40	30	12	20	11	2	56175



- (2) The square box structure composed from orthogonally stiffened plates with halved rolled I-section stiffeners and with an optimized width of  $b_0 = 4500$  mm has the minimum cost of  $K = \$76990$  (Farkas and Jármai 2008b),
- (3) The square box structure with walls of cellular plates with halved rolled I-section stiffeners loaded by a slightly different compression force (30000 instead of 34000 kN) with an optimized width of  $b_0 = 4700$  mm has the minimum cost of  $K = \$60430$  (Farkas and Jármai 2008a).
- (4) The present solution with  $N_x = 30000$  kN and walls of cellular plates with RHS stiffeners of optimized width of 4100 mm has the minimum cost of  $K = \$62432$ .

The difference between the solutions of (3) and (4) can be explained by the difference between the bending stiffnesses of RHS and halved rolled I-sections.

It can be concluded that the cellular box column with halved rolled I-section stiffeners is the most economic structural version, since cellular plates have much higher torsional stiffness than the plates stiffened one side.



## **8.1 Minimum Cost Design for Various Diameters of a Ring-Stiffened Cylindrical Shell Loaded by External Pressure**

### **Abstract**

The problem is to find the optimum dimensions of a ring-stiffened circular cylindrical shell subject to external pressure, which minimize the structural cost. The calculation shows that the cost decreases when the shell diameter decreases. The decrease of diameter is limited by a fabrication constraint that the diameter should be minimum 2 m to make it possible the welding and painting inside of the shell.

### **8.1.1 Introduction**

Cylindrical shells are used in various engineering structures, e.g. in pipelines, off-shore structures, columns and towers, bridges, silos etc. The shells can be stiffened against buckling by ring-stiffeners or stringers or orthogonally. The effectiveness of stiffening depends on the kind of load. Many cases of loads and stiffening have been investigated by realistic numerical structural models and design aspects have been concluded by cost comparisons of optimized structural versions (Farkas and Jármai 1997, 2003, 2008).

Since in Eurocodes design method for stiffened shell buckling is not given, the design rules of Det Norske Veritas (DNV 2002) are used. In this new investigation newer DNV shell buckling formulae are applied.

Optimum design of ring-stiffened cylindrical shells has been treated in (Pappas and Allentuch 1974, Pappas and Morandi 1980). Results of model experiments for cylindrical shells used in offshore oil platforms have been published by Harding (1981). Cho and Frieze (1988) have compared the proposed strength formulation with DNV rules, British Standard BS 5500 and experimental results.

The tripping of open section ring-stiffeners is treated by Huang and Wierzbicki (1993). Buckling solutions for shells with various end conditions, stiffener geometry and under various pressure distributions have been presented by Wang et al. (1997) and by Tian et al. (1999).

In (Akl et al 2002) the adopted approach aims at simultaneously minimizing the shell vibration, associated sound radiation, weight of the stiffening rings as well as the cost of the stiffened shell. The production cost as well as the life cycle and maintenance costs are computed using the Parametric Review of Information for Costing and Evaluation (PRICE) model (PRICE System, Mt.Laurel, N.J. 1999) without any detailed cost data.

In the optimization process the optimum values of shell diameter and thickness as well as the number and dimensions of ring-stiffeners are sought to minimize the structural volume or cost. In order to avoid tripping welded square box section stiffeners are used, their side length and thickness of plate elements should be optimized.

Besides the constraints on shell and stiffener buckling the fabrication constraints can be active. To make it possible the welding of stiffeners inside the shell the minimum shell diameter should be fixed (2000 mm). The calculations show that the volume and cost decreases when the shell diameter is decreased. Thus, the shell diameter can be the fixed minimum value. Another fabrication constraint is the limitation of shell and plate thickness (4 mm).

The remaining unknown variables can be calculated using the two buckling constraints and the condition of volume or cost minimization. The relation between the side length and plate thickness of ring-stiffeners is determined by the local buckling constraint. To obtain the optimum values of variables a relative simple systematic search method is used.

The cost function contains the cost of material, assembly, welding and painting and is formulated according to the fabrication sequence.

### 8.1.2 Characteristics of the Optimization Problem

*Given data:* external pressure intensity  $p = 0.5 \text{ N/mm}^2$ , safety factor  $\gamma = 1.5$ , shell length  $L = 6000 \text{ mm}$ , steel yield stress  $f_y = 355 \text{ MPa}$ , elastic modulus  $E = 2.1 \times 10^5 \text{ MPa}$ , Poisson ratio  $\nu = 0.3$ , density  $\rho = 7.85 \times 10^{-6} \text{ N/mm}^3$ , the cost constants are given separately.

*Unknown variables:* shell radius  $R$ , shell thickness  $t$ , number of spacing between ring-stiffeners  $n$ , thus, the spacing between stiffeners is  $L_r = L/n$ , the side length of the square box section stiffener  $h_r$ , the thickness of stiffener plate parts  $t_r$ .

### 8.1.3 Constraint on Shell Buckling

According to the DNV rules (2002)

$$\sigma = \frac{\eta p R}{t} \leq \frac{f_y}{\sqrt{1 + \lambda^4}}, \lambda = \sqrt{\frac{f_y}{\sigma_E}} \quad (8.1)$$

$$\sigma_E = \frac{C \pi^2 E}{12(1 - \nu^2)} \left( \frac{t}{L_r} \right)^2 \quad (8.2)$$

$$C = \psi \sqrt{1 + \left( \frac{\rho_1 \xi}{\psi} \right)^2}, \psi = 4, \rho_1 = 0.6 \quad (8.3)$$

$$\xi = 1.04 \sqrt{Z}, Z = \frac{L_r^2}{R t} \sqrt{1 - \nu^2} \quad (8.4)$$

### 8.1.4 Constraint on Ring-Stiffener Buckling

The moment of inertia of the effective stiffener cross-section should be larger than the required one

$$I_x \geq I_{req} \quad (8.5)$$

The effective shell length between ring-stiffeners is the smaller of

$$L_e = \frac{1.56\sqrt{Rt}}{1 + 12\frac{t}{R}} \text{ or } L_r \quad (8.6)$$

The distance of the gravity centre of the effective ring-stiffener cross-section (Fig.8.1)

$$y_E = \frac{L_e t \left( h_r + \frac{t + t_r}{2} \right) + h_r t_r (h_r + t_r)}{3t_r h_r + L_e t} \quad (8.7)$$

The moment of inertia of the effective stiffener cross-section

$$I_x = \frac{t_r h_r^3}{6} + 2t_r h_r \left( \frac{h_r + t_r}{2} - y_E \right)^2 + h_r t_r y_E^2 + \frac{L_e t^3}{12} + L_e t \left( h_r + \frac{t + t_r}{2} - y_E \right)^2 \quad (8.8)$$

The relation between  $h_r$  and  $t_r$  is determined by the local buckling constraint

$$t_r \geq \delta h_r, \delta = \frac{1}{42\varepsilon}, \varepsilon = \sqrt{\frac{235}{f_y}} \quad (8.9)$$

For  $f_y = 355$   $\delta = 1/34$ , the required  $t_r$  is rounded to the larger integer, but  $t_{rmin} = 4$  mm.

The required moment of inertia

$$I_{req} = \frac{\eta R R_0^2 L_r}{3E} \left[ 1.5 + \frac{3E y_E 0.005 R}{R_0^2 \left( \frac{f_y}{2} - \sigma \right)} \right] \quad (8.10)$$

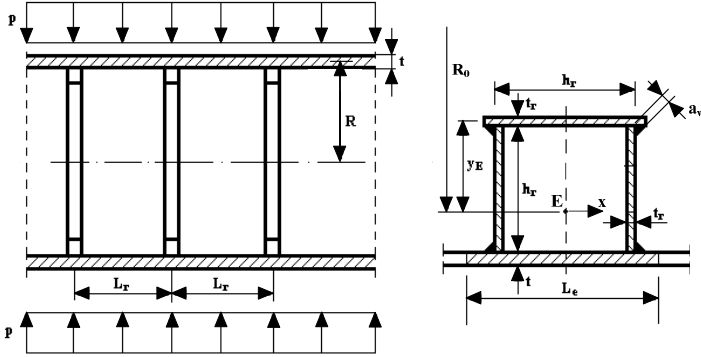


Fig. 8.1 Ring-stiffened cylindrical shell loaded by external pressure

### 8.1.5 The Cost Function

The cost function contains the cost of material, assembly, welding and painting and is formulated according to the fabrication sequence.

The cost of assembly and welding is calculated using the following formula (Farkas and Jármay 1997, 2003, 2008)

$$K_w = k_w \left( C_1 \Theta \sqrt{\kappa \rho V} + 1.3 \sum_i C_{wi} a_{wi}^n C_{pi} L_{wi} \right) \quad (8.11)$$

where  $k_w$  [\$/min] is the welding cost factor,  $C_1$  is the factor for the assembly usually taken as  $C_1 = 1 \text{ min/kg}^{0.5}$ ,  $\Theta$  is the factor expressing the complexity of assembly, the first member calculates the time of the assembly,  $\kappa$  is the number of structural parts to be assembled,  $\rho V$  is the mass of the assembled structure.

The second member estimates the time of welding,  $C_w$  and  $n$  are the constants given for the specified welding technology and weld type,  $C_p$  is the factor of welding position (for downhand 1, for vertical 2, for overhead 3),  $L_w$  is the weld length, the multiplier 1.3 takes into account the additional welding times (deslagging, chipping, changing the electrode).

The fabrication sequence is as follows:

- (a) Welding the unstiffened shell from curved plate parts of dimensions 6000x1500 mm and of number

$$n_p = \frac{2R\pi}{1500},$$

which should be rounded to the larger integer. Use butt welds of length

$$L_{w1} = n_p L, \quad \Theta = 3, \kappa_1 = n_p, V_1 = 2R\pi L t, k_w = 1, \quad (8.12)$$

welding technology SAW (submerged arc welding)

$$\text{for } t = 4\text{-}15 \text{ mm } C_{W1} = 0.1346 \times 10^{-3} \text{ and } n_1 = 2, \quad (8.13a)$$

$$\text{for } t > 15 \text{ mm } C_{W1} = 0.1033 \times 10^{-3} \text{ and } n_1 = 1.9, \quad (8.13b)$$

$$K_{W1} = k_W \left( \Theta \sqrt{\kappa_1 \rho V_1} + 1.3 C_{W1} t^{n_1} L_{W1} \right). \quad (8.14)$$

(b) Welding the ring-stiffeners separately from 3 plate parts with 2 fillet welds (GMAW-C –gas metal arc welding with  $\text{CO}_2$ ):

$$K_{W2} = k_W \left( \Theta \sqrt{3 \rho V_2} + 1.3 \times 0.3394 \times 10^{-3} a_W^2 L_{W2} \right) \quad (8.15)$$

where

$$V_2 = 4\pi h_r t_r \left( R - \frac{h_r}{2} \right) + 2\pi h_r t_r (R - h_r) \quad (8.16)$$

$$L_{W2} = 4\pi (R - h_r), a_W = 0.7 t_r \quad (8.17)$$

(c) Welding the  $(n+1)$  ring-stiffeners into the shell with 2 circumferential fillet welds (GMAW-C)

$$K_{W3} = k_W \left( \Theta \sqrt{(n+2) \rho V_3} + 1.3 \times 0.3394 \times 10^{-3} a_W^2 L_{W3} \right) \quad (8.18)$$

where

$$V_3 = V_1 + (n+1)V_2, L_{W3} = 4R\pi(n+1) \quad (8.19)$$

Material cost

$$K_M = k_M \rho V_3, k_M = 1 \text{ \$/kg} \quad (8.20)$$

Painting cost

$$K_P = k_P S_P, k_P = 28.8 \times 10^{-6} \text{ \$/mm}^2, \quad (8.21)$$

$$S_P = 2R\pi L + 2R\pi [L - (n+1)h_r] + 2\pi (R - h_r) h_r (n+1) + 4\pi \left( R - \frac{h_r}{2} \right) h_r (n+1) \quad (8.22)$$

The total cost

$$K = K_M + K_{W1} + (n+1)K_{W2} + K_{W3} + K_P \quad (8.23)$$

### 8.1.6 Results of the Optimization

In the following the minimum cost design is obtained by a systematic search using a MathCAD algorithm.

For a shell thickness  $t$  the number of stiffeners  $n$  is determined by the shell buckling constraint (Eq. 8.1) and the stiffener dimensions ( $h_r$  and  $t_r$ ) are determined by the stiffener buckling constraint (Eq. 8.5).

The search results for  $R = 1851$  and  $1500$  (Tables 8.1 and 8.2) show that the volume and cost decreases when the radius is decreased. Thus, the realistic optimum can be obtained by taking the radius as small as possible. This minimum radius is determined by the requirement that the internal stiffeners should easily be welded inside of shell, i.e.  $R_{\min} = 1000$  mm. Therefore the more detailed search is performed for this radius (Table 8.3).

**Table 8.1** Systematic search for  $R = 1850$  mm. Dimensions are in mm. The minimum cost is marked by bold letters.

$t$	$n$	$\sigma < \sigma_{\text{adm}}$ MPa	$h_r$	$t_r$	$I_x > I_{\text{req}}$ $\times 10^{-4}$ mm <sup>4</sup>	$V \times 10^{-5}$ mm <sup>3</sup>	$K$ \$
11	7	126<152	180	6	3352>3341	10490	18770
12	6	115<143	180	6	3530>3502	10830	18640
13	5	106<124	190	6	4245>4014	11290	18650
14	4	99<109	200	6	5050>4888	11710	<b>18620</b>
15	4	92<121	200	6	5252>4718	12400	19390

**Table 8.2** Systematic search for  $R = 1500$  mm. Dimensions are in mm. The minimum cost is marked by bold letters.

$t$	$n$	$\sigma < \sigma_{\text{adm}}$ MPa	$h_r$	$t_r$	$I_x > I_{\text{req}}$ $\times 10^{-4}$ mm <sup>4</sup>	$V \times 10^{-5}$ mm <sup>3</sup>	$K$ \$
8	10	140<157	160	5	1745>1616	6830	13890
9	8	125<140	160	5	1590>1550	6870	13250
10	6	112<115	160	5	1995>1885	7130	<b>12900</b>
11	5	102<106	150	5	2109>2102	7480	12950
12	5	93<120	160	5	2217>2003	8050	13570

It can be seen from Table 8.3 that the optima for minimum volume and minimum cost are different. It is caused by the larger value of fabrication (welding and painting) cost. The details of the cost for  $K = \$ 7221$  are given in Table 8.4.

**Table 8.3** Systematic search for  $R = 1000$  mm. Dimensions are in mm. The optima are marked by bold letters.

$t$	$n$	$\sigma < \sigma_{\text{adm}}$ MPa	$h_r$	$t_r$	$I_x > I_{\text{req}}$ $\times 10^{-4}$ mm <sup>4</sup>	$V \times 10^{-5}$ mm <sup>3</sup>	$K$ \$
5	16	150<156	110	4	402>364	3192	8338
6	12	125<141	100	4	353>296	<b>3177</b>	7631
7	9	107<123	100	4	387>336	3343	7321
8	7	94<111	100	4	419>400	3579	7244
9	5	83<90	110	4	572>557	3854	<b>7221</b>
10	4	75<82	120	4	759>703	4186	7419
11	3	68<69	130	4	982>953	4505	7598



**Table 8.4** Details of the minimum cost in \$. (The sum of the welding and painting costs is \$4196).

$K_M$	$K_{W1}$	$(n+1)K_{W2}$	$K_{W3}$	$K_P$	$K$
3025	673	474	665	2384	7221

### 8.1.7 Conclusions

The structural volume and the cost decrease when the shell radius is decreased. Thus, the shell radius should be taken as small as possible. The minimum radius is determined by the limitation that the internal ring-stiffeners should be welded into the shell ( $R_{\min} = 1000$  mm).

The shell thickness and the number of ring-stiffeners can be calculated using the constraint on shell buckling. In order to avoid ring-stiffener tripping, welded square box section rings are used. The dimensions of the rings can be determined from the constraint on ring-stiffener buckling. The constraints on buckling are formulated according to the newer DNV design rules.

In the cost function the costs of material, assembly, welding and painting are formulated. The welding cost parts are calculated according to the fabrication sequence. The optima for minimum volume and minimum cost are different, since the fabrication cost parts are relatively high as compared to the whole cost.

The ring-stiffening is very effective, since in the case of  $n = 1$  (only 2 end stiffeners) the required shell thickness is  $t = 18$  mm, the volume is  $V = 7144 \times 10^{-3}$  mm<sup>3</sup> and the cost is  $K = \$10450$ , i.e. the cost savings achieved by ring-stiffeners is  $(10450 - 7221)/10450 \times 100 = 31\%$ .

## 8.2 Cost Comparison of Optimized Unstiffened Cylindrical and Conical Shells for a Cantilever Column Loaded by Axial Compression and Bending

### Abstract

The problem is to find the optimum dimensions of a cantilever column loaded by compression and bending. The column is constructed as circular or conical unstiffened shell. In both cases the cost minimum is not limited by a fabrication constraint. The cost comparison of both structural versions shows the most economic one.

### 8.2.1 Introduction

Columns or towers are used in many engineering structures, e.g. in buildings, wind turbine towers, piers of motorways, etc. They can be constructed as rectangular boxes or shells. Walls of boxes can be designed from stiffened plates or cellular plates. Shells can be unstiffened or stiffened circular or conical. A ring-stiffened conical shell is treated for external pressure in the case of equidistant stiffening (Farkas and Jármai 2008).

Previous studies have shown that, when the constraint on horizontal displacement of the column top is not active, the unstiffened circular shell can be cheaper than that of stringer stiffened one. In the present study the unstiffened circular shell is compared to the slightly conical one to show the economy of conical shells over the circular ones.

In previous studies the fabrication has been realized by using 3 m long plate elements to form unstiffened shell elements. In the present study 1.5 m wide plate elements are used. Therefore, the shell thicknesses can be varied in more shell parts. With equidistant shell elements of the same thickness the fabrication can be realized more easily.

The optimal thickness for each shell element is calculated from the shell buckling constraint according to the Det Norske Veritas (2002) design rules.

In the previous studies the fabrication sequence is designed so that the circumferential welds have been realized for the completely assembled shell. In order to ease the welding inside the shell the fabrication is changed and it is supposed that these welds are welded successively. Thus the next 1.5 m wide shell part is welded to the previous longer structure and so the number of assembled parts is always 2.

Firstly, the conical shell is optimized by using different radii with a constant inclination angle. Secondly, this angle is changed to show its effect. Thirdly, the optimal circular shell radius is sought to minimize the cost.

### 8.2.2 Constraint on Conical Shell Buckling

According to the DNV rules (2002) the buckling of conical shells is treated like buckling of an equivalent circular cylindrical shell.

The thickness, the average radius and the length of the  $i^{\text{th}}$  equivalent shell part are

$$t_{ei} = t_i \cos \alpha, R_{ei} = \frac{R_i + R_{i+1}}{2 \cos \alpha}, L_{ei} = \frac{L_i}{\cos \alpha}. \quad (8.24)$$

The inclination angle is defined by

$$\tan \alpha = \frac{R_{\max} - R_0}{L_0} \quad (8.25)$$

The sum of the axial and bending stresses should be smaller than the critical buckling stress

$$\sigma_{ai} + \sigma_{bi} = \frac{N_F}{2R_i \pi_{ei}} + \frac{H_F \left( \sum_{j=0}^{i-1} L_j + \frac{L_i}{2} \right)}{R_i^2 \pi_{ei}} \leq \sigma_{cri} = \frac{f_y}{\sqrt{1 + \lambda_i^4}} \quad (8.26)$$

where the reduced slenderness

$$\lambda_i^2 = \frac{f_y}{\sigma_{ai} + \sigma_{bi}} \left( \frac{\sigma_{ai}}{\sigma_{Eai}} + \frac{\sigma_{bi}}{\sigma_{Ebi}} \right) \quad (8.27)$$

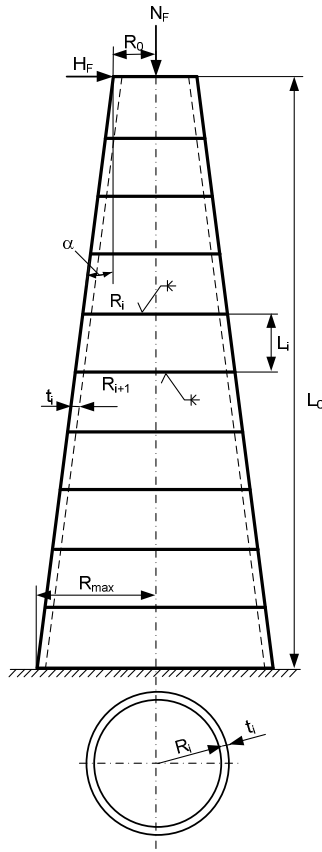


**Fig. 8.2** Conical shell cantilever column loaded by axial compression and bending

The elastic buckling stress for the axial compression is

$$\sigma_{Eai} = C_{ai} (1.5 - 50\beta) \frac{\pi^2 E}{10.92} \left( \frac{t_{ei}}{L_{ei}} \right)^2 \quad (8.28)$$

$$C_{ai} = \sqrt{1 + (\rho_{ai} \xi_i)^2}, \rho_{ai} = 0.5 \left( 1 + \frac{R_{eai}}{150 t_{ei}} \right)^{-0.5} \quad (8.29)$$

$$\xi_i = 0.702 Z_i, Z_i = \frac{L_{ei}^2 \sqrt{1 - \nu^2}}{R_{eai} t_{ei}}, \nu = 0.3 \quad (8.30)$$

The elastic buckling stress for bending is

$$\sigma_{Ebi} = C_{bi} (1.5 - 50\beta) \frac{\pi^2 E}{10.92} \left( \frac{t_{ei}}{L_{ei}} \right)^2 \quad (8.31)$$

$$C_{bi} = \sqrt{1 + (\rho_{bi} \xi_i)^2}, \rho_{bi} = 0.5 \left( 1 + \frac{R_{eai}}{300t_{ei}} \right)^{-0.5} \quad (8.32)$$

Note that the residual welding distortion factor  $1.5 - 50\beta = 1$  when  $t > 9$  mm. The detailed derivation of it is treated in (Farkas and Jármai 2003).

### 8.2.3 The Cost Function

The cost function contains the cost of material, forming of plate parts to conical or circular shell elements, welding and painting and is formulated according to the fabrication sequence.

The material cost is given by

$$K_M = k_M \rho V, k_M = 1.0 \$ / kg, \rho = 7.85 \times 10^{-6} \quad (8.33)$$

$$V = 2\pi \sum_{i=1}^{10} R_{eai} L_{ei} t_i \quad (8.34)$$

The cost of forming of plate parts into conical or circular shell elements

$$K_F = k_F \Theta \sum_{i=1}^{10} e^{\mu_i},$$

$$\mu_i = 6.8582513 - 4.52721t_i^{-0.5} + 0.009531996(2R_{eai})^{0.5}. \quad (8.35)$$

The coefficient for the complexity of assembly is  $\Theta = 3$ . The specific fabrication cost factor is taken as  $k_F = 1.0 \$ / \text{min}$ .

For a shell element 3 axial butt welds are needed (GMAW-C –Gas Metal Arc Welding with  $\text{CO}_2$ ).

$$K_{W0i} = k_F \left( \Theta \sqrt{\kappa \rho V_i} + 1.3 \times 0.152 \times 10^{-3} t_i^{1.94} 3L_{ei} \right) \quad (8.36)$$

The number of assembled elements is  $\kappa = 3$ .

Cost of welding of circumferential welds between shell elements. The welding is performed successively, so one weld is connecting only two parts in each fabrication step.

$$K_{Wi} = k_F \left( \Theta \sqrt{2\rho \left( \sum_{j=1}^{i-1} V_j + V_i \right)} + 1.3 \times 0.152 \times 10^{-3} t_i^{1.94} 2\pi R_i \right) \quad (8.37)$$

Cost of painting

$$K_p = k_p 4\pi \frac{R_{\max} + R_0}{2} L_0, k_p = 28.8 \times 10^{-6} \text{ \$/mm}^2. \quad (8.38)$$

The total cost

$$K = K_M + K_F + \sum_{i=1}^{10} K_{W0i} + \sum_{i=1}^{10} K_{Wi} + K_p \quad (8.39)$$

### 8.2.4 Numerical Data and Results

$L_0 = 15$  m, this height is divided in 10 shell parts, each length of  $L_i = 1500$  mm. This uniform length is selected for easy fabrication.  $N_F = 3400$  kN,  $H_F = 0.1N_F$ ,  $f_y = 355$  MPa,  $E = 2.1 \times 10^5$  MPa.

The calculation is performed by using a MathCAD algorithm. Results are given in Tables 8.5, 8.6 and 8.7.

**Table 8.5** Cost parts (\$) of conical shells of inclination angle  $2.86^\circ$  for different radii (mm)

$R_0$	$R_{\max}$	$K_M$	$K_{F0}$	$K_{W0}$	$K_W$	$K_P$	$K$
750	1500	26300	19895	9702	14750	6107	76754
850	1600	25660	19360	8300	13753	6650	73723
1050	1800	<b>24750</b>	18492	6536	12300	7736	69814
1250	2000	24790	17974	5664	11796	8822	<b>69046</b>
1450	2200	25320	17709	5191	11640	9907	69767
1650	2400	26090	17565	4881	11754	10990	71280

In Table 8.5 the minimum material cost (volume) and total cost are marked by bold letters. It can be seen that the minimum volume and minimum cost correspond to different radii. This difference is caused by high fabrication costs. The optimum is found, since the decrease of radii causes increase of thicknesses, which increases the material and welding cost, on the other hand the increase of radii causes increase of material and painting cost.

**Table 8.6** Cost parts (\$) of conical shells of different inclination angles (the average radius is 1625 mm)

Angle	$R_0$	$R_{\max}$	$K_M$	$K_{F0}$	$K_{W0}$	$K_W$	$K_P$	$K$
$4.38^\circ$	1050	2200	24870	17961	5676	11582	8822	<b>68911</b>
$6.65^\circ$	750	2500	25160	18246	5920	11424	8822	69572

The thicknesses for the optimal conical shell of inclination angle  $4.38^\circ$  are from above as follows: 18, 19, 20 and all others 21 mm.

**Table 8.7** Cost parts (\$) of circular shells for different radii. The minimum cost is marked by bold letters.

$R_0=R_{\max}$	$K_M$	$K_{F0}$	$K_{W0}$	$K_W$	$K_P$	$K$
1450	25750	18661	7070	13640	7872	72993
1650	25500	17960	5825	12393	8957	<b>70635</b>
1750	25500	17920	5596	12385	9500	70901
1850	25730	17809	5333	12250	10040	71162

The thicknesses for the optimal circular shell of radius 1650 mm are as follows: 14, 15, 17, 18, 20, 21, 23, 24, 26 and 27 mm.

## 8.2.5 Conclusions

The following fabrication aspects are considered: the change of shell thickness is designed in equal distances, the circumferential welds are welded successively to ease the welding inside of the shell, only integer numbers are used for shell thicknesses.

The structural volume or components of cost vary with radii in such manner that for both circular or conical unstiffened shells optimum radius can be found.

Three inclination angles of conical shell have been investigated and one of them was optimal.

The comparison of conical and circular shells shows that the cost of optimal conical shell is lower than that of circular one, but the difference is not very large  $(70635-68911)/70635 \times 100 = 2.8\%$ .

## 8.3 Conical Shell with Non-equidistant Ring-Stiffening Loaded by External Pressure

### Abstract

The problem is to design a slightly conical shell loaded in external pressure with non-equidistant ring-stiffeners of welded square box section. The optimum shell thickness is found, which minimizes the cost function and fulfils the design constraints. The length of each shell segment is calculated from the shell buckling constraint. The dimensions of ring-stiffeners for each shell segment are determined on the basis of the ring buckling constraint. The ring-stiffening is very effective, since the unstiffened shell needs a large thickness, which is unrealistic for fabrication.

### 8.3.1 Introduction

Minimum cost design has been worked out for ring-stiffened conical shell with equidistant ring-stiffening in (Farkas and Jármai 2008).

Ghazijahani and Showkati (2011) have described experiments on conical shell models. The measured buckling pressures have been lower than the predicted values. This differences have been caused by initial imperfections. It can be concluded that these low buckling stresses can be avoided by using ring stiffeners.

In the present study we select the following structural characteristics: steel, slightly conical shell, ring-stiffeners of welded square box section to avoid tripping, non-equidistant stiffening, external pressure, welding. Design rules of Det Norske Veritas (2002) are applied for shell and stiffener buckling constraints.

The variables to be optimized are as follows: length of shell segments for a given shell thickness (Fig. 8.3), dimensions of ring-stiffeners ( $h_i$ ,  $t_{ri}$ ). Stiffeners should be used at the ends of the shell, thus, two stiffeners are used in the first shell segment. The ring stiffeners are placed in a small distance from the circumferential welds connecting two segments to allow the inspection of welded joints, this is marked in Fig. 8.3 by dotted lines.

The cost function includes the cost of material, assembly, welding and painting and is formulated according to the fabrication sequence.

The optimization process has the following parts:

- (a) design of each shell segment length for a given shell thickness using the shell buckling constraint,
- (b) design of ring-stiffeners for each shell segment using the stiffener buckling constraint,
- (c) cost calculation for each shell segment and for the whole shell structure.

These design steps should be carried out for a series of shell thicknesses. On the basis of calculated costs the optimum solution corresponding to the minimum cost can be determined.

### 8.3.2 Design of Shell Segment Lengths

According to DNV rules (2002), for shell segments between two ring-stiffeners of radii  $R_i$  and  $R_{i+1}$  the buckling constraint valid for circular cylindrical shells with equivalent radius

$$R_{ei} = \frac{R_{i+1} + R_i}{2 \cos \alpha}, \cos \alpha = \frac{1}{\sqrt{\tan^2 \alpha + 1}} \quad (8.40)$$

$$\tan \alpha = \frac{R_{n+1} - R_1}{L_0}, R_{i+1} = L_i \tan \alpha + R_i \quad (8.41)$$

and equivalent thickness

$$t_{ei} = t_i \cos \alpha \quad (8.42)$$

The normal stress due to external pressure in a shell segment should be smaller than the critical buckling stress

$$\sigma_i = \frac{\gamma_b p R_i}{t_{ei}} \leq \sigma_{cri} = \frac{f_{y1}}{\sqrt{1 + \lambda_i^4}}, \quad \lambda_i = \sqrt{\frac{f_{y1}}{\sigma_{Ei}}} \quad (8.43)$$

$$\sigma_{Ei} = \frac{C_i \pi^2 E}{12(1 - \nu^2)} \left( \frac{t_{ei}}{L_{ei}} \right)^2, \quad L_{ei} = \frac{L_i}{\cos \alpha} \quad (8.44)$$

where

$$C_i = 4 \sqrt{1 + \left( \frac{0.6 \xi_i}{4} \right)^2}, \quad \xi_i = 1.04 \sqrt{Z_i}, \quad Z_i = \frac{L_{ei}^2}{R_{ei} t_{ei}} \sqrt{1 - \nu^2} \quad (8.45)$$

Using Eqs (8.44), Eq.(8.45) can be written in the form of

$$C_i = 4 \sqrt{1 + 0.023214 \frac{L_{ei}^2}{R_{ei} t_{ei}}} \quad (8.46)$$

From the shell buckling constraint Eq. (8.43) the unknown  $L_i$  can be calculated using a Mathcad program.

### 8.3.3 Design of a Ring-Stiffener for Each Shell Segment

For ring-stiffeners a square box section welded from 3 parts is selected to avoid tripping, which is dangerous failure mode for open-section stiffeners (Fig.8.3).

The constraint on local buckling of the compressed stiffener flange according to Eurocode 3 (2009) is expressed by

$$t_{ri} \geq \delta h_{i,1} / \delta = 42 \varepsilon, \quad \varepsilon = \sqrt{235 / f_y} \quad (8.47)$$

for  $f_y = 355 \text{ MPa}$   $1/\delta = 34$ .

Calculating with Eq.(8.47) as equality, the only unknown for a square ring-stiffener is the height  $h_i$ . This dimension can be determined from the stiffener buckling constraint relating to the required moment of inertia of a stiffener section about the axis  $x$  of the point E, which is the gravity centre of the cross-section including the 3 stiffener parts and the effective part of the shell (Fig.8.3).

$$I_{xi} \geq I_{reqi} = \frac{\gamma_b p R_i R_{ei}^2 L_{efi}}{3E} \left[ 2 + \frac{3E y_{Ei} 0.005 R_i}{R_{ei}^2 (f_{y1} / 2 - \sigma_i)} \right] \quad (8.48)$$





$$R_{Ei} = R_i - \left( h_i + \frac{t_i}{2} + \frac{\partial h_i}{2} - y_{Ei} \right) \quad (8.52)$$

The required  $h_i$  can be calculated from Eq.(8.48).

### 8.3.4 The Cost Function

The cost function is formulated according to the fabrication sequence as follows.

- (1) Forming of 3 plate elements for shell segments into slightly conical shape ( $K_{F0}$ ).
- (2) Welding 3 curved shell elements into a shell segment with GMAW-C (gas metal arc welding with  $\text{CO}_2$ ) butt welds ( $K_{F1}$ ).
- (3) Welding of  $n+1$  ring-stiffeners each from 3 elements with 2 GMAW-C fillet welds ( $K_{F2}$ ).
- (4) Welding of a ring-stiffener into each shell segment with 2 GMAW-C fillet welds ( $K_{F3}$ ).
- (5) Assembly of the whole stiffened shell structure from  $n$  shell segments ( $K_{F4A}$ ).
- (6) Welding of  $n$  shell segments to form the whole shell structure with  $n-1$  circumferential GMAW-C butt welds ( $K_{F4W}$ ).
- (7) Painting of the whole shell structure from inside and outside ( $K_P$ ).

The total cost includes the cost of material, assembly, welding and painting

$$K = K_M + K_{F0} + K_{F1} + K_{F2} + K_{F3} + K_{F4} + K_P \quad (8.53)$$

$$K_M = k_M \rho V, k_M = 1.0\$ / \text{kg} \quad (8.54)$$

The volume of the whole structure includes the volume of shell segments ( $V_{li}$ ) and ring-stiffeners ( $V_{ri}$ )

$$V = \sum_{i=1}^n V_{li} + \sum_{i=1}^{n+1} V_{ri} \quad (8.55)$$

$$K_{F0i} = k_F \Theta e^{\mu}, \mu = 6.8582513 - 4.527217 t_i^{-0.5} + 0.009541996 (2R_{ei})^{0.5}$$

$$K_{F0} = \sum_{i=1}^n K_{F0i} \quad (8.56)$$

where the factor of fabrication difficulty is taken as  $\Theta = 3$  and the steel density is  $\rho = 7.85 \times 10^{-6} \text{ kg/mm}^3$ .

$$K_{F1i} = k_F \left[ \Theta \sqrt{3\rho V_{li}} + 1.3 \times 0.152 \times 10^{-3} t_i^{1.9358} \times 3 L_{ei} \right], \quad K_{F1} = \sum_{i=1}^n K_{F1i} \quad (8.57)$$

$$V_{li} = 2\pi R_{ei} L_{ei} t_i \quad (8.58)$$

$$K_{F2i} = k_F \left[ \Theta \sqrt{3\rho V_{ri}} + 1.3 \times 0.3394 \times 10^{-3} a_{wi}^2 \times 4\pi (R_i - h_i) \right] \quad (8.59)$$

where

$$V_{ri} = 4\pi r_i h_i (R_i - h_i / 2) + 2\pi r_i h_i (R_i - h_i)$$

and the fillet weld size  $a_{wi} = 0.7\delta h_i$ .

$$K_{F3i} = k_F \left[ \Theta \sqrt{2\rho V_{3i}} + 1.3 \times 0.3394 \times 10^{-3} a_{wi}^2 \times 4\pi R_i \right], \quad V_{3i} = V_{li} + V_{ri} \quad (8.60)$$

$$K_{F4} = K_{F4A} + K_{F4W}, \quad K_{F4A} = k_F \Theta \sqrt{n\rho V}, \quad K_{F4W} = \sum_{i=2}^n K_{F4Wi} \quad (8.61)$$

$$K_{F4Wi} = 1.3 k_F \times 0.152 \times 10^{-3} t_i^{1.9358} \times 2\pi R_i \quad (8.62)$$

$$K_p = K_{p1} + \sum_{i=1}^{n+1} K_{pi}, \quad K_{p1} = k_p 4\pi \frac{R_{\max} + R_l}{2} L_0 \quad (8.63)$$

$$K_{pi} = k_p 4\pi h_i (R_i - h_i / 2) \quad (8.64)$$

$$k_p = 2 \times 14.4 \times 10^{-6} \text{ \$/mm}^2.$$

### 8.3.5 Numerical Data

Total shell length  $L = 15000$ , side radii  $R_{\min} = R_l = 1850$  and  $R_{\max} = R_{n+1} = 2850$  mm, yield stress of steel  $f_y = 355$  MPa, with a safety factor for yield stress  $f_{yl} = f_y/1.1$ , external pressure intensity

$p = 0.5$  MPa, safety factor for loading  $\gamma_b = 1.5$ , Poisson ratio  $\nu = 0.3$ , elastic modulus  $E = 2.1 \times 10^5$  MPa.

### 8.3.6 Results of the Optimization

The detailed calculations are carried out for shell thicknesses  $t_i = 14$ -20 mm. The corresponding material and total costs are summarized in Table 8.8.

**Table 8.8** The material and total costs in \$ for investigated shell thicknesses. The optima are marked by bold letters.

$t_i$ mm	$K_M$	$K$
14	<b>28490</b>	82280
16	29620	76150
18	32390	<b>75040</b>
20	38170	80120

**Table 8.9** Main dimensions (in mm) of the optimum shell structure ( $t = 18$  mm)

$R_i$	$L_i$	$h_i$	$t_{ri}$
1850	2630	121	4
2025	2376	134	4
2183	2189	146	5
2329	2044	158	5
2465	1927	170	5
2593	1831	182	6
2715	1750	194	6
2832	(1680)	207	7

It can be seen that the optimum shell thickness for material cost is 14 and for total cost 18 mm. This difference is caused by the fact that the fabrication (assembly, welding and painting) cost represents a large amount of total cost. The cost data show that, in the fabrication cost a significant part has the forming of plate elements into shell shape, welding and painting.

In order to characterize the dimensions of the optimum structure, the main data are given in Table 8.9.

### 8.3.7 Conclusions

The length of each shell segment is calculated from the shell buckling constraint. This constraint is similar to that for circular cylindrical shells, but equivalent thickness and segment length is used according to the DNV design rules (2002).

The dimensions of ring-stiffeners for each shell segment are determined on the basis of the ring buckling constraint. This constraint is expressed by the required moment of inertia of the ring-stiffener cross-section.

The cost function includes the cost of material, forming of plate elements into shell shape, assembly, welding and painting. The fabrication cost function is formulated according to the fabrication sequence. The forming, welding and painting costs play an important role in the total cost.

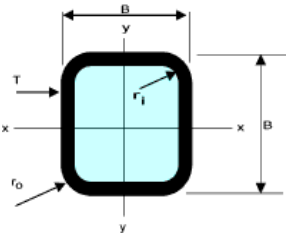
The cost difference between the maximum and minimum cost in the investigated range of is  $(82280-75040)/82280 \times 100 = 9\%$ , thus, a significant cost savings can be achieved by optimization.

The ring-stiffening is very effective, since the unstiffened shell needs a thickness of 42 mm, which is unrealistic for fabrication.

The shell with equidistant ring-stiffening has been optimized in (Farkas and Jármai 2008) resulting the minimum cost of \$79210. This means that the shell with non-equidistant stiffening is by 5% cheaper.

# Appendix A

## Square Hollow Sections Cold Formed BS EN 10219:1997



*M* = Weight; *A* = Cross-section area; *I* = Moment of inertia; *W* = Section modulus; *i* = Radius of gyration; *I<sub>t</sub>* = Torsion modulus; Theoretical density = 7.85 kg/dm<sup>3</sup>.

The cross-sectional properties have been calculated by using nominal dimensions *H*, *B* and *T* and corner outer radius *R*.

- R* = 2.0 x *T*, when *T* ≤ 6.0 mm.
- R* = 2.5 x *T*, when 6.0 mm < *T* ≤ 10.0 mm.
- R* = 3.0 x *T*, when *T* > 10.0 mm.

<i>H</i> x <i>B</i> mm	<i>T</i> mm	<i>M</i> kg/m	<i>A</i> mm <sup>2</sup> x 10 <sup>2</sup>	<i>I<sub>x</sub></i> = <i>I<sub>y</sub></i> mm <sup>4</sup> x 10 <sup>4</sup>	<i>W<sub>x</sub></i> = <i>W<sub>y</sub></i> mm <sup>3</sup> x 10 <sup>3</sup>	<i>i<sub>x</sub></i> = <i>i<sub>y</sub></i> mm x 10	<i>I<sub>t</sub></i> mm <sup>4</sup> x 10 <sup>4</sup>
25 x 25	2.0	1.36	1.74	1.48	1.19	0.92	2.53
25 x 25	2.5	1.64	2.09	1.69	1.35	0.90	2.97
25 x 25	3.0	1.89	2.41	1.84	1.47	0.87	3.33
30 x 30	2.0	1.68	2.14	2.72	1.81	1.13	4.54
30 x 30	2.5	2.03	2.59	3.16	2.10	1.10	5.40
30 x 30	3.0	2.36	3.01	3.50	2.34	1.08	6.15
40 x 40	2.0	2.31	2.94	6.94	3.47	1.54	11.28
40 x 40	2.5	2.82	3.59	8.22	4.11	1.51	13.61
40 x 40	3.0	3.30	4.21	9.32	4.66	1.49	15.75
40 x 40	4.0	4.20	5.35	11.07	5.54	1.44	19.44
50 x 50	2.0	2.93	3.74	14.15	5.66	1.95	22.63
50 x 50	2.5	3.60	4.59	16.94	6.78	1.92	27.53

$H \times B \text{ mm} \quad T \text{ mm} \quad M \text{ kg/m} \quad A \text{ mm}^2 \times 10^2 \quad I_x = I_y \text{ mm}^4 \times 10^4 \quad W_x = W_y \text{ mm}^3 \times 10^3 \quad i_x = i_y \text{ mm} \times 10 \quad I_t \text{ mm}^4 \times 10^4$							
50 x 50	3.0	4.25	5.41	19.47	7.79	1.90	32.13
50 x 50	4.0	5.45	6.95	23.74	9.49	1.85	40.42
50 x 50	5.0	6.56	8.36	27.04	10.82	1.80	47.46
60 x 60	2.0	3.56	4.54	25.14	8.38	2.35	39.79
60 x 60	2.5	4.39	5.59	30.34	10.11	2.33	48.66
60 x 60	3.0	5.19	6.61	35.13	11.71	2.31	57.09
60 x 60	4.0	6.71	8.55	43.55	14.52	2.26	72.64
60 x 60	5.0	8.13	10.36	50.49	16.83	2.21	86.42
70 x 70	2.5	5.17	6.59	49.41	14.12	2.74	78.49
70 x 70	3.0	6.13	7.81	57.53	16.44	2.71	92.42
70 x 70	4.0	7.97	10.15	72.12	20.61	2.67	118.52
70 x 70	5.0	9.70	12.36	84.63	24.18	2.62	142.21
80 x 80	2.5	5.96	7.59	75.15	18.79	3.15	118.52
80 x 80	3.0	7.07	9.01	87.84	21.96	3.12	139.93
80 x 80	4.0	9.22	11.75	111.04	27.76	3.07	180.44
80 x 80	5.0	11.30	14.36	131.44	32.86	3.03	217.83
80 x 80	6.0	13.20	16.83	149.18	37.29	2.98	252.07
90 x 90	2.5	6.74	8.59	108.55	24.12	3.56	170.26
90 x 90	3.0	8.01	10.21	127.28	28.29	3.53	201.42
90 x 90	4.0	10.50	13.35	161.92	35.98	3.48	260.80
90 x 90	5.0	12.80	16.36	192.93	42.87	3.43	316.26
90 x 90	6.0	15.10	19.23	220.48	49.00	3.39	367.76
100 x 100	2.5	7.53	9.59	150.63	30.13	3.96	235.21
100 x 100	3.0	8.96	11.41	177.05	35.41	3.94	278.68
100 x 100	4.0	11.70	14.95	226.35	45.27	3.89	362.01
100 x 100	5.0	14.40	18.36	271.10	54.22	3.84	440.52
100 x 100	6.0	17.00	21.63	311.47	62.29	3.79	514.16
100 x 100	7.1	19.40	24.65	340.13	68.03	3.71	589.17
100 x 100	8.0	21.40	27.24	365.94	73.19	3.67	644.51
100 x 100	10.0	25.60	32.57	411.08	82.22	3.55	749.84
110 x 110	2.5	8.31	10.59	202.38	36.80	4.37	314.86
110 x 110	3.0	9.90	12.61	238.34	43.33	4.35	373.51
110 x 110	4.0	13.00	16.55	305.94	55.62	4.30	486.47
110 x 110	5.0	16.00	20.36	367.95	66.90	4.25	593.60
110 x 110	6.0	18.90	24.03	424.57	77.19	4.20	694.85
120 x 120	3.0	10.80	13.81	312.35	52.06	4.76	487.72
120 x 120	4.0	14.30	18.15	402.28	67.05	4.71	636.57

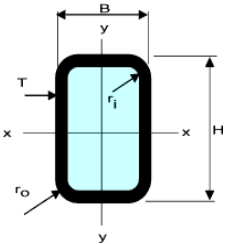
<i>H x B mm T mm M kg/m A mm<sup>2</sup> x 10<sup>2</sup> I<sub>x</sub> = I<sub>y</sub> mm<sup>4</sup> x 10<sup>4</sup> W<sub>x</sub> = W<sub>y</sub> mm<sup>3</sup> x 10<sup>3</sup> i<sub>x</sub> = i<sub>y</sub> mm x 10 I<sub>t</sub> mm<sup>4</sup> x 10<sup>4</sup></i>							
120 x 120	5.0	17.60	22.36	485.47	80.91	4.66	778.50
120 x 120	5.6	19.50	24.82	532.25	88.71	4.63	860.31
120 x 120	6.0	20.80	26.43	562.16	93.69	4.61	913.46
120 x 120	7.1	23.80	30.33	623.30	103.88	4.53	1056.01
120 x 120	8.0	26.40	33.64	676.88	112.81	4.49	1162.95
120 x 120	8.8	28.60	36.48	719.88	119.98	4.44	1252.41
120 x 120	10.0	31.80	40.57	776.81	129.47	4.38	1376.41
140 x 140	4.0	16.80	21.35	651.62	93.09	5.52	1023.32
140 x 140	5.0	20.70	26.36	790.56	112.94	5.48	1255.76
140 x 140	5.6	23.00	29.30	869.55	124.22	5.45	1390.71
140 x 140	6.0	24.50	31.23	920.43	131.49	5.43	1478.77
140 x 140	7.1	28.30	36.01	1031.40	147.34	5.35	1718.74
140 x 140	8.0	31.40	40.04	1126.77	160.97	5.30	1900.84
140 x 140	8.8	34.20	43.52	1205.03	172.15	5.26	2055.40
140 x 140	10.0	38.10	48.57	1311.67	187.38	5.20	2273.90
150 x 150	4.0	18.00	22.95	807.82	107.71	5.93	1264.76
150 x 150	5.0	22.30	28.36	982.12	130.95	5.89	1554.13
150 x 150	6.0	26.40	33.63	1145.91	152.79	5.84	1832.69
150 x 150	7.1	30.50	38.85	1289.35	171.91	5.76	2134.21
150 x 150	8.0	34.00	43.24	1411.83	188.24	5.71	2364.08
150 x 150	8.8	36.90	47.04	1513.12	201.75	5.67	2560.17
150 x 150	10.0	41.30	52.57	1652.53	220.34	5.61	2839.24
150 x 150	12.5	48.70	62.04	1817.44	242.33	5.41	3320.84
160 x 160	4.0	19.30	24.55	987.17	123.40	6.34	1541.45
160 x 160	5.0	23.80	30.36	1202.36	150.29	6.29	1896.32
160 x 160	6.0	28.30	36.03	1405.48	175.69	6.25	2238.90
160 x 160	7.1	32.70	41.69	1587.01	198.38	6.17	2611.42
160 x 160	8.0	36.50	46.44	1741.23	217.65	6.12	2896.58
160 x 160	8.8	39.70	50.56	1869.59	233.70	6.08	3140.82
160 x 160	10.0	44.40	56.57	2047.67	255.96	6.02	3490.29
160 x 160	12.0	50.90	64.86	2224.36	278.05	5.86	3996.72
160 x 160	12.5	52.60	67.04	2275.04	284.38	5.83	4113.99
180 x 180	5.0	27.00	34.36	1736.87	192.99	7.11	2724.16
180 x 180	6.0	32.10	40.83	2036.52	226.28	7.06	3222.65
180 x 180	7.1	37.20	47.37	2312.84	256.98	6.99	3768.11
180 x 180	8.0	41.50	52.84	2545.86	282.87	6.94	4188.56
180 x 180	8.8	45.20	57.60	2741.73	304.64	6.90	4550.90



$H \times B \text{ mm} \quad T \text{ mm} \quad M \text{ kg/m} \quad A \text{ mm}^2 \times 10^2 \quad I_x = I_y \text{ mm}^4 \times 10^4 \quad W_x = W_y \text{ mm}^3 \times 10^3 \quad i_x = i_y \text{ mm} \times 10 \quad I_t \text{ mm}^4 \times 10^4$							
180 x 180	10.0	50.70	64.57	3016.80	335.20	6.84	5073.57
180 x 180	12.5	60.50	77.04	3406.43	378.49	6.65	6049.85
200 x 200	5.0	30.10	38.36	2410.09	241.01	7.93	3763.30
200 x 200	6.0	35.80	45.63	2832.75	283.27	7.88	4458.81
200 x 200	7.1	41.60	53.05	3231.60	323.16	7.81	5222.90
200 x 200	8.0	46.50	59.24	3566.25	356.63	7.76	5815.18
200 x 200	8.8	50.80	64.64	3849.59	384.96	7.72	6327.89
200 x 200	10.0	57.00	72.57	4251.06	425.11	7.65	7071.73
200 x 200	12.5	68.30	87.04	4859.42	485.94	7.47	8501.74
220 x 220	6.0	39.60	50.43	3813.36	346.67	8.70	5976.18
220 x 220	7.1	46.10	58.73	4366.03	396.91	8.62	7009.86
220 x 220	8.0	51.50	65.64	4828.01	438.91	8.58	7814.84
220 x 220	8.8	56.30	71.68	5221.35	474.67	8.53	8514.01
220 x 220	10.0	63.20	80.57	5782.46	525.68	8.47	9532.77
220 x 220	12.5	76.20	97.04	6673.98	606.73	8.29	11529.63
250 x 250	6.0	45.20	57.63	5672.00	453.76	9.92	8842.52
250 x 250	7.1	52.80	67.25	6521.74	521.74	9.85	10387.69
250 x 250	8.0	59.10	75.24	7229.20	578.34	9.80	11597.77
250 x 250	8.8	64.60	82.24	7835.39	626.83	9.76	12652.72
250 x 250	10.0	72.70	92.57	8706.67	696.53	9.70	14197.22
250 x 250	12.5	88.00	112.04	10161.31	812.91	9.52	17282.65
260 x 260	6.0	47.10	60.03	6404.54	492.66	10.33	9969.77
260 x 260	7.1	55.00	70.09	7372.75	567.13	10.26	11716.64
260 x 260	8.0	61.60	78.44	8178.02	629.08	10.21	13086.86
260 x 260	8.8	67.30	85.76	8869.18	682.24	10.17	14282.62
260 x 260	10.0	75.80	96.57	9864.65	758.82	10.11	16035.47
260 x 260	11.0	81.90	104.37	10475.62	805.82	10.02	17497.85
260 x 260	12.5	91.90	117.04	11547.88	888.3	9.93	19553.31
300 x 300	6.0	54.70	69.63	9963.67	664.24	11.96	15433.82
300 x 300	7.1	63.90	81.45	11516.13	767.65	11.89	18161.09
300 x 300	8.0	71.60	91.24	12800.69	853.38	11.84	20311.84
300 x 300	8.8	78.40	99.84	13910.50	927.37	11.80	22194.64
300 x 300	10.0	88.40	112.57	15519.37	1034.62	11.74	24965.66
300 x 300	12.5	108.00	137.04	18348.13	1223.21	11.57	30600.78

# Appendix B

## Rectangular Hollow Section Cold Formed BS EN 10219:1997



<i>H x B</i> <i>mm</i>	<i>T</i> <i>mm</i>	<i>A mm<sup>2</sup> x</i> <i>10<sup>2</sup></i>	<i>I<sub>x</sub> mm<sup>4</sup> x</i> <i>10<sup>4</sup></i>	<i>W<sub>x</sub> mm<sup>3</sup> x</i> <i>10<sup>3</sup></i>	<i>i<sub>x</sub> mm x</i> <i>10</i>	<i>I<sub>y</sub> mm<sup>4</sup> x</i> <i>10<sup>4</sup></i>	<i>W<sub>y</sub> mm<sup>3</sup> x</i> <i>10<sup>3</sup></i>	<i>i<sub>y</sub> mm x</i> <i>10</i>	<i>I<sub>yt</sub> mm<sup>4</sup> x</i> <i>10<sup>4</sup></i>
40 x 20	2.0	2.14	4.05	2.02	1.38	1.34	1.34	0.79	3.45
40 x 20	2.5	2.59	4.69	2.35	1.35	1.54	1.54	0.77	4.06
40 x 20	3.0	3.01	5.21	2.60	1.32	1.68	1.68	0.75	4.57
40 x 30	2.0	2.54	5.49	2.75	1.47	3.51	2.34	1.18	7.07
40 x 30	2.5	3.09	6.45	3.23	1.45	4.10	2.74	1.15	8.47
40 x 30	3.0	3.61	7.27	3.63	1.42	4.60	3.07	1.13	9.72
50 x 30	2.0	2.94	9.54	3.81	1.8	4.29	2.86	1.21	9.77
50 x 30	2.5	3.59	11.30	4.52	1.77	5.05	3.37	1.19	11.74
50 x 30	3.0	4.21	12.83	5.13	1.75	5.70	3.80	1.16	13.53
50 x 30	4.0	5.35	15.25	6.10	1.69	6.69	4.46	1.12	16.53
60 x 40	2.0	3.74	18.41	6.14	2.22	9.83	4.92	1.62	20.70
60 x 40	2.5	4.59	22.07	7.36	2.19	11.74	5.87	1.60	25.14
60 x 40	3.0	5.41	25.38	8.46	2.17	13.44	6.72	1.58	29.28
60 x 40	4.0	6.95	30.99	10.33	2.11	16.28	8.14	1.53	36.67
60 x 40	5.0	8.36	35.33	11.78	2.06	18.43	9.21	1.48	42.85
70 x 50	2.0	4.54	31.48	8.99	2.63	18.76	7.50	2.03	37.45
70 x 50	2.5	5.59	38.01	10.86	2.61	22.59	9.04	2.01	45.75
70 x 50	3.0	6.61	44.05	12.59	2.58	26.10	10.44	1.99	53.62
70 x 50	4.0	8.55	54.67	15.62	2.53	32.22	12.89	1.94	68.07

$H \times B$ mm	$T$ mm	$A \text{ mm}^2 \times$ $10^2$	$I_x \text{ mm}^4 \times$ $10^4$	$W_x \text{ mm}^3 \times$ $10^3$	$i_x \text{ mm} \times$ $10$	$I_y \text{ mm}^4 \times$ $10^4$	$W_y \text{ mm}^3 \times$ $10^3$	$i_y \text{ mm} \times$ $10$	$I_{yt} \text{ mm}^4 \times$ $10^4$
70 x 50	5.0	10.36	63.46	18.13	2.48	37.20	14.88	1.90	80.77
80 x 40	2.0	4.54	37.36	9.34	2.87	12.72	6.36	1.67	30.88
80 x 40	2.5	5.59	45.11	11.28	2.84	15.26	7.63	1.65	37.58
80 x 40	3.0	6.61	52.25	13.06	2.81	17.56	8.78	1.63	43.88
80 x 40	4.0	8.55	64.79	16.20	2.75	21.49	10.74	1.59	55.24
80 x 40	5.0	10.36	75.11	18.78	2.69	24.59	12.30	1.54	64.97
80 x 60	2.5	6.59	60.13	15.03	3.02	38.61	12.87	2.42	75.07
80 x 60	3.0	7.81	70.05	17.51	3.00	44.89	14.96	2.40	88.35
80 x 60	4.0	10.15	87.92	21.98	2.94	56.12	18.71	2.35	113.12
80 x 60	5.0	12.36	103.28	25.82	2.89	65.66	21.89	2.31	135.53
90 x 50	2.5	6.59	70.26	15.61	3.27	28.24	11.29	2.07	65.30
90 x 50	3.0	7.81	81.85	18.19	3.24	32.74	13.10	2.05	76.67
90 x 50	4.0	10.15	102.71	22.82	3.18	40.71	16.28	2.00	97.70
90 x 50	5.0	12.36	120.60	26.80	3.12	47.37	18.95	1.96	116.47
100 x 40	2.5	6.59	79.32	15.86	3.47	18.78	9.39	1.69	50.52
100 x 40	3.0	7.81	92.34	18.47	3.44	21.67	10.84	1.67	59.05
100 x 40	4.0	10.15	115.70	23.14	3.38	26.69	13.35	1.62	74.53
100 x 40	5.0	12.36	135.60	27.12	3.31	30.76	15.38	1.58	87.92
100 x 50	2.5	7.09	91.20	18.24	3.59	31.06	12.42	2.09	75.39
100 x 50	3.0	8.41	106.46	21.29	3.56	36.06	14.42	2.07	88.56
100 x 50	4.0	10.95	134.14	26.83	3.50	44.95	17.98	2.03	112.99
100 x 50	5.0	13.36	158.19	31.64	3.44	52.45	20.98	1.98	134.87
100 x 50	6.0	15.63	178.75	35.75	3.38	58.67	23.47	1.94	154.20
100 x 60	2.5	7.59	103.09	20.62	3.69	46.88	15.63	2.49	103.25
100 x 60	3.0	9.01	120.57	24.11	3.66	54.65	18.22	2.46	121.67
100 x 60	4.0	11.75	152.58	30.52	3.60	68.68	22.89	2.42	156.27
100 x 60	5.0	14.36	180.77	36.15	3.55	80.83	26.94	2.37	187.86
100 x 60	6.0	16.83	205.30	41.06	3.49	91.20	30.40	2.33	216.44
100 x 80	2.5	8.59	126.86	25.37	3.84	90.17	22.54	3.24	165.84
100 x 80	3.0	10.21	148.81	29.76	3.82	105.64	26.41	3.22	196.12
100 x 80	4.0	13.35	189.47	37.89	3.77	134.17	33.54	3.17	253.79
100 x 80	5.0	16.36	225.94	45.19	3.72	159.61	39.90	3.12	307.55
100 x 80	6.0	19.23	258.39	51.68	3.67	182.1	45.53	3.08	357.38
120 x 40	2.5	7.59	126.71	21.12	4.09	22.30	11.15	1.71	63.77
120 x 40	3.0	9.01	148.04	24.67	4.05	25.79	12.89	1.69	74.56
120 x 40	4.0	11.75	186.89	31.15	3.99	31.90	15.95	1.65	94.23
120 x 40	5.0	14.36	220.81	36.80	3.92	36.93	18.46	1.60	111.35

$H \times B$ <i>mm</i>	<i>T</i> <i>mm</i>	$A \text{ mm}^2 \times$ $10^2$	$I_x \text{ mm}^4 \times$ $10^4$	$W_x \text{ m}^3 \times$ $10^3$	$i_x \text{ mm} \times$ $10$	$I_y \text{ mm}^4 \times$ $10^4$	$W_y \text{ mm}^3 \times$ $10^3$	$i_y \text{ mm} \times$ $10$	$I_{yt} \text{ mm}^4 \times$ $10^4$
120 x 40	6.0	16.83	249.97	41.66	3.85	40.97	20.49	1.56	125.97
120 x 50	2.5	8.09	143.97	23.99	4.22	36.70	14.68	2.13	96.03
120 x 50	3.0	9.61	168.58	28.10	4.19	42.69	17.08	2.11	112.87
120 x 50	4.0	12.55	213.82	35.64	4.13	53.43	21.37	2.06	144.22
120 x 50	5.0	15.36	253.89	42.32	4.07	62.62	25.05	2.02	172.44
120 x 50	6.0	18.03	288.99	48.16	4.00	70.36	28.14	1.98	197.55
120 x 60	2.5	8.59	161.23	26.87	4.33	55.15	18.38	2.53	132.57
120 x 60	3.0	10.21	189.12	31.52	4.30	64.40	21.47	2.51	156.34
120 x 60	4.0	13.35	240.74	40.12	4.25	81.25	27.08	2.47	201.12
120 x 60	5.0	16.36	286.97	47.83	4.19	95.99	32.00	2.42	242.23
120 x 60	6.0	19.23	328.01	54.67	4.13	108.77	36.26	2.38	279.67
120 x 80	2.5	9.59	195.75	32.63	4.52	105.19	26.30	3.31	215.82
120 x 80	3.0	11.41	230.20	38.37	4.49	123.43	30.86	3.29	255.47
120 x 80	4.0	14.95	294.59	49.10	4.44	157.29	39.32	3.24	331.24
120 x 80	5.0	18.36	353.14	58.86	4.39	187.78	46.94	3.20	402.27
120 x 80	6.0	21.63	406.06	67.68	4.33	215.03	53.76	3.15	468.54
120 x 80	7.1	24.65	442.06	73.68	4.24	234.41	58.60	3.08	535.11
120 x 80	8.0	27.24	475.83	79.31	4.18	251.66	62.92	3.04	584.04
120 x 80	8.8	29.44	501.79	83.63	4.13	264.84	66.21	3.00	623.54
120 x 80	10.0	32.57	534.14	89.02	4.05	281.14	70.29	2.94	675.59
120 x 100	2.5	10.59	230.27	38.38	4.66	174.40	34.88	4.06	309.43
120 x 100	3.0	12.61	271.27	45.21	4.64	205.28	41.06	4.04	367.01
120 x 100	4.0	16.55	348.43	58.07	4.59	263.24	52.65	3.99	477.84
120 x 100	5.0	20.36	419.31	69.88	4.54	316.27	63.25	3.94	582.86
120 x 100	6.0	24.03	484.11	80.68	4.49	364.56	72.91	3.89	682.04
140 x 60	2.5	9.59	236.55	33.79	4.97	63.43	21.14	2.57	162.67
140 x 60	3.0	11.41	278.08	39.73	4.94	74.16	24.72	2.55	191.92
140 x 60	4.0	14.95	355.59	50.80	4.88	93.81	31.27	2.51	247.13
140 x 60	5.0	18.36	425.89	60.84	4.82	111.16	37.05	2.46	297.97
140 x 60	6.0	21.63	489.19	69.88	4.76	126.34	42.11	2.42	344.46
140 x 70	2.5	10.09	260.18	37.17	5.08	89.30	25.51	2.98	213.11
140 x 70	3.0	12.01	306.24	43.75	5.05	104.69	29.91	2.95	251.99
140 x 70	4.0	15.75	392.60	56.09	4.99	133.18	38.05	2.91	326.02
140 x 70	5.0	19.36	471.48	67.35	4.94	158.71	45.35	2.86	395.06
140 x 70	6.0	22.83	543.10	77.59	4.88	181.44	51.84	2.82	459.09
140 x 80	3.0	12.61	334.40	47.77	5.15	141.23	35.31	3.35	317.07
140 x 80	4.0	16.55	429.60	61.37	5.10	180.42	45.10	3.30	411.6

$H \times B$ mm	$T$ mm	$A \text{ mm}^2 \times 10^2$	$I_x \text{ mm}^4 \times 10^4$	$W_x \text{ mm}^3 \times 10^3$	$i_x \text{ mm} \times 10$	$I_y \text{ mm}^4 \times 10^4$	$W_y \text{ mm}^3 \times 10^3$	$i_y \text{ mm} \times 10$	$I_{yt} \text{ mm}^4 \times 10^4$
140 x 80	5.0	20.36	517.06	73.87	5.04	215.94	53.99	3.26	500.51
140 x 80	6.0	24.03	597.00	85.29	4.98	247.96	61.99	3.21	583.80
150 x 50	2.5	9.59	254.08	33.88	5.15	45.17	18.07	2.17	127.74
150 x 50	3.0	11.41	298.55	39.81	5.12	52.65	21.06	2.15	150.22
150 x 50	4.0	14.95	381.39	50.85	5.05	66.16	26.47	2.10	192.14
150 x 50	5.0	18.36	456.29	60.84	4.99	77.87	31.15	2.06	230.05
150 x 50	6.0	21.63	523.47	69.80	4.92	87.89	35.16	2.02	263.99
150 x 100	3.0	14.41	460.64	61.42	5.65	247.64	49.53	4.15	507.20
150 x 100	4.0	18.95	594.60	79.28	5.60	318.57	63.71	4.10	661.63
150 x 100	5.0	23.36	719.20	95.89	5.55	384.02	76.80	4.05	808.68
150 x 100	6.0	27.63	834.69	111.29	5.50	444.19	88.84	4.01	948.34
150 x 100	7.1	31.75	926.59	123.55	5.40	493.46	98.69	3.94	1095.51
150 x 100	8.0	35.24	1008.13	134.42	5.35	535.65	107.13	3.90	1205.89
150 x 100	8.8	38.24	1073.93	143.19	5.30	569.53	113.91	3.86	1298.14
150 x 100	10.0	42.57	1161.70	154.89	5.22	614.41	122.88	3.80	1425.87
160 x 70	4.0	17.35	549.03	68.63	5.63	150.62	43.04	2.95	389.66
160 x 70	5.0	21.36	661.61	82.70	5.57	179.88	51.39	2.90	472.53
160 x 70	6.0	25.23	764.83	95.60	5.51	206.09	58.88	2.86	549.60
160 x 70	8.0	32.04	908.72	113.59	5.33	243.26	69.50	2.76	683.68
160 x 80	3.0	13.81	463.81	57.98	5.80	159.03	39.76	3.39	380.34
160 x 80	4.0	18.15	597.71	74.71	5.74	203.54	50.89	3.35	494.10
160 x 80	5.0	22.36	721.69	90.21	5.68	244.11	61.03	3.30	601.34
160 x 80	6.0	26.43	836.01	104.5	5.62	280.89	70.22	3.26	702.06
160 x 80	7.1	30.33	922.59	115.32	5.52	310.11	77.53	3.20	805.54
160 x 80	8.0	33.64	1001.22	125.15	5.46	334.95	83.74	3.16	882.33
160 x 80	8.8	36.48	1063.96	132.99	5.40	354.52	88.63	3.12	945.41
160 x 80	10.0	40.57	1146.34	143.29	5.32	379.81	94.95	3.06	1030.69
160 x 90	3.0	14.41	500.79	62.60	5.90	206.79	45.95	3.79	465.40
160 x 90	4.0	18.95	646.39	80.80	5.84	265.54	59.01	3.74	606.16
160 x 90	5.0	23.36	781.77	97.72	5.79	319.52	71.00	3.70	739.70
160 x 90	6.0	27.63	907.19	113.40	5.73	368.91	81.98	3.65	866.01
160 x 90	7.1	31.75	1005.64	125.70	5.63	409.20	90.93	3.59	997.94
160 x 90	8.0	35.24	1093.73	136.72	5.57	443.46	98.55	3.55	1096.54
160 x 90	8.8	38.24	1164.66	145.58	5.52	470.82	104.63	3.51	1178.47
180 x 100	4.0	21.35	926.04	102.89	6.59	373.89	74.78	4.18	853.85
180 x 100	5.0	26.36	1124.20	124.91	6.53	451.77	90.35	4.14	1044.79
180 x 100	5.6	29.30	1236.96	137.44	6.50	495.69	99.14	4.11	1155.01

$H \times B$ mm	$T$ mm	$A \text{ mm}^2 \times 10^2$	$I_x \text{ mm}^4 \times 10^4$	$W_x \text{ mm}^3 \times 10^3$	$i_x \text{ mm} \times 10$	$I_y \text{ mm}^4 \times 10^4$	$W_y \text{ mm}^3 \times 10^3$	$i_y \text{ mm} \times 10$	$I_{yt} \text{ mm}^4 \times 10^4$
180 x 100	6.0	31.23	1309.61	145.51	6.48	523.83	104.77	4.10	1226.68
180 x 100	7.1	36.01	1463.36	162.60	6.38	585.55	117.11	4.03	1419.69
180 x 100	8.0	40.04	1598.49	177.61	6.32	637.47	127.49	3.99	1565.24
180 x 100	8.8	43.52	1709.13	189.90	6.27	679.66	135.93	3.95	1687.64
180 x 100	10.0	48.57	1859.47	206.61	6.19	736.41	147.28	3.89	1858.62
180 x 120	4.0	22.95	1049.97	116.66	6.76	563.81	93.97	4.96	1160.17
180 x 120	5.0	28.36	1277.37	141.93	6.71	683.97	111.00	4.91	1423.83
180 x 120	6.0	33.63	1491.34	165.70	6.66	796.30	132.72	4.87	1676.88
180 x 120	7.1	38.85	1675.73	186.19	6.57	895.15	149.19	4.80	1949.25
180 x 120	8.0	43.24	1835.33	203.93	6.51	978.44	163.07	4.76	2156.35
180 x 120	8.8	47.04	1967.28	218.59	6.47	1047.00	174.50	4.72	2332.35
180 x 120	10.0	52.57	2148.80	238.76	6.39	1140.81	190.13	4.66	2581.64
180 x 120	12.5	62.04	2352.37	261.37	6.16	1252.33	208.72	4.49	3001.38
200 x 80	4.0	21.35	1046.02	104.60	7.00	249.80	62.45	3.42	663.60
200 x 80	5.0	26.36	1269.09	126.91	6.94	300.44	75.11	3.38	808.38
200 x 80	6.0	31.23	1477.42	147.74	6.88	346.74	86.69	3.33	944.77
200 x 80	7.1	36.01	1645.72	164.57	6.76	385.82	96.45	3.27	1086.19
200 x 80	8.0	40.04	1795.76	179.58	6.70	418.23	104.56	3.23	1191.77
200 x 80	8.8	43.52	1918.00	191.80	6.64	444.20	111.05	3.19	1279.19
200 x 80	10.0	48.57	2083.06	208.31	6.55	478.48	119.62	3.14	1398.83
200 x 100	4.0	22.95	1199.71	119.97	7.23	410.78	82.16	4.23	985.38
200 x 100	5.0	28.36	1459.25	145.93	7.17	496.94	99.39	4.19	1206.29
200 x 100	6.0	33.63	1703.31	170.33	7.12	576.91	115.38	4.14	1417.03
200 x 100	7.1	38.85	1910.04	191.00	7.01	646.95	129.39	4.08	1641.19
200 x 100	8.0	43.24	2090.84	209.08	6.95	705.36	141.07	4.04	1810.72
200 x 100	8.8	47.04	2239.93	223.99	6.90	753.08	150.62	4.00	1953.68
200 x 100	10.0	52.57	2444.40	244.44	6.82	817.74	163.55	3.94	2154.13
200 x 100	12.5	62.04	2658.89	265.89	6.55	892.15	178.43	3.79	2473.75
200 x 120	5.0	30.36	1649.42	164.94	7.37	750.14	125.02	4.97	1652.00
200 x 120	6.0	36.03	1929.20	192.92	7.32	874.35	145.72	4.93	1946.73
200 x 120	7.1	41.69	2174.35	217.44	7.22	985.77	164.30	4.86	2264.63
200 x 120	8.0	46.44	2385.92	238.59	7.17	1078.97	179.83	4.82	2507.04
200 x 120	8.8	50.56	2561.86	256.19	7.12	1156.05	192.67	4.78	2713.55
200 x 120	10.0	56.57	2805.73	280.57	7.04	1262.14	210.36	4.72	3007.03
200 x 120	12.5	67.00	3099.00	310.00	6.80	1397.00	233.00	4.57	3514.00
220 x 120	5.0	32.36	2082.19	189.29	8.02	816.31	136.05	5.02	1884.69
220 x 120	6.0	38.43	2439.12	221.74	7.97	952.40	158.73	4.98	2221.88

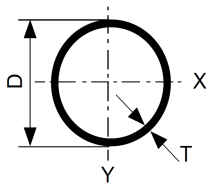
$H \times B$ <i>mm</i>	<i>T</i> <i>mm</i>	$A \text{ mm}^2 \times$ $10^2$	$I_x \text{ mm}^4 \times$ $10^4$	$W_x \text{ mm}^3 \times$ $10^3$	$i_x \text{ mm} \times$ $10$	$I_y \text{ mm}^4 \times$ $10^4$	$W_y \text{ mm}^3 \times$ $10^3$	$i_y \text{ mm} \times$ $10$	$I_{yt} \text{ mm}^4 \times$ $10^4$
220 x 120	7.1	44.53	2756.35	250.58	7.87	1076.39	179.40	4.92	2586.02
220 x 120	8.0	49.64	3029.40	275.40	7.81	1179.49	196.58	4.87	2864.35
220 x 120	8.8	54.08	3257.58	296.14	7.76	1265.09	210.85	4.84	3101.90
220 x 120	10.0	60.57	3575.79	325.07	7.68	1383.47	230.58	4.78	3440.33
250 x 100	5.0	33.36	2553.76	204.30	8.75	609.85	121.97	4.28	1620.11
250 x 100	6.0	39.63	2992.34	239.39	8.69	709.63	141.93	4.23	1904.54
250 x 100	8.0	51.24	3714.08	297.13	8.51	875.06	175.01	4.13	2438.66
250 x 100	10.0	62.57	4384.17	350.73	8.37	1021.08	204.22	4.04	2909.59
250 x 150	5.0	38.36	3304.18	264.33	9.28	1507.95	201.06	6.27	3284.54
250 x 150	6.0	45.63	3885.56	310.84	9.23	1768.35	235.78	6.23	3885.80
250 x 150	7.1	53.05	4426.62	354.13	9.13	2014.87	268.65	6.16	4542.75
250 x 150	8.0	59.24	4885.79	390.86	9.08	2219.25	295.90	6.12	5050.45
250 x 150	8.8	64.64	5274.44	421.96	9.03	2391.51	318.87	6.08	5488.32
250 x 150	10.0	72.57	5825.01	466.00	8.96	2634.20	351.23	6.02	6120.70
250 x 150	12.5	87.04	6632.67	530.61	8.73	3002.33	400.31	5.87	7314.55
260 x 140	6.0	45.63	4081.53	313.96	9.46	1567.27	223.90	5.86	3646.18
260 x 140	7.1	53.05	4647.40	357.49	9.36	1784.54	254.93	5.8	4258.54
260 x 140	8.0	59.24	5128.80	394.52	9.30	1964.15	280.59	5.76	4731.08
260 x 140	8.8	64.64	5536.06	425.85	9.25	2115.26	302.18	5.72	5137.89
260 x 140	10.0	72.57	6112.65	470.20	9.18	2327.67	332.52	5.66	5724.07
260 x 140	12.5	87.04	6949.76	534.60	8.94	2648.36	378.34	5.52	6820.62
260 x 180	6.0	50.43	4855.87	373.53	9.81	2763.43	307.05	7.4	5565.69
260 x 180	7.1	58.73	5555.85	427.37	9.73	3162.31	351.37	7.34	6522.55
260 x 180	8.0	65.64	6145.21	472.71	9.68	3493.23	388.14	7.29	7266.68
260 x 180	8.8	71.68	6647.10	511.32	9.63	3774.33	419.37	7.26	7911.95
260 x 180	10.0	80.57	7363.31	566.41	9.56	4174.13	463.79	7.20	8850.30
300 x 100	5.0	38.36	4065.22	271.01	10.29	722.77	144.55	4.34	2043.80
300 x 100	6.0	45.63	4776.79	318.45	10.23	842.35	168.47	4.30	2403.46
300 x 100	7.1	53.05	5422.43	361.50	10.11	953.92	190.78	4.24	2787.39
300 x 100	8.0	59.24	5977.86	398.52	10.05	1044.77	208.95	4.20	3080.34
300 x 100	8.8	64.64	6446.06	429.74	9.99	1120.18	224.04	4.16	3329.01
300 x 100	10.0	72.57	7106.03	473.74	9.90	1224.41	244.88	4.11	3681.00
300 x 100	12.5	87.04	8009.59	533.97	9.59	1373.92	274.78	3.97	4291.50
300 x 150	6.0	51.63	6073.51	404.90	10.85	2079.57	277.28	6.35	4988.47
300 x 150	7.1	60.15	6946.90	463.13	10.75	2377.98	317.06	6.29	5834.16
300 x 150	8.0	67.24	7683.57	512.24	10.69	2622.95	349.73	6.25	6490.59
300 x 150	10.0	82.57	9209.37	613.96	10.56	3125.03	416.67	6.15	7878.65

<i>H x B</i> <i>mm</i>	<i>T</i> <i>mm</i>	<i>A mm<sup>2</sup> x</i> <i>10<sup>2</sup></i>	<i>I<sub>x</sub> mm<sup>4</sup> x</i> <i>10<sup>4</sup></i>	<i>W<sub>x</sub> m<sup>3</sup> x</i> <i>10<sup>3</sup></i>	<i>i<sub>x</sub> mm x</i> <i>10</i>	<i>I<sub>y</sub> mm<sup>4</sup> x</i> <i>10<sup>4</sup></i>	<i>W<sub>y</sub> mm<sup>3</sup> x</i> <i>10<sup>3</sup></i>	<i>i<sub>y</sub> mm x</i> <i>10</i>	<i>I<sub>yt</sub> mm<sup>4</sup> x</i> <i>10<sup>4</sup></i>
300 x 150	12.5	99.54	10594.23	706.28	10.32	3594.78	479.30	6.01	9451.90
300 x 200	6.0	57.63	7370.23	491.35	11.31	3962.19	396.22	8.29	8115.23
300 x 200	7.1	67.25	8468.59	564.57	11.22	4553.17	455.32	8.23	9524.48
300 x 200	8.0	75.24	9389.27	625.95	11.17	5041.67	504.17	8.19	10626.50
300 x 200	8.8	82.24	10178.28	678.55	11.12	5459.26	545.93	8.15	11585.67
300 x 200	10.0	92.57	11312.70	754.18	11.05	6057.73	605.77	8.09	12987.13
300 x 200	12.5	112.04	13178.86	878.59	10.85	7059.94	705.99	7.94	15767.68
400 x 200	6.0	69.63	14789.35	739.47	14.57	5091.63	509.16	8.55	12068.52
400 x 200	7.1	81.45	17067.90	853.40	14.48	5874.74	587.47	8.49	14169.41
400 x 200	8.0	91.24	18974.42	948.72	14.42	6517.08	651.71	8.45	15820.22
400 x 200	8.8	99.84	20619.13	1030.96	14.37	7068.92	706.89	8.41	17259.78
400 x 200	10.0	112.57	23002.65	1150.13	14.30	7864.40	786.44	8.36	19368.49
400 x 200	12.5	137.04	27100.50	1355.02	14.06	9260.46	926.05	8.22	23594.07



# Appendix C

## Circular Hollow Section EN 10210-2



A = Cross-section area; I = Moment of inertia; W = Section modulus; i = Radius of gyration.

It = Torsion modulus;n Wt = Section modulus in torsion; Theoretical density = 7.85 kg/dm<sup>3</sup>.

The cross-sectional properties have been calculated by using nominal dimensions D and T.

Theoretical density = 7.85 kg/dm<sup>3</sup>.

<i>D mm</i>	<i>T mm</i>	<i>A mm<sup>2</sup> x 10<sup>2</sup></i>	<i>I mm<sup>4</sup> x 10<sup>4</sup></i>	<i>W mm<sup>3</sup> x 10<sup>3</sup></i>	<i>i mm x 10</i>	<i>I<sub>t</sub> mm<sup>4</sup> x 10<sup>4</sup></i>	<i>W<sub>t</sub> mm<sup>3</sup> x 10<sup>3</sup></i>
26.9	2.0	1.56	1.22	0.91	0.88	2.44	1.81
26.9	2.5	1.92	1.44	1.07	0.87	2.88	2.14
26.9	2.6	1.98	1.48	1.10	0.86	2.96	2.20
33.7	2.0	1.99	2.51	1.49	1.12	5.02	2.98
33.7	2.5	2.45	3.00	1.78	1.11	6.00	3.56
33.7	2.6	2.54	3.09	1.84	1.10	6.19	3.67
33.7	3.0	2.89	3.44	2.04	1.09	6.88	4.08
33.7	3.2	3.07	3.60	2.14	1.08	7.21	4.28
42.4	2.0	2.54	5.19	2.45	1.43	10.38	4.90
42.4	2.5	3.13	6.26	2.95	1.41	12.52	5.91
42.4	2.6	3.25	6.46	3.05	1.41	12.93	6.10
42.4	2.9	3.60	7.06	3.33	1.40	14.11	6.66
42.4	3.0	3.71	7.25	3.42	1.40	14.49	6.84

<i>D mm</i>	<i>T mm</i>	<i>A mm<sup>2</sup> x 10<sup>2</sup></i>	<i>I mm<sup>4</sup> x 10<sup>4</sup></i>	<i>W mm<sup>3</sup> x 10<sup>3</sup></i>	<i>i mm x 10</i>	<i>I<sub>y</sub> mm<sup>4</sup> x 10<sup>4</sup></i>	<i>W<sub>y</sub> mm<sup>3</sup> x 10<sup>3</sup></i>
42.4	3.2	3.94	7.62	3.59	1.39	15.24	7.19
42.4	4.0	4.83	8.99	4.24	1.36	17.98	8.48
48.3	2.0	2.91	7.81	3.23	1.64	15.62	6.47
48.3	2.5	3.60	9.46	3.92	1.62	18.92	7.83
48.3	2.6	3.73	9.78	4.05	1.62	19.55	8.10
48.3	3.0	4.27	11.00	4.55	1.61	22.00	9.11
48.3	3.2	4.53	11.59	4.80	1.60	23.17	9.59
48.3	4.0	5.57	13.77	5.70	1.57	27.54	11.40
60.3	2.0	3.66	15.58	5.17	2.06	31.16	10.34
60.3	2.5	4.54	18.99	6.30	2.05	37.99	12.60
60.3	2.9	5.23	21.59	7.16	2.03	43.18	14.32
60.3	3.0	5.40	22.22	7.37	2.03	44.45	14.74
60.3	3.2	5.74	23.47	7.78	2.02	46.94	15.57
60.3	4.0	7.07	28.17	9.34	2.00	56.35	18.69
60.3	5.0	8.69	33.48	11.10	1.96	66.95	22.21
76.1	2.0	4.66	31.98	8.40	2.62	63.96	16.81
76.1	2.5	5.78	39.19	10.30	2.60	78.37	20.60
76.1	2.9	6.67	44.74	11.76	2.59	89.48	23.52
76.1	3.0	6.89	46.10	12.11	2.59	92.19	24.23
76.1	4.0	9.06	59.06	15.52	2.55	118.11	31.04
76.1	5.0	11.17	70.92	18.64	2.52	141.84	37.28
76.1	6.3	13.81	84.82	22.29	2.48	169.64	44.58
88.9	2.5	6.79	63.37	14.26	3.06	126.75	28.51
88.9	3.0	8.10	74.76	16.82	3.04	149.53	33.64
88.9	3.2	8.62	79.21	17.82	3.03	158.41	35.64
88.9	4.0	10.67	96.34	21.67	3.00	192.68	43.35
88.9	5.0	13.18	116.37	26.18	2.97	232.75	52.36
88.9	6.0	15.63	134.94	30.36	2.94	269.88	60.72
88.9	6.3	16.35	140.24	31.55	2.93	280.47	63.10
101.6	2.5	7.78	95.61	18.82	3.50	191.22	37.64
101.6	3.0	9.29	113.04	22.25	3.49	226.07	44.50
101.6	3.6	11.08	133.24	26.23	3.47	266.47	52.46
101.6	4.0	12.26	146.28	28.80	3.45	292.57	57.59
101.6	5.0	15.17	177.47	34.93	3.42	354.94	69.87
101.6	6.0	18.02	206.68	40.68	3.39	413.35	81.37
101.6	6.3	18.86	215.07	42.34	3.38	430.13	84.67
108.0	2.5	8.29	115.35	21.36	3.73	230.69	42.72
108.0	3.0	9.90	136.49	25.28	3.71	272.98	50.55

$D$ mm	$T$ mm	$A$ mm <sup>2</sup> x 10 <sup>2</sup>	$I$ mm <sup>4</sup> x 10 <sup>4</sup>	$W$ mm <sup>3</sup> x 10 <sup>3</sup>	$i$ mm x 10	$I_y$ mm <sup>4</sup> x 10 <sup>4</sup>	$W_y$ mm <sup>3</sup> x 10 <sup>3</sup>
108.0	3.6	11.81	161.06	29.83	3.69	322.11	59.65
108.0	4.0	13.07	176.95	32.77	3.68	353.91	65.54
108.0	5.0	16.18	215.06	39.83	3.65	430.12	79.65
108.0	6.0	19.23	250.91	46.46	3.61	501.81	92.93
108.0	6.3	20.13	261.23	48.38	3.60	522.46	96.75
114.3	2.5	8.78	137.26	24.02	3.95	274.52	48.03
114.3	3.0	10.49	162.55	28.44	3.94	325.10	56.88
114.3	3.6	12.52	191.98	33.59	3.92	383.97	67.19
114.3	4.0	13.86	211.07	36.93	3.90	422.13	73.86
114.3	5.0	17.17	256.92	44.96	3.87	513.84	89.91
114.3	6.0	20.41	300.21	52.53	3.83	600.42	105.06
114.3	6.3	21.38	312.71	54.72	3.82	625.43	109.44
127.0	2.5	9.78	189.53	29.85	4.40	379.06	59.70
127.0	3.0	11.69	224.75	35.39	4.39	449.50	70.79
127.0	4.0	15.46	292.61	46.08	4.35	585.23	92.16
127.0	5.0	19.16	357.14	56.24	4.32	714.28	112.48
127.0	6.0	22.81	418.44	65.90	4.28	836.88	131.79
127.0	6.3	23.89	436.22	68.70	4.27	872.44	137.39
133.0	2.5	10.25	218.27	32.82	4.61	436.54	65.64
133.0	3.0	12.25	258.97	38.94	4.60	517.93	77.88
133.0	4.0	16.21	337.53	50.76	4.56	675.05	101.51
133.0	5.0	20.11	412.40	62.02	4.53	824.81	124.03
133.0	6.0	23.94	483.72	72.74	4.50	967.43	145.48
133.0	6.3	25.08	504.43	75.85	4.49	1008.86	151.71
139.7	3.0	12.88	301.09	43.11	4.83	602.18	86.21
139.7	4.0	17.05	392.86	56.24	4.80	785.72	112.49
139.7	5.0	21.16	480.54	68.80	4.77	961.08	137.59
139.7	6.0	25.20	564.26	80.78	4.73	1128.52	161.56
139.7	6.3	26.40	588.62	84.27	4.72	1177.24	168.54
139.7	8.0	33.10	720.29	103.12	4.66	1440.58	206.24
139.7	10.0	40.75	861.89	123.39	4.60	1723.79	246.78
152.4	3.0	14.08	393.01	51.58	5.28	786.03	103.15
152.4	4.0	18.65	513.73	67.42	5.25	1027.46	134.84
152.4	5.0	23.15	629.54	82.62	5.21	1259.08	165.23
152.4	6.0	27.60	740.56	97.19	5.18	1481.13	194.37
152.4	6.3	28.92	772.96	101.44	5.17	1545.92	202.88
159.0	3.0	14.70	447.42	56.28	5.52	894.84	112.56
159.0	4.0	19.48	585.33	73.63	5.48	1170.67	147.25

<i>D mm</i>	<i>T mm</i>	<i>A mm<sup>2</sup> x 10<sup>2</sup></i>	<i>I mm<sup>4</sup> x 10<sup>4</sup></i>	<i>W mm<sup>3</sup> x 10<sup>3</sup></i>	<i>i mm x 10</i>	<i>I<sub>y</sub> mm<sup>4</sup> x 10<sup>4</sup></i>	<i>W<sub>y</sub> mm<sup>3</sup> x 10<sup>3</sup></i>
159.0	5.0	24.19	717.88	90.30	5.45	1435.75	180.60
159.0	6.0	28.84	845.19	106.31	5.41	1690.37	212.63
159.0	6.3	30.22	882.38	110.99	5.40	1764.76	221.98
168.3	3.0	15.58	532.28	63.25	5.85	1064.57	126.51
168.3	3.2	16.60	565.74	67.23	5.84	1131.47	134.46
168.3	4.0	20.65	697.09	82.84	5.81	1394.18	165.68
168.3	4.5	23.16	777.22	92.36	5.79	1554.43	184.72
168.3	5.0	25.65	855.85	101.70	5.78	1711.69	203.41
168.3	6.0	30.59	1008.69	119.87	5.74	2017.39	239.74
168.3	6.3	32.06	1053.42	125.18	5.73	2106.84	250.37
168.3	8.0	40.29	1297.27	154.16	5.67	2594.54	308.32
168.3	10.0	49.73	1563.98	185.86	5.61	3127.97	371.71
193.7	4.0	23.84	1072.79	110.77	6.71	2145.58	221.54
193.7	5.0	29.64	1320.23	136.32	6.67	2640.46	272.63
193.7	6.0	35.38	1559.72	161.05	6.64	3119.45	322.09
193.7	6.3	37.09	1630.05	168.31	6.63	3260.09	336.61
193.7	8.0	46.67	2015.54	208.11	6.57	4031.07	416.22
193.7	10.0	57.71	2441.59	252.10	6.50	4883.18	504.20
193.7	12.5	71.16	2934.31	302.97	6.42	5868.62	605.95
219.1	4.0	27.03	1563.84	142.75	7.61	3127.67	285.50
219.1	4.5	30.34	1747.24	159.49	7.59	3494.48	318.98
219.1	5.0	33.63	1928.04	176.00	7.57	3856.08	351.99
219.1	6.0	40.17	2281.95	208.30	7.54	4563.89	416.60
219.1	6.3	42.12	2386.14	217.81	7.53	4772.28	435.63
219.1	8.0	53.06	2959.63	270.16	7.47	5919.26	540.33
219.1	10.0	65.69	3598.44	328.47	7.40	7196.88	656.95
219.1	12.5	81.13	4344.58	396.58	7.32	8689.16	793.17
244.5	6.0	44.96	3198.53	261.64	8.43	6397.07	523.28
244.5	8.0	59.44	4160.45	340.32	8.37	8320.89	680.65
244.5	10.0	73.67	5073.15	414.98	8.30	10146.29	829.96
244.5	12.5	91.11	6147.42	502.86	8.21	12294.83	1005.71
273.0	4.0	33.80	3058.25	224.05	9.51	6116.50	448.09
273.0	5.0	42.10	3780.81	276.98	9.48	7561.63	553.97
273.0	6.0	50.33	4487.08	328.72	9.44	8974.17	657.45
273.0	6.3	52.79	4695.82	344.02	9.43	9391.64	688.03
273.0	8.0	66.60	5851.71	428.70	9.37	11703.43	857.39
273.0	10.0	82.62	7154.09	524.11	9.31	14308.18	1048.22
273.0	12.5	102.30	8697.45	637.18	9.22	17394.90	1274.35

<i>D mm</i>	<i>T mm</i>	<i>A mm<sup>2</sup> x 10<sup>2</sup></i>	<i>I mm<sup>4</sup> x 10<sup>4</sup></i>	<i>W mm<sup>3</sup> x 10<sup>3</sup></i>	<i>i mm x 10</i>	<i>I, mm<sup>4</sup> x 10<sup>4</sup></i>	<i>W, mm<sup>3</sup> x 10<sup>3</sup></i>
323.9	4.0	40.20	5143.16	317.58	11.31	10286.33	635.15
323.9	5.0	50.09	6369.42	393.30	11.28	12738.85	786.59
323.9	6.0	59.92	7572.47	467.58	11.24	15144.93	935.16
323.9	6.3	62.86	7928.90	489.59	11.23	15857.79	979.18
323.9	8.0	79.39	9910.08	611.92	11.17	19820.16	1223.84
323.9	10.0	98.61	12158.34	750.75	11.10	24316.68	1501.49
323.9	12.5	122.29	14846.53	916.74	11.02	29693.05	1833.47

# Appendix D

## British Universal Beams

Dimensions:	BS 4-1: 2005	UB 127-914
	ASTM A 6/A 6M - 12	UB 1016
Tolerances:	EN 10034: 1993	UB 127-914
	ASTM A 6/A 6M - 12	UB 1016

Surface condition: according to EN 10163-3: 2004, class C, subclass 1.

Characteristics of rolled UB profiles.

**Table D.1** Characteristics of the selected rolled UB profiles (Sales program Commercial sections)

<i>UB Profile</i>	<i>h</i> [mm]	<i>b</i> [Mm]	<i>t<sub>w</sub></i> [mm]	<i>t<sub>f</sub></i> [mm]	<i>A<sub>s</sub></i> [mm <sup>2</sup> ]	<i>I<sub>y</sub></i> x10 <sup>-4</sup> [mm <sup>4</sup> ]
152x89x16	152.4	88.7	4.5	7.7	2032	834
178x102x19	177.8	101.2	4.8	7.9	2426	1356
203x133x25	203.2	133.2	5.7	7.8	3187	2340
254x102x25	257.2	101.9	6.0	8.4	3204	3415
305x102x28	308.7	101.8	6.0	8.8	3588	5366
356x127x39	353.4	126.0	6.6	10.7	4977	10172
406x140x46	403.2	142.2	6.8	11.2	5864	15685
457x152x60	454.6	152.9	8.1	13.3	7623	25500
533x210x92	533.1	209.3	10.1	15.6	11740	55230
610x229x113	607.6	228.2	11.1	17.3	14390	87320
686x254x140	683.5	253.7	12.4	19.0	17840	136300
762x267x173	762.2	266.7	14.3	21.6	22040	205300
838x292x194	840.7	292.4	14.7	21.7	24680	279200
914x305x224	910.4	304.1	15.9	23.9	28560	376400
1016x305x349	1008.1	302	21.1	40.0	44420	722300
1016x305x393	1016.0	303	24.4	43.9	50020	807700

Sizes and dimensions of different cross-sections are from Arcelor catalogue (*Sales program Commercial sections*), Ruukki, Roymech, etc.

[http://www.arcelormittal.com/sections/fileadmin/redaction/4-Library/1-Sales\\_programme\\_Brochures/Sales\\_programme/ArcelorMittal\\_EN\\_FR\\_DE.pdf](http://www.arcelormittal.com/sections/fileadmin/redaction/4-Library/1-Sales_programme_Brochures/Sales_programme/ArcelorMittal_EN_FR_DE.pdf), access January 06, 2013.

<http://www.ruukki.com/~media/Files/Steel-products/Tubular-products-and-cold-formed-steel-sections-data-sheets/Ruukki-Hollow%20sections-dimensions-cross-sectional-properties.pdf> access January 22, 2013.

<http://www.directsteelsales.com.au/steel-products/shs-squares/square-hollow-section-shs/> access January 22, 2013.

[http://www.roymech.co.uk/Useful\\_Tables/Sections/SHS\\_cf.html](http://www.roymech.co.uk/Useful_Tables/Sections/SHS_cf.html)  
access January 22, 2013.

# References

## **Chapter 1** *Experiences with the Optimum Design of Steel Structures*

- Farkas, J.: New welded storage tanks for fluids covered by soil. *Gép* 14(4), 139–142 (1962) (in Hungarian)
- Farkas, J.: Optimum design of metal structures. Akadémiai Kiadó/Horwood, Budapest/Chichester (1984)
- Farkas, J., Jármai, K.: Analysis and optimum design of metal structures. Brookfield, Balkema, Rotterdam (1997)
- Farkas, J., Jármai, K.: Economic Design of Metal Structures. Millpress, Rotterdam (2003)
- Farkas, J., Jármai, K.: Optimum design of a welded stringer-stiffened steel cylindrical shell subject to axial compression and bending. *Welding World* 49(5-6), 85–89 (2005)
- Farkas, J., Jármai, K.: Cost comparison of a tubular truss and a ring-stiffened shell structure for a wind turbine tower. In: Packer, J.A., Willibald, S. (eds.) *Tubular Structures XI. Proc. 11th Int. Symposium and IIW Int. Conf. on Tubular Structures*, Québec City, Canada, pp. 341–349. Taylor & Francis, London (2006)
- Farkas, J., Jármai, K.: Design and optimization of metal structures. Horwood Publishing, Chichester (2008)
- Farkas, J., Jármai, K.: Minimum cost design of a square box column composed from orthogonally stiffened welded steel plates. In: Jármai, K., Farkas, J. (eds.) *Int. Conf. Proc. Design, Fabrication and Economy of Welded Structures*, Miskolc, Hungary, pp. 61–70. Horwood Publishing, Chichester (2008a)
- Farkas, J., Jármai, K.: Square box column composed from welded cellular plates. In: Farkas, J., Jármai, K. (eds.) *Design and Optimization of Metal Structures*, pp. 253–261. Horwood, Chichester (2008b)
- Farkas, J., Jármai, K.: Minimum cost design of a welded steel square cellular plate supported at four corners. In: Farkas, J., Jármai, K. (eds.) *Design and Optimization of Metal Structures*, pp. 157–165. Horwood, Chichester (2008c)
- Farkas, J., Jármai, K., Snyman, J.A.: Global minimum cost design of a welded square stiffened plate supported at four corners. *Struct. Multidisc. Optim.* 40, 477–489 (2010)
- Rondal, J., Maquoi, R.: On the optimal thickness of centrically compressed columns with square hollow sections, TU Budapest, Faculty of Civil Engineering, Dept. of Mechanics, 58 p. (1981)
- Schmit Jr., L.A.: Structural design by systematic synthesis. In: *Proc. 2nd Conf. Electronic Computation*, pp. 105–132. Am. Soc. Civ. Eng., New York (1960)
- Schmit Jr., L.A.: Structural optimization – some key ideas and insights. In: Atrek, E., Gallagher, R.H., et al. (eds.) *New Directions in Optimum Structural Design*, pp. 1–45. Wiley & Sons, Chichester (1984)



- Thompson, J.M.T., Hunt, G.W.: Dangers of structural optimization. *Eng. Opt.* 1(2) (1974)
- Timár, I.: Vibration damping and optimum design using SUMT method of sandwich beams. Doctor dissertation University of Miskolc (1977) (in Hungarian)
- Uys, P.E., Farkas, J., Jármai, K., van Tonder, F.: Optimisation of a steel tower for a wind turbine structure. *Eng. Struct.* 29, 1337–1342 (2007)

## **Chapter 2** *Newer Mathematical Methods in Structural Optimization*

- Annamalai, N.: Cost optimization of welded plate girders. Dissertation, Purdue Univ. Indianapolis, Ind. (1970)
- Box, M.J.: A new method of constrained optimization and a comparison with other methods. *Computer Journal* 8, 42–52 (1965)
- Das, S., Suganthan, P.N.: Criteria for CEC 2011 Competition on Testing Evolutionary Algorithms on Real World Optimization Problems, Technical Report (December 2010)
- Dasgupta, D. (ed.): *Artificial Immune Systems and Their Applications*. Springer-Verlag, Inc. Berlin (January 1999) ISBN 3-540-64390-7
- De Castro, L., Timmis, J.: *Artificial Immune Systems: A New Computational Intelligence Approach* (2001) ISBN 1-85233-594-7
- De Jong, K.: An analysis of the behavior of a class of genetic adaptive systems, Doctoral dissertation, University of Michigan (1975)
- Dorigo, M., Di Caro, G., Gambardella, L.M.: Ant algorithms for discrete optimization. *Artificial Life* 5(3), 137–172 (1999)
- Dulikravich, G.S., Martin, T.J., Dennis, B.H., Foster, N.F.: Multidisciplinary Hybrid Constrained GA Optimization. In: Miettinen, K., Makela, M.M., Neittaanmaki, P., Periaux, J. (eds.) *EUROGEN 1999 - Evolutionary Algorithms in Engineering and Computer Science: Recent Advances and Industrial Applications*, ch. 12, May 30–June 3, pp. 231–260. John Wiley & Sons, Ltd., Jyväskylä (1999)
- Egorov, I.N.: Indirect Optimization Method on the Basis of Self-Organization. In: *Proceedings of Optimization Techniques and Applications (ICOTA 1998)*, vol. 2, pp. 683–691. Curtin University of Technology, Perth (1998)
- Egorov, I.N., Kretinin, G.V., Leshchenko, I.A.: Multicriteria Optimization of Time Control Laws of Short Take-Off and Vertical Landing Aircraft Power Plant, ASME paper 97-GT-263 (1997)
- Egorov, I.N., Kretinin, G.V.: Multicriterion Stochastic Optimization of Axial Compressor. In: *Proceedings of ASME COGEN-TURBO-VI*, Houston, Texas (1992)
- Fan, Y., Sarkar, S., Lasdon, L.: Experiments with successive quadratic programming algorithms. *J. Optim. Theory Appl.* 56, 359–383 (1988)
- Farkas, J., Jármai, K.: *Analysis and optimum design of metal structures*, 347 p. Balkema Publishers, Brookfield, Rotterdam (1997)
- Farkas, J., Jármai, K.: *Economic design of metal structures*, 340 p. Millpress Science Publisher, Rotterdam (2003) ISBN 90 77017 99 2
- Farkas, J., Jármai, K.: *Design and optimization of metal structures*, 328 p. Horwood Publishers, Chichester (2008)
- Farkas, J., Jármai, K., Snyman, J.A.: Global minimum cost design of a welded square stiffened plate supported at four corners. In: *7th World Congress on Structural and Multidisciplinary Optimization, WCSMO 2007, COEX, Seoul, Korea, May 21–25. Proceedings on CD*, A 0381, pp. 1057–1066 (2007a)

- Farkas, J., Jármai, K., Kožuh, Z.: Cost minimization of an orthogonally stiffened welded steel plate subject to static and fatigue load. *Welding in the World* 51(special issue), 357–366 (2007b)
- Farkas, J., Jármai, K., Orbán, F.: Cost minimization of a ring-stiffened conical shell loaded by external pressure. In: 60th Annual Assembly of International Institute of Welding, Dubrovnik, Croatia, IIW-Doc. XV-1248-07, XV-F-80-07, July 1-8, 9 p. (2007c)
- Farkas, J., Simões, M.C., Jármai, K.: Minimum cost design of a welded stiffened square plate loaded by biaxial compression. *Structural and Multidisciplinary Optimization* 29(4), 298–303 (2005)
- Farmer, J.D., Packard, N., Perelson, A.: The immune system, adaptation and machine learning. *Physica D* 2, 187–204 (1986)
- Fiacco, A.V., McCormick, G.P.: Nonlinear sequential unconstrained minimization technique. John Wiley and Sons, Inc., New York (1968)
- Fourie, P.C., Groenwold, A.A.: Particle swarm in size and shape optimisation. In: Proceedings of International Workshop on Multidisciplinary Design Optimization, Pretoria, South Africa, August 7-10, pp. 97–106 (2000)
- Goldberg, D.E.: Genetic algorithms in search, optimization & machine learning. Addison-Wesley Publ. Company, Inc. (1989)
- Golomb, S.W., Baumert, L.D.: Backtrack programming. *J. Assoc. Computing Machinery* 12, 516–524 (1965)
- Groenwold, A.A., Snyman, J.A.: Global optimization using dynamic search trajectories. *J. Global Optimiz.* 24, 51–60 (2002)
- Himmelblau, D.M.: Applied nonlinear programming. Mc Graw-Hill Book Co., New York (1971)
- Jármai, K.: Single- and multicriteria optimization as a tool of decision support system. *Computers in Industry* 11(3), 249–266 (1989a)
- Jármai, K.: Application of decision support system on sandwich beams, verified by experiments. *Computers in Industry* 11(3), 267–274 (1989b)
- Jármai, K.: Particle swarm method as a new tool for structural optimization. *Journal of Computational and Applied Mechanics* 6(2), 207–226 (2005)
- Jármai, K., Farkas, J.: Minimum cost design of a cellular plate loaded by uniaxial compression. *Structural and Multidisciplinary Optimization* 48, 835–843 (2012), doi:10.1007/s00158-011-0725-9, ISSN 1615-147X
- Kennedy, J.: The particle swarm: social adaptation of knowledge. In: Proceedings of the International Conference on Evolutionary Computation, pp. 303–308. IEEE, Piscataway (1977)
- Kennedy, J., Eberhart, R.C.: Particle swarm optimization. In: Proc. IEEE Int'l Conf. on Neural Networks IV, pp. 1942–1948. IEEE service center, Piscataway (1995)
- Koski, J.: Multicriteria structural optimization. In: Adeli, H. (ed.) *Advances in Design Optimization*, ch. 6. Chapman and Hall, London (1994)
- Kota, L., Jármai, K.: Efficient algorithms for optimization of objects and systems. *Pollack Periodica*, 12 p. (2013) (submitted article), [http://akkrt.hu/55/folyoirat/termekek/muszaki\\_tudomanyok/pollack\\_periodica](http://akkrt.hu/55/folyoirat/termekek/muszaki_tudomanyok/pollack_periodica)
- Liang, J.J., Suganthan, N., Deb, K.: Novel Composition Test Functions for Numerical Global Optimization. In: Proceedings of the 2005 IEEE Swarm Intelligence Symposium, SIS 2005, pp. 68–75 (2005)

- Millonas, M.M.: Swarms, phase transitions, and collective intelligence. In: Langton, C.G. (ed.) *Artificial Life III*. Addison Wesley, Reading (1994)
- Mittcell, M.: *An introduction to genetic algorithms*. The MIT Press (1998)
- Molga, M., Smutnicki, C.: *Test functions for optimization needs* (2005), <http://www.zsd.ict.pwr.wroc.pl/files/docs/functions.pdf>
- Mordecia, A.: *Nonlinear Programming: Analysis and Methods*. Dover Publishing (2003) ISBN 0-486-43227-0
- Ostfeld, A.: *Ant colony optimization methods and applications*. InTech Publishers (2011) ISBN 978-953-307-157-2
- Ostyczka, A.: *Multicriterion Optimization in Engineering*. Ellis Horwood, Chichester (1984)
- Ostyczka, A.: *Computer aided multicriterion optimization system*. International Software Publishers, Krakow (1992)
- Pareto, V.: *Cours d'economie politique*, vols. I and II. F. Rouge, Lausanne (1896)
- Rao, S.S.: *Optimisation theory and applications*. Wiley Eastern Limited, New Delhi (1984)
- Rosenbrock, H.H.: An automatic method for finding the greatest or least value of a function. *Computer Journal* 3, 175–184 (1960)
- Rozvany, G.I.N.: *Topology Optimization in Structural Mechanics*. Springer (1997) ISBN 3211829075
- Siddall, J.N.: *Optimal engineering design (Mechanical engineering)*, 536 p. Marcell Dekker (1982) ISBN-13: 978-0824716332
- Simões, L.M.C., Negrão, J.H.J.O.: Optimization of cable-stayed bridges with box-girder decks. *Advances in Engineering Software* 31(6), 417–423 (2000)
- Snyman, J.A.: An improved version of the original leap-frog dynamic method for unconstrained minimization LFOP1(b). *Applied Mathematical Modelling* 7, 216–218 (1983)
- Snyman, J.A.: *Practical mathematical optimization, An introduction to basic optimization theory and classical and new gradient based algorithms*, 257 p. Springer, Heidelberg (2005) ISBN-10: 0-387-29824-X
- Storn, R.: Constrained optimization. *Dr. Dobb's Journal*, 119–123 (May 1995)
- Storn, R., Price, K.: *Differential evolution – simple and efficient adaptive scheme for global optimization over continuous spaces*. Technical Report TR-95-012, ICSI (1995)
- Tímár, I., Horváth, P., Borbély, T.: Optimierung von profilierten Sandwichbalken. *Stahlbau* 72(2), 109–113 (2003)
- Uys, P.E., Farkas, J., Jármai, K., van Tonder, F.: Optimisation of a wind turbine tower structure. *Journal of Engineering Structures* 29(7), 1337–1342 (2007)
- Wei, S., Leung, H.: A Novel Ranking Method Based on Subjective Probability Theory for Evolutionary Multiobjective Optimization. *Mathematical Problems in Engineering* 2011, Article ID 695087, 10 pages (2011), doi:10.1155/2011/695087
- Yang, X.S.: *Nature-Inspired Metaheuristic Algorithms*. Frome: Luniver Press (2008) ISBN 1-905986-10-6
- Yang, X.S.: *Mathematical Modeling with Multidisciplinary Applications*. John Wiley & Sons (2012) ISBN 1-118-29441-6
- Zhou, J.L., Tits, A.L.: An SQP Algorithm for Finely Discretized Continuous Minimax Problems and Other Minimax Problems with Many Objective Functions. *SIAM J. on Optimization* 6(2), 461–487 (1996)

### Chapter 3 *Cost Calculations*

- Bader, M.G.: Selection of composite materials and manufacturing routes for cost effective performance. *Composites: Part A* 33, 913–934 (2002)
- Catalog (2012),  
[http://www.advanced-composites.co.uk/data\\_catalogue/catalogue%20files/sm/SM1010-INTRO%20TO%20ADV%20COMPS-Rev06.pdf](http://www.advanced-composites.co.uk/data_catalogue/catalogue%20files/sm/SM1010-INTRO%20TO%20ADV%20COMPS-Rev06.pdf) (access December 2012)
- Cost studio (2012),  
[http://www.acoste.org.uk/uploads/EMC\\_seminars/COST-STUDIO-example.pdf](http://www.acoste.org.uk/uploads/EMC_seminars/COST-STUDIO-example.pdf) (access December 2012)
- Bodt, H.J.M.: *The Global Approach to Welding Costs*. The Netherlands Institute of Welding, The Hague (1990)
- COSTCOMP, Programm zur Berechnung der Schweisskosten. Deutscher Verlag für Schweissttechnik, Düsseldorf (2002)
- Farkas, J., Jármai, K.: *Analysis and Optimum Design of Metal Structures*. Balkema Publishers, Rotterdam (1997)
- Farkas, J., Jármai, K.: *Economic design of metal structures*, 340 p. Millpress Science Publisher, Rotterdam (2003)
- Farkas, J., Jármai, K.: *Design and optimization of metal structures*, p. 328. Horwood Publishers, Chichester (2008) ISBN: 978-1-904275-29-9
- Glijnis, P.C.: Private communication (1999)
- Happio, J.: Feature-based costing method for skeletal steel structures based on the process approach, 99 p. Tampere University of Technology, Publication 1027, UniPrint TTY (2012) ISBN 978-95215-2785-2
- Jalkanen, J.: *Tubular truss optimization using heuristic algorithms*, PhD. Thesis, 104 p. Tampere University of Technology, Finland (2007)
- Jármai, K., Farkas, J.: Cost calculation and optimization of welded steel structures. *Journal of Constructional Steel Research* 50(2), 115–135 (1999)
- Jármai, K., Farkas, J., Uys, P.: Optimum design and cost calculation of a simple frame with welded or bolted corner joints. *Welding in the World* 48(1-2), 42–49 (2004)
- Klansek, U., Kravanja, S.: Cost estimation, optimization and competitiveness of different composite floor systems – Part 1. Self manufacturing cost estimation of composite and steel structures. *Journal of Constructional Steel Research* 62(5), 434–448 (2006a)
- Klansek, U., Kravanja, S.: Cost estimation, optimization and competitiveness of different composite floor systems – Part 2. Optimization based competitiveness between the composite I beams, channel-section and hollow-section. *Journal of Constructional Steel Research* 62(5), 449–462 (2006b)
- Ott, H.H., Hubka, V.: Vorausberechnung der Herstellkosten von Schweiss-konstruktionen (Fabrication cost calculation of welded structures). In: *Proc. Int. Conference on Engineering Design ICED*, Hamburg, pp. 478–487. Heurista, Zürich (1985)
- Pahl, G., Beelich, K.H.: Kostenwachstumsgesetze nach Ähnlichkeits-beziehungen für Schweiss-verbindingen. *VDI-Bericht* (457), 129–141 (1992)
- Tímár, I., Horváth, P., Borbély, T.: Optimierung von profilierten Sandwichbalken. *Stahlbau* 72(2), 109–113 (2003)
- Tizani, W.M.K., Yusuf, K.O., Davies, G., Smith, N.J.: A knowledge based system to support joint fabrication decision making at the design stage – Case studies for CHS trusses. In: Farkas, J., Jármai, K. (eds.) *Tubular Structures VII*, pp. 483–489. Rotterdam-Brookfield, Balkema (1996)

## Chapter 4 *Beams and Columns*

- Choi, S.K., Burgess, I.W., Plank, R.J.: Structural behaviour of unrestrained composite truss systems in fire. In: Lamas, A., Simoes da Silva L. (eds.) *Proceedings of Third European Conference on Steel Structures*, Coimbra, Portugal, vol. II, pp. 1459–1468 (2002)
- Eurocode 1: Actions on structures. Part 1-2, General actions. Actions on structures exposed to fire (2005)
- Eurocode 3: Design of steel structures. Part 1-2, General rules. Structural fire design (2005)
- Eurocode 3. Design of steel structures. Part 1-1, General structural rules (2005)
- Farkas, J., Jármai, K.: *Analysis and optimum design of metal structures*. Balkema, Rotterdam (1997)
- Farkas, J., Jármai, K.: *Economic design of metal structures*. Millpress, Rotterdam (2003)
- Farkas, J., Jármai, K.: *Design and optimization of metal structures*. Horwood, Chichester (2008)
- Franssen, J.M., Schleich, J.B., Cajot, L.G.: A simple model for the fire resistance of axially loaded members according to Eurocode 3. *J. Constr. Steel Res.* 35, 49–69 (1995)
- Knobloch, M., Fontana, M., Frangi, A.: On the interaction of global and local buckling of square hollow sections in fire. In: *5th Internat. Conference on Coupled Instabilities in Metal Structures*, CMIS, Sydney, Australia, pp. 587–594 (2008)
- Vila Real, P.M.M., Simoes da Silva, L., Lopes, N., Franssen, J.M.: Fire resistance of unconstrained welded steel beams submitted to lateral-torsional buckling. In: *Proceedings of 4th European Conference on Steel and Composite Structures*, Maastricht, The Netherlands, vol. C. 5-1-119-126. Verlag Mainz, Aachen (2005)

## Chapter 5 *Tubular Trusses*

- Adeli, H., Balasubramanyan, K.V.: *Expert systems for structural design*. Prentice-Hall, Englewood Cliffs (1988)
- BS 5400: Part 3: Steel, concrete and composite bridges. Code of practice for design of steel bridges. BSI, London (1982)
- EN 10219-2: Cold formed circular hollow section profiles. European Committee for Standardization, CEN (2006)
- Eurocode 3. Design of steel structures. Part 3-1: Towers, masts and chimneys. Towers and masts (2006)
- Eurocode 3, EN 1993-1-1: Design of steel structures. Part 1.1. General rules and rules for buildings. European Committee for Standardization, CEN (2005)
- Farkas, J., Jármai, K.: *Analysis and optimum design of metal structures*. Balkema, Rotterdam-Brookfield (1997)
- Farkas, J., Jármai, K.: *Economic design of metal structures*. Millpress, Rotterdam (2003)
- Farkas, J., Jármai, K.: *Design and optimization of metal structures*. Horwood Publishing, Chichester (2008)
- Farkas, J.: *Optimum design of metal structures*. Horwood, Chichester (1984)
- Gil, L., Andreu, A.: Shape and cross-section optimization of a truss structure. *Comp. Struct.* 79, 681–689 (2001)
- Glijnis, P.C.: Southern African Institute of Steel Construction. Personal communications, Johannesburg, South Africa (1999)
- Hasancebi, O., Erbatur, F.: Layout optimization of trusses using simulated annealing. *Advances Eng. Software* 33, 681–696 (2002)

- Hasegawa, A., Abo, H., et al.: Optimum cross-sectional shapes of steel compression members with local buckling. *Proc. JSCE Struct. Eng./ Earthquake Eng.* 2, 121–129 (1985)
- Jármai, K., Snyman, J.A., Farkas, J.: Application of novel constrained optimization algorithms to the minimum volume design of planar CHS trusses with parallel chords. *Eng. Optim.* 36(4), 457–471 (2004)
- Kaveh, A., Talatahari, S.: Particle swarm optimizer, ant colony strategy and harmony search scheme hybridized for optimization of truss structures. *Comp. Struct.* 87, 267–283 (2009)
- Kripakaran, P., Gupta, A., Baugh Jr., J.W.: A novel optimization approach for minimum cost design of trusses. *Comp. Struct.* 85, 1782–1794 (2007)
- Lamberti, L.: An efficient simulated annealing algorithm for design optimization of truss structures. *Comp. Struct.* 86, 1936–1953 (2008)
- Makris, P.A., Provatidis, C.G.: Weight minimization of displacement-constrained truss structures using a strain energy criterion. *Comp. Methods Appl. Mech. Eng.* 191, 2159–2177 (2002)
- MSZ 151-1: Overhead lines for power transmission (2000) (in Hungarian)
- MSZ 151-3: Overhead lines for power transmission. Supports (1988) (in Hungarian)
- Šilih, S., Kravanja, S.: Topology, shape and standard sizing optimization of trusses using MINLP optimization approach. In: Jármai, K., Farkas, J. (eds.) *Design, Fabrication and Economy of Welded Structures*. Int. Conf. Proc. 2008, Miskolc, Hungary, pp. 143–150. Horwood, Chichester (2008)
- Rao, G.V.: Optimum designs for transmission line towers. *Comp. Struct.* 57(1), 81–92 (1995)
- Rao, N.P., et al.: Investigation of transmission line tower failures. *Eng. Failure Anal.* 17, 1127–1141 (2010)
- Rao, N.P., Knight, G.M.S., Mohan, S.J., Lakshmanan, N.: Studies on failure of transmission line towers in testing. *Eng. Struct.* 35, 55–70 (2012)
- Rondal, J., Würker, K.G., Dutta, D., Wardenier, J., Yeomans, N.: *Structural stability of hollow sections*. TÜV Rheinland, Köln (1992)
- Simoes da Silva, L., et al.: Structural assessment of current steel design models for transmission and telecommunication towers. *J. Construct. Steel Res.* 61, 1108–1134 (2005)
- Simos, G., Christos, M., Konstantinos, K., Baniotopoulos, C.C.: Trusses classification according to robustness criteria. In: Graz, A.O., et al. (eds.) *Proc. Conf. Eurosteel 2008*, vol. B, pp. 1849–1854. ECCS, Brussels (2008)
- Static design procedure for welded hollow section joints, International Institute of Welding, IIW Document XV-1329-09 (2009)
- Taniwaki, K., Ohkubo, S.: Optimal synthesis method for transmission tower truss structures subjected to static and seismic loads. *Struct. Multidisc. Optim.* 26, 441–454 (2004)
- Tong, W.H., Liu, G.R.: An optimization procedure for truss structures with discrete variables and dynamic constraints. *Comp. Struct.* 79, 155–162 (2001)
- Wardenier, J., Kurobane, Y., Packer, J.A., Dutta, D., Yeomans, N.: *Design guide for circular hollow section (CHS) joints under predominantly static loading*. TÜV Rheinland, Köln (1991)

## Chapter 6 *Frames*

- American Petroleum Institute (API), *Draft Recommended Practice 2A-LRFD*, 1st edn. (1989)
- DAST Richtlinie 016, Deutscher Ausschuss für Stahlbau. *Bemessung und konstruktive Gestaltung von Tragwerken aus dünnwandigen kaltgeformten Bauteilen* (1986)

- Eurocode 3, Design of steel structures. Part 1-1: General rules and rules for buildings. EN 1993-1-1 (2009)
- Eurocode 3, Part 1.8. Design of joints. EN 1993-1-8 (2002)
- Eurocode 8, EN 1998-1. Design of structures for earthquake resistance. Part 1. General rules, seismic actions and rules for buildings (2008)
- Farkas, J., Jármai, K.: Analysis and optimum design of metal structures. Balkema, Rotterdam-Brookfield (1997)
- Glushkov, G., Yegorov, I., Yermolov, V.: Formulas for designing frames. MIR Publishers, Moscow (1975)
- Jain, A.K., Goel, S.C., Hanson, R.D.: Hysteretic cycles of axially loaded steel members. J. Struct. Div. Proc. Am. Soc. Civ. Eng. 106, 1777–1795 (1980)
- Kurobane, Y., et al.: Design guide for structural hollow section column connections. TÜV-Verlag, Köln (2004)
- Lee, S., Goel, S.C.: Seismic behaviour of hollow and concrete filled square tubular bracing members. Research Report UMCE 87-11. Department of Civil Engineering, University of Michigan, Ann Arbor (1987)
- Liu, Z., Goel, S.C.: Cyclic load behavior of concrete-filled tubular braces. J. Struct. Eng. Proc. Am. Soc. Civ. Eng. 114, 1488–1506 (1988)
- Longo, A., Montuori, R., Piluso, V.: Plastic design of seismic resistant V-braced frames. J. Earthquake Eng. 12, 1246–1266 (2008)
- Matsumoto, T., Yamashita, M., et al.: Post-buckling behavior of circular tube brace under cyclic loadings. In: Safety Criteria in Design of Tubular Structures, Tokyo, Architectural Institute of Japan, pp. 15–25 (1987)
- Medhekar, M.S., Kennedy, D.J.L.: Seismic evaluation of single-storey steel buildings. Can. J. Civ. Eng. 26, 379–394 (1999a)
- Medhekar, M.S., Kennedy, D.J.L.: Seismic response of two-storey buildings with concentrically braced steel frames. Can. J. Civ. Eng. 26, 497–509 (1999b)
- Moghaddam, H., Hajirasolahi, L., Doostan, A.: Optimum seismic design of concentrically braced steel frames: concepts and design procedures. J. Constr. Steel Res. 61(2), 151–166 (2005)
- Mualla, I.H., Belev, B.: Performance of steel frames with a new friction damper device under earthquake excitation. Eng. Struct. 24, 365–371 (2002)
- Nonaka, T.: Approximation of yield condition for the hysteretic behavior of a bar under repeated axial loading. Int. J. Solids Struct. 13, 637–643 (1977)
- Ochi, K., Yamashita, M., et al.: Local buckling and hysteretic behavior of circular tubular members under axial loads. J. Struct. Constr. Eng. AIJ 417, 53–61 (1990) (in Japanese)
- Papadrakakis, M., Loukakis, K.: Elastic-plastic hysteretic behavior of struts with imperfections. Eng. Struct. 9, 162–170 (1987)
- Popov, E.P., Black, R.G.: Steel struts under severe cyclic loadings. J. Struct. Div. Proc. Am. Soc. Civ. Eng. 107, 1857–1881 (1981)
- Prathuangsit, D., Goel, S.C., Hanson, R.D.: Axial hysteresis behavior with end restraints. J. Struct. Div. Proc. ASCE 104, 883–896 (1978)
- Ragni, L., Zona, A., Dall'Asta, A.: Analytical expressions for preliminary design of dissipative bracing systems in steel frames. J. Constr. Steel Res. 67, 102–113 (2011)
- Roeder, C.W., Lumpkin, E.J., Lehman, D.E.: A balanced design procedure for special concentrically braced frame connections. J. Constr. Steel Res. 67, 1760–1772 (2011)
- Shibata, M.: Analysis of elastic-plastic behavior of a steel brace subjected to repeated axial force. Int. J. Solids Struct. 18, 217–228 (1982)

- Static design procedure for welded hollow section joints, Recommendations Int. Inst. Welding (IIW)-Document XV-1329-09, IIW-Doc. XV-E-09-400. International Institute of Welding (2009)
- Supple, W.J., Collins, I.: Post-critical behaviour of tubular struts. *Eng. Struct.* 2, 225–229 (1980)
- Zayas, V.A., Mahin, S.A., Popov, E.P.: Ultimate strength of steel offshore structures. In: *Proc. 3rd Int. Conference on Behaviour of Offshore Structures*, Boston, vol. (2), pp. 39–58. Hemisphere Publ. Co., Washington (1982)

## Chapter 7 Stiffened Plates

- Birchfield, J.R.: Welded machines thrive on tough mining. *Welding Design and Fabrication* 54(4), 47–54 (1981)
- Det Norske Veritas (DNV), Buckling strength analysis. Classification Notes No.30.1. Høvik, Norway (1995)
- Det Norske Veritas (DNV), Buckling strength of plates structures. Recommended practice DNV-RP.C201. Høvik, Norway (2002)
- Eurocode 1, Actions on structures. Part 1-3. General actions. Snow loads (2003)
- Eurocode 3, Design of steel structures. Part 1-1. General structural rules (2002)
- Eurocode 3, Design of steel structures. Part 1-5: Plated structural elements (2006)
- Evans, H.R., Shanmugam, N.E.: Simplified analysis for cellular structures. *J. Struct. Eng.* ASCE 110, 531–543 (1984)
- Farkas, J.: Optimum design of metal structures. Ellis Horwood, Chichester (1984)
- Farkas, J.: Discussion to the paper of Evans R, Shanmugam NE. Simplified analysis for cellular structures. *J. Struct. Eng.* ASCE 111(10), 2269–2271 (1985)
- Farkas, J., Jármai, K.: Analysis and optimum design of metal structures. Rotterdam-Brookfield, Balkema (1997)
- Farkas, J., Jármai, K.: Analysis of some methods for reducing residual beam curvatures due to weld shrinkage. *Welding World* 41(4), 385–398 (1998)
- Farkas, J.: Thickness design of axially compressed unstiffened cylindrical shells with circumferential welds. *Welding World* 46(11/12), 26–29 (2002)
- Farkas, J., Jármai, K.: Economic design of metal structures. Millpress, Rotterdam (2003)
- Farkas, J.: Economy of welded stiffened steel plates and cylindrical shells. *J. Comput. Appl. Mech. (Univ. Miskolc)* 6(2), 183–205 (2005)
- Farkas, J., Jármai, K.: Optimum design and cost comparison of a welded plate stiffened on one side and a cellular plate both loaded by uniaxial compression. *Welding World* 50(3-4), 45–51 (2006)
- Farkas, J., Jármai, K.: Economic orthogonally welded stiffening of a uniaxially compressed steel plate. *Welding World* 51(7-8), 74–78 (2007)
- Farkas, J., Jármai, K.: Design and optimization of metal structures. Horwood, Chichester (2008a)
- Farkas, J., Jármai, K.: Minimum cost design of a square box column composed from orthogonally stiffened welded steel plates. In: Jármai, K., Farkas, J. (eds.) *Proc. Int. Conf. on Design, Fabrication and Economy of Welded Structures*, Miskolc, pp. 61–70 (2008b)
- Ge, H., Gao, S., Usami, T.: Stiffened steel box columns. Part 1. Cyclic behaviour. *Earthquake Eng. Struct. Dyn.* 29, 1691–1706 (2000)
- Haroutel, J.: Soudage laser de structures sandwich métalliques du type Norsial. *Soudage Techn. Conn.*, 25–31 (January-February 1982)



- Hirota, T., Sakimoto, T., Yamao, T., Watanabe, H.: Experimental study on hysteretic behaviour of inverted L-shaped steel bridge piers filled with concrete. In: Loughlan, J. (ed.) *Proc. 4th Int. Conf. on Thin-walled Structures*, Loughborough, UK, pp. 373–380. Institute of Physics Publ., Bristol (2004)
- Krack, M., Secanell, M., Mertiny, P.: Cost optimization of a hybrid composite flywheel rotor with a split-type hub using combined analytical/numerical models. *Struct. Multidisc Opt.* 44(1), 57–73 (2011), doi:10.1007/s00158-010-0573-z
- Kravanja, S., Zula, T., Klansek, U.: The MINLP approach to cost optimization of structures. In: *Int. Conf. Proc. of the Design, Fabrication and Economy of Welded Structures*, Miskolc, Hungary, pp. 89–96. Horwood, Chichester (2008)
- Kuzminov, S.A.: *Welding deformations of ship structures*. Sudostroenie, Leningrad (1974) (in Russian)
- Masubuchi, K.: *Analysis of welded structures*. Pergamon Press, Oxford (1980)
- Nakai, H., Kitada, T., Miki, T.: An experimental study on ultimate strength of thin-walled box stub-columns with stiffeners subjected to compression and bending. *Proc. JSCE Structural Eng. / Earthquake Eng.* 2(2), 87–97 (1985)
- Ohga, M., Takemura, S., Imamura, S.: Nonlinear behaviours of round corner steel box-section piers. In: Loughlan, J. (ed.) *Proc. 4th Int. Conf. on Thin-walled Structures*, Loughborough, UK, pp. 365–372. Institute of Physics Publ., Bristol (2004)
- Okerblom, N.O., Demyantsevich, V.P., Baikova, I.P.: *Design of fabrication technology of welded structures*. Sudpromgiz, Leningrad (1963) (in Russian)
- Paik, J.K., Thayamballi, A.K.: *Ultimate limit state design of steel-plates structures*. John Wiley and Sons Ltd., Chichester (2003)
- Pavlovic, L., Krajnc, A., Beg, D.: Cost function analysis in the structural optimization of steel frames. *Struct. Multidisc Opt.* 28(4), 286–295 (2004)
- Pettersen, E.: *Analysis and design of cellular structures*. University of Trondheim, Norwegian Institute of Technology, Trondheim (1979)
- Shanmugam, N.E., Evans, H.R.: A grillage analysis of the nonlinear and ultimate load behavior of cellular structures under bending loads. *Proc. Inst. Civ. Eng. Part 2* 71, 705–719 (1984)
- Shanmugam, N.E., Balendra, T.: Free vibration of thin-walled multi-cell structures. *Thin-walled Struct.* 4, 467–483 (1986)
- Sahmel, P.: Statische und konstruktive Probleme bei Hilfsvorrichtungen zum Transport schwerer Behälter. *Fördern Heben* 28, 844–847 (1978)
- Sales program, Commercial sections. Arcelor Mittal. Long Carbon Europe (2007)
- Sarma, K.C., Adeli, H.: *Life-cycle cost optimization of steel structures*. Wiley Publishers (2002), doi:10.1002/nme.549
- Steinhardt, O.: Berechnungsmodelle für ausgesteifte Kastenträger. In *Beiträge zum Beulproblem bei Kastenträgerbrücken*. Deutscher Ausschuss für Stahlbau. Berichtsheft 3, 27–35 (1975)
- Timoshenko, S., Woinowsky-Krieger, S.: *Theory of plates and shells*. McGraw Hill, New York (1959)
- Usami, T., Gao, S., Ge, H.: Stiffened steel box columns. Part 2. Ductility evaluation. *Earthquake Eng. Struct. Dyn.* 29, 1707–1722 (2000)
- Vaynberg, D.V., Vaynberg, E.D.: *Calculation of plates*. Kiev, Budivelnik (1970) (in Russian)
- Vinokurov, V.A.: *Welding stresses and distortion*. The British Library, Boston Spa (1977) (translated from Russian)

- Williams, D.G.: Analysis of doubly plated grillage under inplane and normal loading. PhD Thesis. Imperial College, London (1969)
- Yamao, T., Matsumara, S., Hirayae, M., Iwatsubo, K.: Steel tubular bridge piers stiffened with inner cruciform plates under cyclic loading. In: Loughlan, J. (ed.) Proc. 4th Int. Conf. on Thin-walled Structures, Loughborough, UK, pp. 357–364. Institute of Physics Publ., Bristol (2004)

## **Chapter 8** *Cylindrical and Conical Shells*

- Akl, W., Ruzzen, M., Baz, A.: Optimal design of underwater stiffened shells. Struct. Multi-disc. Optim. 23, 297–310 (2002)
- Cho, S.R., Frieze, P.A.: Strength formulation for ring-stiffened cylinders under combined axial loading and radial pressure. J. Constr. Steel Res. 9, 3–34 (1988)
- Det Norske Veritas, Buckling strength of shells. Recommended Practice DNV-RP-C202. Høvik, Norway (2002)
- Eurocode 3, Design of steel structures. Part 1-1: General structural rules. Brussels, CEN (2009)
- Farkas, J., Jármai, K.: Analysis and optimum design of metal structures, Rotterdam, Brookfield, Balkema (1997)
- Farkas, J., Jármai, K.: Economic design of metal structures. Millpress, Rotterdam (2003)
- Farkas, J., Jármai, K.: Design and optimization of metal structures. Horwood Publishing, Chichester (2008a)
- Farkas, J., Jármai, K.: Minimum cost design of a conical shell – External pressure, non-equidistant stiffening. In: Ofner, R., et al. (eds.) Proceedings of the Eurosteel 2008 5th European Conference on Steel and Composite Structures Graz Austria, vol. B, pp. 1539–1544. ECCS European Convention for Constructional Steelwork, Brussels (2008b)
- Ghanbari, G.T., Hossein, S.: Experiments on conical shell reducers under uniform external pressure. J. Constr. Steel Res. 67, 1506–1515 (2011)
- Harding, J.E.: Ring-stiffened cylinders under axial and external pressure loading. Proc. Inst. Civ. Engrs. Part 2 71, 863–878 (1981)
- Huang, J., Wierzbicki, T.: Plastic tripping of ring stiffeners. J. Struct. Eng. Proc. Am. Soc. Civ. Eng. 119(5), 1622–1642 (1993)
- Pappas, M., Allentuch, A.: Extended capability for automate design of frame-stiffened submersible cylindrical shells. Comput. Struct. 4(5), 1025–1059 (1974)
- Pappas, M., Morandi, J.: Optimal design of ring-stiffened cylindrical shells using multiple stiffener sizes. AIAA J. 18(8), 1020–1022 (1980)
- Tian, J., Wang, C.M., Swaddiwudhipong, S.: Elastic buckling analysis of ring-stiffened cylindrical shells under general pressure loading via the Ritz method. Thin-Walled Struct. 35, 1–24 (1999)
- Wang, C.M., Swaddiwudhipong, S., Tian, J.: Buckling of cylindrical shells with general ring-stiffeners and lateral pressure distributions. In: Choi, C.K., et al. (eds.) Proceedings of the Seventh Internat. Conf. Computing in Civil and Building Engng., Seoul, Korea, vol. 1, pp. 237–242 (1997)

# Subject Index

## A

- Absorbed energy of braces 110
- Area of the stable hysteretic loop 116
- Assembly desk constructed from orthogonally stiffened plate 150

## B

- Box column with cellular plate walls 200

## C

- Calculation of welding times 30–32, 34, 35
- Cantilever column loaded by axial compression and bending 219
- Conical shell 219
  - Constraint on shell buckling 219
  - Cost of forming of plate parts into shell elements 221
- Comparison of circular and conical shells 223
- Cantilever tubular truss
  - Minimum volume design 63
  - Minimum cost design 66
- Cellular plate orthogonally stiffened loaded by uniaxial compression 193
- Minimum cost design 193
- Bending and torsional stiffness 195
- Check for strength of a tubular truss joint 88
- Circular floor constructed from stiffened sectorial plates 182
- Minimum cost design of a sectorial plate 183
- Optimum design of radial beams 188

- Optimal number of radial beams 190
- Cost comparison with unstiffened plate version 191
- Comparison of optimum solutions 7–11
- Comparison of standard and modified PSO algorithms 23
- Compressed and bent columns 7
- Stringer stiffened cylindrical shell 7
- Square box 7
- Conical shell loaded by external pressure with non-equidistant ring-stiffening 223
- Design of shell segment lengths 224
  - Buckling constraint 225
  - Design of ring stiffeners 225
  - Cost function 227
- Cost function
  - of welded box beam 46
  - of tubular trusses 80
  - of welded stiffened sectorial plates 164, 168
  - of cellular plate 198
  - of box column with cellular plate walls 205
  - of ring-stiffened cylindrical shell 215
  - of ring-stiffened conical shell 227
- Cost of cutting and grinding of CHS strut ends 40, 81
- Cost comparison
  - of trusses with N or rhombic bracing 97
  - of optimum solutions 7–11
  - of stiffened and unstiffened sectorial plates 172
  - of square box column walls 208
  - of circular and conical shells 223
- Cost of fire protection 53

Intumescent paint 53  
 Plasterboard 53  
 Cost of materials 30  
 Cutting times 33, 36, 38

## D

Design by routine 5  
 Advantages and disadvantages 5  
 Design of stiffened plates 1

## E

Energy-absorbing capacity of a strut  
 116

## F

Fabrication constraints 3  
 Fabrication cost 30  
 Firefly algorithm 16  
 Fire resistant design  
   Centrally compressed welded box  
     column 50  
   Bent box beam 54  
 Fixed storage tank roof constructed from  
   stiffened sectorial plates 174  
   Design of welded stiffened sectorial  
     plates 176  
   Design of radial beams 179

## G

Grid effect in an orthogonally welded  
 stiffened plate 148

## I

Interaction of overall buckling and  
 fatigue 6  
 Interaction of two instabilities 6  
 IOSO (Indirect Optimization on Self-  
   Organization) technique 24

## L

Laser cutting times 36, 37  
 Laser welding times 33, 35

## M

Minimum cost design for fire resistance  
 47  
   Critical temperature method 48  
   Overall buckling constraint in fire  
     51  
     Local buckling constraint in fire 52  
 Modification of PSO algorithm 21

## N

Nonlinear programming problem 16

## O

Optimum design 6  
   Advantages and disadvantages 6  
   truss structures 11  
   building frames 11  
   industrial applications 11  
 Optimum design of trusses 61–107  
   deflection constraint 69  
 Orthogonally stiffened plate 144  
   Minimum cost design for deflection  
     constraint 144  
   Residual welding deflection from  
     longitudinal welds 145  
   Assembly desk of square symmetry  
     150  
   Design with and without grid effect  
     159  
 Overall buckling check of compression  
   rods 80

## P

Particle swarm algorithm (PSO) 19  
 Plasma cutting times 38, 39  
 Postbuckling behaviour of frame  
   bracing 112  
 Ring stiffened cylindrical shell loaded  
   by external pressure 212  
   Constraint on shell buckling 213  
   Constraint on stiffener buckling 214  
   Cost function 215

## S

School of structural optimization 2  
 Sectorial plate design 154  
 Seismic design of a portal frame with X-  
   bracing 116

Absorbed energy of cyclically loaded  
braces 116  
Stable hysteretic loop 116  
Postbuckling behaviour of braces  
112  
Area of the stable hysteretic loop  
116  
Energy-absorbing capacity of a strut  
116  
Calculation of elastic sway 120  
Stress constraint for columns and  
beams 123, 124  
Joint between beam and brace 125  
Welded frame corner 128  
Seismic design of a V-braced 3D multi-  
story frame 129  
Simply supported tubular truss 75  
Optimum design for displacement  
constraint 75  
Square box column with cellular plate  
walls 200  
Constraint on overall buckling of a  
wall 203  
Constraint on horizontal  
displacement of column top 205  
Cost function 205  
Cost comparison of different wall  
structures 208  
Stiffened circular cylindrical shell 212  
Stiffened conical shell 223  
Stiffened sectorial plates 157  
Storage tank roof 174  
Structural optimization system 2, 3  
Structural synthesis 1, 3  
SUMT mathematic method 2  
Surface preparation time 39

## T

Thermal and waterjet cutting cost 34  
Transmission line tower of tubular truss  
98  
Loads 99  
Optimization process 104  
Volume and cost function 105  
Optimum truss angle 105  
Optimum mass 107  
Comparison with the Rao's tower  
107  
Tubular trusses with N and rhombic  
bracing 86

Constraints on stress, buckling and  
deflection 94  
Cost functions 89  
Cost comparison of N and rhombic  
bracing 96  
Tubular truss column 70  
Parallel chords 70  
Non-parallel chords 72

## V

V-braced 3D multi-story frame 129  
Design of CHS bracings 132  
Design of beams, columns and beam-  
to-column joints 135–140  
Joints of braces to the frame 140  
Vertical storage tank roof 1, 3

## W

Waterjet cutting times 37  
Welded box beam 43  
Minimum cross-sectional area design  
44  
Cost function 46  
Minimum cost design 46  
Welded box beam minimum cost design  
for fire 47  
Unprotected beam with stress  
constraint 55  
Protected beam with stress constraint  
57  
Unprotected beam with deflection  
constraint 57  
Protected beam with deflection  
constraint 58  
Welded stiffened sectorial plate 157  
Non-equidistant tangential stiffening  
160  
Equidistant tangential stiffening,  
stepwise varying base plate  
thickness 167  
Equidistant tangential and radial  
stiffeners 170  
Cost comparison with unstiffened  
plate 172  
Welding times  
for 1/2V and V butt welds 31  
for K and X butt welds 32  
Wind turbine tower 9